

Catalysis By Some Pillared Montmorillonites

Thesis submitted to the
Cochin University of Science And Technology
in partial fulfilment of the
requirements for the degree of

Doctor of Philosophy
In
Chemistry

In the Faculty of Science

By

RAHNA K. SHAMSUDEEN

Department of Applied Chemistry
Cochin University of Science And Technology
Kochi - 682 022

December - 2001

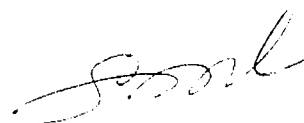
*Remembering each and every one who stood with me
in times of shine and shade throughout
my research period.....*

...to my loving ikka and moloos

CERTIFICATE

This is to certify that the thesis herewith is an authentic record of research work carried out by Ms. Rahna K. Shamsudeen under my supervision, in partial fulfilment of the requirements for the degree of Doctor of Philosophy of Cochin University of Science and Technology, and further that no part thereof has been presented before for any other degree.

Kochi-682 022
13th December 2001

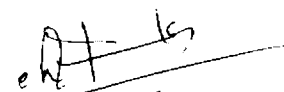


Dr. S. SUGUNAN
(Supervising teacher)
Professor in Physical Chemistry
Department of Applied Chemistry
Cochin University of Science and Technology
Kochi-682 022

DECLARATION

I hereby declare that the work presented in this thesis entitled “**Catalysis by Some Pillared Montmorillonites**” is entirely original and was carried out by me independently under the supervision of Dr. S. Sugunan, Professor in Physical Chemistry, Department of Applied Chemistry, Cochin University of Science and Technology, Kochi-22, Kerala, India, and has not been included in any other thesis submitted previously for the award of any degree.

Kochi-22
13th December 2001



Rahna K. Shamsudeen

Acknowledgements

" I bow before the sovereign Alchemist that in a trice transmutes life's leaden metal into gold"

- Omar Khayyam

With extreme pleasure, I express my sincere and deep sense of gratitude and obligation to my supervising guide, Prof. (Dr.) S. Sugunan, Head of the Department of Applied Chemistry, for his valuable guidance, research training, constant encouragement and timely suggestions throughout my research period. I shall ever remain grateful to him.

I would like to thank Dr. P. Madhavan Pillai and Dr. K.K. Mohammed Yusuff, former Heads of the Department, for providing the necessary facilities for research.

I take this opportunity to thank all the teaching and non-teaching staff of the Department of Applied Chemistry for their help and goodwill on all occasions. Special thanks are due to Mrs. Indira Devi, Section Officer, for her valuable support in office proceedings. I acknowledge with thanks the help rendered by Dr. P. Indrasenan, Professor and Head, Department of Chemistry, University of Kerala and by Dr. M. B. Talawar, HEMRL, Pune, for providing me the necessary thermogravimetric data.

Dr. Jyothi T. M. has always been constantly encouraging and sincerely helping my work by his valuable and timely suggestions, provoking my research interest. I place on record here my sincere gratitude to him. I am deeply indebted and profoundly grateful to Dr. C. G. Ramankutty for his immense assistance, critical scrutiny of the manuscript and constant encouragement during my research period, especially during the thesis writing months.

I am extremely thankful to my former labmates Dr. Renuka N.K. and Dr. K. Sree Kumar and my present labmates Suja, Deepa, Nisha, Sreeja Ajith, Manju, Smitha, Fincy, Bejoy, Sunaja and Sanjay for their sincere cooperation and encouragement throughout my work. But for their lively company, my life in the lab would have been dull. My thanks to all my friends in the Department of Applied Chemistry for their goodwill and cooperation on all occasions. I remember with heart-felt thanks the help rendered by Mr. Gopimenon, Mr. Kashmiri, Mr. Joshi and other technical staff of USIC, CVSAT and Mr. Suresh, Chemito, for their readiness to help me on occasions of technical difficulties. I extend my special thanks to my friends in the Department of Physics for their readiness to help on various occasions.

I would like to apologise to my dear ikka and little daughter for the many hours of my time spent on research instead of with them. No words can express my depth of gratitude towards my ikka. He has been rendering me his wholehearted support and was always ready to suffer any difficulties for the completion of my Ph. D work. To our families, I owe the moral support that they extended throughout my work.

The financial support granted by CSIR, New Delhi is gratefully acknowledged.

Rahna K. Shamsudeen

CONTENTS

Chapter 1	Introduction and Literature Survey	Page No.
1.0	Introduction.....	1
1.1	Homogeneous and Heterogeneous Catalysis.....	1
1.2	Heterogeneous Catalysis.....	2
1.3	Classification of Heterogeneous Catalysts.....	3
1.4	Solid Acid-base Concept in Heterogeneous Catalysis.....	3
1.5	Clays.....	5
1.5.1	Structure of Clays.....	6
1.5.2	Classification of Clay Minerals.....	8
1.5.3	Structural Formula for Clays.....	11
1.6	Smectites.....	12
1.6.1	Unique Properties of Smectites.....	13
1.7	Montmorillonite.....	15
1.8	Modification on Clays.....	16
1.9	Pillared Clays.....	17
1.9.1	Basic Pillaring Mechanism.....	18
1.9.2	Preparation of Pillared Clays-Variou Pillaring Agents.....	20
1.10	Aluminium Pillaring.....	22
1.11	Iron Pillaring.....	24
1.12	Chromium Pillaring.....	25
1.13	Other Pillared Clays.....	26
1.14	Mixed Pillared Clays.....	26
1.14.1	Mixed Fe-Al Pillared Clays.....	27
1.14.2	Mixed Cr-Al Pillared Clays.....	30
1.14.3	Other Mixed Metal/Al Pillared Clays.....	32
1.15	Physical Characteristics of Pillared Clays.....	33
1.15.1	Porosity-Influence of Drying.....	34
1.15.2	Thermal Stability of Pillared Clays.....	35
1.16	Chemical Properties of Pillared Clays-Acidity.....	36
1.16.1	Determination of Acidity.....	38
1.16.2	Catalytic Test Reactions for Acidity.....	40
1.17	Vanadium Impregnation over Clays.....	42
1.18	Catalysis by Pillared Clays.....	43
1.19	Reactions Selected for the Present Study.....	46
1.20	Main Objectives of the Present Work.....	49
	References.....	52
Chapter 2	Experimental	
2.0	Introduction.....	64
2.1	Preparation of Catalysts.....	64
2.1.1	Preparation of Single Oxide Pillared Montmorillonites.....	64
2.1.2	Preparation of Mixed Oxide Pillared Montmorillonites.....	65
2.1.3	Preparation of Vanadia Impregnated Iron-Pillared Montmorillonites.....	65
2.2	Notations of Catalysts.....	66
2.3	Characterisation Techniques.....	66
2.3.1	Energy Dispersive X-Ray Fluorescence Analysis (EDX).....	66
2.3.2	X-Ray Diffraction Analysis (XRD)..	67

2.3.3	BET Surface Area and Pore Volume Measurements.....	68
2.3.4	Infrared Spectroscopy.....	70
2.3.5	Thermogravimetric Analysis.....	71
2.3.6	Acidity Determination Studies.....	71
2.4	Catalytic Activity Measurements.....	74
2.4.1	Liquid Phase Reactions.....	74
2.4.2	Vapour Phase Reactions.....	75
	References.....	79
Chapter 3	Textural and Acidic Properties	
3.0	Introduction.....	80
3.1	Energy Dispersive X-Ray Fluorescence Analysis (EDX).....	80
3.2	X-Ray Diffraction Analysis (XRD)..	83
3.2.1	XRD of Single Metal Oxide Pillared Systems.....	83
3.2.2	Stability of the Pillared Structure Assigned from XRD Data...	85
3.2.3	XRD of Mixed Pillared Systems.	88
3.2.4	XRD of Vanadia Impregnated Iron-Pillared Montmorillonites.	90
3.3	Visible Spectroscopy of Chromium and Mixed Chromium-Aluminium Pillaring Solutions.....	92
3.4	BET Surface Area and Pore Volume Measurements.....	94
3.5	Infrared Spectroscopy.....	97
3.6	Thermogravimetric Analysis.....	100
3.7	Acidity Studies.....	100
3.7.1	Evaluation of Brønsted Acidity-Adsorption of 2,6-Dimethylpyridine.....	100
3.7.2	Electron Accepting Studies using Perylene-Evaluation of Lewis Acidity.....	105
3.7.3	Temperature Programmed Desorption of Ammonia (TPD).....	110
3.8	Cumene Conversion Reaction as a Test Reaction for Acidity...	113
3.8.1	Process Optimisation.....	114
3.8.2	Catalyst Comparison.....	118
3.8	Cyclohexanol Decomposition Reaction as a Test Reaction for Acidity.....	124
3.9.1	Process Optimisation	125
3.9.2	Catalyst Comparison	128
	References.....	131
Chapter 4	Catalytic Activity of Pillared Clays in Liquid Phase and Vapour Phase Alkylation and Acylation Reactions	
4.0	Friedel-Crafts reactions.....	134
4.1	Benzoylation of Toluene.....	136
4.1.1	Benzoylation of Toluene with Benzyl Chloride.....	136
4.1.2	Benzoylation of Toluene with Benzyl Alcohol.....	148
4.1.3	Influence of Benzylating Agent.....	157
4.2	Benzoylation of Toluene.....	158
4.2.1	Influence of Molar ratio.....	159
4.2.2	Influence of Catalyst Composition.....	160
4.2.3	Mechanism of Benzoylation Reaction.....	162
4.3	Alkylation of Aniline.....	164
4.3.1	Process Optimisation.....	166

4.3.2	Catalyst Comparison.....	170
	References.....	175
Chapter 5	Pillared Clays as Efficient Catalysts for Liquid Phase Catalytic Wet Peroxide Oxidation of Phenol	
5.0	Introduction.....	178
5.1	Process Optimisation.....	181
5.1.1	Effect of Reaction Temperature.....	181
5.1.2	Effect of Solvent.....	183
5.1.3	Effect of Amount of H ₂ O ₂	186
5.1.4	Effect of Reaction Time.....	187
5.2	Catalytic Reaction over Various Fe-Al Pillared Montmorillonites.....	188
5.3	Mechanism of Phenol Hydroxylation.....	189
5.4	Catalytic Activity Studies over Other Systems.....	191
	References.....	194
Chapter 6	Summary and Conclusions	
6.1	Summary of the Work.....	196
6.2	Conclusions.....	198
	Further Scope for the Work.....	200

PREFACE

Heterogeneous catalysis is an interdisciplinary area since it is based on solid state chemistry and physics, materials chemistry and engineering, surface science, analytical chemistry, theoretical chemistry, reaction kinetics and mechanisms and reaction engineering. It has not only become the basis of industrial and environmental chemistry during this century, but also its scientific foundation has been developing with ever increasing speed. Because of the great importance of acid catalysts in the petrochemical industry, extensive research work has been carried out during the last three decades concerning the fundamental and applied aspects of catalysis by acids. There is now renewed interest in the field of pillared clays since they are microporous materials with high surface area and they have a close resemblance with zeolites. The interesting architecture of pillared clays can be tuned by varying the interlayer distance. In addition, the chemical functions such as Brønsted and Lewis acidity can be modified by various techniques. By virtue of their acidic properties, they can be promising catalysts in acid catalysed reactions.

In the present study, we have prepared and evaluated the physical and chemical properties and catalytic activities of various single, mixed and modified pillared montmorillonites. The single oxide pillared clays include Al-, Fe- and Cr-pillared montmorillonites. The mixed oxide pillared montmorillonites such as Fe-Al and Cr-Al pillared systems with various Fe(Cr)/Al ratios are also prepared. Modification of iron-pillared system is done by vanadia impregnation. Characterisation using various physico-chemical techniques and a detailed study of acidic properties are also carried out. Major part of our work is oriented to evaluate the catalytic activity of the pillared systems towards certain important catalytic reactions. Our samples are found to be excellent catalysts for the reactions namely Friedel-Crafts benzylation and benzylation, methylation of aniline and catalytic wet peroxide oxidation of phenol.

The thesis is organised into six chapters. The first chapter deals with the brief introduction and literature survey on pillared clays and their catalysis. Second chapter expounds the materials and methods employed in the work. Results and discussion regarding the characterisation and activity studies are described in subsequent chapters. Last chapter includes the summary of the investigation and the conclusions drawn from the work.

Introduction And Literature Survey

1.0 Introduction

Catalysis has a profound beneficial impact on industry and more importantly on society in the 21st century. It is the most important technology in environmental protection. The successful exploration of a material as a catalyst eliminates or minimises the use and release of environmentally hazardous substances, which are responsible for environmental pollution. Furthermore, catalysis plays a vital role in providing fuels, commodity/fine chemicals and pharmaceuticals. Today, more than 60% of all chemical products and almost 90% of chemical processes are based on catalysis, attesting to the pervasive presence and necessity of this discipline throughout the chemical industry.

The term catalysis was introduced as early as 1836 by J.J. Berzelius in which he assumed that catalysis possesses special powers that can influence the affinity of chemical substances. A definition that is valid still today was proposed by Ostwald in 1895. He defined a catalyst as a substance that accelerates a chemical reaction without affecting the position of equilibrium. This definition includes the possibility of small loss of catalyst or its activity during the course of the reaction. However, the catalyst affects only the rate of the reaction, it changes neither the thermodynamics of the reaction nor the equilibrium position.

1.1 Homogeneous and Heterogeneous Catalysis

In chemical industry, two major catalytic processes namely homogeneous and heterogeneous, have been widely employed. Each of these catalytic processes possesses its own advantages and disadvantages. Homogeneous systems often perform better selectivity, activity and reproducibility. However, they are more vulnerable to extraneous materials. The cost of production is very high owing to their low thermal stability and shorter catalyst lifetime, which is a serious drawback from an industrial point of view. The advantages of heterogeneous catalytic processes include the easy separation of the final reaction mass from the catalyst, reusability of

the catalyst and the possibility of continuous operation in a reactor without interruption. Also, heterogeneous processes are more environmentally benign and have little disposal problems, in comparison with homogeneous catalysis. Thus there is a strong impetus for the synthesis of new heterogeneous systems to replace the existing homogeneous systems and this has become a challenging task in the catalytic field.

1.2 Heterogeneous Catalysis

The field of heterogeneous catalysis is one of the most rapidly expanding areas in chemistry. In heterogeneous catalysis, the reactants and catalysts are present in different phases. Usually, the catalyst is a solid and the reactants are either liquids or gases. The heterogeneous catalyst provides an alternate reaction path with a lower energy of activation. The process of heterogeneous catalysis involves the following steps:

- (i) Diffusion of the reactants to the surface of the catalyst,
- (ii) Adsorption of the reactants on the surface,
- (iii) Reaction on the surface,
- (iv) Desorption of the products from the surface and
- (v) Diffusion of the products away from the catalyst.

Of these, (ii) and (iii) are the most important steps. A catalyst can be effective only when the adsorption of the reactant(s) on the surface of the catalyst is not very strong and the desorption of the product(s) is fast. Very strong interaction of the reactants and products on the surface only 'poisons' the catalyst. Adsorption generally is not uniform across a solid surface. Adsorption and therefore catalysis occurs primarily at certain favourable locations called 'active sites'.

The properties of a heterogeneous catalyst for industrial use may be classified into two categories [1].

- (i) Properties that determine directly the catalytic activity and reactivity. Here factors such as bulk and surface chemical composition, local microstructure and phase composition are important.

(ii) Properties that ensure their successful implementation in the catalytic process. These include thermal and mechanical stability, porosity, shapes and dimension of catalyst particles.

In short, a commercial heterogeneous catalyst should be stable, active and selective and should have sufficiently high surface area, good porosity and stable mechanical strength.

1.3 Classification of Heterogeneous Catalysts

Heterogeneous catalysts are classified into several ways. Based on their physicochemical nature, they are generally classified as

- a) Metal oxides: Simple, mixed, supported and modified metal oxides
- b) Supported metals/bimetallic catalysts
- c) Zeolites/molecular sieves
- d) Clays and hydrotalcites
- e) Solid supported heteropolyacids

They are also classified on the basis of their function as

- a) Shape selective catalysts
- b) Phase transfer catalysts
- c) Redox catalysts
- d) Acid-base catalysts

Apart from these two classifications, heterogeneous catalysts are also described as structure sensitive and structure insensitive, based on their behaviour in a particular reaction. Rates of structure sensitive catalytic reactions alter markedly when the crystallite size of the system is changed, whereas rate is independent of crystallite size in structure insensitive reactions.

1.4 Solid Acid-Base Concept in Heterogeneous Catalysis

A major part of the industrial chemical reactions such as catalytic cracking, hydration, dehydration, hydrolysis, isomerisation, etc. come under the acid-base reaction category. These types of reactions are accelerated under the influence of an acid or a base. The elementary step in these reactions is the characteristic transfer of proton or the production of heteropolar donor-acceptor pair [2]. Acid-base property

of a heterogeneous surface is thus an important factor in determining the catalytic efficiencies for these reactions.

Many materials possess inherent acid-base centres. An exhaustive list of various solid acids and bases is tabulated by Tanabe [3] who defined a solid acid as one on which the colour of a basic indicator changes concomitant with its chemisorption and a solid base as one on which the colour of an acidic indicator changes as a result of chemisorption. Various solid acids include the naturally occurring clay minerals, zeolites, silica-alumina and various metal oxides, sulphates, sulphides, phosphates and halides. These solid acids have usually been employed as catalysts on various acid catalysed reactions. Surface hydroxyl groups and co-ordinatively unsaturated metal cations are responsible for the surface acidity. Surface hydroxyl groups originating from incomplete dehydration act as Brönsted acid sites. They may dissociate to protonate an adsorbed base. Brönsted acid sites are present only when surface hydroxyl groups are available. Exposed co-ordinatively unsaturated (CUS) cations may act as Lewis acid sites. The strength of these acid sites depends on the charge and size of the cations.

Extensive studies on heterogeneous cracking catalysts undertaken during 1950s revealed that the essential feature of cracking catalysts is acidity, and therefore, generation of acidic sites on the solids was extensively studied. As a result, amorphous silica-alumina was utilised as a cracking catalyst for a long time. Presently, zeolites have replaced almost all kinds of catalysts in cracking. Good correlation between the total amount of acid (Lewis+Brönsted) and catalytic activities has been found in many cases. For example, the rates of both catalytic decomposition of cumene [4] and polymerisation of propylene [5] over $\text{SiO}_2\text{-Al}_2\text{O}_3$ catalysts were found to increase with increasing acid amounts.

In contrast to the extensive studies of heterogeneous acidic catalysts, fewer efforts have been given to the study of heterogeneous basic catalysts. Pines *et al.* first reported the study of heterogeneous basic catalysts [6]; sodium metal dispersed on alumina acted as an effective catalyst for double bond migration of alkenes.

The various types of heterogeneous basic catalysts [7] are,

a) single component metal oxides such as oxides of alkali, alkaline earth and rare earth metals.

- b) alkali ion-exchanged and alkali ion added zeolites
- c) alkali metal ions supported on alumina, silica or alkaline earth oxide
- d) clay minerals such as hydrotalcites, sepiolite and chrysotile
- e) non-oxides such as KF supported on alumina, lanthanide imide and nitride on zeolite.

In addition to the above mentioned catalysts, a number of materials have been reported to act as heterogeneous base catalysts. Except for non-oxide catalysts, the basic sites are believed to be surface oxygen atoms. These oxygen atoms can interact with a proton. Apart from the double bond migration of 1-butene as reported by Pines *et al.* [6], several other reactions such as alcohol dehydrogenation to aldehydes or ketones, hydrogenation of olefins, amination of conjugated dienes, Meerwin-Ponndorf-Verley (MPV) reduction, side chain alkylation of aromatics, aldol condensation, etc. also come under the base catalysed reactions.

In our investigation, clay based systems are chosen as heterogeneous catalysts. Thus, it is now the turn of clay catalysts that are to be discussed in detail. A detailed discussion on clays is given below.

1.5 Clays

Clays are a group of silicate minerals composed of aluminium and/or magnesium hydroxides along with silica. Clay minerals are loosely described as aluminosilicates. They are usually produced as a result of the process of weathering, hydrothermal alteration or diagenesis.

Majority of these minerals have layer structures and are therefore called phyllosilicates. But some clay minerals have chain or ribbon structures and are called inosilicates (for example, pyroxenes). Disorder in one or two dimensions and interlayering produce many clay mineral species which are intermediate between the wholly crystalline and amorphous forms. Owing to their weak tendency to crystallise, clay minerals are usually of colloidal grain size. These are widespread in both continental and marine clays in soils and in hydrothermal products.

1.5.1 Structure of Clays

In clay minerals, the layer silicates, the extremely stable SiO_4 tetrahedral structural unit has polymerised to form two-dimensional sheets. These

two-dimensional tetrahedral sheets of composition T_2O_5 (T-tetrahedral cation) are formed by the linkage of individual tetrahedral unit with neighbouring tetrahedron by sharing three of the oxygens (basal oxygen) at the corners of the tetrahedra [8] as illustrated in Figure 1.1(a). The continuous linkage through these basal oxygen results in a hexagonal mesh pattern as shown in Figure 1.1(b). It should be noted that SiO_4 is also capable of polymerising one dimensionally using only two oxygens to form chains or ribbons as in the case of inosilicates, and even by sharing all its corner oxygen to form a three-dimensional structure such as quartz which is a tectosilicate. So far as clay minerals are concerned, it is the fact that each tetrahedron has a spare oxygen, unshared in the sheet, which is of importance. This fourth oxygen, called apical oxygen, of course points normally away from the tetrahedral sheet. These oxygens are linked to the other main structural element involved in the crystal. This element is an octahedral sheet formed from oxygen and metal ions, as shown in Figure 1.1(c). Most often, the latter are Al or Mg. Like tetrahedra, octahedra too can polymerise in two dimensions (Figure 1.1 (c)), in this case, by the sharing of four oxygens. Apart from aluminium and magnesium, Fe^{2+} and Fe^{3+} are also commonly found in naturally occurring clays, but other appropriately sized cations such as Ti, V, Mn, Li, Co, Ni and Zn are present in individual minerals.

The tetrahedral sheet (Tet) of polymerised SiO_4 units and the octahedral sheet (Oct) are the basic building blocks of most clay minerals. It turns out to be geometrically possible for oxygens to be shared between the two types of sheets lying one on top of the other. However, there is a degree of distortion and strain in the resulting lattice since the octahedral sheet unit is commonly smaller than the tetrahedral sheet unit. The oxygen involved are the apical from the tetrahedral sheet and those unshared octahedral ions normal to the octahedral sheet; the result is that the oxygen of the Si-O becomes the oxygen of the Al-OH, producing the link Si-O-Al, as shown in Figure 1.2. It can be seen from this structure that the tetrahedral sheet has no further spare apical oxygen, so it is not possible for another octahedral sheet to come under the tetrahedral sheet in order to form Oct-Tet-Oct sandwich. However, it is clearly possible for another tetrahedral sheet to condense on the top of the octahedral sheet, as the latter has spare OH groups, to form Tet-Oct-Tet layers. This is shown schematically in Figure 1.3. Tet-Oct-Tet is now a

completed layer structure, a lamella about 1nm thick, incapable of further growth by condensation in the 'c' plane.

Perhaps the best known fact about clays is that the majority of these carry a net negative charge due to isomorphous substitution of lower valency cations for the higher, within the structure. This often comes about during their formation in 'dirty' geochemical environments, when ion size, rather than either valency or even chemical identity determines substitution in either tetrahedral or octahedral spaces in the oxygen framework. The resulting negative charge in the lattice is electrically balanced in the natural state by adsorption at the surface of various positively

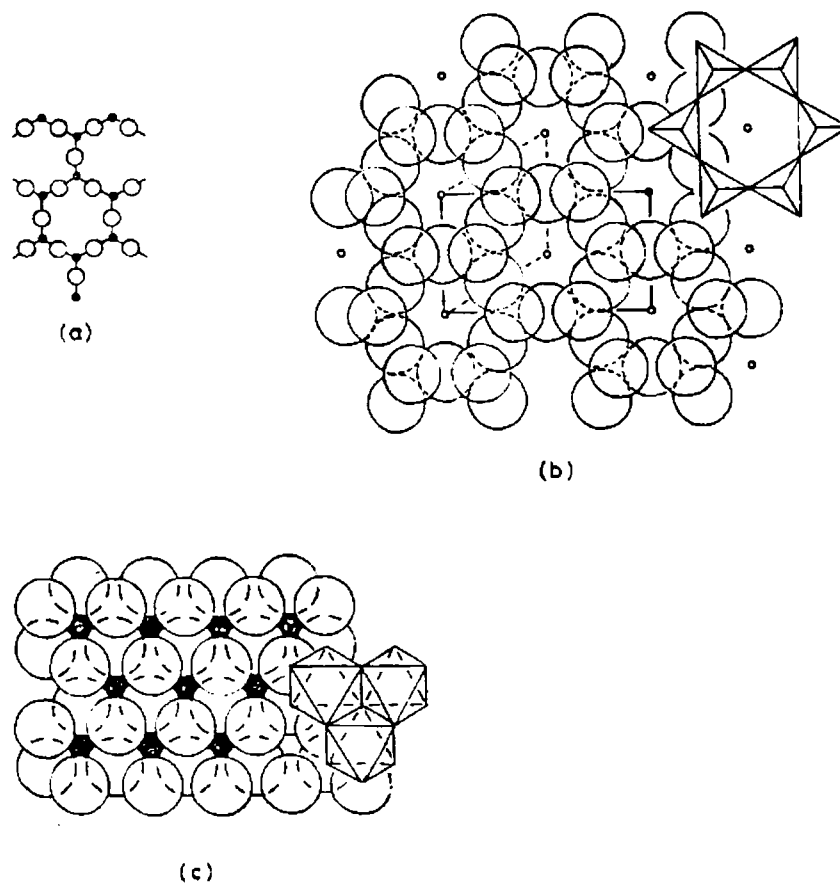


Figure 1.1 (a) Hexagonal mesh pattern formed by the linkage of basal oxygens of silicon tetrahedral (b) plan view of ideally hexagonal tetrahedral sheet. Alternative hexagonal (dashed line) and orthogonal cells (full lines) are shown connecting lattice points and (c) octahedral sheet

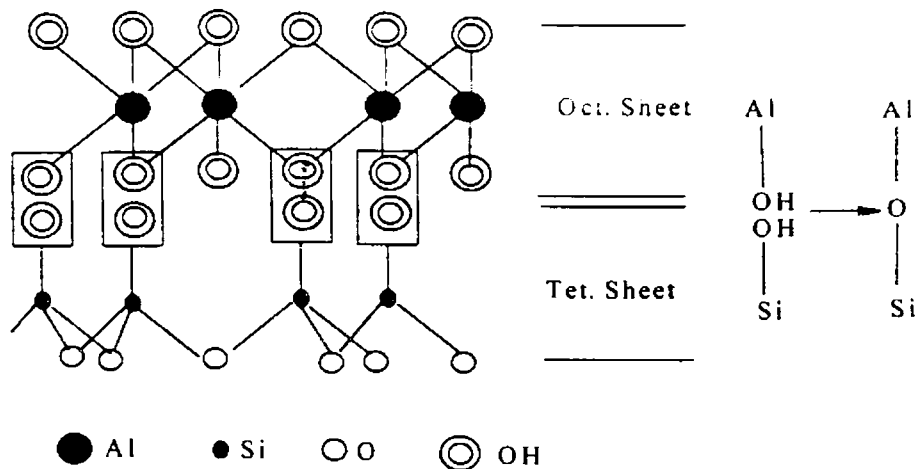


Figure 1.2 Diagrammatic representation of condensation of octahedral and tetrahedral sheets

charged species from the solution. In other words, the two-dimensional oxy anions are separated by layers of cations which are either hydrated or unhydrated. These interlayer cations are capable, in the right conditions, of holding the individual lamellae face to face, so that assemblages of them act together, either chemically and/or physically. Hence, even a suspension of a clay mineral in water may consist of a wide range of crystal sizes, depending upon the history of the sample and the strength of the links provided by the hydrated cation. The presence of water molecules forces the lamellae apart, and this weakens the net forces of attraction compared to the situation in which a bare (small) cation balances the charge close to both surfaces. Thus we can say that as the hydration of the cation in the interlayer increases, the net force of keeping the lamellae together becomes weaker. When this is a bare and small cation, the lamellae will be tightly held together. The best example of a cation, which does not hydrate easily and can balance charge in this way, is potassium and this is found most exclusively in the mica group of minerals.

1.5.2 Classification of Clay Minerals

The phyllosilicate clay minerals can be conveniently classified on the basis of layer type, layer charge per unit cell and types of inter layer [9]. Based on the charge possessed by the clay layers, the clay minerals can be classified into 8 major groups, as shown in Table 1.1. The layer charge can vary from zero to as large as four and the clay groups are accordingly named. On the basis of layer types, clay minerals can be classified into two as 1:1 clays and 2:1 clays. In 1:1 clays, one clay layer is

formed by the assemblage of one tetrahedral sheet with one octahedral sheet to form a double layer. In such clays, the uppermost unshared plane of anions in the octahedral sheets consists only of OH groups (Fig. 1.2). In 2:1 clays, an octahedral sheet is sandwiched between two tetrahedral sheets facing each other to form a three sheet complex (Fig. 1.3). In order to accomplish this linkage, the upper tetrahedral layer must be inverted so that its apical oxygen points down and can be shared with the octahedral layer below (Fig. 1.3). Both octahedral anion planes are then of the same O and OH composition.

On the basis of the octahedral sheet type, each of the eight major groups can be subdivided into two sub-groups, namely dioctahedral and trioctahedral clay minerals. The various individual clay minerals coming under each subgroup are described in Table 1.1. In a unit cell formed from 20 oxygens and 4 hydroxyl groups, there are eight tetrahedral sites and six octahedral sites. When two-thirds of the octahedral sites (i.e., 4 sites) are occupied by cations, the mineral is classified as a dioctahedral phyllosilicate. When all the octahedral sites are occupied by cations, the clay mineral is called a trioctahedral phyllosilicate.

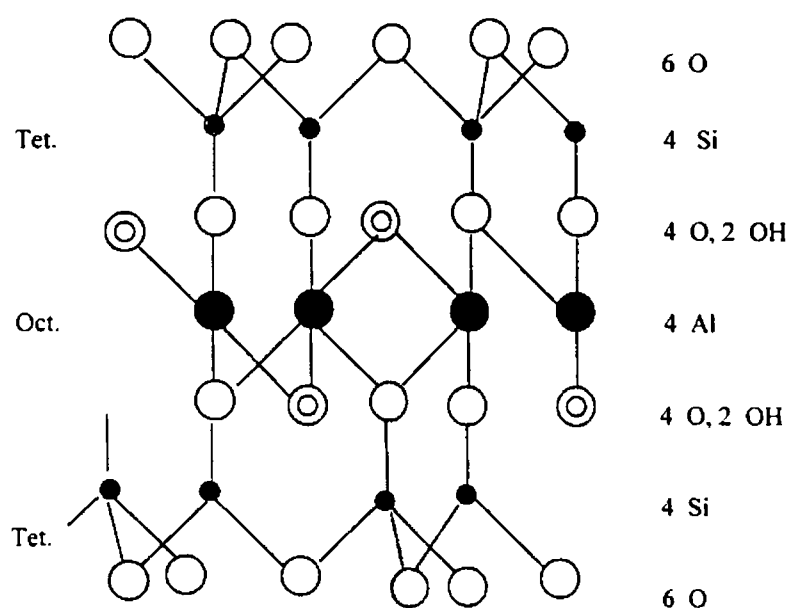


Figure 1.3 Diagrammatic representation of a 2:1 Tet.-Oct.-Tet. clay structure

Table 1.1 Classification and nomenclature of clay types (phyllosilicates)

Group name	Layer charge (x)	Layer type	Octahedral occupancy	Sub-group	Species
Serpentine-Kaolin	Very low or zero	1:1	Tri-	Serpentines	Chrysotile
			Di-	Kaolins	Kaolinite, dickite
Talc-Pyrophyllite	zero	2:1	Tri-	Talcs	Talc
			Di-	Pyrophyllites	Pyrophyllite
Smectites	Low ($0.6 < x < 1.2$)	2:1	Tri-	Saponites	Saponite, hectorite
			Di-	Montmorillonites	Montmorillonite, biedillite
Vermiculite	Medium ($1.2 < x < 1.8$)	2:1	Tri-	Trioctahedral Vermiculites	Trioctahedral Vermiculites
			Di-	Diocahedral Vermiculites	Diocahedral Vermiculites
Mica	High ($x \approx 2$)	2:1	Tri-	Trioctahedral micas	Phlogopite, biotite
			Di-	Diocahedral micas	Muscovite, illite
Brittle mica	Very high ($x \approx 4$)	2:1	Tri-	Trioctahedral brittle micas	Clintonite
			Di-	Diocahedral brittle micas	Margarite
Chlorite	Variable	2:1	Tri-	Trioctahedral chlorites	Chlinochlore
			Di-	Diocahedral chlorites	Dondassite
Sepiolite-Palygorskite	Variable	2:1	Tri-	Sepiolites	Sepiolite
			Di-	Palygorskites	Palygorskite

1.5.3 Structural Formula for Clays

The composition of a 1:1 mineral like kaolinite could be written relative to the proportion of oxides, i.e., as $\text{Al}_2\text{O}_3 \cdot 2\text{SiO}_2 \cdot 2\text{H}_2\text{O}$, but this is virtually devoid of structural information. It is better to take the unit cell as the basic quantity, then express the formula as $(\text{Si}_4)^{\text{IV}}(\text{Al}_4)^{\text{VI}}\text{O}_{10}(\text{OH})_8$. This tells us at once about the cation occupancy of the tetrahedral sheet (superscript IV) and the octahedral sheet (superscript VI). All the 1:1 clay mineral will have the same anion group, $\text{O}_{10}(\text{OH})_8$. Similarly, the anion group is invariant for 2:1 mineral and is $\text{O}_{20}(\text{OH})_4$. A unit cell representation such as $(\text{Si}_8)^{\text{IV}}(\text{Al}_4)^{\text{VI}}\text{O}_{20}(\text{OH})_4$ reveals that the clay mineral is a dioctahedral 2:1 type. Out of the six octahedral sites, only four are occupied and it is by Al. A unit cell representation such as $(\text{Si}_8)^{\text{IV}}(\text{Mg}_6)^{\text{VI}}\text{O}_{20}(\text{OH})_4$ tells that the clay is of a 2:1 trioctahedral type in which tetrahedral cations are Si^{4+} and octahedral cations are Mg^{2+} . Idealised structural formula for some dioctahedral and trioctahedral 2:1 phyllosilicates [10] along with the isomorphous substitutions are given in Table 1.2.

Table 1.2 Idealised structural formulae for some dioctahedral and trioctahedral 2:1 phyllosilicates

Mineral group	Dioctahedral	Trioctahedral
Pyrophyllite -Talc	Pyrophyllite: $[\text{Al}_4\text{O}](\text{Si}_8\text{O})\text{O}_{20}(\text{OH})_4$	Talc: $[\text{Mg}_6\text{O}](\text{Si}_8\text{O})\text{O}_{20}(\text{OH})_4$
Smectites	Montmorillonite: $\text{M}^{n+}_{x/n} \cdot y\text{H}_2\text{O}(\text{Si}_8\text{O})[\text{Al}_{4-0-x}\text{Mg}_x]\text{O}_{20}(\text{OH})_4$ Biedillite: $\text{M}^{n+}_{x/n} \cdot y\text{H}_2\text{O}(\text{Si}_{8-0-x}\text{Al}_x)[\text{Al}_4\text{O}]\text{O}_{20}(\text{OH})_4$ Nontronite $\text{M}^{n+}_{x/n} \cdot y\text{H}_2\text{O}(\text{Si}_{8-0-x}\text{Al}_x)[\text{Fe}_{4\text{O}}]\text{O}_{20}(\text{OH})_4$	Hectorite: $\text{M}^{n+}_{x/n} \cdot y\text{H}_2\text{O}(\text{Si}_8\text{O})[\text{Mg}_{6-0-x}\text{Li}_x]\text{O}_{20}(\text{OH.F})_4$ Saponite: $\text{M}^{n+}_{x/n} \cdot y\text{H}_2\text{O}(\text{Si}_{8-0-x}\text{Al}_x)[\text{Mg}_6\text{O}]\text{O}_{20}(\text{OH})_4$
Micas	Muscovite: $\text{K}_2(\text{Si}_{6\text{O}}\text{Al}_{2\text{O}})[\text{Al}_4\text{O}]\text{O}_{20}(\text{OH})_4$	Phlogopite: $\text{K}_2(\text{Si}_{6\text{O}}\text{Al}_{2\text{O}})[\text{Mg}_6\text{O}]\text{O}_{20}(\text{OH})_4$

Pyrophyllite and talc (Table 1.2) are made up of neutral clay layers, so that no exchangeable cations (M^{n+}) can be accommodated in the interlamellar region. Separate clay layers are therefore rather loosely bound via weak dipolar and van Der Waals forces. The five other sheet silicates, collectively known as smectites, listed in the table bear a net negative charge on the Tet-Oct-Tet framework, as a result of isomorphous substitution. In montmorillonite, some of the Al^{3+} in the octahedral sub-lattice are replaced by Mg^{2+} ions; in hectorite, some of the Mg^{2+} in the octahedral

sub-lattice are replaced by Li^+ . With beidellite and saponite, the isomorphous substitution takes place in the tetrahedral sub-lattice. M^{n+} appearing in the structural formula are the residual negative charge compensating cations, which are usually Na^+ , Ca^{2+} , Mg^{2+} , etc., situated in the interlamellar space.

1.6 Smectites

Smectite clay minerals are the most important among the various clays discussed above, from a catalysis point of view. Smectite clays or their modified forms were used extensively as commercial catalysts until the mid 1960s, when they were replaced by more thermally stable and selective zeolite catalysts. Smectite clays are still used today as commercial catalysts but only in minor quantities. For example, oleic acid dimerisation is best accomplished with a smectite clay catalyst [11]. Recent advances in the various modifications possible on smectite clays have rekindled interest in these minerals as catalysts or catalyst supports.

Figure 1.4 schematically illustrates the oxygen framework of a smectite clay mineral. The oxygen atoms define upper and lower sheets of tetrahedral sites and a central sheet of octahedral sites. Isomorphous substitution of octahedral or tetrahedral ions imparts a net negative charge to the clay layers. Typically the positive charge deficiency in the layers of smectites ranges from 0.4 to 1.2 e^- per Si_8O_{20} [12].

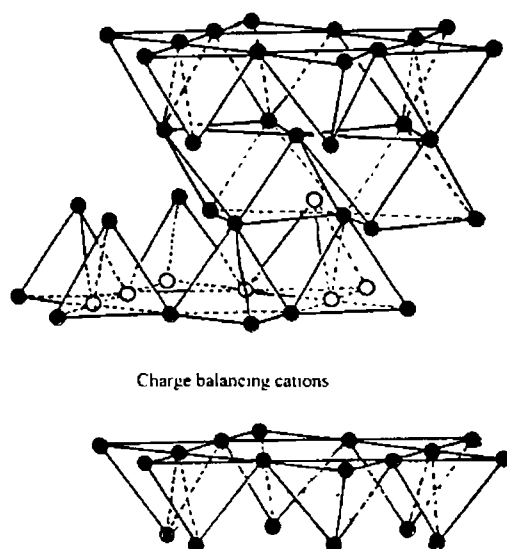


Figure 1.4 Schematic representation of a smectite clay mineral

The layer charge in octahedrally charged smectites is distributed over all oxygens in the framework, but that of tetrahedrally charged smectites is more localised [10]. Octahedrally charged smectites tend to be turbostratic, i.e., the layers are randomly stacked with respect to the in-plane 'a' and 'b' axes of adjoining layers. Tetrahedrally charged smectites tend to exhibit greater three-dimensional order [13,14].

1.6.1 Unique Properties of Smectites

Smectite clays possess a combination of cation exchange, intercalation and swelling properties which make them unique.

a) Cation Exchange Capacity (CEC): Cation exchange capacity refers to the exchange capability of the interlayer cations present in the clay by other cations. Exchange of Na^+ and Ca^{2+} ions in the pristine smectite clays can be done with hydrated transition metal ions as well as robust cations. The essence of this phenomenon is that the cations of the interlamellar space have no fixed sites in the lattice and hence if the mineral is immersed in an electrolyte, exchanges governed by the principle of equivalence will take place between the external and internal cations. That is, the hydrated cations on the interlamellar surface of the native minerals can be replaced with almost any desired cation by utilising simple ion exchange methods. With large complex cations, the extent of ion replacement may be size limited [10]. The cation exchange capacity of some smectite minerals is given in Table 1.3.

b) Intercalation: Intercalation is the insertion of a guest species in the interlayer region of the layered solid with preservation of the layered structure. The material obtained is called an intercalated solid. Neutral molecules other than water also can be intercalated between the silicate layers of smectites. Several binding mechanisms may operate in the intercalation processes [15-17]. One particularly important mechanism involves complex formation between the exchange cations and the intercalant, as in the binding of pyridine to Cu^{2+} exchange forms of smectites [18]. Another important intercalation mechanism is the reaction of the hydrated cation functioning as a Brønsted acid and the intercalant acting as a base as in the case of binding of ammonia as ammonium ion in Mg-montmorillonite [19]. Intercalation can be proven by XRD pattern, which must unambiguously show an increase in the spacing between adjacent layers.

Table 1.3 Cation exchange capacity of some 2:1 phyllosilicates

Mineral	CEC, mEq/100 g
Pyrophyllite	0
Talc	0
<u>Smectites</u>	
Montmorillonite	60-120
Biedillite	60-120
Nontronite	60-120
Hectorite	60-120
Saponite	60-120

c) Swelling: The most important property of smectites from the standpoint of catalyst design is their ability to expand beyond a single molecular layer of intercalant. Swelling is a reversible process that occurs, for example, upon hydration of the interlamellar cations. The extent of interlayer swelling depends on the nature of the swelling agent, the exchange cation, the layer charge and the location of the layer charge. The Li^+ and Na^+ exchange forms of the minerals are particularly susceptible to swelling by water [14, 20, 21]. As the interlayer water content of Na-smectites is increased with increasing partial pressure, a more or less constant interlayer spacing corresponding to monolayer formation is observed. After this, the spacing jumps abruptly to a value corresponding to two intercalated water layers. Further swelling of the interlayers due to osmotic forces is observed when the minerals are immersed in liquid water.

The hydrated cations being more voluminous, a lattice expansion is noted in the [001] direction. The process is reversible and the lattice contracts to its previous value when dehydrated at intermediate temperatures of 573-673K. Swelling provides access to the exchange ions on the basal surface and facilitates the ion exchange process.

The factors on which the degree of swelling depends are (a) layer charge and (b) nature of the exchangeable cations.

Layer Charge: In smectite minerals, the ionic interlayer bond forces are variable and these depend on the charge density on the triple layer and magnitude of the surface (grain size). The magnitude of the negative excess charge (related to charge density) is proportional to the degree of substitution which in turn is different from one mineral to another. The bond force increases as charge density increases, but the increase is much slower at small grain size than at large ones [22]. The bond force represents resistance to expansion (resistance to swelling). Water cannot cause swelling at charge densities beyond a certain limit, when the strong attraction between the silicate sheet and the cations prevent expansion. This limit is stated by White [22] to be $6.7 \times 10^4 \text{esu cm}^{-2}$ (equivalent to 160 mEq/100g in terms of CEC). Charge density is above this limit in micas but lower in smectites. (The charge on a smectite clay can be as low as $0.45 e^-$ per $\text{O}_{20}(\text{OH})_4$ unit).

Nature of exchangeable cation: The nature of the exchangeable cation also plays an important role in expansion of the clay lattice. It was observed by several authors that if a sodium or calcium smectite is transformed into a potassium mineral, swelling is reduced or altogether suppressed [22]. This indicates that the interlayer bond established by the potassium ions is a very strong one.

1.7 Montmorillonite

The most familiar and common member of smectite group is montmorillonite. In montmorillonite, the layer charge arises from the octahedral substitution of Al^{3+} by Mg^{2+} (Table 1.2). It should be noted that in montmorillonite some tetrahedral sites also might be occupied by ions other than Si^{4+} . However, the extent to which this occurs is less than the frequency of substitution of Al^{3+} ions by others in the octahedral sites [23]. It is clear that the Al in the aluminosilicate is the source of the acidic nature of the surface. The surface possesses both Brönsted and Lewis acidic sites. Al^{3+} proxying for Si^{4+} in tetrahedral coordination give rise to a net negative charge. A charge balancing H_3O^+ associated with such tetrahedral Al corresponds to a Brönsted acid site. An Al in the three fold coordination, perhaps occurring at an edge or arising from a Si-O-Al rupturing and dehydroxylation of the Brönsted site would correspond to the Lewis site [24]. The Brönsted and the Lewis sites are shown in Figure 1.5.

By virtue of its acidity and presence of swellable layers, montmorillonite could be modified in several ways and it is used successfully as a solid acid catalyst.

1.8 Modification on Clays

In the history of acid catalysis, clays have played an important role in the past. Acid leaching of the natural smectites led to amorphous aluminosilicate with large acid surface capable of initiating the carbocation chemistry which has so many diverse applications in catalysis. The original Houdry catalyst was prepared in that manner. The intercalation of alkylammonium cations, especially of tetraalkylammonium ions as pioneered by Barrer [25] is an easy process, since the clay

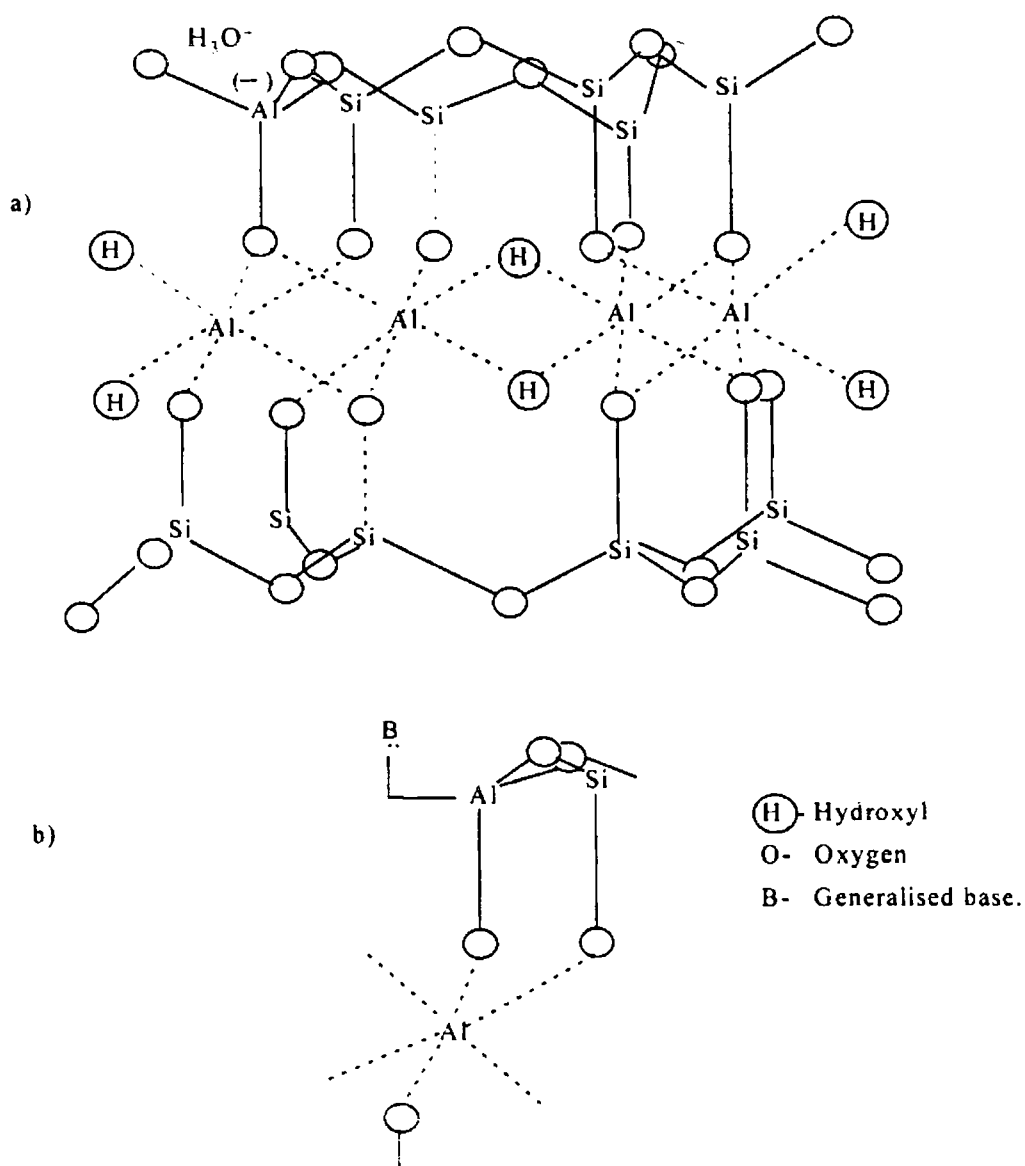


Figure 1.5 a) An off-axis projection of a 2:1 dioctahedral clay mineral with a Brønsted acid site. b) A possible configuration of a Lewis acid site.

lattice is negatively charged and a large surface area becomes available through this process and hence the idea to keep the clay layers “permanently expanded” by intercalating robust inorganic pillars came, though relatively late.

Thus acid activation and intercalation are the main modifications that have been done on clay minerals.

Acid activation: When the phyllosilicate clay minerals are treated with dilute acids, the H^+ ions attack the silicate layers via the interlayer region and exposed edges, thus displacing octahedral ions such as Al^{3+} and Mg^{2+} , which then occupy the interlayer sites. Acid activation causes little damage to the silicate layer and consequently the structure for the centre of the platelet remains intact. The rate of dissolution of the octahedral sheet increases not only with the increasing concentration of the acid, temperature and contact time, but also with increasing Mg content in octahedral sheet [26, 27]. Until 1960s proton exchanged or acid treated clays were used as cracking catalysts. They have also proved to be good catalysts for many industrially important reactions like alkylation [28], dimerisation and polymerisation of unsaturated hydrocarbons [29], Diels-Alder reaction [30], etc.

Intercalation: Because of the ability of the smectite clay minerals to imbibe a variety of cations and neutral molecules, an almost limitless number of intercalates are possible. A class of intercalates incorporates metal complex catalyst between the silicate layers. Although the immobilisation of complex catalysts in clay structures makes it possible to conduct solution-like reactions in the solid state and minimise many of the technical and economic barriers associated with the use of homogeneous solution catalysts, the advantage of catalyst intercalation go beyond immobilisation. By mediating the chemical and physical forces acting on interlayer reactants one can often improve catalytic specificity relative to homogeneous solution.

Another class of smectite intercalation compounds makes use of robust cations as pillars or pillar precursors between the silicate layers. This phenomenon termed as pillaring is our present concern and shall be discussed in detail.

1.9 Pillared Clays

Pillaring is the process by which a layered compound is transformed into a thermally stable microporous material with the retention of the layer structure. The

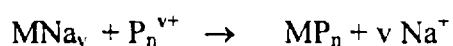
material obtained is called a pillared compound or a pillared layered solid. Thermal stability and porosity distinguish a pillared derivative from an ordinary intercalation compound. The latter can be, but must not be thermally stable. They also may have, but must not have porosity.

The concept of pillaring smectite clays was demonstrated more than 45 years ago by Barrer and MacLeod [31] when they utilised tetraalkylammonium ions to introduce interlayer porosity in montmorillonite. However, the paternity of the idea of “permanently expanding” the clay layers is due to Vaughan, Lussier and Magee [32] and to Brindley and Sempels [33] who, in fact had combined their efforts. Lahav, Shani and Shabtai [34] published a pioneering work and these works were at the origin of a worldwide interest for the so-called pillared clays (PILCs). Pillared clays have a resemblance to zeolites in the sense that both categories of solids are microporous and can easily be transformed into acid catalysts. To some extent, the researchers in the domain of pillared clays were, at least in their early enthusiasm, challenging those in the domain of zeolites.

1.9.1 Basic Pillaring Mechanism

The basic phenomenon used in the preparation of pillared clays is the ion exchange of interlamellar cations by bulky cationic species (oligomer) that act as props to keep the structure open. It is obvious that only swelling clay minerals capable of cation exchange (of course, this condition is satisfied by smectites) can be pillared.

Let M be the symbol representing the clay, and C that of the charge balancing cation of the clay. If P_n^{v+} is a cationic oligomer (a cation with large size and high charge), we can represent the cation exchange process as



If the exchange were the only reaction involved in the pillaring mechanism, the experimental procedure would indeed be simple as in the case with exchanging Na^+ by a quaternary alkylammonium [31], for instance. To get a stable structure such as a pillared clay, the intercalated solid has to be carefully processed further. Treatment of the solid at an elevated temperature is the next step after intercalation. This results in the dehydration and dehydroxylation of the polycation where it

changes to stable oxide clusters. This step is termed as thermal activation (calcination). Thus the robust cations, which are transformed into oxide particles upon calcination, maintain the structure open even after dehydration and calcination and a porous network is created. That is why these particles are named pillars [35]. Upon calcination, the bond between the interlayer species and clay layers is thought to shift from ionic to near covalent, which results in the stabilisation of the porous network, by converting hydroxide pillars to stable oxides [36]. The interlayer distance or the d_{001} spacing of the clay exchanged with the bulky cation will be larger compared to the pristine clay mineral. This d spacing is maintained to be sufficiently large, though a small lowering is there due to dehydroxylation and dehydration of the bulky cation, even after calcination. The process of pillaring is schematically shown in Figure 1.6.

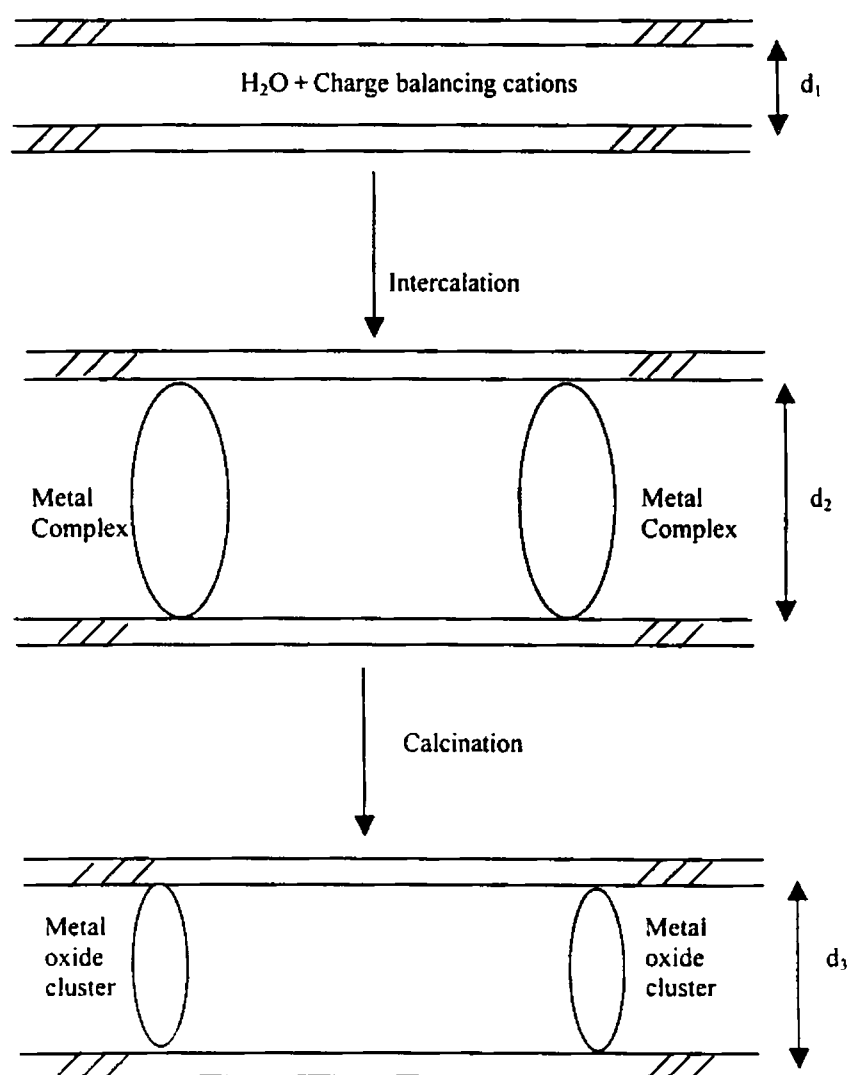


Figure 1.6 Schematic representation of the process of pillaring ($d_1 < d_3 < d_2$)

Thus the solid, stabilised in a temperature range of 400-500°C, is the actual pillared clay. Its structure is essentially turbostratic since the long-range crystalline order is only along the 'c' axis perpendicular to the layers. There is no long-range order along the 'a' and 'b' unit cell axes.

Figure 1.7 is a schematic representation of a pillared clay. There are two important characteristics for a pillared clay and the pore size is determined by these characteristics. First is the distance between the clay layers (d_{001}), which is determined by the size of the pillars, and the second is the lateral separation between the pillars, which is the distance between the pillars as shown in Figure 1.8. The regions between the pillars define pores for adsorption and possible catalysis.

There is now a renewed interest in pillared clays because it is realised that their pore size can be made larger than those of faujasitic zeolites. Moreover, by varying the size of the pillar or the spacing between the pillars or both, one can adjust the pore size to suit a particular application. These pillared clays offer new possibilities for catalysis of large molecules such as those found in residual crude oils.

The highly selective molecular sieving property of clays pillared by hydroxy metal cations requires a regular distribution of pillars and pores in the interlayer region. However, the layer charge distribution in smectite clays is highly irregular, varying as much as by a factor of two from interlayer to interlayer. Thus one should expect a non-uniform distribution of pillars and a range of pore sizes, particularly when the cations are stable to hydrolysis as, for instance, NR_4^+ . Here ion exchange is the sole driving force for intercalation (Figure 1.9 A). With polynuclear hydroxy pillars, however, the ions apparently fill each interlayer region to essentially the same population density regardless of the layer charge (Figure 1.9 B). In this case, the average charge per pillaring cations varies with the extent of hydrolysis and also with the negative charge density of the clay layers and thus a regular spacing between the pillars can be achieved [10].

1.9.2 Preparation of Pillared Clays- Various Pillaring Agents

As discussed in the earlier sections, in order to prepare a pillared clay, we have to first think about the intercalating agent (pillaring agent). Pillaring agent

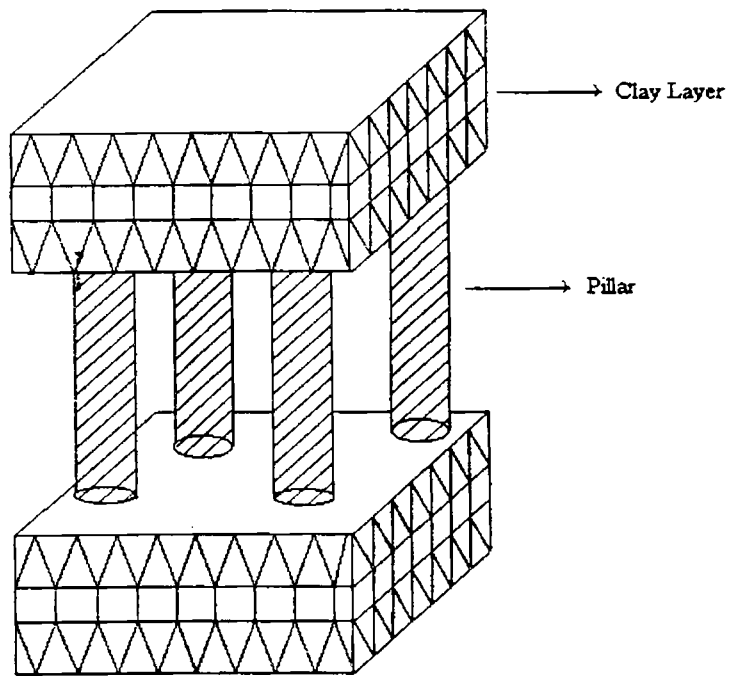


Figure 1.7 Schematic representation of a pillared clay

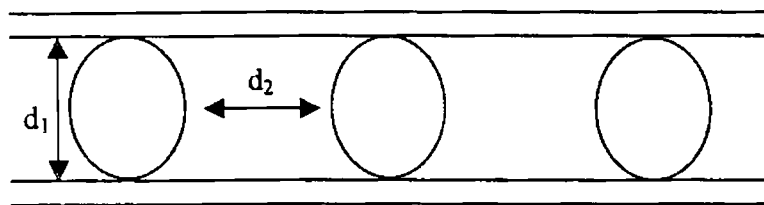


Figure 1.8 Characteristics of a pillared solid; d_1 – gallery height and d_2 – interpillar distance

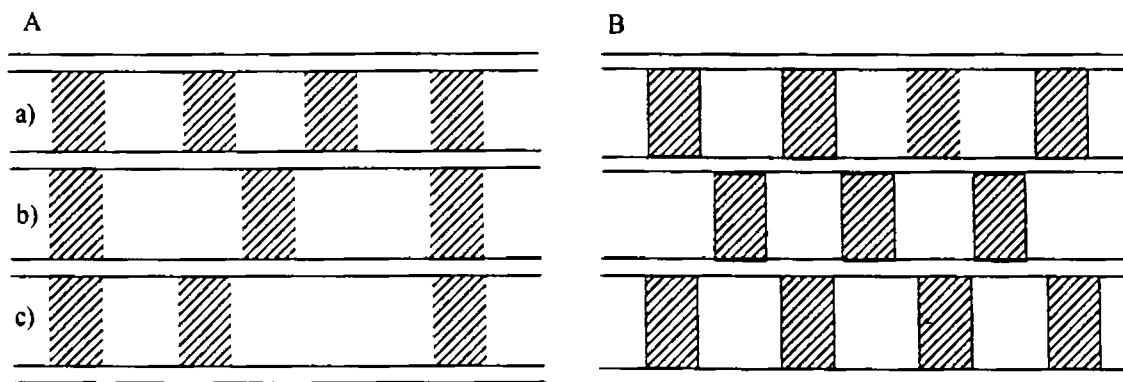


Figure 1.9 A) Irregular and B) regular distribution of pillaring cations in clay interlayers. a) and b) represents irregular spacings from interlayer to interlayer and c) represents irregular spacings within an interlayer

solutions containing substantial concentrations of large polyoxocations are prerequisites for the preparation of pillared clays. Much effort has been expended in finding various pillaring cations, i.e., polyoxocations. The formation of polynuclear cations was first recognised by Bjerrum [37] in his study on the hydrolysis of Cr^{3+} and later for metal ions such as Al^{3+} , Be^{2+} , Ni^{2+} , Pb^{2+} , Zr^{4+} , Hf^{4+} , Ti^{4+} , Fe^{3+} and Ce^{4+} by other workers [38]. While all these cations are reported to form polynuclear species upon hydrolysis, only some of them have been used as pillaring precursors in the preparation of pillared smectites. The various types of polynuclear hydroxy metal cations for pillaring smectites include those of Al [33, 34, 39-43], Zr [44, 45], Si [46], Fe [47-49], Cr [50-52] and Ni [39]. These polynuclear hydroxy cations afford pillared phases with higher free spacings which can reach above 15Å with reasonable stability at high temperatures. Among the various pillared clays, the most widely explored systems are those containing Al and Zr pillars.

1.10 Aluminium Pillaring

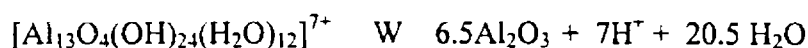
Until now, most of the research on pillared clays has been focused on the aluminium polycations as a pillaring agent. Consequently, the aluminium pillared clays are, by far, the most documented pillared clays. This is because of the fact that the solution chemistry of Al is very well-known and its polymerisation is better understood than that of other cations.

The intercalating solution of aluminium is generally prepared by the partial hydrolysis of an aluminium salt such as aluminium chloride or nitrate by a base such as hydroxide or carbonate. In general terms, hydrolysis refers to the reaction by which solutions of salts are converted to new ionic species or precipitates. For the preparation of the pillaring agent, addition of the base is stopped before precipitation; hence the process is called partial hydrolysis. Soluble polynuclear species may exist under these conditions. Determining the identity and stability of dissolved hydrolysis products is a difficult task. Often they exist over a limited range of pH. Many direct techniques such as NMR [53], X-ray diffraction [54] and Raman spectroscopy [55] and indirect techniques like pH measurements [38] have been applied to the analysis of polymer species in solutions. Small angle X-ray scattering [56] is a powerful technique for the determination of structure, growth and topology of macromolecules.

The OH⁻/M (M = metal, here Al) ratio determines the extent of hydrolysis of the salt. A ratio near 3 results in the complete precipitation of Al³⁺ as Al(OH)₃. In order to get the polycations for pillaring, hydrolysis is ceased, in most cases, near or below an OH⁻/M ratio of 2.5 [57]. Early work using potentiometric techniques [58] suggested the formation of oligomers like Al₆(OH)₁₅³⁺ or Al₈(OH)₂₀⁴⁺. Using small angle X-ray scattering, Raush and Bale [59] suggested the formation of a polymer species, [Al₁₃O₄(OH)₂₄(H₂O)₁₂]⁷⁺ for OH⁻/Al ratios between 1 and 2.5. The structure of this species has been previously described in the solid state by Johansson [60]. ²⁷Al NMR studies have also proven that the complex is most probably this tri-decamer, called a Keggin cation [61-63]. In these partially hydrolysed Al solutions, other species than the Al₁₃ polyoxocation, can also exist, which can be exchanged for the clay interlayer cations, as shown by Sterte and Otterstedt [64]. However, it is now unambiguously and thoroughly explored that the major polycation existing in these solutions is Al₁₃⁷⁺ cation (59, 61-63), whose structure is shown in Figure 1.10. It consists of a central tetrahedral Al surrounded by 12 octahedral Al which can be written as [AlO₄Al₁₂(OH)₂₄(H₂O)₁₂].

An alternate way for the preparation of this polycation is the reaction between aqueous AlCl₃ with Al metal. This is commercially available as aluminium chlorohydrate solution (ACH). It has been demonstrated [65, 66] that these two different types of pillaring agents afforded very similar pillared products in terms of d spacing, composition and surface area. However, Pinnavaia *et al.* have shown that Al₁₃⁷⁺ cations will be the major component in partially hydrolysed solutions whereas ACH solution will contain a range of cations including larger oligomers [65].

Upon thermal activation, the Al₁₃ polycation undergoes dehydroxylation and dehydration to yield Al₂O₃ pillars [10], as shown below.



The amount of Al bound in the interlayer per unit cell varies only within a small range of 2.78 to 3.07, equivalent to approximately one Al₁₃ per 4.2 to 4.6 unit cells, and shows no correlation with the charge of the layer. The absence of a correlation suggests a more or less uniform monolayer of hydrated Al polyoxocations to be present in the interlayer. Bergaoui *et al.* [67] indicated in a recent paper that the

amount of Al never exceeds one Al_{13} per 6 unit cells, due to steric constraints at the solid-liquid interface.

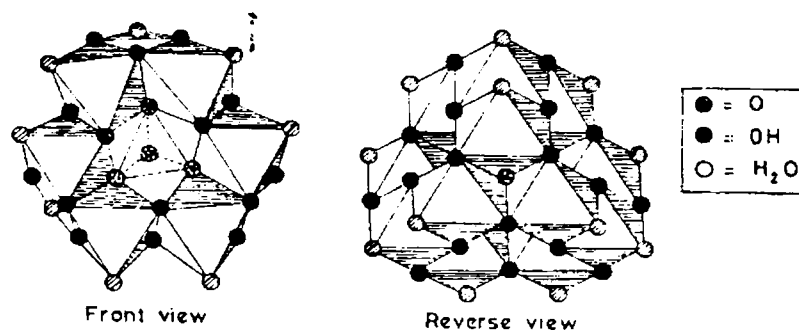
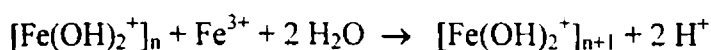


Figure 1.10 Schematic representation of Al_{13} complex

1.11 Iron Pillaring

In contrast to the great majority of work and publications concerning Al or Zr-pillaring, very few papers have been reported for Fe-pillared clays. This is perhaps surprising given that Fe-PILCs are cheaper to prepare and would have not only acidic properties, but would also contain pillars which in themselves may be catalytically active and have redox and magnetic properties [68].

The solution chemistry of Fe is complex. It is well-known that the hydrolysis behaviour of Fe^{3+} is similar to that of Al^{3+} ions in forming polymeric cations [69] and there have been reported attempts to intercalate such ions in the interlayers of smectite clays [48, 70-74]. Iron polymeric species were also prepared by the partial hydrolysis reactions of Fe^{3+} . During the course of hydrolysis, polymerisation of iron typically begins at low pH (<1.5) and propagates by deprotonation of co-ordinated water molecules (olation) and hydroxyl groups (oxolation) [75] as illustrated in the following equations.



The hydrolysis reactions of Fe^{3+} can lead to discrete spherical polycations as large as 30\AA in diameter [68, 76, 77]. Aggregation of the spheres produces rods and eventually rafts of rods. The polymerisation process is dependent on base to metal ratio, temperature, nature of counter ion, pH and other factors [38, 75]. Although the

whole process of the growth of polymeric cations may be brought by prolonged ageing at room temperature or addition of base or ageing at high temperatures, the addition of base is recommended, since this appears to offer the greatest degree of control over the size of the pillaring species. It is also reported that iron oxide pillars can be successfully prepared using trinuclear acetate iron(III), $[\text{Fe}_3(\text{OCOCH}_3)_7\text{OH}]^+$ as a pillaring agent [74]. During thermal treatment of the intercalated clay at an elevated temperature, decomposition of the intercalated ions takes place to yield discrete iron oxide pillars, which prop apart the clay layers.

1.12 Chromium Pillaring

Pillaring agents containing substantial concentrations of large polyoxochromium cations are prerequisites for chromia pillared clays with high spacings. Cr is one among the few cations that form large polyoxospecies, and the hydrolysis chemistry of chromium has been extensively investigated [38,78]. Several small chromium oligomers including dimers, trimers and tetramers have been identified and isolated from solutions at various pH values [79-83]. The existence of much larger chromium polymers is also evidenced in aqueous solutions, but have not yet been isolated and identified [83-85]. Chromium nitrate solutions have a red-purple colour which changes upon increasing basicity to bluish green and finally to deep green. The polymerisation reaction is rather slow at room temperature [38], but quite rapid at 100°C [78, 84]. The bluish green species is identified as a dimer namely $[\text{Cr}_2(\text{OH})_2(\text{H}_2\text{O})_8]^{4+}$ [79, 81, 84] and the deep green species are attributed to higher polymers like trimer [83, 86].

Three different methods were reported for the preparation of chromium oligomers. Pinnavaia *et al.* [87] and Tzou *et al.* [88] prepared CrPILCs with large gallery height with thermal stability up to 500°C, by partially hydrolysing chromium nitrate solutions at 95°C using Na_2CO_3 as base and intercalating clay with this solution. Hydrolysis at a lower temperature of 25°C yielded CrPILCs, but these were thermally unstable above 300°C [51]. A different way to prepare Cr-pillaring solutions comprises of the addition of $\text{Cr}(\text{NO}_3)_3$ solutions in concentrated ammonia (15N), a method attempted and patented by Hopkins *et al.* [89]. Another interesting route describes the reaction of clay suspension with Cr(III) acetate, $\text{Cr}(\text{OAc})_3$, followed by refluxing for 10 days, as attempted by Jiminez-Lopez *et al.* [90] and Dubbin *et al.* [91]. Calcination of the chromium intercalated clays in air or N_2

always resulted in gallery collapse above 300°C and this was attributed to the air oxidation of chromium to more mobile oxidation states [88] and also to the abrupt release of protons [91]. Calcination under NH_3 is an effective treatment for this difficulty since ammonia can retain the protons during calcination and also the presence of NH_4^+ apparently stabilises Cr^{3+} [92], making it more resistant to oxidation.

1.13 Other Pillared Clays

Apart from Al^{3+} , Fe^{3+} and Cr^{3+} pillaring of clays, pillaring with polycations formed upon the hydrolysis of Zr^{4+} , Ti^{4+} , Ga^{3+} , Ni^{2+} and Si^{4+} has also been reported [93-97]. Pillared clays with niobium and tantalum have also been reported [98]. Dissolution of zirconyl chloride in water leads to the formation of a tetramer with Zr as a Zr_4^{8+} species and this cation is thought to transform to ZrO_2 pillars in Zr-PILC [99]. Similar to Al, Ga also forms the major cation in Ga_{13}^{7+} form upon partial hydrolysis of Ga^{3+} salt [100-102]. For silicon pillaring, an Si_8 polymer is employed.

1.14 Mixed Pillared Clays

So far we have discussed the intercalation of smectite clays by oxides of a single metal. The process increases the surface area, thermal stability and acidity of the parent clay mineral. The maintenance of a well-defined porous network up to relatively high temperature along with the presence of acid sites immediately suggested outstanding potential catalytic applications for these solids. Since the early eighties, research has been conducted to improve the thermal and hydrothermal stability and catalytic properties of single oxide pillared clay systems. As a result, the intercalation of clays with solution containing two or more cations has been widely studied. Various metals have been described in combination with Al polyoxocations, the most important of these being Fe, Ga, Cr and Zr [102-118]. Usually, the first cation polymerises easily (Al is the most studied), whereas the addition of a small molar fraction of a second cation tries to improve the thermal, adsorptive and/or catalytic properties of the final solids.

Two different strategies have been employed for the preparation of mixed pillared systems. Cation exchange of the clay with one metal ion followed by intercalation with the polyoxocation of the other metal is one route. The other method comprises of the preparation of polyoxocations of both metals in the

always resulted in gallery collapse above 300°C and this was attributed to the air oxidation of chromium to more mobile oxidation states [88] and also to the abrupt release of protons [91]. Calcination under NH_3 is an effective treatment for this difficulty since ammonia can retain the protons during calcination and also the presence of NH_4^+ apparently stabilises Cr^{3+} [92], making it more resistant to oxidation.

1.13 Other Pillared Clays

Apart from Al^{3+} , Fe^{3+} and Cr^{3+} pillaring of clays, pillaring with polycations formed upon the hydrolysis of Zr^{4+} , Ti^{4+} , Ga^{3+} , Ni^{2+} and Si^{4+} has also been reported [93-97]. Pillared clays with niobium and tantalum have also been reported [98]. Dissolution of zirconyl chloride in water leads to the formation of a tetramer with Zr as a Zr_4^{8+} species and this cation is thought to transform to ZrO_2 pillars in Zr-PILC [99]. Similar to Al, Ga also forms the major cation in Ga_{13}^{7+} form upon partial hydrolysis of Ga^{3+} salt [100-102]. For silicon pillaring, an Si_8 polymer is employed.

1.14 Mixed Pillared Clays

So far we have discussed the intercalation of smectite clays by oxides of a single metal. The process increases the surface area, thermal stability and acidity of the parent clay mineral. The maintenance of a well-defined porous network up to relatively high temperature along with the presence of acid sites immediately suggested outstanding potential catalytic applications for these solids. Since the early eighties, research has been conducted to improve the thermal and hydrothermal stability and catalytic properties of single oxide pillared clay systems. As a result, the intercalation of clays with solution containing two or more cations has been widely studied. Various metals have been described in combination with Al polyoxocations, the most important of these being Fe, Ga, Cr and Zr [102-118]. Usually, the first cation polymerises easily (Al is the most studied), whereas the addition of a small molar fraction of a second cation tries to improve the thermal, adsorptive and/or catalytic properties of the final solids.

Two different strategies have been employed for the preparation of mixed pillared systems. Cation exchange of the clay with one metal ion followed by intercalation with the polyoxocation of the other metal is one route. The other method comprises of the preparation of polyoxocations of both metals in the

intercalating solution by the co-hydrolysis of a solution containing both the cations with a base [50, 105, 111]. The latter mentioned method is usually employed to prepare mixed pillared clays.

1.14.1 Mixed Fe-Al Pillared Clays

Fe-Al pillared clays have been extensively studied because iron oxide pillars have potential interesting magnetic properties [103]. Secondly, reduced iron, present as finely dispersed metallic domains within the pillared clay structure, may exhibit useful catalytic properties in, for example, Fischer-Tropsch reactions [104, 112].

Preparation of intercalating solutions containing Fe and Al and successful pillaring of montmorillonite with these solutions have been reported in a detailed study by Lee *et al.* [113]. Co-hydrolysis of a solution containing Al/Fe ratio of 2.5 with Na_2CO_3 as a base was employed for the preparation of intercalating solutions. Pillared solids with basal spacings up to 16.7 Å and specific surface areas of $250 \text{ m}^2\text{g}^{-1}$, stable up to 400°C were obtained while using mixed solutions. From Mössbauer spectral studies of these solids, they could find that the iron preferentially decorated the surface of the alumina pillars. Although the formation of $[\text{Al}_{12.5}\text{Fe}_{0.5}\text{O}_4(\text{OH})_{24}]^{7+}$ polycations was postulated by these authors, they did not find any evidence of mixed pillared clays intercalated with species containing iron and aluminium in the same complex, but found that intercalation was rather with discrete alumina and iron oxide pillars. They also observed that the mixed pillars could not be reduced due to the strong interaction between the iron and the support, viz, the Al pillar, whereas, in pillared clays containing a mixture of iron pillars and alumina pillars, small metallic particles in the form of pancake-shaped domains were formed between the unaffected alumina pillars, upon reduction.

Kirisci *et al.* have studied Fe-Al pillared montmorillonites, characterising the solids mainly by Mossbaeur spectroscopy and H_2 -TPR [114-117]. Contradictory to the postulation by Lee *et al.* [113], no evidence was found for isomorphous substitution of iron for aluminum in the Al_{13}^{7+} Keggin-type cations. These authors suggested that a co-hydrolysis of Fe and Al occurred and that the Fe^{3+} cations were not able to occupy any site in the Al_{13} cluster. Instead, mixed pillars containing Al_{13}^{7+} cations and hydrous iron oxide oligomers were found. Al/Fe ratios from 2.25 to 2.5 were used and they found that the basal spacings (18-19 Å) and the specific

surface areas ($163\text{-}301\text{ m}^2\text{g}^{-1}$) depended on the amount of Fe in the intercalating solutions.

The intercalation of montmorillonite with mixed solutions containing Fe and Al has been reported by Lenarda *et al.* [118-120]. The solids showed basal spacings of $17.5\text{-}19.0\text{ \AA}$ and specific surface areas of $176\text{-}240\text{ m}^2\text{g}^{-1}$ after calcination at 400°C . They found that these iron containing solids have a high oxidising activity and strongly acidic properties which was confirmed by testing these for the dehydrogenation of 2-propanol to acetone. Comparison with Ru-Al solids was also attempted and it was found that Fe-Al solids were superior to Ru-Al systems.

Bergaua *et al.* have also studied the synthesis and catalytic properties of Fe-Al pillared laponite [121-124]. Basal spacings of about 18 \AA were obtained, although, in some samples, only a wide band instead of a clear peak was observed. Chemical analysis and H_2 -TPR experiments showed the presence of two iron species, in the mixed pillars and outside pillars. The authors proposed the formation of mixed $\text{Al}_{13-x}\text{Fe}_x$ pillars, based on the Fe content of the pillared solids. Al-Fe pillars in alumina rich samples were particularly active for a syngas conversion reaction, showing high selectivities to light olefins, probably due to the presence of FeAl_xO_y mixed oxides. These are more stable with respect to sintering and carbide formation than the other catalysts containing supported iron particles. They could also report that the iron rich pillars showed catalytic properties similar to those of conventional supported iron catalysts. The same authors have recently reported [125] the synthesis of Fe and Fe/Al pillared montmorillonites with large basal spacings, up to 76 \AA , using different mixtures of Al_{13} and of a polycation prepared by reaction of FeCl_3 and Na_2CO_3 as pillaring species. The specific surface areas reached values between 148 and $246\text{ m}^2\text{g}^{-1}$ and specific pore volumes between 0.18 and $0.24\text{ cm}^3\text{g}^{-1}$.

Zhao *et al.* [126] have also described the intercalation of a montmorillonite with mixed solutions of Al/Fe, as well as with solutions containing only Al or Fe. Ratios from 0.1 to 2.0 were used yielding solids with basal spacings of $15.5\text{-}19.8\text{ \AA}$ and specific surface areas of $170\text{-}237\text{ m}^2\text{g}^{-1}$. Various characterisation techniques such as IR spectra of adsorbed pyridine, temperature programmed desorption (TPD) of *n*-butylamine, Mössbauer spectroscopy and H_2 -TPR were used to elucidate the properties of the catalysts. They have concluded that the incorporation of Fe into an

alumina pillar decreases the Brönsted acid concentration and the surface acid strength of the resulting pillared clays.

De Stefanis *et al.* [127] investigated the adsorption of several molecules on an Al-pillared Zenith montmorillonite (AZA) and an Al/Fe pillared Zenith montmorillonite (FAZA) and also their catalytic properties. The adsorption of cyclic (aromatic and non-aromatic) and linear chain/cyclic non-aromatic hydrocarbons, among others, was studied. Mixtures such as hexane-hexene, hexane-heptane and cyclohexane-hexene were used and their separation could be performed at 200-350°C. Aromatic chlorohydrocarbons could also be separated. The catalytic activity of these solids towards isopropanol decomposition reaction was carried out by Ladavos *et al.* [128]. The iron containing solids showed specific surface areas of 205-207 m²g⁻¹, total pore volume of 0.142-0.148 cm³g⁻¹ and 2.2x10¹⁸ acid sites per square metre. The activity for isopropanol decomposition was high (AZA was more active than FAZA), but lower than that of iron-free clays. The products were mainly propene and diisopropyl ether, with a selectivity to propene of 0.8-0.9, irrespective of the reaction temperature.

Catalytic transformation of the gases evolved during the thermal decomposition of high-density polyethylene (HDPE) was carried over AZA and FAZA solids by Breen and Last (129). Thermal decomposition of the plastic yielded n-alkanes, alk-1-enes, alk-x-enes, and α ,C-dienes in the range C₄-C₂₀. These products were catalytically converted into light gases and aromatic species such as toluene, xylene, trimethylbenzene and tetramethylbenzenes. When using AZA and FAZA as catalysts a large yield of aromatics was observed. The high production of aromatics over AZA and FAZA pillared clays suggested the presence of dehydrocyclisation sites associated with the pillars.

Colombo and Violante [130] have described the effect of ageing on the nature of mixed hydroxy Fe-Al montmorillonite. Fe/Al ratios from 0.1-10 were used. Specific surface areas up to 316 m²g⁻¹ and basal spacings of 18.2 Å were observed. Up to 4.55 wt% of Fe was fixed by the pillared solids. The degree of interlayering was always greater in the samples with Fe/Al ratios between 0.5 and 4.0. Gibbsite and haematite, with traces of goethite or non crystalline Fe oxides were detected depending on the ratios used. Bakes *et al.* [131] have prepared an Fe-Al pillared

montmorillonite using an intercalating solution containing equal amounts of Al and Fe chlorides (Fe/Al=1.0). About 4 wt% of Al and 17 wt% of Fe were found to be fixed by the solid during intercalation. A basal spacing of only 15.6 Å was obtained and it reduced to 12.6 Å upon calcination at 500°C. A maximum value for the specific surface area of 127 m²g⁻¹ (which is comparatively low), was reached. The nature of the Al-Fe oxides in the pillars was studied by Mössbauer spectroscopy under both oxidising and reducing conditions. When calcined in air, aluminium-substituted maghemite was formed, which was converted to aluminium-substituted magnetite following H₂ reduction. The reduction led to decomposition of the pillars, which did not sinter during subsequent oxidising stages.

1.14.2 Mixed Cr-Al Pillared Clays

Incorporation of Cr into alumina pillared clay or the preparation of mixed Cr-Al pillared systems has attracted considerable attention due to the catalytic electron transfer properties and acidic properties of chromium. A comparative study of mixed Fe-Al and Cr-Al pillared systems has shown that an uptake of up to 5.64 wt% of Fe and 10.2 wt% of Cr were taking place during the pillaring process respectively [105]. Due to the lesser fixing of Cr into the clays, Cr-Al pillared systems were found to be more stable towards acid attack compared to Fe-Al systems [105]. A study of the mixed Cr-Al solids by DRS and EPR [50] showed that Cr(III) cations existed in two different environments, in the micropore structure and in the pillars. When chromium is exchanged before aluminium pillaring, it is believed that it is present in the micropores and when intercalated with a solution containing both Cr and Al oligomers, Cr is present in the pillars. These solids were subjected to catalytic activity studies towards n-decane hydrocracking. The activity of mixed Cr-Al systems were distinctly higher than that of single Al pillared clay. The activity depended on the location of Cr(III) cations in the clay. Pillar-bound Cr yielded the highest stabilities and catalytic activities.

Lenarda *et al.* [132] have studied the activity of Cr-Al pillared clays in the vapour-phase deep oxidation of chlorinated hydrocarbons. A sample with a basal spacing of 18.2 Å and specific surface area of 350 m²g⁻¹ showed higher activity than a chromia-pillared clay for the combustion of methylene chloride, a refractory halocarbon, in the 300-400°C temperature range.

Studies of Zhao *et al.* [106] on Cr-Al pillared montmorillonites led to the conclusion that Cr/Al ratios greatly affected the pillar structure, the surface area, the acidity and the thermal stability of the pillared clay. The surface acidity and thermal stability increased when the amount of Al was increased in the intercalating solution. The pillars obtained with a Cr/Al ratio < 1 had a Keggin structure similar to that of a hydroxy Al pillared clay and chromium was mostly dispersed in the alumina pillars and was easily oxidised. On the contrary, large polyoxochromium complexes similar to those of hydroxy Cr-pillared clay were obtained for Cr/Al ≥ 1 and Cr(III) was easily converted to α -Cr₂O₃. The authors proposed a moderately strong interaction between Cr and Al in the pillars, enhanced for low Cr/Al ratios. Catalytic activity for the disproportionation of 1,2,4-trimethylbenzene was also found to be higher for mixed Cr-Al systems when compared with single pillared systems.

Toranzo *et al.* have pillared a saponite with aluminium-chromium solutions containing different Al/Cr ratios [107, 133, 134]. The solids containing both Al and Cr cations had properties intermediate between pure Al and pure Cr pillared clays. In particular, the thermal stability strongly depended on the amount of Al fixed by the solids, reaching 500°C when Al/Cr ratios > 1 were used. Pure Cr-pillared system was not thermally stable above 200°C whereas pure Al pillared system was found to be thermally stable up to 600°C. The specific surface area and the porous structure of the pillared solids were also closely related to the thermal stability. These clays were used in the deep oxidation of acetone, reaching 100% conversion to CO₂ at 300-340°C. For a given amount of Cr₂O₃ fixed in the solids, which is assumed to be the catalytically active phase, the activity strongly depended on the acetone accessibility to this phase (i.e., on the surface area and the porous structure of the solids, both of which are related to the amount of Al pillars in the pillared clay). This is a good example of the co-operative effect between two cations on at least two important properties of the final solids, namely the thermal stability and the catalytic activity.

Kirisci *et al.* [135] have prepared Cr/Al pillared montmorillonites with various Cr/Al ratios. Basal spacings of 18.4-19.1 Å and specific surface areas of 152-265 m²g⁻¹ were obtained. These authors investigated the presence of chromium in the pillars, finding that Cr³⁺ cations did not incorporate into the structure of the

Al_{13} polycations, nor were there isomorphous substitution of Cr. ^{27}Al NMR studies always showed an $\text{Al}^{\text{oct}}/\text{Al}^{\text{tet}}$ ratio close to 12, irrespective of the presence of chromium. However, possible polymerisation of Cr^{3+} was not investigated. The pillared solids were tested in the oxidation of 1-phenyl-1-propanol to propiophenone.

1.14.3 Other Mixed Metal/Al Pillared Clays

Extensive studies on Ga/Al, Si/Al and Zr/Al pillared clay systems have also been reported. Gallium is known to have dehydrogenation properties [102, 136]. Furthermore, the tetrahedral site in the Al_{13} structure is rather distorted due to the relatively smaller size of the aluminium cation. Replacement by a slightly larger cation, such as gallium or zinc, would increase the stability of this Keggin structure [107]. Studies of Bradley and co-workers [102, 107, 137, 138] revealed that in the Keggin cation of mixed Ga-Al polymer, one central tetrahedral Ga is surrounded by 12 Al octahedra. The increase in symmetry due to the incorporation of Ga in the Al Keggin structure is reflected in the thermal stability which increases in the order Ga PILC < Al PILC < Ga-Al PILC. In catalytic reactions, Ga_{13} pillared clays mainly exhibited dehydrogenation, whereas Al- and Ga-Al pillared clays showed strong cracking activity in addition to dehydrogenation [92].

Different preparation routes were followed by different authors for the preparation of mixed silica/alumina pillared clays. Initially Gaaf *et al.* [139] employed refluxing of a mixture of aluminium chlorohydrate and sodium silicate for 24 hours. Occelli [108, 109] used commercially available sub-micron positively charged colloidal particles of alumina-coated silica and Sterte and Shabtai [140] employed the hydrolysis of a mixture of orthosilicic acid and AlCl_3 with NaOH for getting hydroxy silico-aluminium oligomer. The acidity of mixed Si/Al pillared clays is found to be considerably higher than the acidity of Al pillared clays and also increased with increasing Si/Al ratio of the pillars [140]. This is due to the formation of acidic surface silanol groups. These clays exhibited a higher cracking activity and disproportionation/alkylation activity compared to Al pillared clays [141].

Mixed Zr/Al pillared clays have mainly been prepared by the research group of Occelli [108-110, 142] using commercially available zirconyl-alumino halohydroxy complexes like REZAL 67 or RETZEL 36G. The resulting solid exhibited a basal spacing of 17.3 Å and BET surface area of $250 \text{ m}^2\text{g}^{-1}$. The cracking

activity for gas oil conversion was found to be higher for these solids compared to Al pillared clays.

Apart from the above discussed mixed metal/Al pillared clays, other systems such as UO_2/Al [143], Cu-Al (144, 145), Mo-Al [146-147], etc. have also been reported. Al free mixed systems such as Fe-Cr and Fe-Zr pillared clays were also reported [148-151]. It is to be mentioned that during our literature survey, we could find only limited number of reports in mixed pillared clays containing pillars with more than two metal cations [152-154].

1.15 Physical Characteristics of Pillared Clays

The d_{001} spacing, the pore-size distribution, the specific surface area and the thermal stability are the essential physical characteristics of pillared clays. These properties will depend on the exchange and distribution of the cations within the particle of the clay. These will, in turn, depend on the presence of other cations, the concentration and pH of the pillaring solution. Generally many ionic species differing in charge and size are present in the intercalating solution. The cation exchange process must then be described as a competition between these ions and the original cations of the clay. The selectivity of cation exchange in silicates depends on both the charge and size of the cations. The selectivity is higher for highly charged cations and the rate of exchange is expected to be lower for bulkier species. The initial cations of the clay also exhibit some influence on pillaring [36]. Better intercalation is observed when the initial cations of the clay bear a higher positive charge. This influence can readily be explained by the competition between these initial cations and the pillaring agent. The competition between Na^+ and the polyoxocation possessing a high charge such as $+7$, is much more favourable to the incorporation of the polyoxocation than the competition between a highly charged ion like Ce^{3+} and the polycation. In the absence of a strong competitor, the exchange takes place rapidly. But in presence of ions like Ce^{3+} or Ce^{4+} , a homogeneous distribution of the polycation results and hence a large surface area is obtained.

In theory, the concentration of the pillaring agent should also have an influence on the distribution of the cations. Whatever the nature of the pillar, getting a pillared clay with an interlayer spacing of at least about 16 Å and specific surface area of at least $150 \text{ m}^2\text{g}^{-1}$ after calcination at 500°C always requires a critical

concentration of the pillaring agent. This critical concentration depends upon the nature of the pillaring agent and the clay. Studies have revealed that the concentration of the polyoxocation is mostly dependent on the OH⁻/metal ratio and much less on the total metal concentration. At higher concentration of the pillaring agent, the competition between the macro cation and the other cations is decreased and the distribution of the pillars should be less homogeneous.

The pH will have an influence on the equilibrium of formation of the polymer and the competitive exchange with the protons and will affect the concentrations of the macro cation and thus the distribution of cations.

1.15.1 Porosity- Influence of Drying

The purpose of pillaring layered materials is to introduce microporosity and to enable permanent access to the intracrystal gallery spaces. The porous properties of pillared clays are thus of primary importance. The drying conditions of a polyoxocation-exchanged clay, influence surface area and pore structure [65]. Air-drying leads to the reorganisation of edge-to-face and edge-to-edge aggregates (delaminated) to face-to-face aggregates. Thus zeolite like products which do not adsorb 1,3,5-triethylbenzene or perfluorotributyl amine with kinetic diameters of 9.2 and 10.4 Å [65] are obtained. In contrast, freeze-dried clays show an appreciable adsorption for these two molecules indicating the presence of wider pores resulting in a 'house of cards' structure. In the 'house of cards' structure, edge-to-face and edge-to-edge arrangement is predominant whereas in well-pillared system face-to-face arrangement is predominating. The different types of aggregations are shown in Figure 1.11. The method of drying is thus believed to control the porosity of the resulting material. It should be added that the particle size of the clay is also an important factor for the pore structure of the pillared product. Clays with small particle size like laponite and certain saponites tend to yield delaminated rather than truly pillared products upon intercalation with polycation [155, 156].

The size of the micropores is relatively difficult to estimate. The height of the micropores is easily obtained from X-ray diffraction. However, the interpillar distance (discussed in section 1.9.1) is difficult to be evaluated because pillared clays

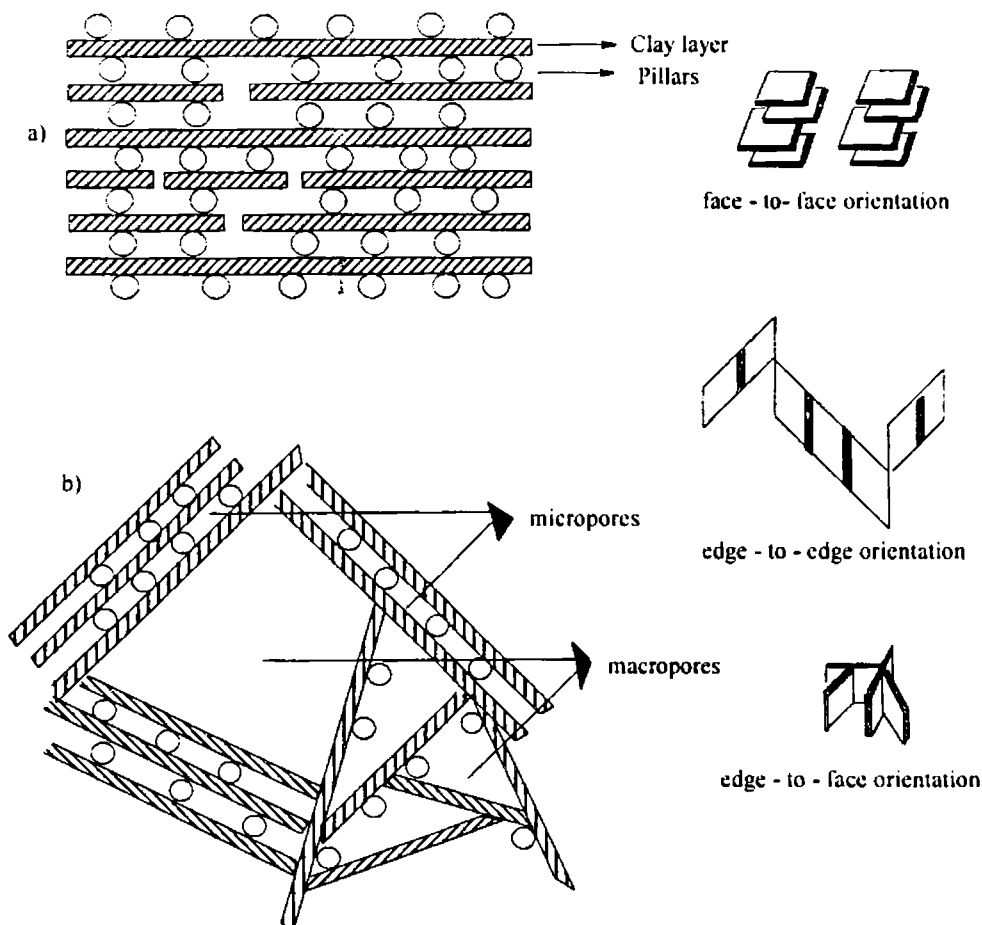


Figure 1.11 Schematic representation of (a) a lamellar and (b) a 'house-of-cards' like aggregation

are not crystallographically ordered in the 'in-plane' direction. N_2 adsorption and Xe-NMR [157] can also provide estimation of pore size but the values again are in the range of the pore height rather than the interpillar distance. However, through an X-ray diffraction study and a thermodynamic study of xenon and krypton adsorption in pillared montmorillonite, an inter pillar distance of 1.8 nm was obtained [158].

1.15.2 Thermal Stability of Pillared Clays

If pillared clays are to be used as catalysts for reactions such as cracking, these should have good thermal and hydrothermal resistance. The hydrothermal stability of montmorillonites has long been known to depend on the nature of the interlayer cations [159]. Two factors appear to control the thermal and hydrothermal stability of pillared clays namely, the density of the pillars and their distribution within the particle. The best hydrothermal stability reported to date concerns a clay

intercalated by hydroxy silico-aluminium ions. After 6 h. at 1033 K in 1 atm. of steam, this clay retains a surface area of $165 \text{ m}^2\text{g}^{-1}$ compared to an initial surface area of $353 \text{ m}^2\text{g}^{-1}$ after calcination at 810 K [44].

The thermal stability of the pillared clays is associated with the dehydroxylation of the clay lattice. Dehydroxylation of the clay lattice of pristine clay minerals occurs above 600°C , but that of pillared minerals occurs much below this temperature. Thermal activation (calcination) is always the necessary final step in the preparation of the pillared clay. Upon calcination, the pillars are first dehydrated and their structure is modified accordingly. This does not involve clay lattice reconstruction, at least when calcination is carried out below the temperature at which the clay octahedral layer dehydroxylates. It should be stated that pillaring lowers the dehydroxylation temperature of the clay lattice. During the activation process, the water and protons are removed from the pillar. They may react in different ways with the clay sheet. For instance, protons can migrate inside the clay lattice and interact with the OH groups within the octahedral sheet. Moreover, when sheets are propped apart by pillars, water molecules nucleated within the octahedral layer do not experience the diffusion barrier that they meet in migrating within a collapsed structure. The result is to lower the dehydroxylation temperature of the pillared clay [160].

1.16 Chemical Properties of Pillared Clays - Acidity

Smectite surfaces are acidic. This results from the high degree of dissociation of water of hydration of the cation and is a consequence of the bidimensional structure [161, 162]. It is well-known that the residual water molecules belonging to the hydration shell of exchangeable cations are very acidic [160]. The exchangeable cation-clay association is like a cation-anion association but the "anion" namely the clay lattice, has an infinite radius of curvature. Thus, the electric field created by the cation strongly polarises a hydration water molecule in the first co-ordination shell. One of the protons is probably delocalised on the network of water filling the space between the cations, while the remaining OH⁻ remain co-ordinated to the cation. The acidic properties of pillared clays have been studied by many authors with several well established and useful techniques. In pillared clays, acidity can originate from the clay layer sheets and pillars [163]. There is a general agreement on the existence of both Lewis and Brønsted acidic sites on pillared montmorillonites. Structurally

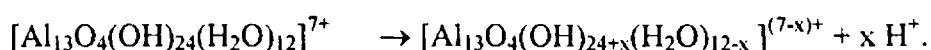
montmorillonite comprises a central sheet of octahedrally co-ordinated aluminium and magnesium in the form of their oxides and hydroxides sandwiched between two sheets containing tetrahedrally co-ordinated silicon essentially in the form of its oxide. The Brönsted acidity for both montmorillonite and pillared montmorillonite is provided mainly by structural OH groups in the 2:1 layers. The strong dependence of Brönsted acidity on the structural OH groups has been evidenced [163]. Al(VI)-O-Al(VI) and Al(VI)-O-Mg linkages comprise most of the structural OH groups of pillared clays and only a small part of the structural OH groups can become Brönsted acid sites during adsorption. The linkage of Al(VI)-O-Mg compared with the linkage of Al(VI)-O-Al(VI), seems more liable to donate H^+ by transferring negative charge to Mg atoms which are located in the dioctahedral sheet. Hall [164] and Davidtz [165] pointed out that co-ordinatively unsaturated Al exposed at crystal edges, may become either Brönsted acid sites or Lewis acid sites. However, their contributions are limited by the site density.

Apart from the acidic sites present in the clay layers, acidic sites can exist on the surface of the pillars also. There is a general agreement on the presence of higher proportion of Lewis acidic sites than Brönsted acidic sites in pillared clays [166-169]. In calcined pillared clays, the pillars are metal oxide clusters and hence the contribution of pillars to the acidity of the pillared clays is mainly of Lewis type. However, there are reports showing the unavoidable contribution of Brönsted acidic sites by the pillars [170-172]. Occelli [170, 171] found by IR studies that Al-pillared Na-bentonite showed a doublet in the OH stretching region indicating the existence of two types of hydroxyls- one vibrating at 3650 cm^{-1} and the other at 3700 cm^{-1} . The former vibration was assigned to the lattice OH and the latter was believed to be associated with the pillar hydroxy groups. The spectra of Al pillared Ca-bentonite also showed two types of bands in the OH region. However, at cracking temperatures and in the absence of H_2O , pillared bentonite have acidity predominantly of the Lewis type.

In calcined pillared clays, Brönsted acidity is found to disappear slowly during the process of thermal activation [163]. This disappearance of Brönsted acidity upon calcination is often attributed to a migration of the protons of the interlayer space into the clay lattice sites where the negative charge originates. These sites are in the octahedral sheet in the case where the octahedral isomorphous

substitution occurs and in the tetrahedral sheet in the case where there is tetrahedral isomorphous substitution. The loss of Brönsted acidity of a pillared clay is much faster than that for an unpillared clay since the former loses its structural OH groups much more easily upon heating than the original clay mineral [163]. Figueras [36] have explained several categories of acidic sites, which indeed are known to exist at the surface.

1. One type may be connected with the initial sites of ion exchange, not occupied by the pillars that represent approximately 30% of the initial exchange capacity of the clay.
2. A second type could be the Si-O-Al(IV) linkages.
3. A third type can be connected with the pillars since it is widely admitted that hydrolytic reactions of the following type can occur.



The co-existence of these different types of acidity complicates the situation, and the localisation of the acid sites is hence much more difficult than in the case of well crystallised structures such as zeolites.

1.16.1 Determination of Acidity

In general, pillaring of clays enhances the acidity and the pillars have been assumed to generate Lewis acid sites [163]. Adsorption of bases such as ammonia, pyridine or aliphatic amines like n-butyl amine has been used for the determination of the acidity of the solid surfaces [173]. These bases, after chemisorption on acidic surfaces, interact with acidic protons, electron acceptor sites and hydrogen from neutral or weakly acidic hydroxyl groups.

In situ IR spectroscopy studies of pyridine and ammonia adsorbed solid provide the best information regarding the nature of interaction between adsorbed bases and the acid sites on the surface of the solid. Different peaks are obtained for different association of the base with the surface. A quantitative determination of the two types of acidities can be done by measuring the area of the IR absorption peaks. The band at 1545 cm^{-1} was considered as characteristic of Brönsted acidity and the band at $1456\text{-}1448 \text{ cm}^{-1}$ of Lewis acidity when the solid is adsorbed with pyridine. As to pillared montmorillonites, Tichit *et al.* [174] observed that Brönsted acidity is

weak as pyridinium ion disappears upon thermal treatments above 570 K, whereas Lewis sites are strong and hold pyridine up to 750 K and it is concluded that the acidity of pillared clays as a whole is comparable to that of zeolite-Y. Flego *et al.* [153] also detected acid sites of both Brønsted and Lewis types by pyridine adsorption of Al, Ce and Al-Ce-Mg PILCs. They have observed a shift in Lewis absorption peak due to a change in the environment of the Lewis sites. The acidic properties of Cr-Al pillared system was studied by Zhao *et al.* [106] and those of Fe-Al system was studied by Storaro *et al.* [118] using pyridine IR technique. Shabtai *et al.* investigated the acidity of Ce-Al pillared smectite [175] by ammonia and pyridine adsorption, using IR and indicated that the acidity decreased with reducing pillar density.

Temperature programmed desorption of ammonia (TPD) is another useful and well exploited technique for investigating the acidity of solid surfaces. This enables one to evaluate the total acidity and its distribution (concentration and strength). However, this technique lacks the detection of the distinction between Lewis and Brønsted acid sites [176]. The already adsorbed ammonia over the catalyst surface is subjected to desorption at different temperatures and is assigned to weak, medium and strong acid sites. The distribution of acid sites among the various regions is thus possible from the ammonia TPD method.

The acid contents of Al, Al-Cr and Cr-pillared derivatives of montmorillonites and saponites were established by Moreno *et al.* [177] by TPD method. They observed that the pillared saponites exhibited higher acid contents than the pillared montmorillonite, regardless of the nature of the pillar. Narayanan *et al.* extensively studied the TPD of ammonia over various solid acid catalysts [178, 179]. Acidity study of Al pillared samples of various OH/Al ratios and also a comparison of acidity of Ce, Al pillared and Ce-Al pillared montmorillonites [178] were reported. The total acidity and its distribution in the three temperature regions (weak, medium and strong) for Al pillared sample were almost the same for OH/Al ratios of 1.5, 2.0 and 2.25. They also observed that pillared samples have much stronger acidity than parent and Ce-exchanged montmorillonite. The total acidity of Al pillared and Ce-Al pillared montmorillonites were found to be almost the same but their distribution was different. Acidity was almost equally distributed in Ce-Al pillared sample whereas Al pillared sample showed comparatively more sites in the strong region.

Canizares *et al.* [180] have also used this technique for the comparison of acidity of various single oxide pillared systems and mixed oxide pillared systems. They have observed a maximum acidity for CrPILC and minimum for FePILC. Likewise, it was observed that pillared clays with mixed oxide pillars of Al and Fe have higher acidity than those with single oxide pillars.

Other methods of determining acidity of solid acids include adsorption studies of aromatic molecules such as substituted benzenes [181-183], comparative adsorption studies of pyridine, piperidine and 2,6-dimethylpyridine [184,185], perylene adsorption studies [186] and calorimetric methods [173].

Adsorption studies of aromatic molecules owing to their poor basicities, are useful to detect the strongest acidic sites present in the catalyst. Liu and Hsu [187] showed that substituted benzenes could be used as adsorbates to evaluate superacidity of solid catalysts. Comparison between the adsorption of pyridine and piperidine gives a measure to obtain strong acidic sites and total acidic sites respectively. Adsorption of 2,6-dimethylpyridine helps to detect Brønsted acidic sites owing to its selective adsorption over these sites, which is attributed to the steric hindrance imparted by the two methyl groups. On the contrary, adsorption of perylene helps to determine the electron acceptor sites, i.e., the Lewis acidic centres in presence of Brønsted acidic sites [173].

1.16.2 Catalytic Test Reactions for Acidity

The acidity of catalyst surface can also be estimated using appropriate test reactions. The most widely used examples include decomposition of alcohols, cracking of alkyl aromatic hydrocarbons and isomerisation of alkenes [173].

a) Cracking of Alkyl Aromatics- Cumene Cracking

The cracking of alkyl aromatic hydrocarbons is a very specific reaction. The aromatic nucleus of the molecule such as cumene is practically inert towards fragmentation. The splitting of C-C bond is thus limited to the non-aromatic part of the hydrocarbon and the most sensitive part for the reaction is the $C_{\text{arom}}-C_{\text{aliph}}$ bond as shown below.

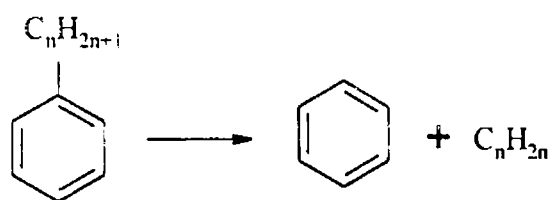


Figure 1. 12 Cracking of alkyl aromatic hydrocarbons

Cumene is a convenient model compound for the catalytic studies, because it undergoes different reactions over different types of active sites [188-190]. The conversion of cumene proceeds in two ways (a) cracking to benzene and (b) dehydrogenation to α -methylstyrene. Cracking to benzene proceeds over Brønsted acid sites through a carbocation mechanism [188, 191]. The other product of this cracking reaction is propene. Dehydrogenation reaction of cumene occurs on Lewis acid sites to convert it to α -methylstyrene [192]. Selectivity towards cracking products is directly proportional to the Brønsted acidic sites whereas selectivity towards dehydrogenation reaction is proportional to Lewis sites. Thus it is possible to estimate and compare both the Brønsted and Lewis acid sites in a catalyst through the study of cumene conversion reaction.

b) Decomposition of Alcohols- Cyclohexanol Decomposition

The most important properties of a metal oxide from a catalysis point of view are its acidity, basicity and redox properties. Alcohol decomposition reactions are quite interesting and useful since more than one parameter can be established by doing a single reaction. A good deal of information about both the acidic and basic sites present in the catalyst can be obtained by carrying out alcohol decomposition reaction. The reaction proceeds through different routes on different active sites. The nature of the active site, whether it is acidic or basic, can then be identified by examining the products of the reaction. The amphoteric nature of alcohols permits their interaction with acidic and basic centres. Hence, in a metal oxide containing both acidic and basic sites, the alcohols can interact with both the centres. Different interactions lead to different reactions.

It was observed that both dehydration and dehydrogenation of alcohols are catalysed by metal oxides. Dehydration leads to the formation of the olefin with the elimination of water and dehydrogenation leads to the formation of an aldehyde (in the case of primary alcohols) or a ketone (in the case of secondary alcohols) with the

elimination of hydrogen. Many authors ascribe the dehydration activity of oxides to their surface acidity, whereas the dehydrogenation reaction is related to their surface basicity [193-199]. Thus the selectivity exhibited by a catalyst is related to its surface acid-base properties. In cyclohexanol decomposition reaction, dehydration yields cyclohexene and dehydrogenation yields cyclohexanone.

1.17 Vanadium Impregnation over Clays

Supported vanadium oxide catalysts are important in industrial processes [200-202]. Use of supporting vanadium oxide on another oxide has several advantages over an unsupported oxide, such as higher mechanical strength, better thermal stability and larger surface area. [203]. There are several reports regarding the dispersion of vanadium oxide over basic, amphoteric and acidic oxides [204-206]. It is possible that the dispersion of vanadium oxide as well as the structure can be understood on the basis of acid-base character of the supports used. The basic and amphoteric oxides favour the bidimensional dispersion, often with the formation of compounds. The agglomeration of vanadia species to form crystalline vanadia is favoured with the acid character of the support. The formation of these different types of vanadia species can be accounted as follows. Since vanadia is comparatively acidic, it reacts easily with basic oxides with the preferential formation of vanadates such as ortho and pyrovanadates. But a weaker interaction with the acidic supports favours the aggregation of VO_x leading to the formation of crystalline V_2O_5 .

Vanadium oxide is supported over the oxides usually by the wet impregnation method. The term impregnation denotes a procedure whereby a certain volume of solution containing a compound of the active element is totally adsorbed into the pores of the support. This well exploited method involves the stirring of the support with required amounts of ammonium metavanadate in oxalic acid solution, followed by evaporation to dryness. By employing this method, it is possible to produce any desired loading of V_2O_5 over the support [207].

Except a few reports [208, 209], work on vanadia impregnation over clays is very rare. Over acid activated montmorillonite, namely K10, vanadia loading by wet impregnation method was attempted and compared with vanadia-silica by Narayanan *et al.* [210]. They have inferred that the type of interaction of vanadia with K10 montmorillonite and SiO_2 is different. Vanadia is well dispersed as V_2O_5

crystallites in both the supports. An interaction of vanadia with the support occurs in the case of silica whereas such interaction is absent in montmorillonite K10. An interaction between vanadia and the support leads to the hyperfine splitting of ESR spectra, and is observed with the case of silica but not with K10 montmorillonite.

To our knowledge, there are hardly any reports on vanadia impregnation over pillared clays. In our present investigation, apart from the preparation of various pillared clays, we have also prepared various vanadia loaded pillared clays by the wet impregnation method.

1.18 Catalysis by Pillared Clays

The pillaring of clays increases the accessibility of reactant molecules to the interlayer catalytic sites, resulting in a possibly high catalytic activity. Simultaneously, the interlayer and interpillar distances exert a shape selective effect, which control the diffusion rates of reactants, reaction intermediates and products. A large variety of catalytic reactions such as cracking, disproportionation, alkylation and acylation, methanol conversion, oxidation reactions, etc. have been reported to take place over the pillared clays and most of these reactions are based on the acidic properties of the catalyst. Table 1.4 (on page 48) summarises some of the catalytic reactions attempted on pillared clays.

One of the important catalytic processes based on shape selectivity is the production of *p*-xylene by alkylation of toluene with methanol. The selectivity for the pillared clays in this reaction is surprisingly higher than that of the zeolite, ZSM-5 [210]. However, an opposite result has been reported by Ocelli *et al.* [211]. Alkylation of toluene with ethylene produced *p*-ethyltoluene in equilibrium amounts by use of ALPILC. *p*-Ethyltoluene is a larger molecule than *p*-xylene and therefore, the reaction is shape selectively controlled, for *p*-ethyltoluene to be produced selectively. In the methylation of toluene, the low activity for isomerisation of *p*-xylene seems to lead to a high selectivity for its formation.

Alkylation of 1,2,4-trimethylbenzene with methanol was studied by Mastuda *et al.* [212]. A high selectivity to the 1,2,4,5-tetramethylbenzene isomer was achieved in the absence of methanol, i.e., via disproportionation, while the selectivity decreased with increase in conversion due to isomerisation of the

1,2,4,5-tetramethylbenzene. However, isomerisation of 1,2,4,5-isomer was not observed in alkylation with methanol. Moreover, the increase in methanol content in the feed enhanced the selective formation of 1,2,4,5-tetramethylbenzene isomer. These results indicate that methanol retards isomerisation of 1,2,4,5-tetramethylbenzene isomer once produced, because of preferential adsorption of methanol on acid sites than aromatic hydrocarbon.

Kikutchi *et al.* [213] observed a restricted transition state type shape selectivity in the disproportionation of 1,2,4-trimethylbenzene to yield 1,2,4,5-tetramethylbenzene on pillared clays. When AlPILC having a layer distance of 8 Å was used as a catalyst, 1,2,4,5-tetramethylbenzene and *o*-xylene were produced more abundantly than expected from thermodynamic equilibrium calculations. Preferential formation of the specified isomers was attributed to restricted transition state selectivity.

Shabtai *et al.* [214] have reported that AlPILC is more active for dealkylation and cracking of large organic molecules than Y-type zeolites. The high activity of PILCs has been attributed to the large pore size that allows bulky hydrocarbon molecules to reach the interior active sites. It has also been pointed out by the same authors [215] that higher activity is obtained when rare earth exchanged clays are cross linked rather than ion exchanged subsequent to cross linking.

An interesting outlook on the commercial application of pillared clays has been provided by Ocelli and co-workers. [142, 216, 217]. They showed that gas oil cracking catalysed by pillared clays gave high and selective yields of gasoline under moderate conditions. The activity and selectivity are affected by the nature of clays. Hectorite exhibits a gasoline selectivity and minimises light gas production, although it is not so active as montmorillonite. However, they pointed out some problems like high coke formation and lack of hydrothermal stability while using PILC as a catalyst.

Cracking of cumene and *n*-paraffins were conducted by He *et al.* [163] on AlPILCs. Cumene cracking was carried out as a test reaction for Brønsted acidity by conducting the reaction at 250°C with catalyst preheated at various temperatures. The conversion was found to fall rapidly after treatment at 400°C or above which is due to the loss of structural hydroxyls and Brønsted acidity. When the reaction of

n-heptane was conducted on a dried Al-pillared montmorillonite, cracking was initiated at 120°C and the conversion level increased steadily to a maximum at about 240°C, then decreased with further increase in the reaction temperature. This unusual behaviour can best be explained by the loss of Brønsted acidity of Al-pillared montmorillonite upon heating during reaction. The cracking activities for n-C₁₀ and n-C₁₂ hydrocarbons were also studied and the activities showed a similar trend as that of n-heptane.

Barrault *et al.* [144, 218] have studied the catalytic wet peroxide oxidation of phenol over mixed Al-Fe and mixed Al-Cu pillared clays. The study of the catalytic oxidation by hydrogen peroxide of an aqueous solution of phenol on an Al-Fe pillared clay catalyst has shown that under mild reaction conditions, about 80% of the initial amount of phenol was transformed into CO₂ at 70°C in 2 h under atmospheric pressure [144]. The catalyst leaching remained very low even after three cycles of reaction and represented less than 0.2% of the total amount iron contained in the catalyst. The low leaching and its high catalytic activity showed that mixed Al-Fe pillared catalyst could be one of the most promising catalysts for an industrial depollution process. The same authors observed a high degree of phenol conversion to CO₂ for mixed Al-Cu pillared systems [218]. Castillo *et al.* [219] conducted the phenol oxidation reaction over Ti-pillared montmorillonite. They have observed dihydroxy benzenes such as catechol and hydroquinone and also benzoquinone as the major products. They have studied the influence of solvent as well and the observations are related to the nature of the solvents. Hydroquinone was observed as the major product with a protic solvent such as methanol and catechol was found to be the major product with an aprotic solvent such as acetone.

The use of chromia-alumina pillared saponites as catalysts in the deep oxidation of acetone have been reported [107]. All the Cr-Al pillared saponites were active catalysts for the complete oxidation of acetone, reaching 100% conversion to CO₂ at temperatures ranging from 573 to 613 K. A significant effect of the Al³⁺/Cr³⁺ ratio of the pillared clay on the catalytic activity has been found. The combined effect of this ratio on the chromium dispersion and pillared clay surface areas as well as the saponite intrinsic activity seemed to be the main factors that control catalytic activity.

Selective catalytic reduction (SCR) of NO_x (x=1 or 2) with ammonia is the most efficient technology for its abatement from power plant exhaust gases. SCR has

been extensively studied in recent years because of its environmental importance. Various pillared clay catalysts also have been tried for the reaction. Fe³⁺ exchanged titanium pillared clay catalysts were employed by Long *et al.* [220]. They have proposed a possible reaction scheme also for the SCR reaction on Fe-TiO₂-PILC. Nitrogen originates mainly from the reaction between gaseous or weakly adsorbed NO and adsorbed NH₃ species.

Different ion exchanged AlPILC, ZrPILC and TiPILC were used for selective catalytic reduction of NO by ethylene in presence of O₂ by Yang *et al.* [221]. Cu²⁺ exchanged TiPILC showed the highest activities at temperatures below 370°C, while Cu²⁺ exchanged AlPILC was most active at above 370°C, and both catalysts were substantially more active than Cu-ZSM-5. They have also carried out the deactivation by H₂O and SO₂, and found that both slightly deactivated the SCR activity of Cu-TiPILC whereas severe deactivation was observed for Cu-ZSM-5. Also, the catalytic activity of Cu-TiPILC was found to depend on the method and amount of Cu loading.

Apart from the above, Table 1.4 gives an account of a few more catalytic reactions over pillared clays. However, the great multitude of catalytic studies reported over pillared clays limits us not to make this review exhaustive.

1.19 Reactions Selected for the Present Study

Pillared clays are well-known for their acidic properties. Hence various acid catalysed reactions such as benzylation and benzoylation of toluene and alkylation of aniline are selected for the present study. The efficiency of various pillared clays as catalysts for an oxidation reaction namely catalytic wet peroxide oxidation of phenol is also tested.

a) Friedel-Crafts Alkylations and Acylations

The Friedel-Craft's reactions are of great interest due to their importance and common use in synthetic and industrial chemistry. These are important means for attaching alkyl chains to aromatic rings and are widely used in the synthesis of large number of fine chemicals such as drugs, fragrances, dyes and pesticides [229, 230]. The alkylation and acylation are traditionally performed with alkyl or acyl halides using Lewis acid catalysts such as BF₃ and AlCl₃ or with alcohols using Brønsted

Table 1.4 Some catalytic applications of pillared clays

Pillared system	Catalytic application	Reactants	References
Al, Al-Ga, Ga	Cracking	Cumene	[222]
Al, LA-Al		Cumene	[223]
Al, Si-Al		Cumene	[141]
Al, La-Al		n-Heptane	[224]
Fe, Fe-Al, Al		n-Decane	[111]
Zr, Zr-Al, Al		Gas oil	[142]
Al, Ga-Al	Alkylation	Toluene	[225]
Al		Toluene/methanol	[210]
Al, Al-Zr		Toluene/ethylene	[211]
Al, Al-Zr		1,2,4-Trimethylbenzene/methanol	[211]
Al		1,2,4-Trimethylbenzene/methanol	[212]
La-Al, Al	Disproportionation	1,2,4-Trimethylbenzene	[223]
Al, Si-Al, Si		1,2,4-Trimethylbenzene	[141]
Cr, Cr-Al, Al		1,2,4-Trimethylbenzene	[106]
Cr, Cr-Al, Al	Isomerisation	1-Butene	[132]
Ga-Al		n-Heptane	[226, 227]
Ru-Al, Al	Deep oxidation	Chlorinated hydrocarbons	[120]
Cr-Al, Cr		Chlorinated hydrocarbons	[132]
Cr, Cr-Al, Al		Acetone	[107]
Cr, Cr-Al, Al	Oxidation	1-Phenyl-1-propanol	[107]
Cr, Cr-Al, Al		Cyclohexane	[87]
Cu-Al	Wet peroxide oxidation	Phenol	[218]
Fe-Al		Phenol	[144]
Ti		Phenol	[219]
Fe	Fischer-Tropsch synthesis	CO/H ₂	[228, 48]
Al, Fe-Al	Alcohol decomposition	Isopropanol	[128]
Ti-exchanged	SCR of NO _x	NO _x	[220]
Al, Zr, Ti.		NO _x	[221]

acids, typically H_2SO_4 [231-233]. However, these catalysts pose several problems. The use of these substances involves technological and environmental problems due to their corrosive nature, the difficulty of recycling and the formation of large amounts of harmful wastes, with consequent economic and environmental problems. Although alkylation reaction proceeds in the presence of a catalytic amount of Lewis acid, the acylation reactions require more than a stoichiometric amounts of the traditional Lewis acids, which form complexes with both the acylating reagent and the carbonyl product. This necessitates work-up to decompose the complexes and the catalyst is not reusable. Yet another disadvantage is polyalkylations and rearrangements that are difficult to avoid. One important consequence of the new environmental legislation and the drive towards "clean technology" is the thrust towards the development of "environmentally friendly heterogeneous catalysts" for these reactions. Thus it is highly desirable to develop new processes that can reduce the environmental and economic problems associated with the classical Friedel-Craft's alkylation and acylation catalysts [234, 235]. Active research has been directed at substituting the traditional homogeneous catalysts with acid catalysts such as clay minerals and zeolites [236].

b) Alkylation of Aniline

Alkylation of aniline is industrially very important as the major products of this reaction form the basic raw materials for synthesis of organic chemicals and intermediates in dye stuffs, pharmaceuticals and agro industries. N-alkylated products such as N-methylaniline (NMA), N,N'-dimethylaniline (NNDMA), N-methyl p-toluidine (NMT) and other C-alkylated products (toluidines) are formed during the methylation of aniline. Initially, aniline was alkylated with methanol in the liquid phase using acid or halide as homogeneous catalysts [237]. The use of aluminium alkoxide and strong acids as catalysts has also been reported [238-241]. However, with the varying awareness of environmental issues, various solid acid catalysts have been tried for the reaction. These include oxides, zeolites, AEL type molecular sieves and clays [209, 242-250]. The various alkylating reagents used include olefins, alcohols and dimethyl carbonate [246-248, 251-253].

Aniline alkylation reaction is an acid-catalysed reaction and proceeds through an electrophilic substitution mechanism. The electrophile i.e., the carbocation is

formed from the alkylating agents, viz., olefins, alcohols or alkyl halide with the help of acid sites on the catalyst surface. Alkylation of aniline is a consecutive reaction. N-alkyl aniline is the primary product which is further alkylated to N,N'-dialkylaniline. Direct ring alkylation can also occur. N,N'-dialkylaniline can rearrange to form N-alkyl toluidines via N → C shift [254].

c) Catalytic Wet Peroxide Oxidation of Phenol (CWPO)

Industrial processes and agricultural activities generate a large diversity of waste-water containing organic pollutants. Thus ecologically friendly technology is one of the most important subjects in present-day chemistry, in particular for partial oxidation of organic compounds. Until now, many different solids were proposed as catalysts for the oxidation of various organic compounds in water [144, 255-258]. Phenol constitutes one of the main pollutants to be removed from waste-water. Hence the disposal of phenol by a 'clean' technology is very much advisable. Catalytic Wet Peroxide Oxidation (CWPO) is reported to be a suitable method to achieve a high conversion of the organic pollutants at soft conditions and at the lowest cost [259].

Phenol is a very simple organic compound, easily soluble in water at different conditions of acidity. It will be of added advantage, if this phenol is converted to useful products. The hydroxylation products of phenol namely catechol and hydroquinone (diphenols) are extensively used as photographic developers, ingredients for food and pharmaceutical applications and antioxidants.

1.20 Main Objectives of the Present Work

Pillared clays have attracted considerable attention as catalysts for a variety of acid-mediated reactions. The catalytic properties of pillared clays are a result of the propping apart of the clay structure, thereby increasing the surface area and pore volume, and exposing much of the inter layer region and any acid sites therein to reactant molecules. Furthermore, in addition to expanding the layer structure, the metal oxide pillars are themselves thought to possess a certain amount of acidity and activity.

Owing to the presence of both Brönsted and Lewis acidic centres on pillared clays, they have been used as efficient catalysts for cracking, alkylation, isomerisation, hydroconversion, etc. Addition of a second metal into the pillared clay

structure is known to improve the acidity, thermal stability and catalytic activity of single oxide pillared systems. Our synthetic programme, hence, has focused on the preparation of mixed pillared systems and a comparison with single pillared systems. Furthermore, vanadia is known to improve the catalytic activity of metal oxides that act as supports for vanadia. Reports of vanadia impregnation over clays are very sparse.

In the present work, we report the preparation and characterisation of single, mixed and vanadia loaded pillared montmorillonites. Al^{3+} , Fe^{3+} and Cr^{3+} , are known to be acidic. Hence their individual and mixed pillaring solutions are selected for pillaring the parent clay, namely montmorillonite. We are interested and curious about their catalytic behaviour towards certain industrially important reactions, which are discussed in the section 1.19.

The main objectives of the present work can be summarised as

- To modify a naturally occurring clay mineral, namely montmorillonite through pillaring.
- To synthesise single metal oxide pillared montmorillonites such as Al-pillared, Fe-pillared and Cr-pillared montmorillonites. Another major objective is to synthesise mixed metal oxide pillared clays namely Fe-Al and Cr-Al pillared montmorillonites with various Fe/Al (Cr/Al) ratios.
- To investigate the influence of vanadia loading over iron pillared montmorillonite.
- A thorough characterisation study of all the prepared catalytic systems for an understanding of their textural characteristics is another objective. Various characterisation techniques include EDX, XRD, IR, BET surface area and pore volume measurements and TG studies.
- To explore the acidic character of all the catalysts through various independent techniques such as thermodesorption study of 2,6-dimethylpyridine, adsorption of perylene, temperature programmed desorption (TPD) of ammonia, decomposition of cyclohexanol and cumene conversion test reaction.

- To investigate the catalytic efficiency of the samples towards the industrially important reactions namely Friedel–Craft’s benzylation and benzoylation of toluene.
- To study the aniline methylation reaction which is another industrially important reaction, over all the catalyst systems.
- Phenol is a major water pollutant and its removal by oxidation to harmless/ useful products is highly desirable. So the last objective is to test the efficiency of the catalysts for the wet peroxide oxidation of phenol to industrially important chemicals namely the diphenols.

References

- [1] J.A. Schwarz, C. Contescu and A. Contescu, *Chem. Rev.*, 95 (1995) 477.
- [2] Olegv Krylov, in "Catalysis by Non-metals: Rules for Catalyst Selection", Academic Press, New York.
- [3] K. Tanabe, M. Misono, Y. Ono and H. Hattori, "New Solid Acids and Bases", Kodansha, Tokyo, 1989, p-1.
- [4] M.W. Tamale, *Discuss. Farad. Soc.*, 8 (1950) 270.
- [5] O. Johnson, *J. Phys. Chem.*, 59 (1955) 827.
- [6] H. Pines, J.A Vaseky and V.N. Ipatieff, *J. Amer. Chem. Soc.*, 77 (1961) 6314.
- [7] H. Hattori, *Chem. Rev.*, 95 (1995) 537.
- [8] C.J.B. Mott, *Catal. Today*, 2 (1988) 199.
- [9] S. W. Bailey in "Crystal Structures of Clay Minerals and their X-Ray identification" (G. W. Brindley and G. Brown (Eds.)), Mineralogical Society, Monograph No.5, London, 1980, Chapter 1.
- [10] T. J. Pinnavaia, *Science*, 220 (1983) 365.
- [11] A. Weiss, *Angew. Chem. Ind. Ed. Engl.*, 20 (1981) 850.
- [12] G. Beson, A. Mifsud, C. Tchoubar and J. Mering, *Clays Clay Miner.*, 22 (1974) 379.
- [13] G. W. Brindley in "Crystal Structures of Clay Minerals and their X-Ray Identification", (G. W. Brindley and G. Brown (Eds.)), Mineralogical Society, London, 1980, Chapter 2.
- [14] H. Suquet, C. de la Calle and H. Pezerat, *Clays Clay Miner.*, 23 (1975) 1.
- [15] M. M. Mortland, *Adv. Argon*, 22 (1970) 70.
- [16] M. M. Mortland, *Trans. 9th Int. Cong. Soil Sci.*, 1 (1968) 691.
- [17] R.K.G. Theng, "The Chemistry of Clay-Organic Reactions", Wiley, New York, 1974.
- [18] V. Berkheiser and M. M. Mortland, *Clays Clay Miner.*, 25 (1977) 105.
- [19] K. V. Raman and M.M. Mortland, *ibid*, 16 (1968) 393.
- [20] D. M. MacEwan and M.J. Wilson, in "Crystal Structures of Clay Minerals and their X-Ray Identification", (G. W. Brindley and G. Brown (Eds.)), Mineralogical Society, London, 1980, Chapter 3.
- [21] R. Glaeser and J. Mering, *C. R. Acad. Sci. Ser. D*, 267 (1968) 463.
- [22] Erno Nemezc, "Clay Minerals", Akademiai Kiado, Budapest, 1981, p-41.

- [23] J.M. Thomas and C.R. Theocharis, in " Perspectives in Catalysis" Eds. J.M. Thomas and K. I. Zamarev, London, 1992, p-465.
- [24] Chemistry of Clays and Clay Minerals, Mineralogical Society, Monograph No. 6 Ed. A.C.D. Newman, 1987, p-275.
- [25] R.K. Barrer, *Phil. Trans. R. Soc. London*, 1984, A 311, 333.
- [26] D.A. Morgan, D.B. Shaw, M.J. Sidebottom, T.C. Soon and R.C. Taylor, *J. Amer. Oil Chem. Soc.*, 62 (1985) 292.
- [27] W. Cranquit and G.S. Gardner, *Clays Clay Miner.*, (1959) 292.
- [28] J.H. Clark, A.P. Kybett, D.J. Macquarrite, S.J. Barlow and P. Landon, *J. Chem. Soc. Chem. Commun.*, (1989) 1353.
- [29] J.R. Sohn and M.Y. Park, *Appl. Catal. A Gen.*, 101 (1993) 129.
- [30] C. Cativiela, J.M. Fraile, J.I. Garcia, J.A. Mayoral, F. Figueras, L.C. Menorval and P.J. Alonso, *J. Catal.*, 137 (1992) 394.
- [31] R.M. Barrer and D.M. Macheode, *Trans. Faraday Soc.*, 51 (1955) 1290.
- [32] D.E.W. Vaughan, R.J. Lussier and J.S. Magee, *U S Patent* 3 775 395, 1973. *U S Patent* 3 838 037, 1974; *U K Patent* 1483 466, 1979.
- [33] G. W. Brindley and R. E. Sempels, *Clay Miner.*, 12 (1977) 229.
- [34] N. Lahav, U. Shani and J. Shabtai, *Clays Clay Miner.*, 26 (1978) 107.
- [35] E.M. Farfan-Torres and P. Grange, *J. Chem. Phys.*, 87 (1990) 1547.
- [36] F. Figueras, *Catal. Rev. Sci. Eng.*, 30 (1988) 457.
- [37] N. Bjerrum, *Z. Physik. Chem.*, 59 (1907) 349.
- [38] C.F. Baes and R.E. Mesmer, " The Hydrolysis of Cations", Wiley, New York, 1976.
- [39] S. Yamanaka and G.W. Brindley, *Clays Clay Miner.*, 26 (1978) 21.
- [40] H.M. Mody, P.M. Oza and V.P. Pandya, *Appl. Clay Sci.*, (1993) 53.
- [41] Zhonghua Ge, Danyan Li and T.J. Pinnavaia, *Micropor. Mater.*, 3 (1994) 165.
- [42] S.L. Johns, *Catal Today*, 2 (1988) 209.
- [43] D.E.W. Vaughan. and R.J. Lussier, in "Proc. of the 5th Int. Conf. on Zeolites", Eds. L.V. Rees and Heyden, London, 1980, p-94.
- [44] D.E.W. Vaughan, R.J. Lussier and J.S. Magee. *U S Patent*, 4 176 090 (1979); 4 248 739 (1981).
- [45] S. Yamanaka and G.W. Brindley, *Clays Clay Miner.*, 27 (1979) 119.

- [46] A.G. Vormokov, "Topics in Current Chemistry". Springer-Verlag, Berlin, 1982, p-199.
- [47] S. Yamanaka and M. Hattori, *Catal. Today*, 2 (1988) 261.
- [48] E.G. Rightor, M. Tzou and T.J. Pinnavaia, *J. Catal.*, 130 (1991) 29.
- [49] T.J. Pinnavaia and R. Raythatha, *J. Mol. Catal.*, 27 (1984) 195.
- [50] K.A. Korrado, S.L. Suib, N.B. Skoularikis and R.W. Coughlin, *Inorg. Chem.*, 25 (1986) 4217.
- [51] G.W. Brindley and S. Yamanaka, *Amer. Miner.*, 64 (1979) 830.
- [52] T.J. Pinnavaia, M.S. Tzou and S.V. Landau, *J. Amer. Chem. Soc.*, 107 (1985) 4783.
- [53] J.W. Akitt, N.N. Greenwood, B.L. Kandel Wahl and G.D. Lester, *J. Chem. Soc. Dalton Trans.*, (1972) 604.
- [54] R. Caminiti, G. Licheri, G. Piccalaga, G. Pinna and M. Magini, *Rev. Inor. Chem.*, 1 (1979) 333.
- [55] D.N. Waters and S.M. Henty, *J. Chem. Soc.*, (1977) 243.
- [56] C.J. Brinker, D. E. Clark and D.R. Ulrich, *Mater. Res. Soc., Symp. Proc.*, 32 (1984).
- [57] J.T. Klopogge, D. Seykens, J.B. H. Jansen and J. W. Gens, *Non-Cryst. Solids*, 142 (1992) 94.
- [58] C. Borosset, G. Biedermann and G. Sillen, *Acta. Chem. Scand.*, 8 (1954) 1917.
- [59] W.V. Rausch and H.D. Bale, *J. Chem. Phys.*, 40 (1964) 3391.
- [60] G. Johansson, *Acta. Chem. Scand.*, 14 (1960) 771.
- [61] J.Y. Bottero, J.M. Cases, F. Fiessinger and J.E. Poirier, *J. Phys. Chem.*, 84 (1980) 2933.
- [62] P.M. Bertsch, G.W. Thomas and R.I. Barnhisel, *Soil Sci. Soc. Amer. J.*, 50 (1986) 825.
- [63] P.M. Bertsch, W.J. Layton and R.I. Barnhisel, *Soil Sci. Soc. Amer. J.*, 50 (1986) 1449.
- [64] J.P. Sterte and J.E. Otterstedt, in "Preparation of Catalysts, IV", Eds. B. Delmon, P. Grange, P.A. Jacobs and G. Poncelet, 1987, p-631.
- [65] T.J. Pinnavaia, M.S. Tzou, S.V. Landau and R.H. Raythatha, *J. Mol. Catal.*, 27 (1984) 195.
- [66] D. Plee, Ph. D Thesis. University of Orleans, France, 1984.

- [67] L. Bergaoui, J.F. Lambert, R. Franck, H. Suquet and J.L. Robert, *J. Chem. Soc. Farad. Trans.*, 91 (1995) 2229.
- [68] C.I. Warburton, *Catal. Today*, 2 (1988) 271.
- [69] T.G. Spiro, S.E. Allerton, J. Renner, A. Terzis, R. Bils and P. Saltman, *J. Amer. Chem. Soc.*, 88 (1966) 2721.
- [70] R. Herrera and M. Peech, *Soil Sci. Soc. Amer. Proc.*, 34 (1970) 740.
- [71] D.D. Carstea, *Clays Clay Miner.*, 16 (1968) 231.
- [72] P. Rengasamy and J.M. Oades, *Aust. J. Soil Res.*, 15 (1977) 221.
- [73] P. Rengasamy and J.M. Oades, *Aust. J. Soil Res.*, 15 (1977) 235.
- [74] S. Yamanaka, T. Doi, S. Sako and M. Hattori, *Mater. Res. Bull.*, 19 (1984) 161.
- [75] C.M. Flynn Jr., *Chem. Rev.*, 84 (1984) 31.
- [76] P.J. Murphy, A.M. Posner and J.P. Quirk, *Aust. J. Soil Res.*, 13 (1975) 189.
- [77] P.J. Murphy, A.M. Posner and J.P. Quirk, *J. Coll. Inter. Sci.*, 52 (1975) 229.
- [78] J.E. Earley and R.D. Cannon in "Transition Metal Chemistry", Vol.1, Ed. R. Carlen, Marcel Dekker, New York, 1965, p-34.
- [79] M. Ardon and R.A. Plane, *J. Amer. Chem. Soc.*, 81 (1959) 3197.
- [80] R.W. Kolackowski and R.A. Plane, *Inorg. Chem.*, 3 (1964) 322.
- [81] M. Thompson and R.E. Connick, *Inorg. Chem.*, 20 (1981) 2279.
- [82] E. Finholt, M. Thompson and R.E. Connick, *Inorg. Chem.*, 20 (1981) 4151.
- [83] H. Stünzi and W. Marty, *Inorg. Chem.*, 22 (1983) 2145.
- [84] J.A. Laswick and R.A. Plane, *J. Amer. Chem. Soc.*, 81 (1959) 3564.
- [85] S. Kratovil and E.J. Matijevic, *J. Coll. Inter. Sci.*, 24 (1967) 47.
- [86] H. Stünzi, L. Spiccia, R.P. Rotzinger and W. Marty, *Inorg. Chem.*, 28 (1989) 66.
- [87] T.J. Pinnavaia, M.S. Tzou and S.V. Landau, *J. Amer. Chem. Soc.*, 107 (1985) 4783.
- [88] M. Tzou and T.J. Pinnavaia, *Catal. Today*, 2 (1988) 243.
- [89] P.D. Hopkins, B.L. Meyer and D.M. Van Duch, *U S Patent* 4 452 910 (1984).
- [90] A.J. Lopez, J. Maza-Rodriguez, P. Olivera-Pastor, M. Torres and E.R. Castellon, *Clays Clay Miner.*, 41 (1993) 328.
- [91] W.E. Dubbin, T.B. Goh and D.W. Oscarson, *Clay Miner.*, 42 (1994) 331.
- [92] J. T. Klopogge, *J. Porous Mater.*, 5 (1998) 5.

- [93] S. Yamanaka, T. Yishihara and M. Hattori, *Mater. Chem. Phys.*, 17 (1987) 87.
- [94] A. Bernier, N. F. Admaiai and P. Grange, *Appl. Catal.*, 77 (1991) 269.
- [95] H.L. Del Castillo and P. Grange, *Appl. Catal. A Gen.*, 103 (1993) 23.
- [96] M.A. Matin- Luengo, H. Matins-Carvalho, J. Ladriere and P. Gange, *Clay Miner.*, 24 (1989) 495
- [97] A. Bellaloui, D. Plee and P. Meriaudeau, *Appl. Catal.*, 63 (1990) L 7.
- [98] S.P. Christiano, J. Wang and T. J. Pinnavaia, *Inorg. Chem.*, 24 (1985) 1222.
- [99] G.J.J. Bartley, *Catal. Today.*, 2 (1988) 233.
- [100] S.M. Bradley, R.A. Kydd and R. Yamdagni, *J. Chem. Soc. Dalton Trans.*, (1990) 2653.
- [101] S.M. Bradley and R.A. Kydd, *Catal. Lett.*, 8 (1991) 185.
- [102] S.M. Bradley and R.A. Kydd, *J. Catal.*, 142 (1993) 448.
- [103] D.H. Doff, N.H.J. Gangas, J.E.M. Allan and J.M.D. Coey, *Clay Miner.*, 23 (1988) 367.
- [104] W.Y. Lee and B.J. Tatarchuk, *Hyperfine Interactions*, 41 (1988) 661.
- [105] K.A. Karrado, A. Kostapapas, S.L. Suib and R.W. Coughlin, *Solid State Ionics*, 22 (1986) 117.
- [106] D. Zhao, Y. Yang and X. Guo, *Zeolites* 15 (1995) 58.
- [107] A. Gill, M.A. Vicenti, R. Toranzo, M.A. Banares and L.M. Gandia, *J. Chem. Technol. Biotechnol.*, 72 (1998) 131.
- [108] M.L. Occelli, *J. Mol. Catal.*, 35 (1986) 377.
- [109] M.L. Occelli, in "Proc. Int. Clay. Conf. Denver" 1985 Eds. L.G. Schultz, H. Van Olphen and F.A. Mumpton, (1987) p- 319.
- [110] M.L. Occelli and R.J. Rennard, Prep. Rap. Chem. Soc. 188th Nat. ACS Meeting Div. Fuel Chem., Philadelphia, 1984, Vol. 29, p-30.
- [111] N.D. Skoularikis, R.W. Coughlin, A. Kostapapas, K.A. Karrado and S.L. Suib, *Appl. Catal.*, 39 (1988) 61.
- [112] F. Bergaya, N. Hassoun, L. Gatineau and J. Barrault, in "Scientific Bases for the Preparation of Heterogeneous Catalysts", 5th Int. Symp. Louvain-La-Neuve, Belgium, 1990, Preprint, p-141.
- [113] W.Y. Lee, R.H. Raythatha and B.J. Tatarchuk, *J. Catal.*, 115 (1989) 159.
- [114] I. Kiricsi, A. Molnar, I. Palinko and K. Lazar, *Stud. Surf. Sci. and Catal.*, 94 (1995) 63.

- [115] I. Palinko, K. Lazar, I. Hannus and I. Kirisci, *J. Phys. Chem. Solid*, 57 (1996) 1067.
- [116] J. Valyon, I. Palinko and I. Kirisci, *React. Kinet. Catal. Lett.*, 58 (1996) 249.
- [117] I. Palinko, A. Molnar, J.B. Nagy, J.C. Bertrand, K. Lazar, J. Valyon and I. Kirisci, *J. Chem. Soc. Farad. Trans.*, 93 (1997) 1591.
- [118] L. Storaro, M. Lenarda, R. Ganzerla and A. Rinaldi, *Micropor. Mater.*, 6 (1996) 55.
- [119] M. Lenarda, R. Ganzerla, L. Storaro, S. Enzo and R. Zanoni, *J. Mol. Catal.*, 92 (1994) 201.
- [120] L. Storaro, R. Ganzerla, M. Lenarda and R. Zanoni, *J. Mol. Catal.*, 97 (1995) 139.
- [121] F. Bergaya, N. Hassoun, J. Barraoult and L. Gataineau, *Clay Miner.*, 28 (1993) 109.
- [122] J. Barraoult, C. Zivkov, F. Bergaya, L. Gataineau, N. Hassoun, H. Van Damme and G. Mari, *J. Chem. Soc. Chem. Commun.*, (1988) 1403.
- [123] F. Bergaya and J. Barraoult, in "Pillared Layered Structures: Current trends and Applications" Ed. I. V. Mitcheli, Elsevier, London, 1990, p-167.
- [124] J. Barraoult, L. Gataineau, N. Hassoun and F. Bergaya, *Energy Fuels*, 6 (1992) 760.
- [125] T. Mandalia, M. Crespini, D. Messad and F. Bergaya, *J. Chem. Soc. Chem. Commun.*, (1998) 2111.
- [126] D. Zhao, G. Wang, Y. Yang, X. Guo, Q. Wang and J. Ren, *Clays Clay Miner.*, 41 (1993) 317.
- [127] A. de Steffanis, G. Perrez and A.A.G. Tomlinson, *J. Mater. Chem.*, 4 (1994) 959.
- [128] A.K. Ladavos, P.N. Trikalitis and P.J. Pimonis, *J. Mol. Catal. A Chem.*, 106 (1996) 241.
- [129] C. Breen and P.M. Last, *J. Mater. Chem.*, 9 (1999) 813.
- [130] C. Colombo and A. Violante, *Clay Miner.*, 32 (1997) 55.
- [131] T. Bakas, A. Moukarika, V. Papaefthymiou and A.K. Ladavos, *Clays Clay Miner.*, 42 (1994) 634.
- [132] L. Storaro, R. Ganzerla, L. Lenarda, R. Zanoni, A.J. Lopez, P.O. Pastor and R. Castellon, *J. Mol. Catal. A Chem.*, 115 (1997) 329.

- [133] R. Toranzo, M.A. Vicente and M.A. Banares-Munoz, *Chem. Mater.*, 9 (1997) 1829.
- [134] M.A. Vicente, R. Toranzo, M.A. Banares-Munoz and E. Rodriguez, *An. Quim. Int. Ed.*, 94 (1998) 136.
- [135] I. Kirisci, A. Molnar, I. Palinco, A. Fudala, and J.B. Nagy, *Solid State Ionics*, 101 (1997) 793.
- [136] A. Bellaloui, D. Plee and P. Meriaudeau, *Appl. Catal.*, 63 (1990) L 7.
- [137] S.M. Bradley, R.A. Kydd and R. Yamdagni in “*Proc. Symp. Synthesis and Properties of New Catalysts: Utilisation of Novel Materials, Components and Synthetic Techniques*”, Fall Meeting, MRS Boston, U. S. A., Eds. E.W. Corcoran and M.J. Ledoux, 1990, p-69.
- [138] S.M. Bradley, R.A. Kydd and A.K. Brandt, *Progress in Catalysis*, (1992) 287.
- [139] J. Gaaf, R.A. van Santen, A. Knoester and B. van Wingerden, *J. Chem. Soc. Chem. Commun.*, (1983) 655.
- [140] J. Sterte and J. Shabtai, *Clays Clay Miner.*, 35 (1987) 429.
- [141] D. Zhao, Y. Yang and X. Guo, *Inorg. Chem.*, 31 (1992) 4727.
- [142] M. L. Occelli and D. H. Finseth, *J. Catal.*, 99 (1986) 316.
- [143] S.L. Suib, J.F. Tanguay and M.L. Occelli, *J. Amer. Chem. Soc.*, 108 (1986) 6972.
- [144] J. Barrault, C. Bouchoule, K. Echachoui, N. Frini-Srasra, M. Trabelsi and F. Bergaya, *Appl. Catal. B Environ.*, 15 (1998) 269.
- [145] N. Frini, M. Crepsin, M. Trabelsi, D. Messad and H. van Damme and F. Bergaya, *Appl. Clay Sci.*, 12 (1997) 281.
- [146] A. Gil, Ph. D Thesis, Universidad del Pais Vasco, Spain, 1994.
- [147] A. Gil and M. Montes, *Ind. Eng. Chem. Res.*, 36 (1997) 1431.
- [148] I. Heylon, N. Maes, P. Cool, M. de Bock and E.F. Vansant, *J. Porous Mater.*, 3 (1996) 217.
- [149] N. Maes, I. Heylon, P. Cool and E.F. Vansant, *Appl. Clay Sci.*, 12 (1997) 43.
- [150] I. Heylon and E.F. Vansant, *Micropor. Mater.*, 10 (1997) 41.
- [151] A. Molinard and E.F. Vansant, *Adsorption*, 1 (1995) 49.
- [152] J. Jamis, A. Drljaca, L. Spiccia and T.D. Smith, *Chem. Mater.*, 7 (1995) 2078.
- [153] C. Flego, L. Galasso, R. Millini and I. Kiricsi, *Appl. Catal. A Gen.*, 168 (1998) 323.

- [154] L.M. Gandia, M.A. Vicente, P. Oelker, P. Grange and A. Gil, *React. Kinet. Catal. Lett.*, 64 (1998) 145.
- [155] T. Mastuda, H. Nagashima and E. Kikuchi, *Appl. Catal.*, 45 (1988) 171.
- [156] K. Urabe, H. Sakurai and Y. Izumi, in "Proc. 9th Int. Congr. on Catalysis", Eds. M.J. Phillips and M. Ternam, Chem. Inst. of Canada, Ottawa, 1988, p-1858.
- [157] G. Fetter, D. Tichit, L.C. de Menorval and F. Figueras, *Appl. Catal.*, 65 (1990) L 1.
- [158] I. Gameson, W.J. Stead and T. Rayment, *J. Phys. Chem.*, 95 (1991) 1727.
- [159] L.L. Ames and L.B. Sand, *Amer. Mineralogist*, 43 (1958) 641.
- [160] J.J. Fripiat, *Catal. Today*, 2 (1988) 281.
- [161] J.J. Fripiat, in "Handbook of Heterogeneous Catalysis", Eds. G. Ertl, H. Kozinger, and J. Weitkamp, Vol. I, Germany, 1997, p-387.
- [162] M.M. Mortland and K.V. Raman, *Clays Clay Miner.*, 16 (1968) 398.
- [163] He Ming-Yuan, L. Zhonghui and M. Enze, *Catal. Today*, 2 (1998) 321.
- [164] P.L. Hall, *Clay Miner.*, 15 (1985) 321.
- [165] J.C. Davidtz, *J. Catal.*, 43 (1976) 260.
- [166] D. Tichit, F. Fajula, F. Figueras, J. Bousquet and C. Gueguen, in "Catalysis by Acids and Bases", Eds. B. Imelik *et al.*, Elsevier, Amsterdam, 1985, p-351.
- [167] M.L. Occelli, *Ind. Eng. Chem. Prod. Res. Dev.*, 22 (1983) 55.
- [168] D. Plee, A. Schutz, G. Poncelet and J.J. Fripiat, in "Catalysis by Acids and Bases", Eds. B. Imelik *et al.*, Elsevier, Amsterdam, 1985, p-343.
- [169] J.F. Lambert and G. Poncelet, *Topics Catal.*, 4 (1997) 43.
- [170] J. Kijenski and A. Baiker, *Catal. Today*, 5 (1989) 12.
- [171] M.L. Occelli and R.M. Tindwa, *Clays Clay Miner.*, 31 (1983) 22.
- [172] M.L. Occelli and J.E. Lester, *Ind. Eng. Chem. Prod. Res. Dev.*, 24 (1985) 27.
- [173] J. Shabtai, F.E. Massoth, M. Tokarz, G.M. Tsai and J. Mc Cauley, *Proc. 8th Int. Cong. in Catalysis*, Berlin, 1984, Vol. IV, p-735.
- [174] D. Tichit, F. Fajula, F. Figueras, C. Guegue and J. Bousquet, in "Amer. Chem. Soc. Symp. on FCC", New Orleans, 1987, p-647.
- [175] S. Bodoardo, F. Figueras and E. Garrone, *J. Catal.*, 147 (1994) 223.
- [176] F. Arena, R. Dario and A. Parmaliana, *Appl. Catal. A Gen.*, 170 (1998) 127.
- [177] S. Moreno, R.S. Kou, R. Molina and G. Poncelet, *J. Catal.*, 182 (1999) 174.

- [178] S. Narayanan and K. Deshpande, *Appl. Catal., A Gen.*, 193 (2000) 17
- [179] S. Narayanan and K. Deshpande, *Appl. Catal., A Gen.*, 199 (2000) 1.
- [180] P. Canizares, J.L. Valverde, M.R. Sunkou and C.B. Molina, *Micropor. Mesopor. Mater.*, 29 (1999) 267.
- [181] V. R. Choudary, K.R. Srinivasan and A.P. Singh, *Zeolites*, 10 (1990) 16.
- [182] M. Otremba and W. Zajdel, *React. Kinet. Catal. Lett.*, 51 (1993) 473.
- [183] M. Otremba and W. Zajdel, *React. Kinet. Catal. Lett.*, 51 (1993) 481.
- [184] T. Mishra and K. Parida, *Appl. Catal. A. Gen.*, 166 (1998) 123.
- [185] T. Mishra and K. Parida, *Appl. Catal. A. Gen.*, 174 (1998) 91.
- [186] B.D. Flockart, J.A.N. Scott and R.C. Pink, *Trans. Farad. Soc.*, 62 (1966) 730.
- [187] C.H. Liu and C.Y. Hsu, *J. Chem. Soc. Chem. Commun.*, (1992) 1479.
- [188] H. Pines, "The Chemistry of Catalytic Hydrocarbons Conversions", Academic Press, New York, 1981.
- [189] H. Kozinger, *Adv. Catal.*, 25 (1975) 84.
- [190] J.B. Nagy, J.P. Longe, A. Gourgue, P. Bodurt and Z. Gabelica, "Catalysis by Acids and Bases", Eds. B. Imelik *et al.*, Elsevier, Amsterdam, 1987, p-127.
- [191] J.T. Richardson, *J. Catal.*, 9 (1967) 182.
- [192] E.T. Shao and E. Mc Innich, *J. Catal.*, 4 (1965) 586.
- [193] N. Gaordano, L.Pino, I. Cavillaro, P. Vitavelli and B. S. Rao, *Zeolites*, 7 (1987) 131.
- [194] S. J. Kulakarni, R. Ramachandra Rao, M. Subrahmanyam and A.V. Rama Rao, *J. Chem. Soc. Chem. Commun.*, (1994) 273.
- [195] C.P. Bezouhanova, Chr. Dimitrov, V. Nenova, Yu Kulvachev and H. Lechert, *Stud. Surf. Sci. Catal.*, 49 (1989) 1223.
- [196] F. Figueras, L. Mourgues and Y. Trambouze, *J. Catal.*, 14 (1969) 107.
- [197] Y. Matsumura, K. Hashimoto and S. Yoshida, *J. Catal.*, 117 (1989) 135.
- [198] K. Z. Tomke, *Phys. Chem. N.F.*, 106 (1977) 225.
- [199] H. Vinek, H. Noller, M. Ebel and K. Schwarz, *J. Chem. Soc. Farad. Trans. I.*, 73 (1977) 734.
- [200] D.J. Hucknal, "Selective Oxidation of Hydrocarbons", Academic Press, London, 1974.
- [201] J. Villadsen and H. Livberg, *Catal. Rev. Sci. Eng.*, 17 (1978) 203.
- [202] A. Bielanski and J. Haber, *Catal. Rev. Sci. Eng.*, 19 (1979) 1.

- [203] P.L. Villa in "Catalyst Deactivation" Eds. B. Delmon and G. F. Froment, Elsevier, Amsterdam, 1980, p-103.
- [204] T. Blasco, J. Lopez-Nieto, A. Dejoz and M.I. Vasquet, *J. Catal.*, 159 (1995) 271.
- [205] J.R. Shon, S.G. Cho, Y.I. Pae and S. Hayashi, *J. Catal.*, 159 (1996) 170.
- [206] J.M. Lopez-Neito, G. Kremnik and J.L.G. Fiero, *Appl. Catal.*, 61 (1990) 235.
- [207] G.C. Bond and S. F. Tahir, *Appl. Catal.*, 71 (1991) 1.
- [208] S. Narayanan and K. Deshapande, *Micropor. Mater.*, 11 (1997) 77.
- [209] S. Narayanan and K. Deshapande, *Appl. Catal. A Gen.*, 135 (1996) 125.
- [210] K. Urabe, H. Sakurai and Y. Izumi, *J. Chem. Soc. Chem. Commun.*, (1986) 1074.
- [211] E. Kikuchi and T. Mastuda, *Catal. Today*, 2 (1988) 297.
- [212] T. Mastuda, M. Matsukata, E. Kikuchi and Y. Morita, *Appl. Catal.*, 21 (1986) 297.
- [213] E. Kikuchi, T. Mastuda, H. Fujuki and Y. Morita, *Appl. Catal.*, 11 (1984) 331.
- [214] J. Shabtai, N. Frydman and R. Lazar, *Proc. 6th Int. Cong. Tokyo*, (1976) 660.
- [215] J. Shabtai, R. Lazar and A.G. Oblad, *Proc. 7th Int. Cong. Tokyo*, (1980) 828.
- [216] M. L. Occelli, J.T. Hsu and L.G. Galya, *J. Mol. Catal.*, 35 (1986) 277.
- [217] M. L. Occelli, *Proc. 8th Int. Clay Conf.*, Denver, 1985.
- [218] J. Barrault, M. Abdellaoui, C. Bouchoule, A. Majeste, J.M. Tatibouet, A. Laouloudi, and N.H. Ganags, *Appl. Catal. B Environ.*, 27 (2000) L 225.
- [219] H.D. Castillo, A. Gil and P. Grange, *Clays Clay Miner.*, 44 (1996) 706.
- [220] R.Q. Long and R.T. Yang, *J. Catal.*, 190 (200) 22.
- [221] R.T. Yang, N. Tharappiwattananon, and R.Q. Long, *Appl. Catal. B Environ.*, 199 (1998) 289.
- [222] S.M. Bradley and R.A. Kydd, *J. Catal.*, 141 (1993) 239.
- [223] D. Zhao, Y. Yang and X. Guo, *Mater. Res. Bull.*, 28 (1993) 939.
- [224] F. Gonzalez, C. Pesquera, I. Benito, S. Mendioroz and G. Poncelet, *J. Chem. Soc. Chem. Commun.*, (1992) 491.
- [225] I. Benito, A. del Reigo, M. Martinez, C. Blanco, C. Pesquera and F. Gonzalez, *Appl. Catal. A Gen.*, 180 (1999) 175.
- [226] M.J. Fernando, C. Blanco, I. Benito and F. Gonzalez, *Chem. Mater.*, 8 (1996) 76.

- [227] C. Pesquera, F. Gonzalez, M.J. Fernado, C. Blanco and I. Benito, *React. Kinet. Catal. Lett.*, 55 (1995) 267.
- [228] Y. Kiyozumi, K. Suzuki, S. Shin, K. Ovagu, K. Saito and S. Yamanka, *Jpn. Kokai Tokyo Koho*, 59-216631 (1984).
- [229] H.W. Kouwenhova and H. van Bekkum in "Handbook of Heterogeneous Catalysis" Eds. G. Ertl, H. Kozinger and J. Wietkamp, Vol. 5, p-2358. Weinheim, 1997.
- [230] J. March, "Advanced Organic Chemistry", 4th Edn., Wiley, New York, 1992.
- [231] G.A. Olah, "Friedel-Crafts and Related Reactions", Vols.1-4, Wiley Intersciences, New York, London.
- [232] G.A. Olah, "Friedel-Crafts Chemistry", Wiley-Intersciences, New York, Toronto, 1973.
- [233] G.A. Olah, G.K.S. Prakash and J. Sommer, Super acids, Wiley-Intersciences, New York, Toronto, 1985.
- [234] A. Corma, *Chem. Rev.*, 95 (1995) 559.
- [235] P.B.A. Venuto, *Micropor. Mater.*, 2 (1994) 297.
- [236] J.C. Jansen, E.J. Geyghton, S.L. Njo, H. Van Koningsveld and H. Van Bekkum, *Catal. Today*, 38 (1997) 205.
- [237] A.B. Brown and E.E. Reid, *J. Amer. Chem. Soc.*, 46 (1924) 1836.
- [238] C.E. Andrews, *US patent* 2 073 671.
- [239] A.G. Hill, J.H. Shippe and A.J. Hill, *Ind. Eng. Chem.*, 43 (1951) 1579.
- [240] J.C. Earl and N.G. Hill, *J. Chem. Soc.*, 2 (1947) 973.
- [241] A.K. Bhattacharya and D.K. Nandi, *Ind. Eng. Chem. Prod. Res. Dev.*, 14 (1975) 162.
- [242] A.N. Ko, C.L. Yang, W. Zhu, H. Lin, *Appl. Catal.*, 134 (1996) 53.
- [243] S. Narayanan, B.P. Prasad, V. Viswanathan, *React. Kinet. Catal. Lett.*, 48 (1992) 561.
- [244] M. Rusek, *Proc. 9th Int. Conf. Catal.*, Calgary, Vol. 3, Canada, 1988, 1138.
- [245] R.G. Rice and E.J. John, *J. Amer. Chem. Soc.*, 77 (1955) 4052.
- [246] S. Narayanan, Asima Sultana, K. Krishna, P. Meriaudeau and C. Naccache, *Catal. Lett.*, 34 (1995) 129.
- [247] S. Narayanan, Asima Sultana, K. Krishna, P. Meriaudeau, C. Naccache, A. Aurox and C. Viorner, *Appl. Catal.*, 145 (1996) 337.
- [248] P.S. Singh, R. Bandopadhyay and B.S. Rao, *Appl. Catal.*, 136 (1996) 177.

- [249] S. Narayanan, K. Deshpande and B.P. Prasad, *J. Mol. Catal.*, 81 (1994) L 271.
- [250] S. Narayanan and K. Deshpande, *J. Mol. Catal.*, 104 (1995) L 109.
- [251] R.B. Barode, A.J. Chandradhkar, S. B. Kulakrni and P. Ratnasamy, *Ind. J. Technol.*, 21 (1983) 358.
- [252] Z. Fu and Y. Ono, *Catal. Lett.*, 22 (1993) 277.
- [253] P.R.H.P Rao and P. Massiani, *Catal. Lett.*, 31 (1995) 115.
- [254] S. Prasad and B.S. Rao, *J. Mol. Catal.*, 62 (1990) L 17.
- [255] M. Abdellaoui, J. Barrault, C. Bouchoule, N. Frini-Srasra and F. Bergaya, *J. Chim. Phys.*, 96 (1999) 419.
- [256] M. Falcon, K. Fajerweg, J.N. Foussard, E. Purch-Coster, M.T. Maurette and H. Debellefontaine, *Environ. Technol.*, 16 (1995) 501.
- [257] K. Fajerweg and H. Debellefontaine, *Appl. Catal. B Environ.*, 10 (1996) L 229.
- [258] C. Hemmert, M. Renz and B. Meunier, *J. Mol. Catal.*, 137 (1999) 205.
- [259] F. Luck, *Catal. Today*, 27 (1996) 195.

Experimental

2.0 Introduction

The activity of a catalyst is generally influenced by the method of catalyst preparation and the conditions of pre-treatment, apart from the reaction parameters. Variations in the method of preparation affect the physical and chemical properties of a catalyst and this affects the catalysts' activity profoundly [1]. In the case of pillared clays, the physical and chemical properties of the final pillared solid is extremely sensitive to the preparation history of the samples. Hence the preparation procedure is very crucial to get the catalyst with optimum properties.

In this chapter, the preparation procedures of the various catalysts and their characterisation techniques are discussed in detail.

2.1 Preparation of Catalysts

We have synthesised single oxide pillared montmorillonites such as aluminium-pillared, iron-pillared and chromium-pillared montmorillonites. Mixed pillared systems such as iron-aluminium and chromium-aluminium pillared montmorillonites with various Fe (Cr)/Al ratios were also prepared. Finally, we have impregnated iron-pillared montmorillonite with various amounts of vanadia.

Materials:

1. Montmorillonite (KSF) obtained from Fluka.
2. Aluminium nitrate, ferric nitrate and chromium nitrate obtained from Merck
3. Ammonium metavanadate from s.d. fine chem. ltd.,
4. Sodium carbonate from s.d.fine chem. ltd.

2.1.1 Preparation of Single Oxide Pillared Montmorillonites

The initial step of the pillaring process is the preparation of respective pillaring agents. Pillaring agent for aluminium-pillared montmorillonite was prepared as follows. 0.2 M aluminium nitrate solution was partially hydrolysed using 0.3 M sodium carbonate as the base at a base/metal ratio of 2.0 under vigorous stirring at 70°C for two hours and the stirring was continued for six hours at room

temperature. Then the pillaring agent was flushed with nitrogen to free from carbon dioxide and it was then aged for 24 hours at room temperature. Meanwhile, a 1% suspension of the parent montmorillonite in distilled water was also prepared and kept overnight. The pillaring solution, after ageing was then treated with the clay suspension for six hours at 70°C. Al³⁺ to clay ratio was maintained as 20 mmol g⁻¹ of clay in the final reaction mixture. After reaction, the material was washed until flocculation appeared and it became nitrate free. It was then dried at 110°C, followed by controlled calcination in dry air at 400°C for five hours to get aluminium pillared montmorillonite catalyst.

A similar method was adopted for the synthesis of iron-pillared and chromium- pillared montmorillonites. Ferric nitrate and chromium nitrate were used respectively. All the preparation steps were same, except that chromium pillaring agent was prepared at 95°C and this warm solution was used for pillaring the clay, without ageing.

2.1.2 Preparation of Mixed Oxide Pillared Montmorillonites

Mixed iron-aluminium and chromium-aluminium pillared montmorillonites were prepared by the co-hydrolysis of ferric nitrate or chromium nitrate and aluminium nitrate.

Requisite volumes of 0.2 M Fe(NO₃)₃.9H₂O or Cr(NO₃)₃.9H₂O were added to 0.2 M Al(NO₃)₃ solution to get various solutions with an Fe(Cr)/Al ratio of 0.1, 0.2, 0.3, 0.4, 0.5 and 1.0. Each of these solutions was then partially hydrolysed with sodium carbonate solution so as to acquire a base/metal ratio of 2.0. Further procedures for mixed iron-aluminium pillared montmorillonites were the same as that of iron-pillared montmorillonite. Those for chromium-aluminium pillared montmorillonites were the same as that of chromium-pillared montmorillonite.

2.1.3 Preparation of Vanadia Impregnated Iron-Pillared Montmorillonites

Impregnation of vanadia over iron-pillared montmorillonite was done by the conventional wet impregnation method [2]. 2, 5, 7, 10, 15 and 20 weight percentages of vanadia were added on iron-pillared montmorillonite. Calculated amounts of ammonium metavanadate was dissolved in aqueous oxalic acid solution and stirred with iron-pillared montmorillonite for 3 hours using a magnetic stirrer. Excess

solvent was then evaporated to dryness on a water bath. The material was then dried in an air-oven overnight and calcined at 400°C for five hours.

2.2 Notations of Catalysts

- M - Parent montmorillonite
- AlPM - Aluminium-pillared montmorillonite
- FePM - Iron-pillared montmorillonite
- CrPM - Chromium-pillared montmorillonite
- FeAl_xPM - Mixed iron-aluminium pillared montmorillonite
with Fe/Al ratio = x; (x = 0.1, 0.2, 0.3, 0.4, 0.5 & 1.0)
- CrAl_xPM - Mixed chromium-aluminium pillared montmorillonite
with Cr/Al ratio = x; (x = 0.1, 0.2, 0.3, 0.4, 0.5 & 1.0)
- XVFe - Vanadia impregnated iron-pillared montmorillonite with
X weight % of vanadia loading (X = 2, 5, 7, 10, 15 & 20)

2.3 Characterisation Techniques

2.3.1 Energy Dispersive X-ray Fluorescence Analysis (EDX)

Energy Dispersive X-ray (EDX) fluorescence analysis is one of the most successful method for the qualitative and quantitative elemental analysis of solid samples. The requirements for EDX instrumentation are

- a) Si (Li) detector for receiving undispersed characteristic X-rays from a fluorescing specimen.
- b) multi-channel pulse height analyser for digesting and accumulating the pulses in channels, each channel representing a small range of energy and
- c) powerful microcomputers for the calculation of elemental concentrations.

Principle:

The principle is based on the strong interaction of electrons with matter and their appreciable scattering by quite small clusters. When electrons of appropriate energy impinge on a sample they cause emission of X-rays, whose energies and relative abundance depend upon the composition of the sample. This can be explained as follows. An electron beam from a scanning electron micrograph ejects an electron from an inner shell of the sample atom. The vacancy caused by this removal of the electron is filled by another electron from a higher energy shell.

While falling to the lower energy state, this vacancy-filling electron will emit the difference in energy between the two shells as electromagnetic radiation. Since this energy difference is fairly large for inner shells, the radiation appears as X-rays. As every element has a unique configuration of electron energy levels, the X-ray pattern spectrum will be a unique characteristic of a particular element. Thus from the X-ray pattern obtained, the element can be identified. Additionally, the number of X-rays emitted by an element will be directly proportional to the concentration of that element in the sample. Thus the elemental composition can be determined as well, from the integrated peak areas.

However, the method has some limitations namely, 1) the Si (Li) detector cannot detect elements lighter than sodium and the resolution of low energy radiation is poor and 2) it is not possible to achieve high sensitivities of weak peaks when strong ones are also present.

The attractive feature of this analysis is that the technique is practically non-destructive in most cases and the requirements for sample preparation are minimal.

2.3.2 X-Ray Diffraction Analysis (XRD)

X-ray diffraction is one of the most widely used techniques in the field of heterogeneous catalysis. It is used to study the three dimensional structure of the solid substances, their composition and crystallinity. Transition to different phases, allotropic transformation and purity of the substance can also be identified by this technique. The mean crystallite size of the substance can also be determined from the broadening of an X-ray diffraction peak. The instrumental aspects of the X-ray diffractometer are (i) X-ray generating equipment with Cu or Mo as target (commonly called X-ray tube) associated with high voltage generators and stabilisers, (ii) collimator for limiting the divergence of the rays that reach the crystal and (iii) a filter to reduce the intensity of the line of shorter wavelength. A common target of X-ray tube is Cu and the filter used is Ni.

Principle:

X-ray diffraction method depends upon the wave character of X-rays and the regular spacing of the planes in a crystal. Virtually monochromatic radiation is

obtained by reflecting X-rays from crystal planes. The relationship among the wavelength of the X-ray beam, the angle of diffraction θ , and the distance between each set of atomic planes of the crystal lattice d , is given by Bragg's equation.

The Bragg's equation can be represented as

$$n\lambda = 2d \sin\theta$$

where n is the order of diffraction. Since λ is a constant for a particular source, for a given order of diffraction, d spacing will be inversely proportional to $\sin\theta$.

Montmorillonite, a natural clay is characterised by large platelets with face to face stacking. The distance between two layers of the clay is called the interlayer distance, denoted as d_{001} spacing. The major application of XRD in the field of pillared clays is to determine this d_{001} spacing. During the pillaring process, a lattice expansion is noticed in the 001 direction. This leads to larger d_{001} spacing. Consequently, the 2θ value corresponding to 001 reflection shifts to lower region. Thus from the XRD data, we can see whether expansion and hence pillaring has taken place. From the relative intensities, the extent of pillaring can also be found out.

However, one major disadvantage regarding the application of XRD in the field of smectite clays is that these are poorly crystallised systems and hence usually show only broad XRD patterns, instead of very sharp peaks. Smectite clays exhibit turbostratic stacking, which means that the layers stack flat (face to face) upon one another, but without alignment of the 'ab' planes. This defect contributes to the line broadening of the 001 reflection. While considering pillared clays, differences in pillar density can lead to a distribution of basal spacings. This also will lead to broadened XRD peaks.

The XRD patterns of all the prepared samples were obtained using RIGAKU D/MAX-C instrument with λ equal to 1.5418 Å.

2.3.3 BET Surface Area and Pore Volume Measurements

Determination of surface area is considered to be an important requirement in catalyst characterisation. In spite of various theoretical limitations, the Brunauer-Emmett-Teller (BET) method continues to be widely used for the evaluation of the surface area from adsorption isotherm data. It is now generally agreed that the BET

method is based on an oversimplified model of physisorption and that it is necessary to ensure that certain conditions are fulfilled before any BET area accepted as the true value.

The adsorption of molecules in the first layer is assumed to take place in an array of surface sites of uniform energy. These molecules act as sites for the second layer. This arrangement is extended to multilayer. A Simple isothermal equation is obtained after making the following assumptions.

- a) In all layers after the first, the adsorption-desorption conditions are identical.
- b) In all layers except the first, the energy of adsorption is equal to the condensation energy.
- c) When $P=P_0$, the saturated vapour pressure of the adsorbate, the multilayer has infinite thickness.

The BET equation is conveniently expressed in the form,

$$P / [(P_0 - P) V] = 1 / [V_m C] + [(C - 1) / V_m C] X [P / P_0] \quad \text{where}$$

V_m = volume of the adsorbate required to form a complete monolayer on the surface of unit mass of the adsorbant, defined as monolayer capacity.

V = volume adsorbed at equilibrium pressure, P .

P_0 = saturated vapour pressure of the adsorbate and

C = a constant for a given system at a given temperature and related to the heat of adsorption.

A linear plot of $P / [(P_0 - P) V]$ against P / P_0 values gives slope equal to $(C - 1) / V_m C$ and y-intercept equal to $1 / V_m C$. From the slope and intercept, V_m is calculated.

The specific surface area is obtained after deriving the monolayer capacity (V_m). Multiplying V_m with the average area occupied by the adsorbate molecule (ie., the molecular cross-sectional area - a_m) in the filled monolayer and Avagadro number (N_0) will give the surface area.

$$\text{Surface area (m}^2\text{g}^{-1}\text{)} = (V_m) (a_m) (N_0)$$

Nitrogen gas at 77 K is generally considered to be the most suitable adsorbate for the determination of the surface area of non-porous and porous solids.

The surface areas of all the catalysts were determined by BET nitrogen adsorption at liquid nitrogen temperature using a Micromeritics Flow Prep 060 instrument. Previously activated samples were preheated and degassed at 200°C for two hours under nitrogen flow. The catalyst is then brought to 77 K using liquid nitrogen for adsorbing nitrogen gas at various pressures.

The total pore volumes of the samples were also measured using the same instrument. The pore volume is measured by the uptake of nitrogen at a relative pressure of 0.9.

2.3.4 Infrared Spectroscopy

Vibrational spectroscopies are among the most promising and most widely used methods for catalyst characterisation. This is because very detailed structural information can be obtained from vibrational spectra. In situations where X-ray diffraction techniques are not applicable, vibrational spectroscopy can often provide information on phase transitions, changes in compositions of bulk catalyst materials, their crystallinity and on the nature of functional groups.

Conventional dispersive infrared spectroscopy is gradually being replaced by Fourier Transform Infrared Instrument (FTIR) due to many advantages such as improved spectral quality, higher sensitivity and suitability for use in the low frequency region. The KBr technique is routine for IR transmission-absorption spectroscopy of powdered samples.

Infrared spectroscopy is concerned with the study of molecular vibrations. Upon interaction with infrared radiation, portions of the incident radiation are absorbed at particular wavelengths. The instrumentation part includes radiation sources, optical system and detectors. For the region 200-4000 cm^{-1} the source is usually Nernst glower or Globar or coil of nichrome wire. The optical system consists of two or four plane diffraction gratings with either a fore prism monochromator or infrared filters. Detector can be thermopile, thermistor or pyroelectric materials.

FTIR spectra of the powdered samples were measured by the KBr disk method over the range 4000-400 cm^{-1} . Shimadzu DR 8001 instrument was used for the purpose. The entire frequency range of electromagnetic waves transmitted

through the sample was recorded simultaneously and the output of the detector was fed to a computer, which reinforces the spectrum using Fourier transformation.

For pillared clays, IR is of no special use other than detecting the vibrational bands of different bonds and checking the intensities of OH bands. But for vanadia impregnated pillared samples, this characterisation technique has a prominent role in identifying the dispersed species of vanadium.

2.3.5 Thermogravimetric Analysis

Thermogravimetry (TG) provides the analyst with a quantitative measurement of any weight change associated with a transition. TG directly records the loss in weight of a sample with time while its temperature is raised through a temperature programme. Changes in weight are as a result of the rupture and/or formation of various physical and chemical bonds at elevated temperatures that lead to the evolution of volatile product or the formation of heavier reaction products. The usual temperature range is from ambient to 1200°C with inert atmosphere.

To get the thermogram, the weight is plotted against temperature. From the thermogram we can ascertain dehydration and decomposition and also the thermal stability of the samples.

The method needs a crucible in which the sample is placed and it is attached to an automatic recording balance. The accessories associated with the balance enable to detect the mass change as a result of thermal treatment.

Shimadzu TGA-50 instrument was used for carrying out thermogravimetric studies. About 20 mg of the sample was used and the heating rate was maintained as 10°C / minute in the nitrogen atmosphere. The TG data were computer processed to get the thermograms. The horizontal portion of the thermogram indicates regions where there is no weight loss and that the sample is thermally stable. Curved portions of the graph indicate weight loss.

2.3.6 Acidity Determination Studies

The acid-base character of a catalyst plays the most important role in its catalytic activity towards an organic reaction. Hence, a through understanding of these properties is very essential. It is well documented that smectite clays and their

modified forms are rich in acidic sites and the presence of basic sites are almost nil. The acidity of the solids used as catalysts or catalyst carriers has been the subject of numerous investigations and reviews for nearly four decades [3]. It is well established that the acidity plays a very important role in virtually all organic reactions occurring over solid catalysts. Determination of the strength of the acidic sites on the catalyst as well as their distribution is a necessary requirement to understand the catalytic properties of acidic solids.

It is very well established that clays possess both Brønsted and Lewis acid sites [4, 5]. Infrared spectra of the catalysts after chemisorbing with a basic molecule such as NH_3 or pyridine can clearly distinguish between Lewis and Brønsted acid sites. Also various methods are reported for obtaining the numbers and the strength of Lewis and Brønsted sites independently.

Brønsted and Lewis acid sites play different roles in various types of catalytic reactions and the strength of respective acid sites strongly affects the catalytic performance [6]. Therefore there is a significant motivation to develop easy and reproducible methods for the measurement of Lewis and Brønsted acid sites separately.

We have employed the gravimetric adsorption of 2,6-dimethylpyridine (DMPY) for determination of Brønsted sites. 2,6-Dimethyl pyridine preferentially adsorbs on Brønsted acid sites [7-9]. Electron accepting properties can be correlated with Lewis acidity of the samples and this is determined by perylene adsorption method. Useful information regarding Lewis acidity in presence of Brønsted acidity can be obtained using this procedure [8].

However, the most promising methods of determining acidity are temperature programmed desorption (TPD) and calorimetric measurements [10]. We have employed temperature programmed desorption of ammonia as a single technique to find the total acidity of the systems including both Brønsted and Lewis acidity, but discrimination between the two was not possible here.

Thus a thorough study of the acidity of the prepared systems was done using three independent techniques viz.,

- 1) Adsorption of 2,6-dimethylpyridine followed by its thermodesorption for evaluating Brönsted acidity.
- 2) Perylene adsorption study for evaluating Lewis acidity and
- 3) Temperature programmed desorption of ammonia for investigating total acidity.

a) Adsorption of 2,6-Dimethylpyridine- Evaluation of Brönsted Acidity

Previously activated catalysts were kept in a desiccator saturated with vapours of 2,6 Dimethylpyridine at room temperature for 48 hours. Then the catalysts were subjected to thermogravimetric analysis when the weight loss of the adsorbed sample was monitored for the range 40-500°C at a rate of 20°C/min. The fraction of weight loss in the range 250-500°C was found out and taken as a measure of the Brönsted acidity of the samples.

b) Surface Electron Accepting Properties - Lewis Acidity by Perylene Adsorption

Electron accepting studies were carried out using perylene as the electron donor. The principle is based on the ability of the catalyst surface site to accept electrons from an electron donor, like perylene to form charge transfer complexes and the amount of adsorbed species is measured quantitatively by spectroscopic studies [11,12].

Perylene was obtained from Merck and benzene used as the solvent was obtained from Qualigens. Benzene was purified according to the method reported earlier [13]. The catalysts were activated at 500°C for two hours before each experiment. Different concentrations of perylene in benzene were prepared and stirred with about 0.5 g of the activated catalyst at room temperature for four hours.

Due to adsorption of perylene on the catalyst surface from the solution, its concentration in the solution will be less after adsorption. The difference in concentration before and after adsorption was determined by means of a Shimadzu UV-VIS spectrophotometer. The absorbance were measured at a λ_{max} of 439 nm.

c) Temperature Programmed Desorption of ammonia

The ammonia TPD method is widely employed to characterise the acidity of solid catalysts. However, this method lacks in selectivity because ammonia can titrate acid sites of any strength and type.

The method is based on adsorbing ammonia on solid which is then heated at a programmed rate and the amount of desorbed ammonia is estimated volumetrically. About 0.75 g of the previously activated catalyst was degassed by heating in a stream of nitrogen at 300°C. It was then cooled to room temperature. The ammonia was allowed to be adsorbed on the catalyst by injecting 15 mL of ammonia gas at 27°C and at 1 atmospheric pressure into a stainless steel reactor of 30 cm length and 1 cm diameter in which the catalyst was kept. The catalyst was then heated through a temperature programme in nitrogen flow. At each interval of 100°C, the ammonia desorbed was trapped using nitrogen as the carrier in a stoppered conical flask containing a known excess of 0.025 N sulphuric acid for the temperature range 100 – 600°C. It estimated by the back titration of the excess sulphuric acid using standard NaOH. The amount of ammonia desorbed was distributed in the weak (100-200°C), medium (200-400°C) and strong regions (400-600°C).

2.4 Catalytic Activity Measurements

2.4.1 Liquid Phase Reactions

The liquid phase catalytic reactions performed were benzoylation of toluene, benzylation of toluene and catalytic wet peroxide oxidation of phenol.

All the liquid phase reactions were carried out in a 100 mL/50 mL round bottomed flask equipped with an oil bath, a magnetic stirrer and an air condenser/ water condenser. The oil bath was attached to a dimmerstat so that the temperature of the oil in the oil bath can be adjusted between the room temperature and its boiling point and the temperature required for the reaction can be attained.

a) Benzylation of Toluene

For the benzylation of toluene, both benzyl chloride and benzyl alcohol from s.d fine-chem. ltd were used without further purification. 0.1 g of the activated catalyst was kept in the round-bottomed flask after mixing the alkylating agent and substrate in the desired molar ratio. The temperature of the oil bath was kept at the desired value by means of the dimmer stat. After the reaction time, the catalyst was separated from the reaction medium and the products were analysed using a gas chromatograph fitted with a flame ionisation detector. The analysis conditions are described in Table 2.1.

b) Benzoylation of Toluene

Benzoylation of toluene was carried out in the liquid phase using benzoyl chloride as the acylating agent. Benzoyl chloride was obtained from Merck and was used without further purification. Benzoyl chloride and toluene were mixed in the desired ratio in the round-bottomed flask. 0.1 g of the catalyst was activated at 500°C and put into the flask and the mixture was kept for one hour at the refluxing temperature. The R.B. was fitted with a water condenser. Reaction mixture, freed from the catalyst was analysed for the products. Analysis details are given in Table 2.1.

d) Catalytic Wet Peroxide Oxidation of Phenol (CWPO)

Ecologically friendly technology is one of the most important subject in chemistry, in particular for the partial oxidation of organic compounds. Catalytic wet peroxide oxidation (CWPO) of phenol is a typical example for ecologically friendly technologies by using catalysts, which is widely applied in industrial chemistry for the preparation of catechol and hydroquinone. Moreover, one of the major organic pollutants in waste-water is phenol. We have thus focused to check the efficiency of pillared clays for the room temperature wet oxidation of phenol using H_2O_2 as the oxidising agent.

Phenol and hydrogen peroxide (30%) were obtained from Merck. The catalytic peroxide oxidation was carried out at room temperature in a 50 mL round flask equipped with an air condenser and a magnetic stirrer. 1.097 g of phenol was mixed with 5 mL of water, which was used as the solvent in almost all cases. 5 mL (or the required amounts as the case may be) of 30% H_2O_2 was introduced into the glass reactor in one lot. 0.1 g catalyst, which was previously activated, was added into the reaction mixture and the mixture is magnetically stirred for one hour. The catalyst was then freed from the reaction mixture and the reaction mixture was analysed by GC, the details of which is discussed in Table 2.1.

2.4.2 Vapour Phase Reactions

The applicability of liquid phase reactions is limited due to the impossibility of carrying out the reaction above the boiling point of the least boiling component in the reaction mixture. Reaction at much higher temperatures can be performed using

vapour phase set up where the reactants will be in the vapour state and undergoes reaction over the catalyst surface.

We have performed the cumene conversion reaction, decomposition of cyclohexanol and methylation of aniline over the pillared clay samples in the vapour phase. The reactions were carried out at atmospheric pressure in the fixed-bed, vertical, down-flow quartz reactor placed inside a double-zone furnace. Powdered catalysts were placed at the centre of the reactor in such a way that the catalyst was sandwiched between the layers of inert porcelain beads. The upper part of the reactor serves as a pre-heater. All heating and temperature measurements were performed using a temperature controller and indicator instruments. A thermocouple was positioned at the centre of the catalyst bed to monitor the exact temperature of the catalyst. Before each run, the catalysts were activated at the required temperature in a flow of dry air for two hours. The reactant (single reactant/ mixture of reactants) was fed into the reactor by means of a syringe pump at required feed rate. The products and the unreacted reactant were condensed by means of a cold water circulating condenser and collected from the bottom of the set up at required time intervals. A schematic representation of the whole set up is shown in Figure 2.1.

a) Conversion of Cumene

Exactly 0.5 g of the activated catalyst was placed at the centre of the reactor. cumene obtained from Merck is fed as such into the quartz reactor. The temperatures in the range 350-500°C were selected for the reaction. For comparing the catalytic activities of all the systems, a common temperature of 400°C was selected. Table 2.1 reveals the analysis conditions of the reaction mixture.

b) Decomposition of Cyclohexanol

The amount of catalyst used was exactly 0.5 g, after activation at the required temperature. LR grade cyclohexanol from s.d.fine chem. ltd., was used as such without further purification. The cyclohexanol was fed into the reactor, which is set at the required temperatures before every start of the reaction, with the help of the feed pump. Analysis of the collected sample was done gas chromatographically. Details are shown in Table 2.1.

c) Methylation of Aniline

Exactly 0.4 g of the catalyst was used for performing the reaction. Aniline from Merck was purified according to the reported procedure [13]. Methanol

(Merck) was used as such. Aniline and methanol were mixed in the required molar ratio and the mixture was fed into the reactor. The various aniline to methanol molar ratios studied were in the range 1:1 - 1:9. The temperatures selected were in the range 300-450°C. The products were analysed using Chemito-8610 Gas Chromatograph and the details of the analysis conditions are given in Table 2.1.

Table 2.1 Analysis conditions for the various catalytic reactions.

Catalytic Reaction	Analysis Conditions				
	Column	GC	Temperature programme for column	Injector Temperature	Detector Temperature
Benzylation & Benzoylation of Toluene	SE-30	ChemitoGC-8610	100- 3 – 5-210*	250°C	250°C
Oxidation of phenol	SE-30	ChemitoGC-8510	170-Isothermal	270°C	270°C
Cumene Conversion	SE-30	ChemitoGC-8610	120-Isothermal	250°C	250°C
Cyclohexanol Decomposition	Carbo-wax	ChemitoGC-8510	70- 5-3-170	200°C	200°C
Methylation of Aniline	SE-30	ChemitoGC-8610	140-Isothermal	275°C	275°C

* Initial temperature-duration-rate of increase-final temperature

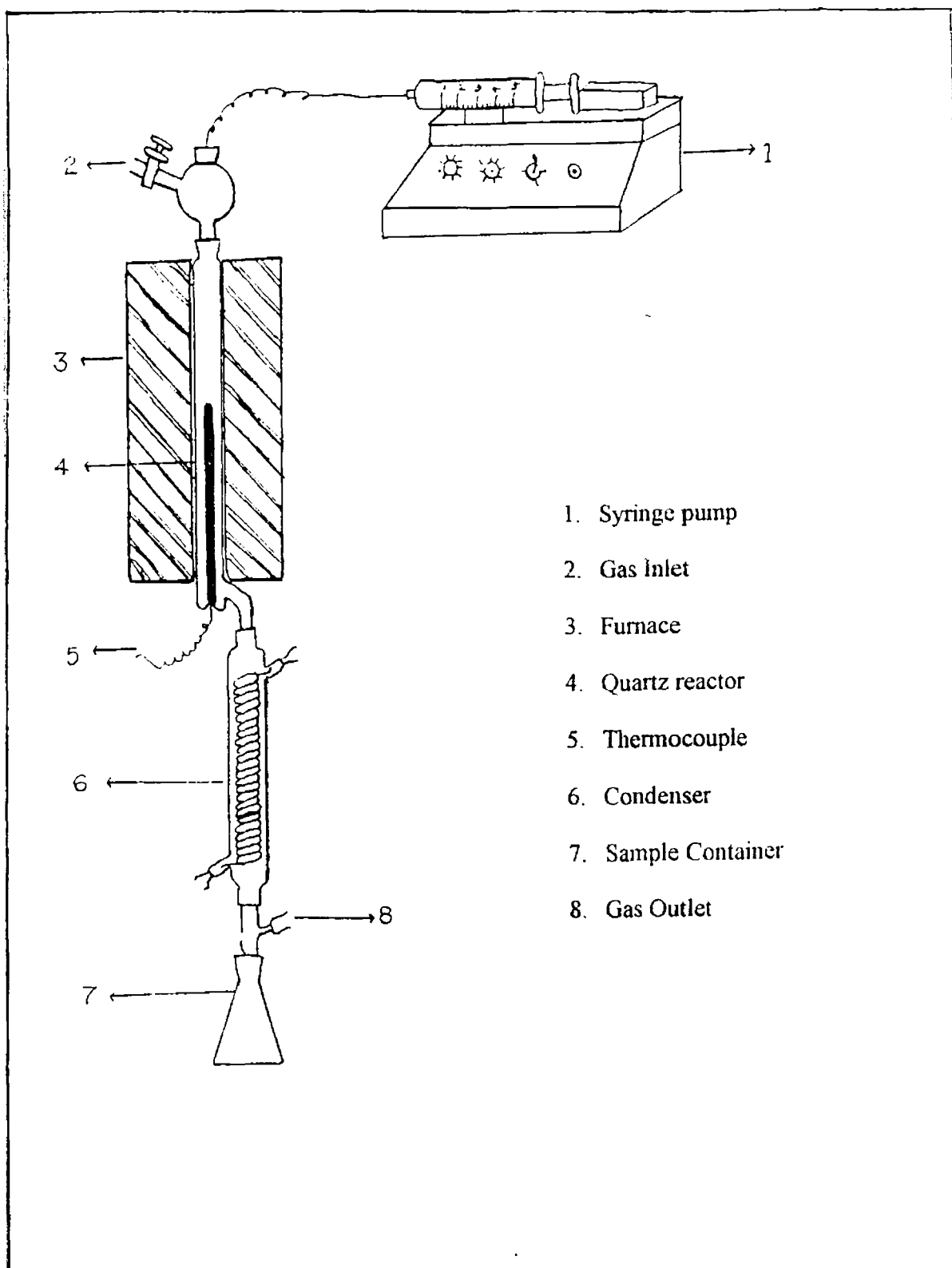


Figure 2.1 Experimental set up for conducting vapour phase reactions at atmospheric pressure.

References

- [1] K. Morikawa, T. Shirasaki and M. Okada, *Adv. Catal.*, 20 (1969) 97.
- [2] K.V. Narayana, A. Venugopal, K.S. RamaRao, V. Venkat Rao, S. Khajamasthan and P. Kanta Rao, *Appl. Catal. A Gen.*, 150 (1997) 269.
- [3] J.P. Bohm and Knozinger, "Catalysis, Science and Technology", (J.R. Anderson, M. Boudart, (Eds.)), Vol.4, Springer Verlag, 1983, p- 39.
- [4] T. J. Pinnavaia, *Science*, 220 (1983) 365.
- [5] F. Figueras, *Catal. Rev. Sci. Eng.*, 30 (1988) 457.
- [6] A. Corma, *Chem. Rev.*, 95 (1995) 559.
- [7] H.A. Bensi, *J. Catal.*, 28 (1973) 176.
- [8] P.A. Jacobs and C.F. Heylen, *J. Catal.*, 34 (1974) 267.
- [9] A. Satsuma, Y. Kamiay, Y. Westi and T. Hattori, *Appl. Catal. A Gen.*, 253 (2000) 194.
- [10] J. Kijenski and A. Baiker, *Catal. Today*, 15 (1989) 1.
- [11] J.J. Rooney and R.C. Pink, *Proc. Chem. Soc.*, (1961) 70.
- [12] B.D. Flockart, J.A.N. Scott and R.C. Pink, *Trans. Farad. Soc.*, 62 (1966) 730.
- [13] L.F. Fiesser and M. Fiesser, "Reagents for organic synthesis", John Wiley, New York, p-125, 1967.

Textural And Acidic Properties

3.0 Introduction

The catalyst systems synthesised were characterised by adopting techniques such as EDX analysis, XRD analysis, surface area and pore volume measurements, infrared spectra, thermogravimetric analysis and acidity determination studies. The results are discussed in the present chapter.

3.1 Energy Dispersive X-ray Fluorescence Analysis (EDX)

The compositions of all the pillared samples and vanadia impregnated samples were determined using EDX analysis, performed over an EDX-JEM-35 instrument (JEOL Co. link system AN-1000 Si-Li detector, sensitivity > 0.1 wt%). The chemical compositions of mixed Fe-Al pillared montmorillonites are shown in Table 3.1. Those of mixed Cr-Al systems are shown in Table 3.2 and the chemical compositions of vanadia impregnated iron-pillared montmorillonite catalysts are shown in Table 3.3.

The silicon and aluminium weight percentages of the parent montmorillonite were 59.57 and 21.05 respectively. The iron weight percentage was 10.73. Pillaring of montmorillonite with Al polyoxocations increased the weight percentage of Al from 21.05 to 29.51% (Table 3.1). Thus an excess of 8.46% Al was fixed by the pillared solid. The drastic decrease of Ca from 3.48 to 0.04% during this pillaring process indicated that the cation exchanged to a great extent was Ca^{2+} . Almost one third of Na^+ was retained after the pillaring process.

Pillaring the montmorillonite with Fe polycations increased its iron content from 10.73 to 29.01%. Here also, the calcium content is reduced remarkably (Table 3.1).

Various pillaring agents were prepared by the co-hydrolysis of aluminium nitrate and ferric nitrate in the Fe/Al ratios 0.1 to 0.5 and 1.0 with sodium carbonate as base. Thus the pillaring agent containing both aluminium and iron polyoxocations were used for pillaring montmorillonite. Pillaring of montmorillonite with a mixture

of Fe and Al polycations increased both Al content and iron content. As the Fe/Al ratio increased from 0.1 to 0.5, there was a clear increase of Fe content, and decrease of Al content was also observed. However, at equimolar concentration of iron and aluminium in the pillaring agent, the amount of iron incorporated was less. Thus maximum uptake of iron was for FeAl_{0.5}PM. The pillaring agent with lower Fe/Al ratios such as 0.1 or 0.2 resembled more to aluminium pillaring agent and the amount of iron incorporated into the solid was less. At a higher Fe/Al ratio of 0.5, more iron was incorporated into the clay sheets than aluminium. However, at a much higher Fe/Al ratio of 1.0, the amount of iron introduced into the clay structure was less than that for the ratio 0.5.

Table 3.1 Chemical composition of the various elements in mixed Fe-Al pillared systems

Catalyst	Weight percentages						
	Si	Al	Fe	Ca	K	Mg	Na
M	59.57	21.05	10.73	3.48	1.86	2.32	0.97
AlPM	56.43	29.51	10.20	0.04	1.59	1.86	0.35
FeAl _{0.1} PM	57.09	27.02	12.81	0.02	1.10	1.39	0.57
FeAl _{0.2} PM	55.58	26.92	14.60	0.10	1.50	1.39	0.37
FeAl _{0.3} PM	54.63	24.01	17.41	0.08	1.57	1.39	0.90
FeAl _{0.4} PM	55.01	22.10	20.08	0.02	1.10	1.07	0.62
FeAl _{0.5} PM	50.97	21.63	24.44	0.04	0.79	1.58	0.52
FeAl _{1.0} PM	53.68	22.42	19.61	0.08	1.47	1.93	0.79
FePM	47.49	20.37	29.01	0.09	1.10	1.57	0.36

Table 3.2 shows the chemical composition of Cr-pillared and mixed Cr-Al pillared montmorillonites. When the parent montmorillonite was pillared with chromium polycations, 19.20% of chromium was fixed into the solid. For aluminium-pillared montmorillonite, the excess aluminium introduced into the solid as a result of pillaring process was 8.46%. For the mixed Cr-Al pillared montmorillonite, chromium was introduced along with aluminium. The chromium weight percentage reached a maximum of 11.73 for CrAl_{0.5}PM. However, further increase of Cr/Al ratio from 0.5 to 1.0, only reduced the chromium content.

An interesting observation while comparing the pillaring process involving iron and chromium pillaring agents was the enhanced replacement of sodium ions, along with calcium ions, during the pillaring process involving chromium. Almost in all cases of mixed Cr-Al systems, there is a considerable reduction in the weight percentage of Na.

Table 3.3 shows the chemical composition of vanadia impregnated iron-pillared montmorillonites. While preparing, adequate amounts of ammonium

Table 3.2 Chemical composition of the various elements in mixed Cr-Al pillared systems

Catalyst	Weight percentages							
	Si	Al	Fe	Cr	Ca	K	Mg	Na
AlPM	56.43	29.51	10.20	0.00	0.04	1.59	1.86	0.35
CrAl _{0.1} PM	56.78	27.09	10.73	2.08	0.10	1.38	1.79	0.05
CrAl _{0.2} PM	56.50	24.95	10.85	4.35	0.23	1.43	1.67	0.00
CrAl _{0.3} PM	57.89	23.82	9.83	5.21	0.21	1.19	1.83	0.01
CrAl _{0.4} PM	57.32	22.26	9.11	6.54	0.10	1.51	1.92	0.24
CrAl _{0.5} PM	57.94	22.88	9.68	11.73	0.00	1.34	1.82	0.01
CrAl _{1.0} PM	55.31	23.98	10.21	7.10	0.24	1.21	1.75	0.20
CrPM	50.80	17.71	9.15	19.20	0.25	1.19	1.73	0.05

Table 3.3 Chemical compositions of vanadia loaded iron-pillared systems

Catalyst	Weight percentages							
	Si	Al	Fe	Ca	K	Mg	Na	V
FePM	47.49	20.37	29.01	0.09	1.10	1.57	0.36	0.00
2VFe	48.23	20.65	25.66	0.10	1.12	1.83	0.43	2.01
5VFe	48.00	19.64	24.02	0.24	1.15	1.53	0.36	4.98
7VFe	46.06	18.92	24.79	0.09	0.84	1.52	0.36	7.40
10VFe	45.10	17.67	23.84	0.12	0.91	1.39	0.41	10.55
15VFe	43.81	16.01	21.84	0.09	1.37	1.51	0.35	15.02
20VFe	41.05	15.31	20.74	0.24	1.07	1.31	0.24	20.04

metavanadate in oxalic acid corresponding to 2, 5, 7, 10, 15 and 20 weight percentages of V were used for impregnation. The EDX data showed that satisfactory impregnation of vanadia took place on the pillared clay.

3.2 X-Ray Diffraction Analysis (XRD)

The XRD patterns of the prepared samples were recorded using Rigaku Model D/Max C instrument. The most important property of a smectite clay (montmorillonite) from the standpoint of catalyst design, is its ability to expand beyond a single molecular layer of intercalant. This swelling capacity along with cation exchange capacity enables the propping up of the layers of the clay with stable metal oxides, which act as pillars. Obviously, this pillar intercalation process increases the interlayer distance and it can be determined from the XRD pattern.

3.2.1 XRD of Single Metal Oxide Pillared Systems

Figure 3.1 shows the XRD patterns of parent montmorillonite (M), aluminium-pillared montmorillonite (AlPM), iron-pillared montmorillonite (FePM) and chromium-pillared montmorillonite (CrPM). Pillared clays are poorly crystallised materials. The broad band obtained in the XRD pattern, instead of sharp peaks, can be attributed to the predominant amorphous nature of the clay. The characteristic d_{001} spacing of the parent montmorillonite (M) is obtained at a 2θ value of 9.00 corresponding to 9.82 Å. For AlPM, this d_{001} value increased to 16.74 Å corresponding to 2θ value of 5.26. For FePM, the interlayer distance was 15.48 Å ($2\theta = 5.72$) and for CrPM, d_{001} was 18.10 Å ($2\theta = 4.87$). Shifting of 2θ values from 9.00 to lower region clearly suggests the expansion of the clay layer, during the pillaring process.

The major aluminium species in the pillaring solution prepared by the partial hydrolysis of Al^{3+} at a base/metal ratio of 2.0 was presumed to be the Al_{13} polymer, $[\text{Al}_{13}\text{O}_4(\text{OH})_{24}(\text{H}_2\text{O})_{12}]^{7+}$ [1]. The interlayer cations are exchanged by this polyoxocation during the pillaring process. Dehydration and dehydroxylation lead to discrete aluminium oxide clusters, which act as pillars, tightly held into the interlayer region. This accompanied the layer expansion and was identified from the XRD pattern.

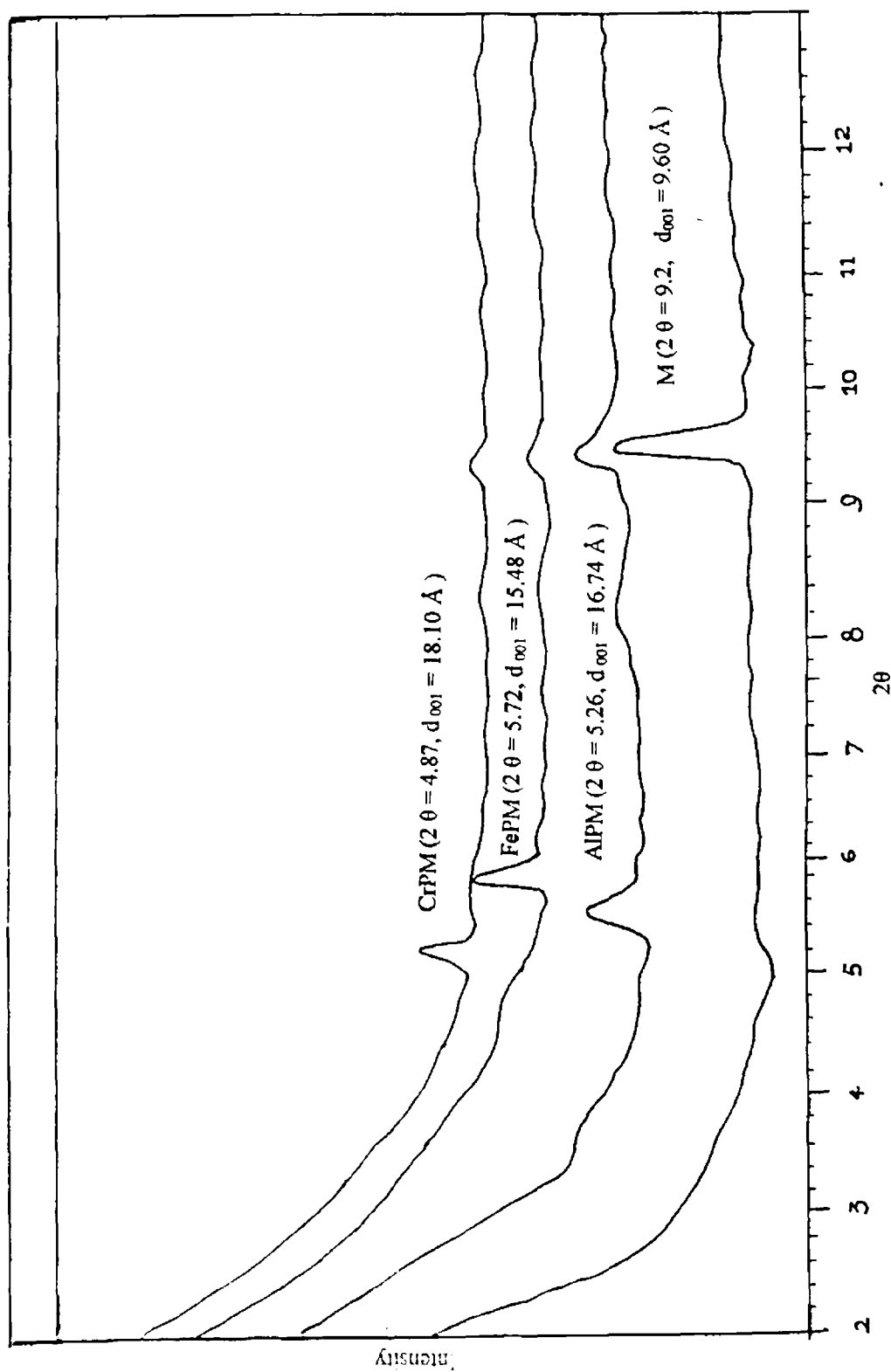


Figure 3.1 XRD Patterns of M, AIPM, FePM and CrPM

Similar reaction took place with iron oligomeric and chromium oligomeric solutions. Various investigations like electrometric measurements [2], conductometric titrations [3], spectrophotometric measurements [4, 5] Raman spectroscopy [6] and magnetic measurements [7] for determining the size and nature of polymeric iron cations revealed that the solution chemistry of Fe is complex. Although the dissolution of Fe(III) salts in water is known to result initially in simple hydrolysis products such as $\text{Fe}(\text{OH})^{2+}$, $\text{Fe}_2(\text{OH})^{2+}$, $\text{Fe}_2(\text{OH})_2^{4+}$ and $\text{Fe}_3(\text{OH})_4^{5+}$ [8, 9], further hydrolysis leads to the formation of discrete spherical polycations. They gradually grow in size and have diameters ranging from 1.5 to 3.0 nm and eventually link up to give rods comprising 2 to 6 spheres. Further hydrolysis eventually results in the precipitation of ferric hydroxide. For the polymeric solution, hydrolysis was stopped before the precipitation. The spherical polycations enter into the swelled clay layer and replaces the interlayer cations. Calcination leads to the propping apart of the layers with stable iron oxide pillars. Thus we prepared an iron-pillared montmorillonite of interlayer distance 15.48 Å.

Chromium pillaring agent contained polycations of chromium such as a dimer $[\text{Cr}_2(\text{OH})_2(\text{H}_2\text{O})_8]^{4+}$ which is bluish green species, higher polymers such as trimers and others [10-12] (more details in section 3.3). Intercalation of the polycation resulted in the larger interlayer distance of 18.10 Å.

3.2.2 Stability of the Pillared Structure Assigned from XRD Data

An investigation by X-ray diffraction reveals the behaviour of the three single pillared solids towards thermal treatment (Tables 3.4-3.6 and Figures 3.2–3.4). Here, by using XRD, we plotted both the intensities of 001 diffraction and the values of d_{001} as a function of pretreatment temperature. The intensity of 001 peak can be regarded as an indication of the stability of the whole structure of pillared montmorillonite while d_{001} is a measure of the distance between the two layers in the pillared montmorillonite.

As the pretreatment temperature increased, no significant change of d_{001} was observed (Figures 3.2-3.4). However, the intensity of d_{001} peak declined sharply as the temperature of calcination increased for AlPM and FePM. The decrease was not so sharp for CrPM as that for AlPM and FePM. More or less similar values of d_{001} for the different pretreatment temperatures in all the cases indicated the stability of the

pillar under thermal treatment. But the decrease in intensity of the d_{001} peak showed that the lattice structure of the pillared montmorillonite is liable to change upon heating.

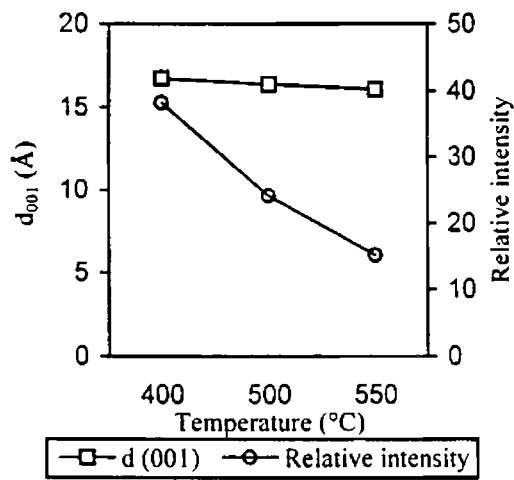
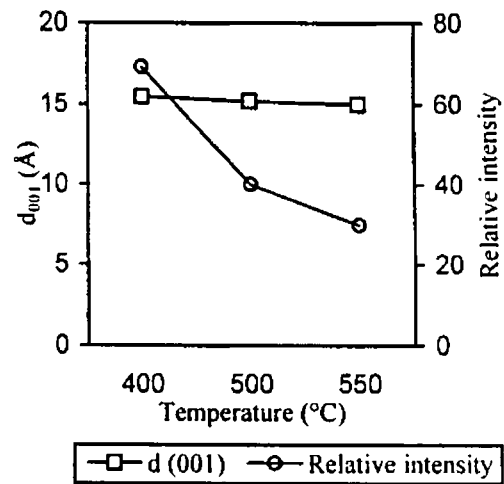
Pillaring or cross-linking is the process of cation exchange in nature. However, the pillars are usually hydroxy polycation with large size and abundant positive charge. During the process of pillaring, while large cations are propping up the interlayer spacing, 7 Na^+ ions in the interlayer space are exchanged by one Keggin ion (in the case of AlPM). Thus the distribution of cations within the interlayer space will be changing greatly. The negative charge and also the structural OH groups of octahedral sheet are mostly located towards the six membered ring formed by silicon tetrahedra in the tetrahedral sheet. Hence the Na^+ cation in the interlayer space will be correspondingly located opposite to, and very possibly blocking, the six membered rings. Thus most structural OH groups are hardly accessible as acidic sites and rather stable during thermal treatment. The pillaring processes release quite a number of Na^+ cations from blocked six member rings and makes many structural OH groups (and possible acidic sites) accessible and liable to elimination on heating. The lattice vacancies caused by the loss of OH groups favour more and more structural shrinkage during thermal treatment and accordingly reduce the thermal stability of pillared clay. For FePM, the extent of pillaring was high, (intensity of 001 diffraction being 69.21) compared to AlPM and CrPM. When the extent of pillaring is high more Na^+ blocking cations from six member rings are liberated and hence the structural shrinkage is more.

Table 3.4 Variation of d spacing and relative intensity with calcination temperature of AlPM

Calcination temperature ($^{\circ}\text{C}$)	d_{001} (\AA)	Relative intensity
400	16.74	38.23
500	16.40	24.13
550	16.10	15.10

Table 3.5 Variation of d_{001} and relative intensity with calcination temperature of FePM

Calcination temperature (°C)	d_{001} (Å)	Relative intensity
400	15.48	69.21
500	15.21	40.11
550	15.00	29.89

**Figure 3.2** Stability pattern by XRD of AIPM.**Figure 3.3** Stability pattern by XRD of FePM**Table 3.6** Variation of d_{001} and relative intensity with calcination temperature of CrPM

Calcination temperature (°C)	d_{001} (Å)	Relative intensity
400	18.10	41.36
500	18.00	38.49
550	17.41	35.94

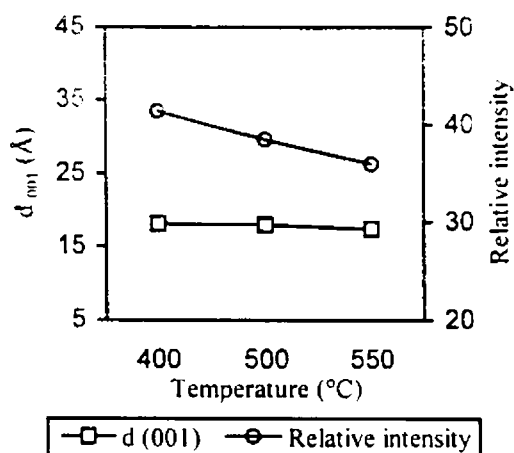


Figure 3.4 Stability pattern by XRD of CrPM

3.2.3 XRD of Mixed Pillared Systems

Table 3.7 shows the XRD details of mixed Fe-Al pillared clays. The d_{001} spacing of AlPM was 16.74 Å. An attempt to introduce iron in order to obtain a mixed pillar system resulted in slight variation in d spacing. For FePM the d spacing was 15.48 Å. For mixed Fe-AlPMs, d_{001} values were intermediate between those of AlPM and FePM. This is in agreement with the results obtained for Zhao *et al.* [13], though in the present case, the difference in d spacing between the various mixed Fe-Al pillared montmorillonites was less prominent. At low Fe/Al ratios the d_{001} was closer to that of AlPM and at high Fe/Al ratios (0.5 and 1.0) the d spacing was closer to that of FePM. These results indicate that the dimension of hydroxy iron-aluminium cross-linking species with Fe/Al in a direction vertical to the smectite layers was similar to that of hydroxy Al_{13} oligomer when Fe/Al ratio is low (≤ 0.4) and the structure of the pillaring species with Fe/Al ratio ≥ 0.5 was similar to that of hydroxy iron oligomer [14]. Zhao *et al.* proved the same observation using ^{27}Al NMR [13]. Canizares and coworkers also concluded that at low metal/Al ratios, the Keggin structure seems to predominate whereas in those with high metal/Al ratios, the resultant structure approaches that of pillared clays with single oxide pillars of the respective metal [15].

Table 3.8 depicts the XRD details of mixed Cr-Al pillared systems. As in the case of mixed Fe-Al systems, the d_{001} values for the mixed Cr-Al systems with low Cr/Al ratios were more similar to that of AlPM. Hence it can be assumed that the pillars obtained with chromo-alumina oligomeric solution having low Cr/Al ratios

Table 3. 7 XRD data of mixed Fe-Al pillared montmorillonites

Catalyst	2 θ (Degree)	d ₀₀₁ (Å)	Relative intensity
M	9.00	9.82	87.42
AlPM	5.26	16.74	38.23
FeAl _{0.1} PM	5.40	16.38	40.45
FeAl _{0.2} PM	5.54	16.01	49.23
FeAl _{0.3} PM	5.46	16.14	51.36
FeAl _{0.4} PM	5.48	16.11	59.32
FeAl _{0.5} PM	5.66	15.62	69.54
FeAl _{1.0} PM	5.53	15.98	57.21
FePM	5.72	15.48	69.21

had a Keggin like structure similar to that of Al oligomeric solution. For CrPM, d₀₀₁ was 18.10 Å and dehydroxylation during the calcination process yielded the large gallery height. At high Cr/Al ratios, the d₀₀₁ spacing was closer to CrPM [16]. This was even applicable to CrAl_{0.4}PM. Hence only at very low Cr/Al ratios (0.1, 0.2 and 0.3) the oligomeric solution resembled that of AlPM.

Table 3. 8 XRD data of mixed Cr-Al pillared montmorillonites

Catalyst	2 θ (Degree)	d ₀₀₁ (Å)	Relative intensity
AlPM	5.26	16.74	38.23
CrAl _{0.1} PM	5.20	17.01	42.32
CrAl _{0.2} PM	5.17	17.04	43.65
CrAl _{0.3} PM	5.10	17.32	42.66
CrAl _{0.4} PM	5.01	17.61	43.00
CrAl _{0.5} PM	5.00	17.66	43.25
CrAl _{1.0} PM	4.99	17.73	39.22
CrPM	4.87	18.10	41.36

Tables 3.7 and 3.8 also show the relative intensities of the d_{001} peak. We can see that the intensities were dependent on the Fe (Cr)/Al ratios. The intensity of the d_{001} peak can be related to the efficiency of pillaring (extent of pillaring) as well as the stability of the systems [17]. As the Fe/Al ratio increased from 0.1 to 0.5, the relative intensity also increased and the introduction of pillars inside the clay layers was maximum when Fe/Al ratio was 0.5. When the ratio increased to 1.0, the intensity decreased. This observation is supported by the EDX data, which showed that maximum incorporation of iron was for the ratio 0.5.

As the Cr/Al ratio increased, the intensity variations were not very significant. The only significant observation was that there was a slight decrease of intensity when the ratio was changed from 0.5 to 1.0 probably due to the lesser incorporation of Cr-Al pillars, as evidenced by the chemical composition data obtained from EDX analysis.

3.2.4 XRD of Vanadia Impregnated Iron-Pillared Montmorillonites

Table 3.9 shows the XRD details of all the vanadia impregnated iron-pillared systems. It is well-known that loading of vanadia over basic oxides results in compound formation such as orthovanadate or pyrovanadate formation [18, 19]. But with acidic oxides, no such compound formation is expected. Instead, V_2O_5 aggregates dispersed over the solid surface are observed [20]. Clays, especially pillared clays are well-known as acidic oxides. Hence dispersion of V_2O_5 over the solid surface was expected. In Table 3.9, X-ray diffraction patterns of FePM and the various vanadia loaded systems, along with pure vanadia are presented. The addition of vanadia up to 7 wt% on iron pillared montmorillonite, did not exhibit any characteristic peak shown by pure V_2O_5 . However, with the increased loading of vanadia of 10 wt% and above, peaks characteristic of vanadia started to appear. It is clear from the Table 3.9 that the intensity of the vanadia peak increased with the vanadia content. We can also note that the peak corresponding to the expansion of layers during pillaring in FePM, becomes weak and it almost disappeared when the vanadia loading reached 10 wt%. These facts suggested the distribution of vanadia on the pillared montmorillonite, as very small crystallites, not detectable by XRD, especially when the vanadia content is 7% or below. The crystallite size of vanadia seems to increase with vanadia loading beyond 7% and becomes detectable by XRD. Studies of vanadia impregnation on silica are thoroughly studied by Narayanan *et al.*

[21]. They could not observe any characteristic peak of V_2O_5 on vanadia loaded silica even up to a weight percentage of 25. They have suggested the formation of V-O-Si species, vanadia being present as V_2O_4 species contributing to the hyperfine splitting in the ESR spectrum. In another publication, Narayanan *et al.* revealed the effect of vanadia loading on K10 montmorillonite, a commercial acid activated clay [22]. Similar to our observation, they also found the fine dispersion of vanadia as V_2O_5 over the montmorillonite clay, vanadia being undetectable by XRD up to a weight percentage of 10. Above that loading, vanadia peaks started to appear in the XRD pattern.

In the present case, we have observed XRD peaks corresponding to vanadia for a weight percent of 7 and above. In [22] the authors confirmed the absence of any interaction of V_2O_5 with the clay surface for the formation of V-O-Si linkage as in the case of silica, by checking the ESR spectra of vanadia impregnated K10 montmorillonite. The ESR spectra did not show any hyperfine splitting and hence such an interaction on the clay surface is ruled out. Thus in our case also, we can conclude that vanadia is finely dispersed as V_2O_5 on the pillared clay surface.

Table 3.9 XRD data of vanadia loaded-iron pillared systems

Catalysts	Position (2 θ) of the XRD peaks
FePM	5.72 (69.21)*, 19.7 (100), 25.2 (30.10)
2VFe	5.71 (51.10), 19.8 (100), 25.1 (27.89)
5VFe	5.72 (38.10), 19.75 (100), 25.1 (26.24)
7VFe	5.71 (26.41), 19.66 (100), 25.15 (28.81)
10VFe	19.66 (100), 25.15 (17.81), 26.10 (26.10), 32.05 (24.10), 35.65 (28.10), 54.01 (24.01)
15VFe	19.91 (100), 25.48 (16.10), 26.18 (28.09), 32.14 (24.51), 35.15 (31.01), 54.08 (22.08)
20VFe	19.76 (100), 25.15 (19.62), 26.04 (31.04), 32.28 (27.91), 35.65 (44.44), 55.01 (28.04)
V_2O_5	20.05 (100), 26.20 (63.87), 32.45 (29.31), 34.45 (45.22), 55.75 (15.52)

* Figures in parenthesis give the relative intensity of the corresponding peak.

3.3 Visible Spectroscopy of Chromium and Mixed Chromium-Aluminium Pillaring Solutions

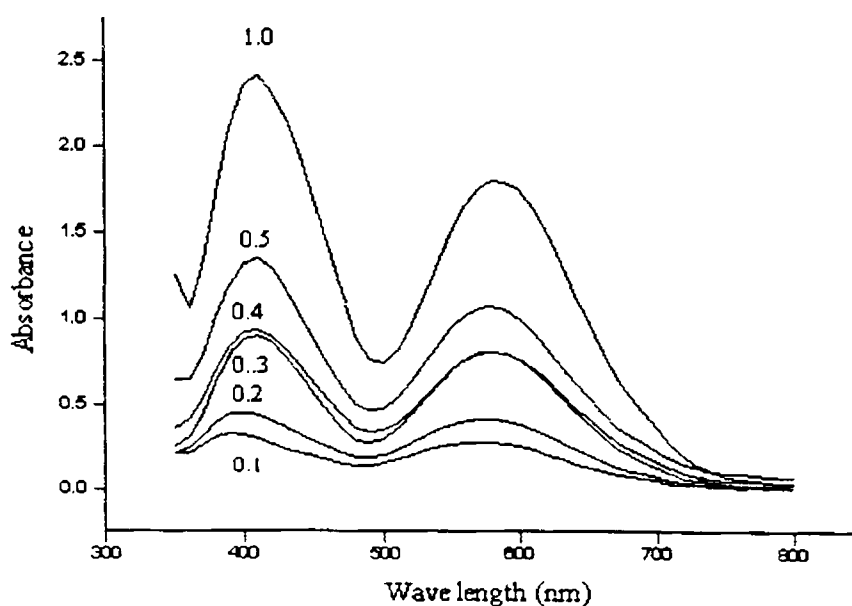
The various pillaring solutions prepared for the synthesis of mixed Cr-Al pillared montmorillonites were subjected to visible spectroscopy. A certain amount of 0.2 M aqueous chromium nitrate was gradually added to the aqueous 0.2 M aluminium nitrate solution, resulting in the product solutions having various Cr/Al ratios. Aqueous 0.2 M sodium carbonate was added to the solutions with constant stirring until a final base/metal ratio of 2 was reached. Visible spectra of these solutions were taken using Shimadzu UV-VIS spectrophotometer for the range 350-800 nm. The spectra are reproduced in Figure 3.5. The positions of the bands are summarised in Table 3.10.

The chemistry of Cr in solution is complicated. While adding base to a solution of Cr^{3+} , the dimer $[\text{Cr}_2(\text{OH})_2(\text{H}_2\text{O})_8]^{4+}$, the trimer $[\text{Cr}_3(\text{OH})_4(\text{H}_2\text{O})_9]^{5+}$, the tetramers $[\text{Cr}_4(\text{OH})_6(\text{H}_2\text{O})_{11}]^{6+}$ and $[\text{Cr}_4(\text{OH})_5\text{O}(\text{H}_2\text{O})_{10}]^{5+}$ and even a pentameric and hexameric polycation, not studied in detail may exist [11, 23, 24]. The solution obtained when dissolving chromium nitrate in water is blue in colour, with two peaks in the visible spectrum at 408 and 576 nm. The addition of base to this solution makes it change to green and for the base/metal ratio 2, the peaks shifted to 420 and 584 nm respectively. The ratio between their extinction coefficient was 1.53 (Table 3.10). Stünzi and Marty [11] in a very thorough study of the solution chemistry of Cr^{3+} , found that the two d-d band maxima (*ca* 420 and 580 nm) and the ratio between the extinction coefficient of these maxima (ϵ_1/ϵ_2) provides information about the polymerisation of Cr species. The positions of the bands and the corresponding ratios of the extinction coefficients for the various polymeric solutions of chromium, obtained by these authors are also furnished in the Table 3.10 so that a comparison between the results obtained for us and for Stünzi and Marty can be made. They obtained bands at 408 and 575 nm ($\epsilon_1/\epsilon_2 = 1.17$) for the monomeric form; 417 and 582 nm ($\epsilon_1/\epsilon_2 = 1.18$) for the dimeric form; 425 and 584 nm ($\epsilon_1/\epsilon_2 = 1.60$) for the trimeric cation and 426 and 580 nm ($\epsilon_1/\epsilon_2 = 1.95$) for the tetrameric polycation. Aluminium and chromium species co-exist in the mixed Cr-Al pillaring solutions. The position of the bands varied depending on the stoichiometry of the pillaring solution. The comparison of the data from these spectra with those reported by Stünzi and Marty indicated that Cr formed only the monomer for the Cr/Al ratios

Table 3.10 Positions of d-d bands and the ratio of their extinction coefficients for the various Cr containing solutions

Cr/Al ratio in the pillaring solution	$\lambda_{1\max}$	$\lambda_{2\max}$	ϵ_1/ϵ_2
0.1	570.0	391.5	1.16
0.2	573.0	397.0	1.12
0.3	580.5	406.5	1.16
0.4	578.0	408.5	1.12
0.5	580.0	412.0	1.20
1.0	583.0	414.0	1.19
∞	584.0	420.0	1.53
#Cr ³⁺	576.0	408.0	1.17
*Monomer	575.0	408.0	1.17
*Dimer	582.0	417.0	1.18
*Trimer	584.0	425.0	1.60
*Tetramer	580.0	426.0	1.95

Solution of chromium nitrate, not hydrolysed by base; *Reproduced from [11]

**Figure 3.5** Visible spectra of mixed Cr-Al pillaring solutions with various Cr/Al ratios.

0.1-0.4 and formed mainly the dimer for the ratios 0.5 and 1.0. The pillaring solution of Cr without Al mainly formed the trimer, $[\text{Cr}_3(\text{OH})_4(\text{H}_2\text{O})_9]^{5+}$.

The different polymerisation degree of Cr depending on the Cr/Al ratio may be explained by the acid properties of both the cations. The cationic radius of Al^{3+} (0.535 Å) is smaller than that of Cr^{3+} (0.615 Å). Hence Al^{3+} is more acidic than Cr^{3+} , having a higher tendency to form hydroxo bridged polynuclear species and easier forming polymeric cations [25]. Moreover, the formation of Al_{13} polycation involves a large amount of OH groups (2.46 OH per aluminium atom), while the formation of chromium polymeric cations involves lower amounts of hydroxyl groups (1.0 and 1.33 OH per chromium atom for the dimer and the trimer respectively). While adding OH to a solution containing both Al^{3+} and Cr^{3+} cations, Al^{3+} first polymerises and only when the polymerisation of this cation is completed does the polymerisation of Cr^{3+} begin. In solution with Cr/Al ratios 0.1-0.4, the large amount of Al^{3+} in the solutions makes it consume all the hydroxyl groups, and Cr^{3+} cannot polymerise. For solution containing Cr/Al ratios 0.5 and 1.0, the amount of Al^{3+} is relatively less and when the polymerisation of this cation finishes, the amount of OH groups is sufficient to permit the dimerisation of chromium, but not the formation of higher polymers.

3.4 BET Surface Area And Pore Volume Measurements

Table 3.11 shows the BET surface areas and the pore volumes of mixed Fe-Al pillared montmorillonites. M has a BET surface area of $6 \text{ m}^2\text{g}^{-1}$ only with a pore volume of $0.0043 \text{ cm}^3\text{g}^{-1}$ after degassing at 200°C . Pillaring with polycation increased the surface area and the pore volume. AIPM has a surface area of $102.5 \text{ m}^2\text{g}^{-1}$ after calcination at 400°C with a pore volume of $0.0888 \text{ cm}^3\text{g}^{-1}$. This suggested efficient pillaring of the parent montmorillonite.

For FePM, still further increase of BET surface area was observed with much higher pore volume ($188.67 \text{ cm}^3\text{g}^{-1}$ and $0.1435 \text{ cm}^3\text{g}^{-1}$ respectively). As the Fe/Al ratio increased from 0.1 to 0.5, surface area and pore volume also increased. Further increase, however, only reduced both. This is consistent with the observation from XRD data and EDX data. $\text{FeAl}_{0.5}\text{PM}$ exhibited maximum surface area ($198 \text{ m}^2\text{g}^{-1}$) and pore volume ($0.1723 \text{ cm}^3\text{g}^{-1}$). Comparing with the single systems, i.e., AIPM and FePM, this catalyst possessed more surface area and pore volume. All other mixed

systems were inferior to FePM with respect to pore volume and surface area. This result pointed towards the fact that the use of a mixture of Fe-Al oligomeric solution with a particular Fe/Al ratio of 0.5 only, can improve the pillared solid in terms of surface area and pore volume.

Table 3. 11 Surface area and pore volumes of mixed Fe-Al pillared montmorillonites

Catalyst	BET Surface area ($\text{m}^2 \text{g}^{-1}$)		Pore volume ($\text{cm}^3 \text{g}^{-1}$) (400°C)
	400°C	500°C	
M	6.60	-	0.0043
AlPM	102.50	88.62	0.0888
FeAl _{0.1} PM	83.01	61.56	0.0559
FeAl _{0.2} PM	103.70	99.87	0.0863
FeAl _{0.3} PM	123.80	116.12	0.0913
FeAl _{0.4} PM	146.80	139.81	0.1213
FeAl _{0.5} PM	198.00	188.60	0.1723
FeAl _{1.0} PM	131.20	101.90	0.0922
FePM	188.67	169.11	0.1435

The surface area and pore volumes of the mixed Cr-Al PMs are shown in Table 3.12. CrPM has a surface area of 96.33 m^2/g with pore volume 0.0731 cm^3/g . The surface area and pore volume of mixed Cr-Al systems do not show any significant difference among each other. The surface area and pore volume data of these systems after treating them at 500°C are also furnished in Table 3.12. All the pillared systems containing Cr showed an interesting property. At a higher pretreatment temperature, the surface area and the pore volumes increased significantly. The surface area increase was due to the creation of more and more pores inside the clay layers when the Cr containing systems are pretreated at high temperatures [26]. Increase in pore volume associated with high temperature treatment also suggests the same reasoning.

Table 3.13 gives the surface area and pore volume of vanadia-impregnated systems. Table shows that there was a continuous decrease of surface area and pore volume due to vanadia addition. It is already seen from XRD data the formation of

Table 3.12 Surface area and pore volumes of mixed Cr-Al pillared montmorillonites

Catalyst	BET Surface area (m ² /g)		Pore volume (cm ³ /g)	
	400°C	500°C	400°C	500°C
AlPM	102.50	88.62	0.0888	0.0784
CrAl _{0.1} PM	106.49	121.21	0.0722	0.0799
CrAl _{0.2} PM	110.54	124.31	0.0748	0.0802
CrAl _{0.3} PM	107.59	118.21	0.0712	0.0781
CrAl _{0.4} PM	113.43	131.18	0.0749	0.0831
CrAl _{0.5} PM	112.19	129.21	0.0752	0.0811
CrAl _{1.0} PM	70.83	92.36	0.0521	0.0684
CrPM	96.33	113.73	0.0699	0.0731

Table 3.13 Surface area and pore volumes of vanadia impregnated iron-pillared montmorillonites

Catalyst	BET surface area (m ² g ⁻¹)	Pore volume (cm ³ g ⁻¹)
FePM	188.67	0.1435
2VFe	124.89	0.1017
5VFe	93.97	0.1040
7VFe	72.37	0.0732
10VFe	36.62	0.0378
15VFe	25.99	0.0344
20VFe	14.63	0.0210

V₂O₅ on FePM while treating it with ammonium metavanadate. The decrease in surface area and pore volume further suggested the intrusion of vanadia species on the pores of FePM. As the percentage of vanadia loading increased, the surface area and pore volume decreased. The surface area of 20VFe was dramatically reduced to 14.63 m²g⁻¹, which suggested almost complete blocking of the pores by the vanadia species. The gradual decrease of surface area and pore volume as the percent of

vanadia loading increased, pointed towards greater intrusion of vanadia inside the pores. Similar results were obtained for Narayanan *et al.* also [27]. The BET surface area of FePM started to decline upon vanadia addition. The pore volumes were also found to decrease upon the increase in vanadia loading. When 2% vanadia is loaded on iron-pillared montmorillonite, the surface area changed from $188.67 \text{ m}^2\text{g}^{-1}$ to $124.89 \text{ m}^2\text{g}^{-1}$, and pore volume changed from 0.1435 to $0.1017 \text{ cm}^3\text{g}^{-1}$ (Table 3.13). Probably vanadia is occupying the micropores present in the iron-pillared clay, thereby reducing the surface area and pore volume. As the percentage of vanadia increased, more vanadia entered into the pores, causing significant reduction in surface area and pore volume. When the vanadia loading reached 20%, the surface area drastically reduced to $14.62 \text{ m}^2\text{g}^{-1}$, suggesting the complete blocking of pores by the vanadia species. Pore volume, consequently reduced to $0.0210 \text{ cm}^3\text{g}^{-1}$. The broadening of the peak corresponding to the pillaring in FePM in the XRD pattern also supports the entrance of V_2O_5 inside the pores of the pillared clay. However, definitely there is the possibility of dispersing V_2O_5 over the clay surface also.

3.5 Infrared Spectroscopy

Figure 3.6 shows the infrared (IR) spectra of parent montmorillonite, single and some mixed pillared samples. Broad band near $3416\text{-}3443 \text{ cm}^{-1}$ indicated the OH group. For the parent montmorillonite, this was a very intense peak. The intensity of this peak considerably reduced for the pillared samples showing the loss of hydroxyl groups upon pillaring followed by calcination at 400°C . For all the pillared samples there were two bands corresponding to the hydroxyl groups, one probably assigned, to the pillar OH group and the other assigned to layer hydroxyl groups [28]. Comparison between the parent montmorillonite and the pillared samples showed that the basic structure of clay was not at all altered during the pillaring process since all the main peaks are retained in the pillared samples.

Figure 3.7 shows the IR spectrum of FePM and those of 2VFe, 5VFe, 7VFe, 10VFe, 15VFe and 20VFe after subtracting the IR spectrum of FePM. This subtraction enables to find out the modification caused by vanadia impregnation alone. The characteristic mode of V_2O_5 at 1020 cm^{-1} (V=O stretching) is shown by the vanadia impregnated FePMs [29]. As the percentage of vanadia increased, the intensity of this peak also increased. Thus the formation of V_2O_5 over FePM was again confirmed by IR spectroscopy.

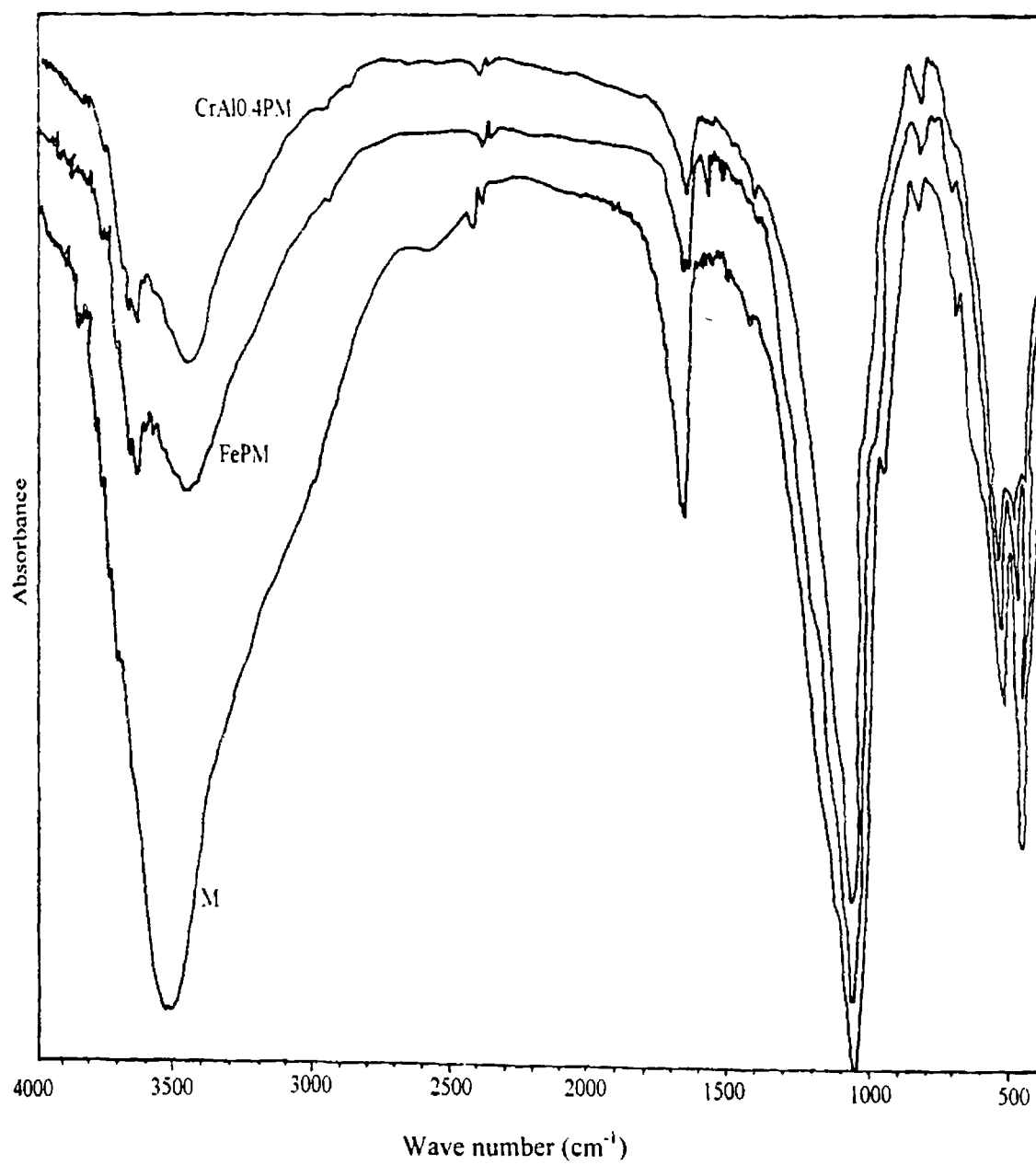


Figure 3.6 IR spectra of M, FePM and CrAl_{0.4}PM

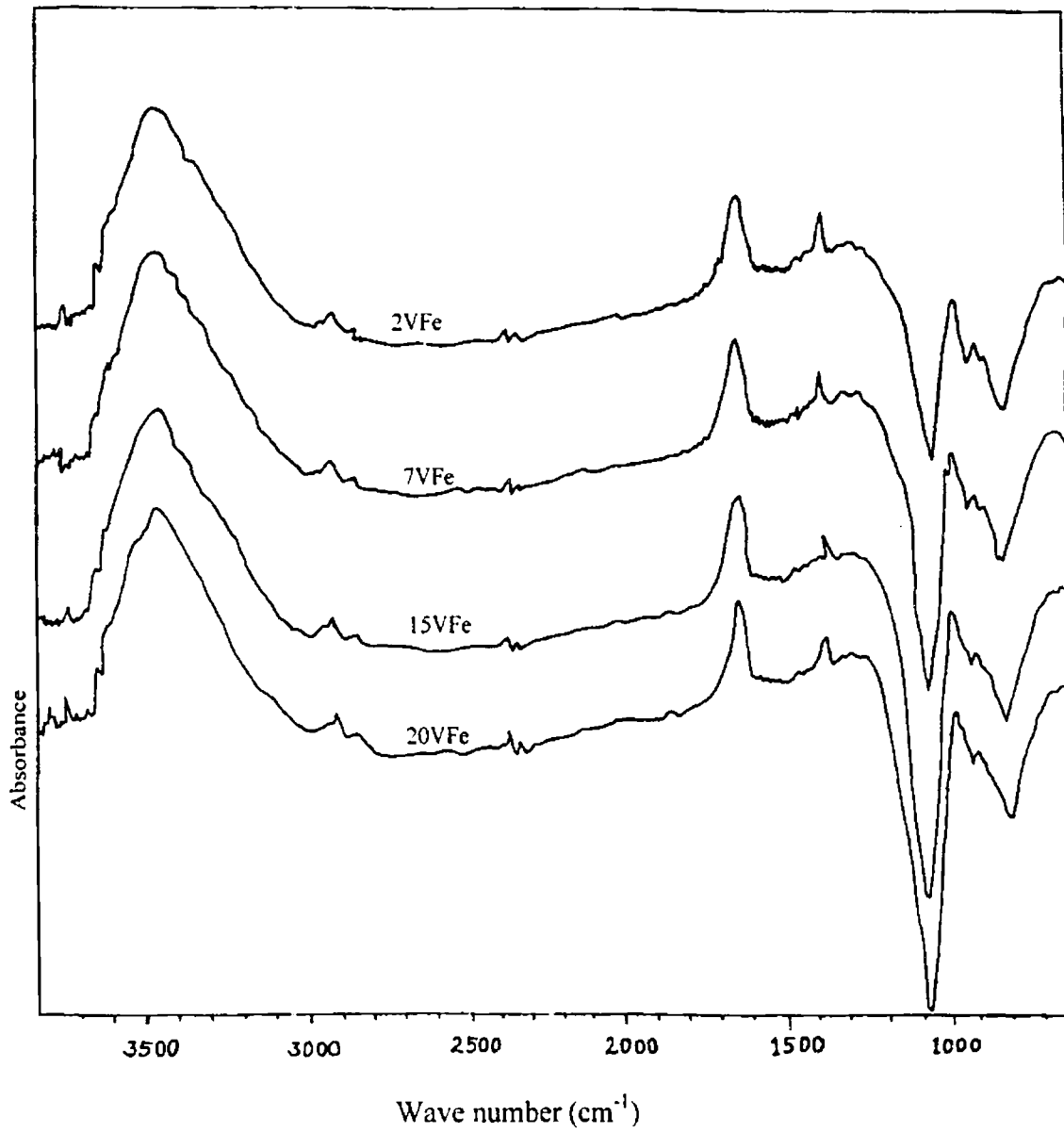


Figure 3.7 IR results of various vanadia loaded iron-pillared montmorillonites after subtracting the IR of FePM

3.6 Thermogravimetric Analysis

The TG-DTG diagrams of some oven-dried samples are shown in Figure 3.8. The sharp dip near 120°C for all the samples indicates a cumulative weight loss corresponding to the removal of physically adsorbed water from the clay structure. For the parent montmorillonite, from 120 to around 500°C, the weight loss was negligible, while after 500°C up to 800°C, there was a significant weight loss. This second weight loss was due to dehydroxylation of the clay structure. For pillared samples also, the major weight loss was near the 120°C region. However, after that also, they showed a continuous loss of weight. This was associated with the formation of the pillars. For FePM, there was a small dip appeared around 300°C and for AlPM, this was around 600°C. This weight loss was due to the dehydroxylation of the clay structure and of any remaining hydroxide from the pillars. For CrPM, the second dip was near 500°C.

Thus the TG curves show that pillared systems lost more weight than their un-pillared counterpart during calcination. More specifically, the parent clay lost a small amount of weight in the range 120-500°C while the pillared clays showed a steady weight loss above 120°C.

3.7 Acidity Studies

3.7.1 Evaluation of Brönsted Acidity- Adsorption of 2,6-Dimethylpyridine

Brönsted and Lewis acid sites play different roles in various types of catalytic reactions, and the strength of the respective acid sites strongly affects the catalytic performance [30]. Therefore, there is significant motivation to develop an easy and reproducible method for the measurement of strength and amount of Brönsted and Lewis acid sites separately. 2,6-Dimethylpyridine (DMPY) is a useful probe molecule for the selective determination of Brönsted acid sites. Several researchers applied DMPY as a probe for Brönsted acid sites [31-34]. DMPY desorbed above 250°C is solely attributed to the Brönsted acid sites. The selective adsorption of DMPY on Brönsted acid sites is attributed to the steric hindrance of the methyl groups [35].

To evaluate the Brönsted acidity of the various samples, we had carried out the adsorption of 2,6-dimethylpyridine (DMPY) over the solids by keeping the calcined samples in a desiccator, inside of which is saturated with vapours of DMPY.

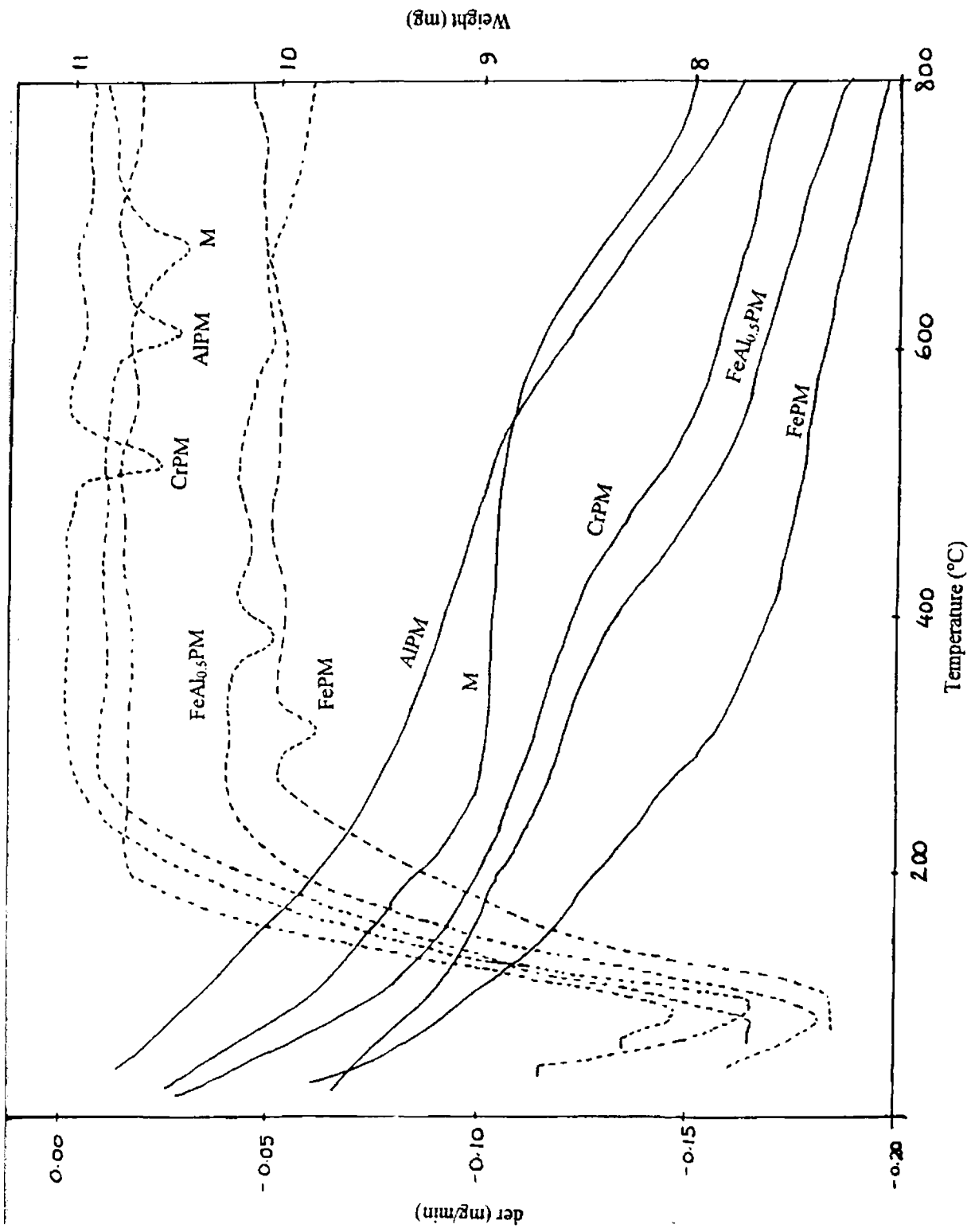


Figure 3.8 TG-DTG curves of Parent and some pillared montmorillonites.

for 48 hours. The samples were then allowed for controlled thermal treatment under nitrogen atmosphere. During this treatment, the adsorbed DMPY will get desorbed from the acid sites. DMPY desorbed above 250°C is proportional to the concentration of Brönsted acidic sites present in the sample.

Figure 3.9 gives the thermodesorption data of mixed Fe-Al systems along with M, FePM and AlPM. All of these catalysts were activated at 500°C. before placing them into the DMPY vapours. The weight loss was due to the desorption of DMPY alone up to 500°C. It is clear that the parent montmorillonite possessed only a very low Brönsted acidity compared to those of pillared systems. This Brönsted acidity can be due to the structural hydroxyl groups of the clay layers. Figure 3.10 shows a schematic structural model of the clay layer of montmorillonite along with pillar intercalation. The location of the possible acid sites can be seen from this figure.

Montmorillonite has an idealised stoichiometric composition corresponding to $(Al_{2-x}Mg_x)Si_4O_{10}(OH)_2$. Structurally it comprises a central sheet containing octahedrally co-ordinated Al and Mg in the form of their oxides and hydroxides sandwiched between two sheets containing tetrahedrally co-ordinated silicon essentially in the form of its oxide. The structural OH groups associated with Al(VI)-O-Al(VI) and Al(VI)-O-Mg linkages are responsible for the Brönsted acidity. However, only a small part of the structural OH groups can become Brönsted sites

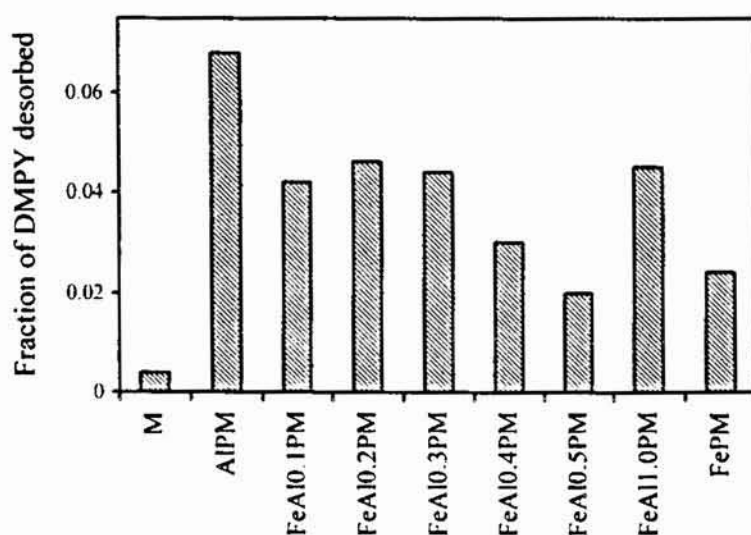


Figure 3.9 Thermodesorption data of DMPY over mixed Fe-Al pillared montmorillonites

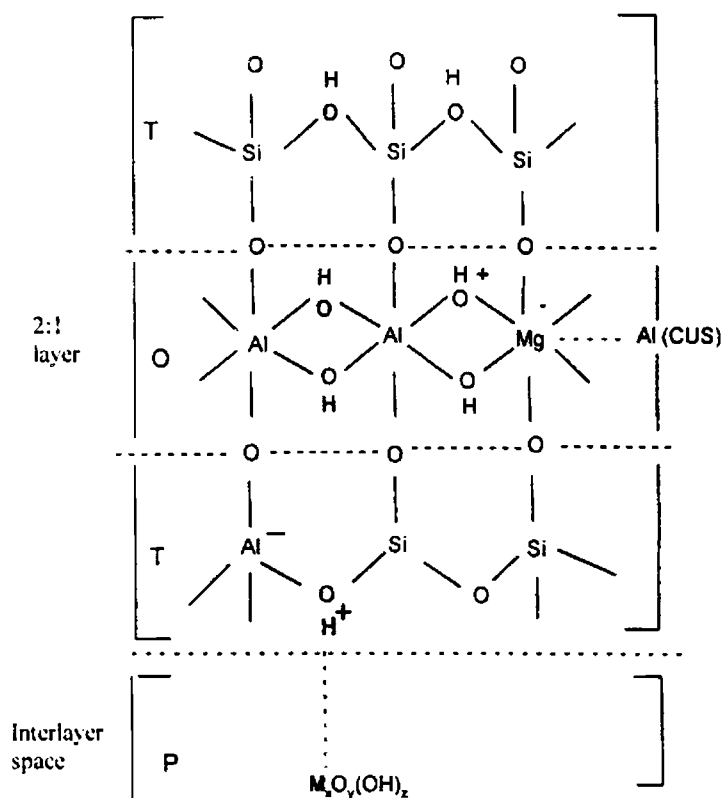


Figure 3.10 Acid sites on the pillared solid; T: - Tetrahedral sheet, O: - Octahedral sheet, P- Pillar and CUS: - Co-ordinatively unsaturated Al.

during adsorption as suggested by the small total Brönsted acidity value of M. The linkage of Al(VI)-O-Al(VI) seems more liable to donate H⁺ by transferring negative charge to Mg atoms, which locate in the dioctahedral sheet. Also, it was shown by Hall [36] and Davidtz [37] that Al (CUS) i.e., co-ordinatively unsaturated Al. exposed at crystal edges can become either Brönsted or Lewis acid sites.

During pillaring, there was a clear enhancement of Brönsted acidity. More amount of DMPY was desorbed at all temperature regions for the pillared samples than the unpillared sample. Though the generally accepted view regarding the acidity of pillared clays is that Lewis acid sites are mainly resident on the metal oxide pillars [28] and Brönsted acid sites are associated with the structural OH groups present on the host clay [28, 38], Bodoaro *et al.* have reported that the pillars can also contribute a significant number of Brönsted acid sites [39]. Also it was observed that AIPM was superior to FePM in this regard. Increasing the Fe/Al ratio decreased the number of sites more or less in a regular fashion up to a ratio of 0.5. Further increase to 1.0, however, caused a positive effect. This observation is

supported by the iron content from the EDX data (Table 3.1) and pillar density from XRD data (Table 3.4). The presence of iron decreased the Brönsted acidity. For $\text{FeAl}_{1.0}\text{PM}$, the amount of iron was less and consequently it possessed a greater Brönsted acidity.

Figure 3.11 gives the thermodesorption data of Cr- and mixed Cr-Al pillared systems. Among these also, AlPM has the highest DMPY adsorption. Incorporation of Cr significantly reduced the DMPY adsorption. $\text{CrAl}_{0.1}\text{PM}$ has only a value of 0.045, which is much less than 0.068, the DMPY adsorption value of AlPM. Further increase of Cr reduced the DMPY adsorption. Hence samples containing more Al possessed more number of Brönsted acidic sites. Low Fe/Al and Cr/Al ratios led to a comparatively high value for DMPY adsorption. Zhao *et al.* also observed that at low Fe/Al and low Cr/Al ratios Brönsted acidic sites were more [13, 16]. These results suggest that the acidity of the pillared clays varied with the pillaring composition.

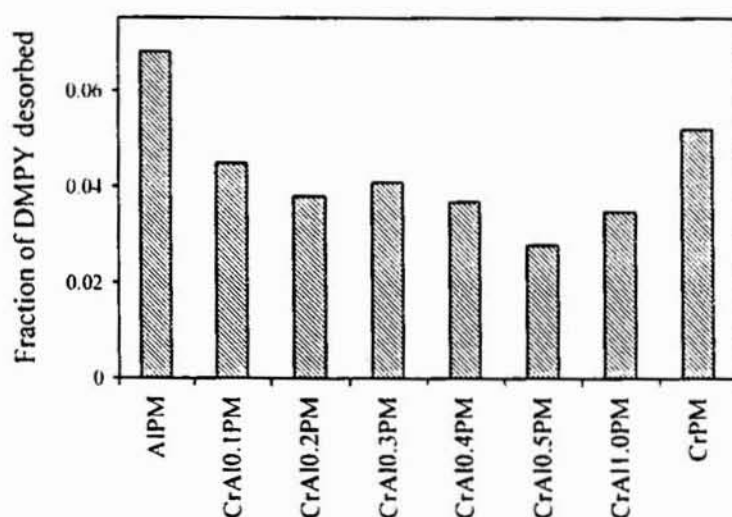


Figure 3.11 Thermodesorption data of DMPY over mixed Cr-Al pillared montmorillonites

Figure 3.12 displays the thermodesorption data of vanadia impregnated iron pillared montmorillonites. Vanadia addition improved the Brönsted acidity for the loading of 5VFe, 7VFe and 10VFe. As the vanadia loading increased from 2%, the amount of DMPY desorbing from the catalyst also increased, up to 7% and then it decreased. We have already seen that vanadia is well dispersed over the clay surface up to the weight percentage of 7. After that only, large crystallites of V_2O_5 formed over the surface. These crystallites entered into the pores and thus reduced the surface area and also pore volume. It is reported that vanadia loading creates

Brönsted acidity, assigned to the V-OH species of crystalline V_2O_5 [40]. The well dispersion of V_2O_5 increased the Brönsted acidity considerably, the case of 7VFe.

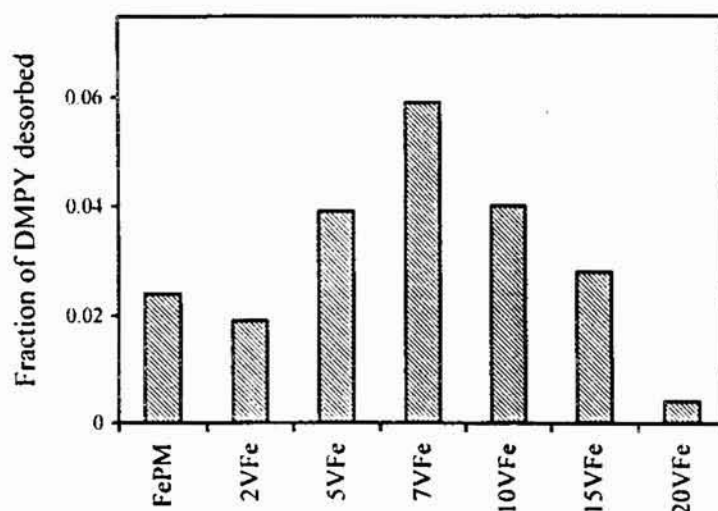


Figure 3.12 Thermodesorption data of DMPY over vanadia loaded iron pillared montmorillonites.

3.7.2 Electron Accepting Studies using Perylene - Evaluation of Lewis Acidity

Apart from the *in situ* IR adsorption of bases such as pyridine or NH_3 , the only procedure suitable to gain qualitative information regarding Lewis acidity in the presence of Brönsted sites is based on the investigation of the ability of the surface to accept a single electron. For the investigation of one-electron acceptor properties of solids, polyaromatic hydrocarbons such as perylene, pyrene and chrysene [41, 42] have mainly been used as electron donors.

The determination of the surface sites which act as acceptors of single electron is based on the measurement of the amount of these adsorbed molecules, which can easily donate one electron. They form charge transfer complexes with surface active sites which exhibit characteristic ESR spectrum, the intensity of the corresponding esr signals being a direct measure of surface active sites. It can also be stated that the investigation of the interaction between one-electron acceptor sites and adsorbed donor molecule is an indirect determination of the electron deficient sites. An alternative method for the determination of active sites through ESR spectra is the spectroscopic monitoring of the amount of electron donor left in the solution after adsorption.

Perylene was used as the electron donor and it was adsorbed at room temperature from a solution in benzene on the previously activated samples. The

pale yellow colour of AIPM changed to a mottled lavender colour due to the adsorption of perylene on the surface. Owing to the dark brown colour of FePM and Fe-AIPMs and the dark green colour of CrPM and Cr-AIPMs, the change in colour of these catalysts due to adsorption of perylene was not clearly visible. Perylene being an electron donor transferred electron to the Lewis acid sites and got itself adsorbed as perylene radical cation [43]. Thus after adsorption, the concentration of perylene in the solution decreased. This decrease was found out using absorbance measurements at λ_{max} equal to 439 nm and corresponds to the amount of perylene getting adsorbed on the surface, which in turn corresponds to the Lewis acidity of the system. As the concentration of perylene used for adsorption was increased, the amount of perylene getting adsorbed on the solid surface also increased. But after a particular concentration of perylene in benzene, the amount of perylene adsorbed remained constant. This constant value is referred to as limiting amount. The limiting amount of perylene indicated the surface electron accepting capacity or in other words, the Lewis acidity of the samples. A clear picture of the adsorption and limiting amount of perylene adsorbed can be obtained by plotting the amount of perylene adsorbed against its equilibrium concentration, as shown in the Figures 3.13 and 3.13a)

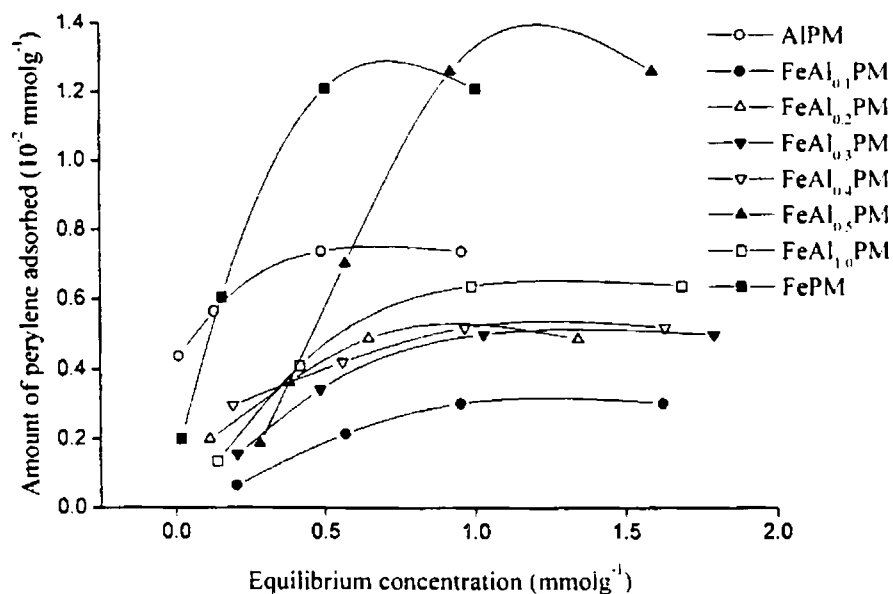


Figure 3.13 Results of perylene adsorption over mixed Fe-Al pillared systems.

These graphs convince a Langmuir type of adsorption over the solid surfaces. The limiting amounts of the various series of systems are shown in Tables 3.14, 3.15 and 3.16. As evident from Table 3.14 and Figure 3.13, the limiting amount obtained for AlPM was significantly lower than that of FePM. This suggested the lower electron accepting capacity and lower Lewis acidity of AlPM compared to FePM. This can be attributed to the intrinsic character of iron pillars which are more Lewis acidic than alumina pillars. An increase on Fe/Al ratio increased the limiting amount, and was found to be maximum for FeAl_{0.5}PM. Among mixed Fe-Al pillared systems, the increase of limiting amount with increasing iron content proposes that the Lewis acidity was proportional to iron content. This suggests that more and more electron accepting centres are associated with iron content of the pillared samples. Only FeAl_{0.5}PM possessed more Lewis acidity than FePM. Thus a mixed system of Fe-Al pillared montmorillonite with Fe/Al ratio 0.5 was superior to the respective single metal oxide pillared systems, in this regard. And it is unambiguous that the presence of iron is responsible for the increase in Lewis acidity.

Table 3.14 Perylene adsorption data over mixed Fe-Al pillared montmorillonites.

Catalyst	Limiting amount (10 ⁻² mmolg ⁻¹)
M	-
AlPM	0.7366
FeAl _{0.1} PM	0.3024
FeAl _{0.2} PM	0.4870
FeAl _{0.3} PM	0.4996
FeAl _{0.4} PM	0.5186
FeAl _{0.5} PM	1.2615
FeAl _{1.0} PM	0.6368
FePM	1.2104

Table 3.15 and Figure 3.13a give the adsorption results for CrPM and mixed Cr-AlPMs. Chromium containing pillared systems exhibited higher Lewis acidity than AlPM. However, no regular gradation in limiting amount with Cr/Al ratio

variation was observed. Any way, we can state that the incorporation of Cr along with alumina pillars enhanced the Lewis acidity, probably due to the intrinsic Lewis acidity of Cr.

Table 3.15 Perylene adsorption data over mixed Cr-Al pillared montmorillonites

Catalyst	Limiting amount (10^{-2} mmol g $^{-1}$)
AlPM	0.7366
CrAl _{0.1} PM	1.1602
CrAl _{0.2} PM	0.9372
CrAl _{0.3} PM	1.2452
CrAl _{0.4} PM	1.2852
CrAl _{0.5} PM	1.1101
CrAl _{1.0} PM	0.9862
CrPM	0.9392

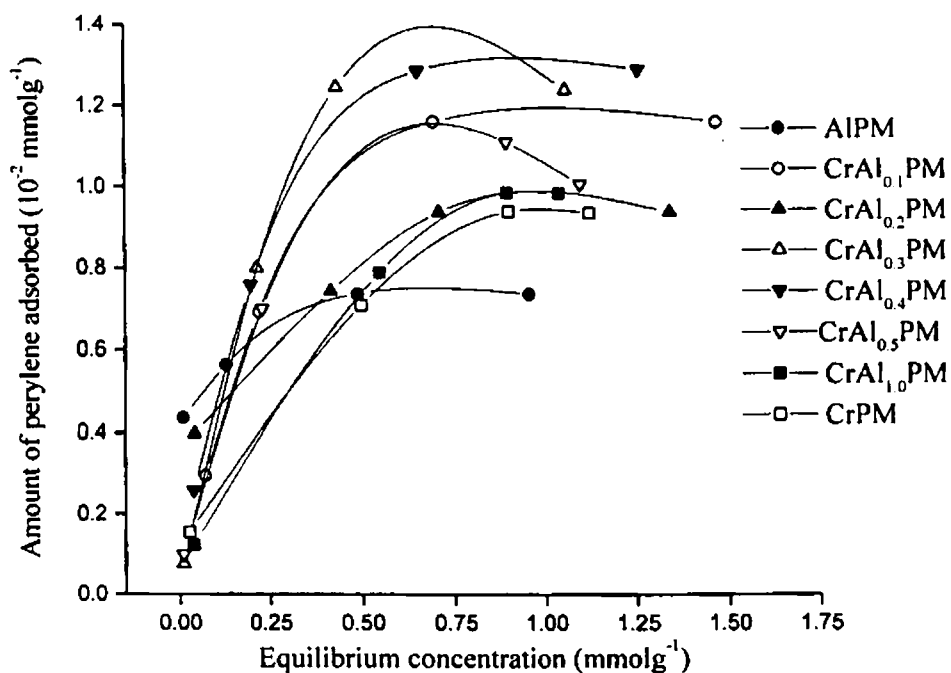


Figure 3.13 α Results of perylene adsorption over mixed Cr-Al pillared systems.

Another simple, but important observation was that the parent montmorillonite was not responding towards perylene adsorption. This observation

is in consonance with the general agreement that the contribution of pillars to the acidity of pillared clays is mainly Lewis type. From the DMPY experiment, we observed that a small adsorption of DMPY took place on M. Thus though parent montmorillonite possessed some Brönsted acidity, it lacks detectable Lewis acidity with perylene. This behaviour can also be attributed to the very low surface area of M also ($6 \text{ m}^2\text{g}^{-1}$).

Table 3.16 present the limiting amount of perylene adsorbed on the vanadia impregnated samples. Vanadia is a very weak acid and exhibits mainly Brönsted acidity [44, 45, 46]. From the IR and XRD studies we had concluded that vanadia is dispersed as V_2O_5 inside the pores and surface of the clay lattice. Now, during the perylene experiments, we observed a significant loss of Lewis sites which are responding to the adsorption of perylene. It can be confirmed that loading of vanadia and there by dispersal of vanadia as V_2O_5 did not enhance the Lewis acidity of iron-pillared systems. Not only that, addition of vanadia significantly reduced perylene adsorption, due to the blocking of surface acidic sites by vanadia species.

Table 3.16 Perylene adsorption over vanadia loaded Fe pillared montmorillonites

Catalyst	Limiting amount ($10^{-2} \text{ mmolg}^{-1}$)
FePM	1.2104
2VFe	1.1010
5VFe	0.9088
7VFe	0.7316
10VFe	0.4140
15VFe	0.3421
20VFe	0.2461

At low vanadium loadings of 2 and 5%, Lewis acidic sites are not very much reduced. But at higher vanadium loadings, Lewis acidity was diminished due to the coverage of catalyst surface with particles of V_2O_5 . At low vanadium loadings, Lewis acidity due to exposed Fe and Al ions were present. Lewis acidity can be assigned to unsaturated vanadium ions also, due to the adsorbed V-oxide on the clay surface to some extent. At high vanadium loadings, crystalline vanadia covers almost the major portions of the clay, and reduced the Lewis acidity.

3.7.3 Temperature Programmed Desorption of Ammonia (TPD)

Among the various basic probe molecules (n-butyl amine, pyridine and ammonia), ammonia is widely employed to characterise the acidity of solid catalysts by the method of temperature programmed desorption. n-butyl amine being a stronger base ($pK_b = 7.00$) can titrate even the weaker acidic sites. But it may not have a considerable access to the various sites, due to its large size. Comparing pyridine and ammonia, ammonia is smaller (kinetic diameter = 2.65 Å) and more basic ($pK_b = 4.77$) than pyridine (kinetic diameter is 5.8 Å and $pK_b = 8.75$). Hence we have chosen ammonia as the probe molecule for conducting the temperature programmed desorption experiments. Apart from titrating acid sites of any strength and type, ammonia molecule can be adsorbed by a hydrogen bond or a dipolar interaction [47, 48].

Table 3.17 give the distribution of acid sites of M, AlPM, FePM and mixed Fe-AlPMs among various regions, determined by TPD of NH_3 . Total acidity is also shown along with the sum of weak and medium sites. Almost all samples showed a maximum of acid sites in the weak acid region. M also possessed a little acidity, mainly from the weaker acid sites. Pillaring with various polyoxocations increased the acidity considerably. Pillaring process (the process by propping up the clay layers) exposes the Brönsted and Lewis acid sites of the layers. Further more, the pillars add acid sites to the already existing hydroxyl groups and to Al. Pillars are known to increase especially the Lewis acidity [49, 50]. Pillaring increased the number of acid sites of various strengths. AlPM has a total acidity of $0.5352 \text{ mmol g}^{-1}$ with 0.3084 in the weak, 0.1814 in the medium and $0.0454 \text{ mmol g}^{-1}$ in the strong acid region. FePM possessed a slightly higher acidity among weak and medium region, but do not differ much from that of AlPM. But FePM clearly possessed much more strong acid sites which is arising from the presence of iron pillars. The variation in the distribution of acidity with respect to variation in Fe/Al ratio, at first sight, seemed very irregular. But quite a clear picture can be obtained, if we count the weak plus medium acidity as a whole and the strong acidity separately. Increasing the Fe/Al ratio from 0.1 to 0.4, the weak plus medium acidity increased, though no regular gradation could be observed when we examine weak and medium acidity separately. Increasing Fe/Al ratio from 0.4 to 0.5 reduced the weak plus medium acidity, but the total acidity was found to be higher for the ratio 0.5, than the

Table 3. 17 Acid site distribution of Fe-Al pillared montmorillonites

Catalyst	Weak (100-200°C)	Medium (200-400°C)	Strong (400-600°C)	Weak + Medium	Total (mmolg ⁻¹)
M	0.01003	0.00600	0.00	0.01603	0.01603
AlPM	0.3084	0.1814	0.0454	0.4898	0.5352
FeAl _{0.1} PM	0.1867	0.1401	0.0992	0.3268	0.4260
FeAl _{0.2} PM	0.2081	0.1207	0.1612	0.3287	0.4898
FeAl _{0.3} PM	0.1370	0.2740	0.1793	0.4110	0.5823
FeAl _{0.4} PM	0.4752	0.4234	0.1811	0.8986	0.8797
FeAl _{0.5} PM	0.3544	0.4807	0.3056	0.8351	1.1407
FeAl _{1.0} PM	0.3090	0.1902	0.0475	0.4992	0.5466
FePM	0.2726	0.1992	0.1163	0.4718	0.5880

ratio 0.4, owing to the fact that the increase from 0.4 to 0.5 greatly increased the strong acidity. Thus when the ratio was changed from 0.4 to 0.5, weak + medium acidity decreased from 0.8986 to 0.8351 mmolg⁻¹ and strong acidity jumped from 0.1811 to 0.3056 mmolg⁻¹. However, further increase of Fe/Al ratio did not cause an increase in acidity. Strong acidity also showed a similar trend. FeAl_{1.0}PM has smaller values in all ranges and total acidity, mainly due to the lesser incorporation of Fe as evidenced from EDX data.

Table 3.18 gives the acidity distribution of Cr-AlPMs. CrPM possessed a total acidity of 0.775 mmolg⁻¹, with 73.75% contribution from weak plus medium region. The total acidity was more than that of AlPM. Thus CrPM is the most acidic among AlPM, FePM and CrPM. CrPM possessed highest acidity in the weak plus medium region, and the least in the strong region. FePM has the maximum strong acidity. Comparing the Brönsted acidity obtained from DMPY adsorption, AlPM was found to be most acidic and FePM was found to be the least acidic. Comparing Lewis acidity obtained from perylene adsorption, FePM was the strongest and AlPM was the weakest one.

As experienced from perylene adsorption, we could not get a regular variation in the distribution of acidity with change in Cr/Al ratio. Mixed Cr-Al systems are

Table 3. 18 Acid site distribution of Cr-Al pillared montmorillonites

Catalyst	Weak (100-200°C)	Medium (200-400°C)	Strong (400-600°C)	Weak + Medium	Total (mmolg ⁻¹)
AlPM	0.3084	0.1814	0.0454	0.4898	0.5352
CrAl _{0.1} PM	0.2677	0.0850	0.1404	0.3526	0.4931
CrAl _{0.2} PM	0.1976	0.0093	0.1517	0.2069	0.3586
CrAl _{0.3} PM	0.1513	0.0091	0.1603	0.1603	0.3207
CrAl _{0.4} PM	0.1010	0.0117	0.1793	0.1127	0.2920
CrAl _{0.5} PM	0.0986	0.0151	0.1082	0.1137	0.2219
CrAl _{1.0} PM	0.2026	0.0964	0.1318	0.2990	0.3309
CrPM	0.3617	0.2040	0.0034	0.5717	0.7751

found to possess enhanced strong acidity when compared with respective single pillared systems i.e., CrPM and AlPM. However, the total acidity of the mixed Cr-Al systems was in between those of CrPM and AlPM.

Another noticeable point while comparing the acidity data obtained from perylene adsorption and NH₃-TPD was the large difference in magnitude of acidity values. Hundred times higher values are obtained from NH₃-TPD than those from perylene measurements. NH₃ being smaller and stronger, can detect almost all types and strengths of acid sites where as perylene being larger, along with its sole ability for binding with electron accepting centres, has access only to certain exposed Lewis sites. Though perylene measures only Lewis acidity, the difference between acidity values of NH₃-TPD and perylene adsorption could not be attributed to Brönsted acidity alone, since this value will be very much higher than that expected for pillared clays in which there is a general agreement of a large excess of Lewis acid sites than Brönsted acid sites [50]. This also suggests that there remained Lewis acid sites undetectable by perylene molecule, the effect of which could be attributed to its large size.

The distribution of acid sites and total acidity values of the various vanadia loaded iron-pillared montmorillonites are shown in Table 3.19. We can see that the total acidity values considerably enhanced upon vanadia loading. We have already seen the increase in Brönsted acidity and decrease in Lewis acidity upon vanadia

addition. Thus we can assign the increase in total acidity as the effect of increasing Brönsted acidity. For 7VFe, the total acidity measured was three times greater than that of the parent iron-pillared montmorillonite. It is evident from the limiting value of perylene adsorbed on the solids, that Lewis acidity decreased. However, we

Table 3.19 Acid site distribution of vanadia impregnated iron-pillared systems.

Catalyst	Weak (100-200°C)	Medium (200-400°C)	Weak + Medium	Strong (400-600°C)	Total
FePM	0.2726	0.1992	0.4718	0.1163	0.5881
2VFe	0.2985	0.1610	0.4595	0.1314	0.5909
5VFe	0.4263	0.4225	0.8488	0.3726	1.2214
7VFe	0.5095	0.8006	1.3101	0.6186	1.9280
10VFe	0.3887	0.2682	0.6569	0.3754	1.0324
15VFe	0.3207	0.1781	0.4988	0.0534	0.5522
20VFe	0.1810	0.1011	0.2821	0.0190	0.3011

cannot rule out the possibility of NH_3 molecule being adsorbed on those Lewis acid sites which perylene molecule could not. It may be suspected that the total acidity values increased when determined by temperature programmed desorption of NH_3 due to this factor also, along with enhancement of Brönsted acidity. The catalysts up to 10 wt% vanadia loading, possessed more acidity than the parent iron pillared montmorillonite, where as 15VFe and 20VFe had lesser number of acidic sites, when determined by NH_3 -TPD method.

3.8 Cumene Conversion Reaction as a Test Reaction for Acidity

Cumene conversion reaction proceeds in two ways. On Brönsted acidic sites, cracking takes place to produce benzene and propene. On Lewis acidic sites dehydrogenation takes place to produce α -methylstyrene [51-53]. Dealkylation to toluene and ethylbenzene can also occur [54]. Thus cumene conversion reaction can be chosen as a test reaction to check the presence of Brönsted and Lewis acid sites and also to correlate the product distribution with acidity data. Hence, the main incentive to carry out cumene conversion reaction was to correlate the activity and selectivity with acidity of the prepared catalysts. The selectivity for cracking relates to Brönsted acidity whereas selectivity for dehydrogenation relates to Lewis acidity.

Thus an attempt to correlate the results obtained from cumene conversion reaction with those of DMPY adsorption and perylene adsorption has been done. In order to optimise the reaction parameters, we have investigated their influence on the reaction.

Cumene cracking reaction was carried out in the vapour phase in a fixed bed, down flow, vertical glass reactor of 2 cm diameter and 40 cm length inside a double zone furnace. 0.5 g catalyst was used in the powder form. The catalyst was activated at required temperatures in air for 2 h before every catalytic run. Cumene obtained from Merck was used as such. It was fed into the reactor by a syringe pump at a desired rate. The products, condensed to liquid by a water condenser, were collected and analysed by GC and identified by the comparison of the GC retention times of the samples with pure components expected during the reaction.

3.8.1 Process Optimisation

In order to study the effect of contact time, reaction temperature and activation temperature, $\text{FeAl}_{0.1}\text{PM}$ was selected as a representative of all the catalysts. To study the effect of contact time, cumene was fed at different flow rates keeping other conditions constant. Similarly, to study the effect of reaction temperature, the temperature of the double zone furnace in which the reactor was kept, was set at different temperatures keeping other conditions alike. The catalyst was activated at different temperatures to elucidate the role of activation temperature on the reaction. The reaction was continued to run for five hours to find out whether the catalyst is prone to deactivation during this reaction.

a) Effect of Flow Rate: A typical activity profile of cumene conversion as a function of feed rate over $\text{FeAl}_{0.1}\text{PM}$ is shown in the Figure 3.14. The reaction was carried out at 400°C and the catalyst was activated at 500°C before use. Benzene, toluene, ethylbenzene, styrene and α -methylstyrene are the observed products. Benzene is the normal cracking product and α -methylstyrene, the dehydrogenation product. Dealkylation and side chain cracking resulted in the formation of ethylbenzene and toluene. Dehydrogenation of ethylbenzene formed during the reaction can result in the formation of styrene. Benzene and α -methylstyrene are

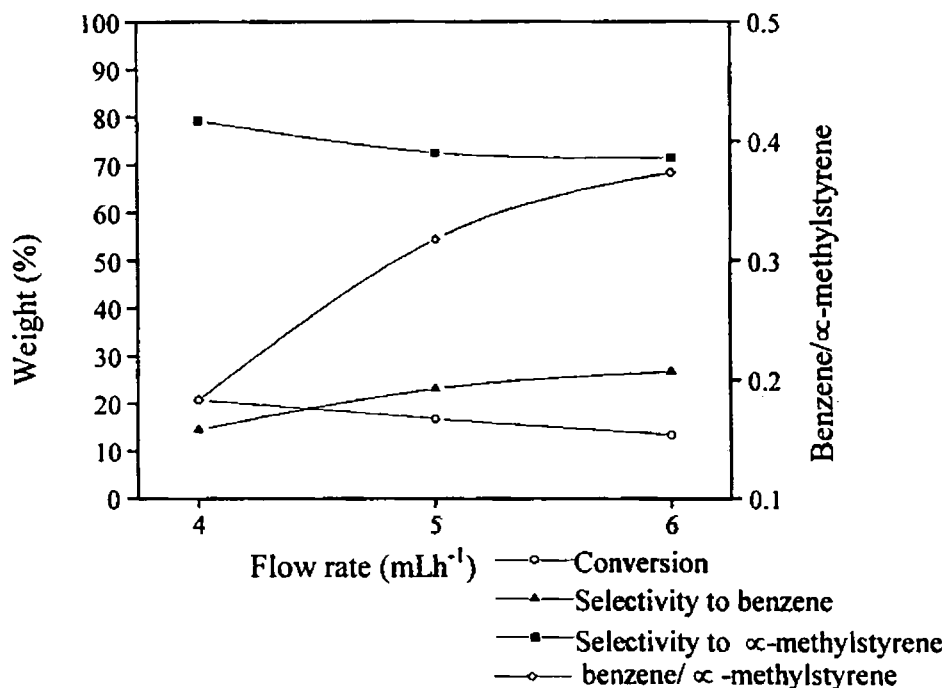


Figure 3.14 Effect of flow rate on the conversion, selectivity and benzene/ α -methylstyrene ratio on cumene conversion reaction. (Reaction conditions: Fe-Al_{0.1}PM- 0.5g, activation temperature- 500°C, reaction temperature-400°C, TOS= 2h)

found to be the major products. As the feed rate increased from 4 to 6 mLh⁻¹, the conversion steadily decreased from 20.73% to 13.36%. At higher flow rates, the contact time will be less and hence the conversion will be less. Maximum selectivity for benzene is obtained at a flow rate of 6 mLh⁻¹. More than 70% selectivity to α -methylstyrene can be explained by pointing out the high temperature of activation of the catalyst. Activation at high temperatures drastically reduces the Brønsted acid sites that are responsible for cracking. The catalyst is possessing large number of Lewis acid sites and hence dehydrogenation was favoured more. The selectivity for other products gradually reduced as the flow rate increased. As contact time decreases (which is a consequence of increasing flow rate), the rate of side reaction also decreased and this resulted in the higher yield of benzene. However, the selectivity for dehydrogenation did not vary much with flow rates and hence the ratio of benzene to α -methyl styrene increased (Figure 3.14).

b) Effect of Reaction Temperature: In another series of experiments, the effect of reaction temperature was studied. Temperatures from 350°C to 500°C were selected. Figure 3.15 shows the influence of reaction temperature on the conversion and

selectivity pattern. As the temperature increased, conversion also increased as expected. The conversion was very low, only about 8.51% at 350°C. The Brönsted

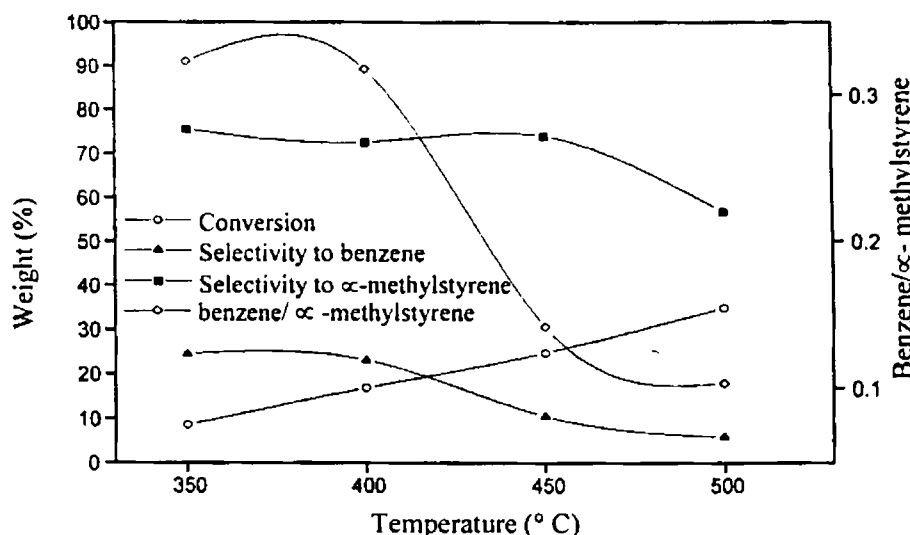


Figure 3.15 Effect of reaction temperature on the conversion and selectivity for cumene conversion. (Reaction conditions: Fe-Al_{0.1}PM-0.5g, activation temperature – 500°C, Flow rate- 5 mLh⁻¹, TOS-2 h.)

acid sites are lost considerably as temperature is increased to 500°C. This resulted in the decrease in selectivity for benzene as the temperature increased. However, selectivity for α-methylstyrene is not much influenced during the temperature range of 350-450°C. Instead, a gradual increase of side products is observed indicative of the side reactions, which occur at high temperatures. At the very high temperature of 500°C, the amount of both α-methylstyrene and benzene were low, as compared to those at other temperatures. Instead, dealkylation occurred at an increased rate to produce other products at this temperature. The sharp decrease in benzene to α-methylstyrene ratio when the temperature changes from 400 to 450°C may be understood in terms of the fact that the Brönsted acid sites got considerably destroyed during this temperature change.

c) Effect of Activation Temperature: The cumene conversion experiments were performed for a series of activation temperatures of the catalyst and the data are shown in the Figure 3.16. As the activation temperature of the catalyst was increased, conversion first increased up to 500°C and then decreased. At higher temperatures of 550 and 600°C, layer collapse of the pillared clay occurred to some extent and this

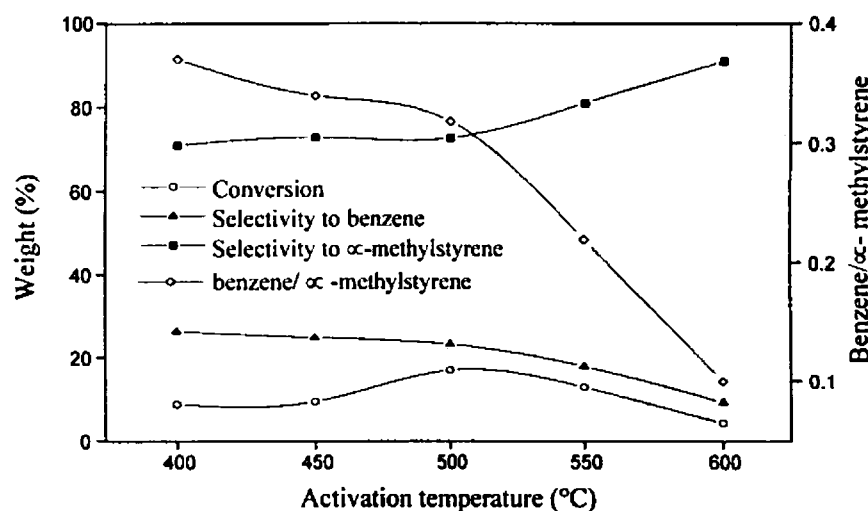


Figure 3.16 Effect of activation temperature on the conversion, selectivity and benzene/ α -methylstyrene ratio for cumene conversion reaction ($\text{FeAl}_{0.1}\text{PM}$ - 0.5 g, reaction temperature – 400°C, Flow rate- 5 mL h^{-1} and TOS= 2 h.)

caused the reduction of surface area. The benzene selectivity gradually decreased due to the gradual loss of Brönsted acid sites as the temperature increased. A concomitant increase in the selectivity for α -methylstyrene was also observed. At higher activation temperatures, dealkylation was not observed, may be due to the structural collapse of the clay. The variation of ratio of benzene to α -methylstyrene from 0.3698 to 0.0995 also suggests the negative effect of temperature on the number of Brönsted acid sites and the temperature independent nature of Lewis sites [51].

d) Effect of Time on Stream - Deactivation Studies

By allowing the reaction to run for five hours, the stability of the catalyst was established. Figure 3.17 show that even after five hours, neither the conversion nor the selectivities vary much. This may be due to the fact that the coke formed during the reaction may not be bulky to block the whole pores of the catalyst [55].

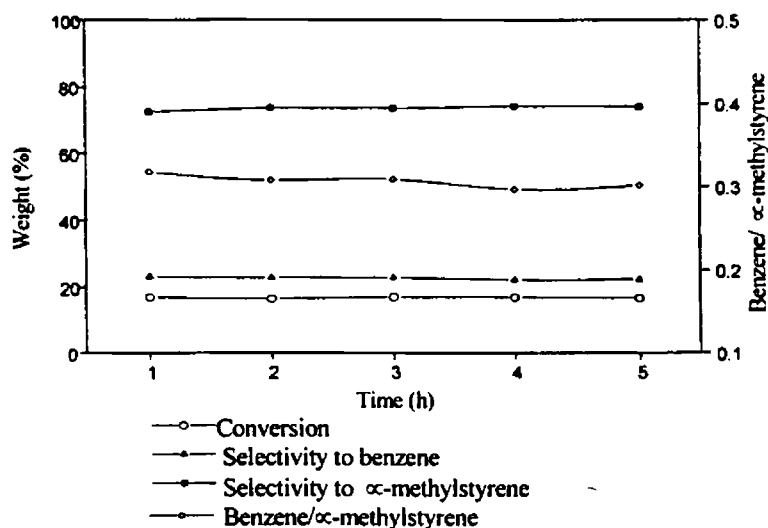


Figure 3.17 Effect of time on stream on the conversion, selectivity and benzene/methyl styrene ratio for cumene conversion reaction ($\text{FeAl}_{0.1}\text{PM}$ - 0.5 g, reaction temperature – 400°C , activation temperature- 500°C and flow rate- 5 mL h^{-1}).

3.8.2 Catalyst Comparison

For carrying out the reaction over various catalysts the reaction was optimised for the following conditions. Activation temperature and reaction temperature were selected as 500°C and 400°C respectively. Flow rate is selected as 5 mLh^{-1} . Reaction temperatures lower than 400°C led to lower percentage conversion and reaction temperatures higher than 400°C led to higher yield for side products. Also, the conversion was maximum at an activation temperature of 500°C . Hence it was selected as the activation temperature for all the catalysts.

The conversion and selectivity for various products are furnished in Table 3.20 for M, AlPM, FePM and mixed Fe-AlPMs. In all the systems, dehydrogenation of cumene to α -methylstyrene was the predominant reaction. Except for AlPM, more than 70% selectivity was observed for α -methylstyrene.

It is noteworthy that M produced α -methylstyrene almost exclusively (selectivity being 96.59%). The conversion, however, was very low. It is well documented that dehydrogenation takes place on Lewis acid sites to give α -methylstyrene. Adsorption experiment showed that M was neutral towards the adsorption of perylene. DMPY got adsorbed on M to a considerable extent.

Table 3.20 Data on cumene conversion reaction over Fe-Al systems (0.5 g catalyst activated at 500°C, reaction temperature – 400°C, flow rate- 5 mL h⁻¹ and TOS= 2 h.).

Catalyst	Conversion (%)	Selectivity for				
		Benzene	Toluene	Ethylbenzene	Styrene	α -methylstyrene
M	1.80	3.14	-	-	-	96.59
AlPM	12.10	38.61	1.08	5.83	1.11	52.37
FeAl _{0.1} PM	16.78	23.06	-	1.97	1.31	72.56
FeAl _{0.2} PM	18.21	19.81	-	0.99	0.31	78.89
FeAl _{0.3} PM	19.00	19.06	-	1.01	0.40	79.53
FeAl _{0.4} PM	21.08	15.41	-	0.81	0.54	83.24
FeAl _{0.5} PM	23.41	6.73	-	0.31	0.16	92.80
FeAl _{1.0} PM	17.34	14.16	-	1.00	0.36	83.48
FePM	18.09	6.31	-	0.43	0.31	92.95

Contrary to these observations, we obtained α -methylstyrene and benzene with percentage selectivity 96.59 and 3.41 respectively for cumene conversion reaction in the case of M. α -methylstyrene formation was attributed to the Lewis acidity imparted by the exchangeable cations present in the clay [54]. Though perylene molecule could not reach these sites to get adsorbed, cumene was able to get adsorbed and undergo reaction, though only to a small extent (conversion very low). From the very low selectivity of benzene, it can be concluded that the exposed clay layer surface was not very active for cracking to benzene. One montmorillonite layer consists of a sheet of aluminium octahedrally co-ordinated by oxy anions and hydroxyls, sandwiched between two silicate sheets. So the exposed surface will be a silicate sheet, which could not provide Brönsted acidity [54].

Catalytic activity for AlPM was 12.10%. Compared to other cases in Table 3.20, AlPM produced a significantly high amount of benzene, the cracking product. This is accountable since this catalyst possessed a comparatively high value

for DMPY adsorption. The Brönsted acid sites were even responsible for an appreciable side chain cracking to produce ethyl benzene and toluene. Dealkylation of cumene to toluene was observed only in the case of AIPM. Dehydrogenation of ethylbenzene, which was formed during the reaction, occurred over the Lewis sites to yield styrene. Anyhow, we can state that the principal reaction taking place was the dehydrogenation of cumene to give α -methylstyrene, since its selectivity was found to be the highest (52.37%).

Incorporation of iron along alumina pillars clearly enhanced the conversion of cumene. Selectivity for benzene decreased and that for α -methylstyrene increased. For iron containing systems, selectivity of α -methylstyrene was found to be in the range 72-93%. This can be attributed to the intrinsic Lewis acidity of iron. AIPM showed a selectivity of 52.37% whereas iron systems exhibited the above range. Increasing Fe/Al ratio from 0.1 to 0.5 increased the conversion from 16.78 to 23.41%. The benzene selectivity decreased and α -methylstyrene selectivity increased. Figure 3.18 shows the trend of Brönsted acidity and selectivity for cracking products among the various Fe-Al systems. It is clear that cracking reaction is dependent on the number of Brönsted acidity. The trend for Brönsted acidity and cracking selectivity follows the same direction (Fig. 3.18). When the Fe/Al ratio was

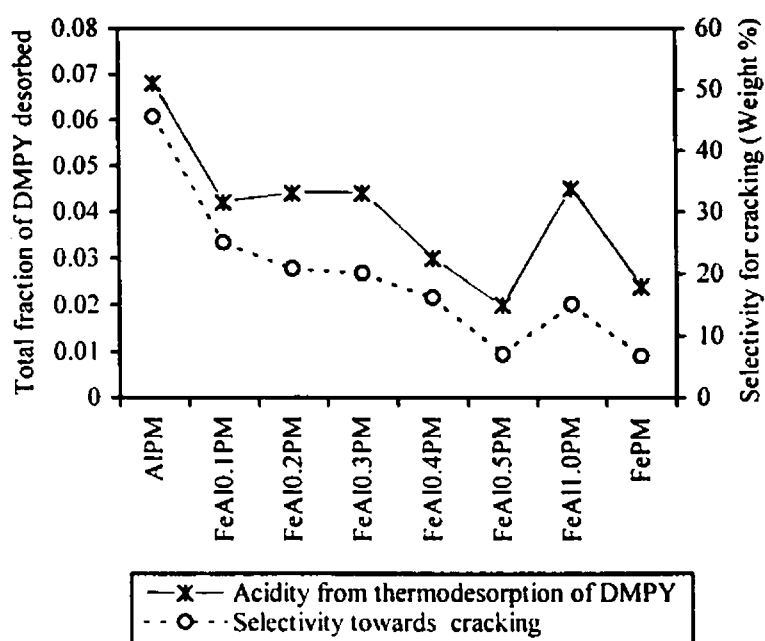


Figure 3.18 Comparison of thermodesorption of DMPY and cracking selectivity for cumene reaction over Fe-Al systems.

increased from 0.5 to 1.0. Brönsted acidity slightly increased and accordingly an increase for cracking products also observed with a concomitant decrease in selectivity for dehydrogenation.

Limiting amount adsorbed from perylene adsorption experiments and the dehydrogenation selectivities of cumene conversion reaction are presented in Figure 3.19. The figure shows that dehydrogenation selectivity was directly proportional to the limiting amount, which amounts the Lewis acid sites. Thus it was concluded that Lewis acid sites were responsible for dehydrogenation. However, a contradiction can be noticed when FePM and FeAl_{0.5}PM were compared. Though the limiting value of FeAl_{0.5}PM was higher than that of FePM, dehydrogenation selectivity was found to be higher for FePM. FePM contains exclusively iron pillars, whereas FeAl_{0.5}PM contained mixed iron-alumina pillars, the latter might have more number of Brönsted acid sites than the former. In effect, this caused a slightly higher yield for cracking products for FeAl_{0.5}PM and hence reduced the yield of the dehydrogenation product. Thus the lower dehydrogenation yield, in spite of its higher Lewis acidity is due to its higher number of Brönsted acid sites. By plotting total

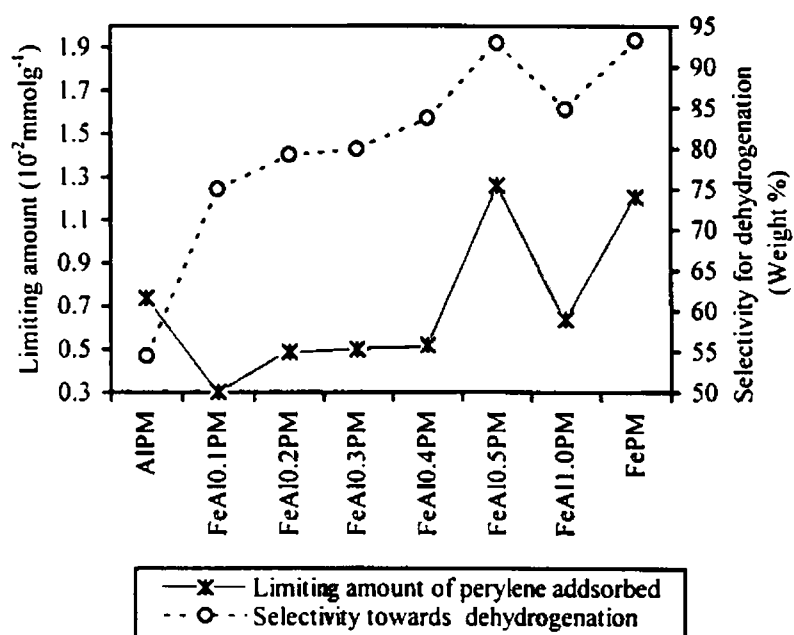


Figure 3.19 Comparison of perylene adsorption data with dehydrogenation selectivity on cumene conversion reaction.

acidity and percentage conversion of various systems in a single graph (Fig 3.20), we can also conclude that conversion is proportional to total acidity. When the Fe/Al

ratio varied from 0.5 to 1.0, the total acidity determined by NH_3 -TPD and Lewis acidity determined by perylene adsorption decreased significantly, whereas Brönsted acidity increased. The decrease in total acidity and Lewis acidity was responsible for

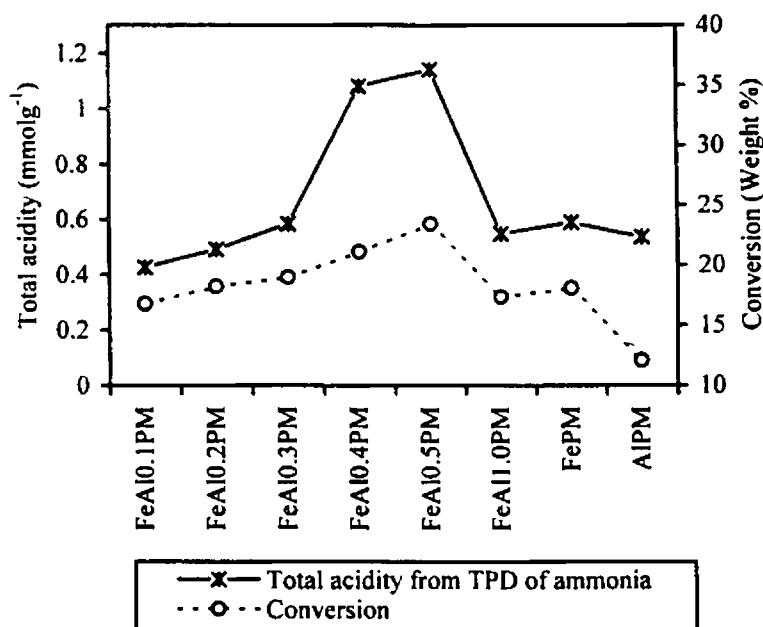


Figure 3.20 Comparison of total acidity from NH_3 -TPD and conversion of cumene.

the decrease in percentage conversion and yield of dehydrogenation products respectively. Though the decrease in total acidity reduced the percentage conversion, the increase in Brönsted acidity enhanced the selectivity of cracking products. This effect is very much pronounced when we compare FePM and AlPM also (Table 3.20).

The results for cumene conversion reaction over mixed Cr-Al systems are presented in Table 3.21. In agreement with the total acidity variation (Table 3.18) for mixed Cr-Al systems, the conversion decreased from the ratio 0.1 to 0.5 and then the percentage conversion slightly increased for the system $\text{CrAl}_{1.0}\text{PM}$. CrPM exhibited higher percentage conversion than the mixed Cr-Al systems and AlPM. It is also worth to note that selectivity for benzene formation was very low in all cases whereas the selectivity for the formation of α -methylstyrene was always around or greater than 85%. Chromia is reported to be a strong Lewis acid [56]. The presence of chromium in the clay lattice was responsible for their high Lewis acidity and hence the dehydrogenation selectivity was high. The comparatively high value of

limiting amount for perylene adsorption also supports that Lewis acidity of Cr containing systems was high.

Table 3.21 Cumene conversion reaction over Cr- Al systems

Catalyst	Selectivity for					
	Conversion	Benzene	Toluene	Ethylbenzene	Styrene	α -methylstyrene
AIPM	12.10	38.61	1.08	5.83	1.11	52.37
CrAl _{0.1} PM	10.84	9.11	-	-	-	90.89
CrAl _{0.2} PM	10.09	10.13	-	-	-	89.87
CrAl _{0.3} PM	8.43	6.31	-	-	-	93.69
CrAl _{0.4} PM	7.01	5.04	-	-	-	94.96
CrAl _{0.5} PM	6.37	5.02	-	-	-	94.98
CrAl _{1.0} PM	6.99	6.94	-	-	-	93.06
CrPM	14.61	14.03	-	0.81	0.41	84.75

Table 3.22 presents the cumene conversion results for the vanadia impregnated systems. Vanadia impregnation increased the catalytic activity only slightly. Higher loading resulted in the decrease of percentage conversion. This can be attributed to the decrease in the acidity for the high loaded samples. Cracking selectivities were found to be very much higher for the systems with high vanadia loadings (22.13-43.62% for 7-20VFe) and correspondingly dehydrogenation selectivities were low for the high loading systems, compared to low loading systems and the parent iron-pillared montmorillonite. Thermodesorption values of DMPY over the solids increased from 2VFe up to 7VFe and then reduced, whereas limiting amount of perylene adsorbed over the solids continued to decrease even from 2VFe. 20VFe directed the reaction almost equally towards cracking and dehydrogenation, and the low percentage conversion was due to the very low surface area and pore volume ($14.63 \text{ m}^2\text{g}^{-1}$ and $0.0210 \text{ cm}^3\text{g}^{-1}$ respectively) and the very low acidity values. The inhibition of Lewis acidity due to the high loading led to the reduction of percentage selectivity of α -methylstyrene significantly while that for cracking (only benzene) increased.

Table 3.22 Cumene conversion reaction over vanadia loaded iron-pillared montmorillonites (0.5 g catalyst activated at 500°C, reaction temperature – 400°C, flow rate- 5 mL h⁻¹ and TOS= 2 h.)

Catalyst	Selectivity for					
	Conversion	Benzene	Toluene	Ethylbenzene	Styrene	α -ethylstyrene
FePM	18.09	6.31	-	0.43	0.31	92.95
2VFe	18.01	7.01	-	0.30	-	92.69
5VFe	20.11	12.34	0.61	0.74	0.24	86.07
7VFe	26.13	19.88	1.31	0.94	0.51	77.36
10VFe	19.99	25.11	0.86	0.31	-	73.72
15VFe	10.61	28.64	-	-	-	71.36
20VFe	4.21	43.62	-	-	-	56.38

3.9 Cyclohexanol Decomposition Reaction as a Test Reaction for Acidity

Cyclohexanol decomposition reaction is usually adopted to check the acid-base property of the catalyst system [57, 58]. The amphoteric character of the alcohol permits its interaction with both acidic and basic centres. As a result of this, dehydration and dehydrogenation are catalysed by the oxide system resulting in the formation of cyclohexene and cyclohexanone respectively [59, 60]. Dehydrogenation takes place with the intervention of both acidic and basic sites and dehydration takes place with the participation of acidic sites only. Figure 3.21 shows the mechanism of formation of cyclohexene and cyclohexanone over the oxide catalyst surface.

The decomposition of cyclohexanol was carried out in the vapour phase. A glass reactor of length 40 cm and diameter 2 cm was used. The liquid products collected were analysed by a Chemito 8610 GC analyser fitted with FID using carbowax column (2 m). Products detected were cyclohexene, cyclohexanone, benzene, methylcyclopentene and cyclohexane. Products such as benzene, methylcyclopentene and cyclohexane were taken together and labelled as 'others' in the tables. However, these three products are due to the further transformation of cyclohexene formed during the reaction.

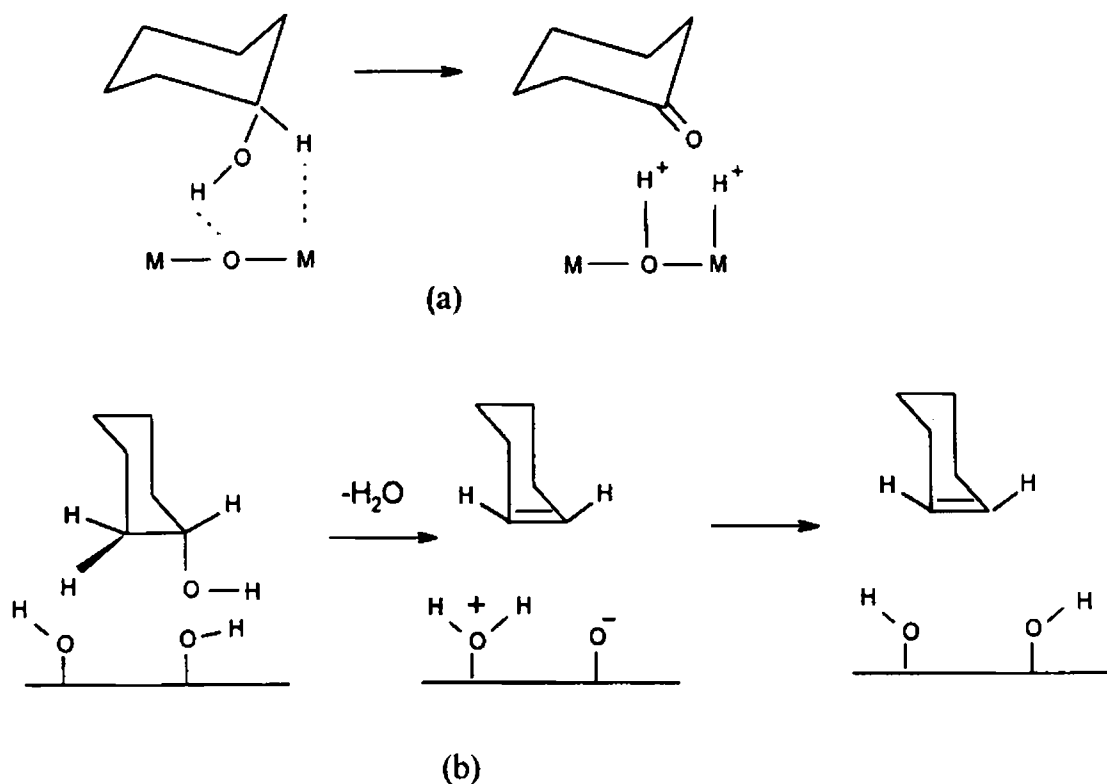


Figure 3.21 Mechanism of (a) dehydrogenation and (b) dehydration of cyclohexanol on oxide surface

The selectivity was calculated as ‘-ene’ selectivity ($C=C$) and ‘-one’ selectivity ($C=O$). ‘Others’ are also included in the ‘-ene’ selectivity, since all of these were formed by the further transformation of cyclohexene. The formation of phenol is reported by the transformation of cyclohexanone [61]. In the present case, no phenol is detected in any instance. Hence ‘others’ can be undoubtedly incorporated in the ‘-ene’ selectivity.

Here, we report the optimisation of the various reaction parameters for the vapour phase decomposition of cyclohexanol over iron-pillared montmorillonite and also the comparison of activity and selectivity of the various catalysts. The results obtained are correlated with the acidity data also.

3.9.1 Process Optimisation

a) Effect of Reaction Temperature: Table 3.23 shows the influence of reaction temperature towards the conversion and selectivity. As the temperature increased, the percentage of conversion also increased. The $C=C$ selectivity was found to be more than 95% at all temperatures. The conversion reached a maximum of 87.82% at a

temperature of 450°C. The formation of cyclohexanone was very little as evident from its yield and selectivity. Cyclohexanone was formed by the involvement of both acidic and basic sites [59, 60]. Though enough number of acidic sites was present, absence of basic sites on the clay surface restricted the formation of cyclohexanone. Negligible amounts of cyclohexanone were formed at all temperatures compared to cyclohexene. As the temperature increased, the yield of 'others' also increased to a large extent (Table 3.23). At higher temperatures, further transformations of cyclohexene were more feasible and this resulted in the higher percentage yield of benzene, cyclohexane and methylcyclopentene.

Table 3.23 Effect of reaction temperature on cyclohexanol decomposition reaction over FePM (Reaction parameters: Catalyst - FePM (0.5 g), flow rate - 5 mLh⁻¹, activation temperature- 500°C, TOS-2h)

Reaction Temp.(°C)	Conversion (%)	Product Distribution (Yield) (%)			Selectivity (%)	
		Cyclohexene	Cyclohexanone	Others	C=C	C=O
250	25.79	23.17	1.08	1.535	95.79	4.21
350	91.26	62.32	1.61	27.33	98.24	1.76
450	97.82	68.66	1.81	27.35	98.15	1.85

b) Effect of Feed Rate: The reaction was carried out at different flow rates viz., 4, 5 and 6 mLh⁻¹ to understand the influence of flow rate on the reaction. As the flow rate increased, conversion gradually reduced. However, no regular pattern for the '-ene' and the '-one' selectivities was seen. Maximum selectivity for C=C was observed at a flow rate of 5 mLh⁻¹. At a flow rate of 4 mLh⁻¹, the yield for cyclohexene was less. This is due to the increased transformation of cyclohexene to other products such as benzene, cyclohexene and methyl cyclopentene, which is evident from the comparatively high yield of 'others' (Table 3.24). At the high flow rate of 6 mLh⁻¹, cyclohexanol may probably wash out the cyclohexene from the catalyst surface and reduces the further transformation of cyclohexene. Hence the yield of 'others' is less.

c) Effect of Activation Temperature: Table 3.25 gives the influence of activation temperature on the reaction. The catalyst was preheated at various temperatures before carrying out the reaction. When the catalyst, dried at 110°C was used as such without calcination, almost 99% selectivity was observed for the formation of

Table 3.24 Effect of flow rate on cyclohexanol decomposition reaction over FePM. (Reaction conditions: FePM (0.5 g), reaction temperature- 350°C, activation temperature -500°C, TOS-2h)

Flow rate (mLh ⁻¹)	Conversion (%)	Product Distribution (Yield) (%)			Selectivity (%)	
		Cyclohexene	Cyclohexanone	Others	C=C	C=O
4	98.22	55.52	5.9	36.8	94.0	6.0
5	91.26	62.32	1.61	27.33	98.24	1.762
6	82.27	73.15	3.9	5.22	94.74	5.26

cyclohexene. The conversion was very low since the catalyst contains only Brönsted acid sites almost exclusively. Lewis acid sites may not be generated at this drying condition. Dehydration and dehydrogenation of the pillars take place and the catalyst acquires conversion was very low since the catalyst contains only Brönsted acid sites almost exclusively. Lewis acid sites may not be generated at this drying condition. Dehydration and dehydrogenation of the pillars take place and the catalyst acquires its actual structure and catalytic activity only after calcination at a higher temperature. Calcination at higher temperature leads to high percentage conversion. In all cases the selectivity for cyclohexanone was found to be negligible while that of cyclohexene was more than 96%.

Table 3.25 Effect of activation temperature on cyclohexanol decomposition reaction over Fe PM (Reaction parameters: Catalyst- 0.5 g, reaction temperature- 350°C, flow rate- 5 mLh⁻¹, TOS- 2 h.)

Activation Temp.(°C)	Conversion (%)	Product distribution (Yield) (%)			Selectivity (%)	
		Cyclohexene	Cyclohexanone	Others	C=C	C=O
110	38.62	38.01	0.61	-	98.5	1.50
300	43.62	35.43	1.37	6.82	96.86	3.14
400	78.69	68.31	1.52	8.86	98.07	1.93
500	91.26	62.32	1.61	27.33	98.24	1.76

d) Effect of Time on Stream

To study the influence of reaction time on the catalyst's stability, three different catalysts were studied under the time on stream condition. FePM, CrPM and 2VFe were selected for the deactivation study. For all the three catalysts, conversion

considerably reduced as the time on stream increased (Figure 3.22). Maximum deactivation was observed for 2VFe and minimum for CrPM. The initial conversion of 92.32% of CrPM reached only 70.23% after the 5th hour of stream whereas that of the 2VFe changed from 90.96 to 39.65%. For FePM, the change was intermediate between these two cases. Deactivation was more for 2VFe compared to other two, may be due to the presence of more strong sites in 2VFe compared with the other two. Strong acidity is associated with faster deactivation of the catalyst.

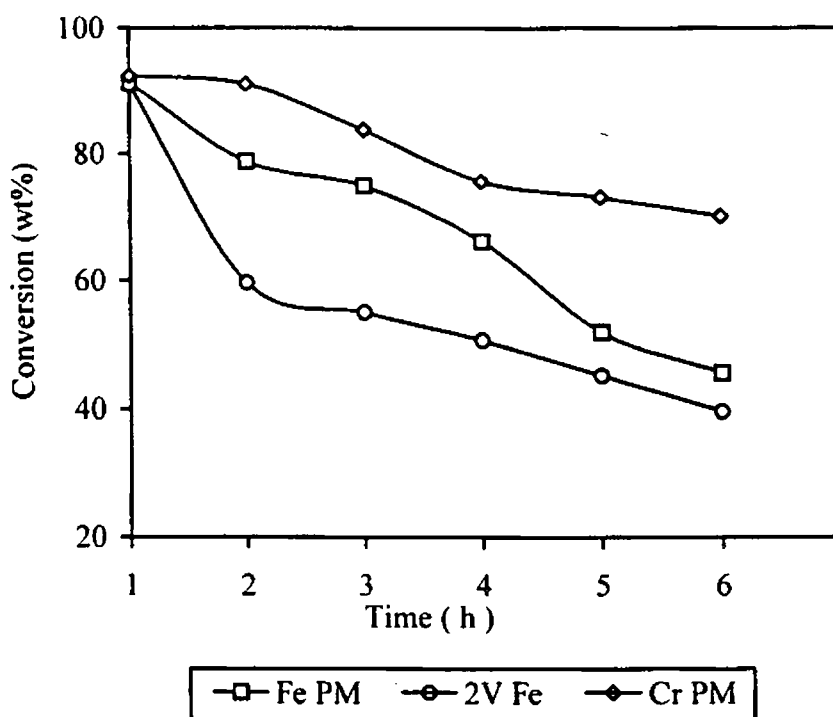


Figure 3.22 Deactivation study for cyclohexanol decomposition reaction over FePM, 2VFe and CrPM. (Reaction parameters: Catalyst- 0.5 g, reaction temperature- 350°C, flow rate- 5 mLh⁻¹, TOS- 2 h.)

3.9.2 Catalyst Comparison

Tables 3.28–3.30 depict the results of decomposition of cyclohexanol over the various systems. Parent montmorillonite, owing to its very low surface area and acidity, displayed only poor activity (Table 3.26). The increase in acidity increased the activity for the modified systems. Though there is a general agreement that the dehydration reaction is favoured by Brönsted acidity, we could not get any direct relationship with Brönsted acidity alone. It seems that the Lewis acidity also plays a major role in deciding the activity, but not alone. Comparing the reaction data with various acidity data, we could find a direct relationship of the activity and

dehydration activity ('-ene' selectivity) with the sum of weak and medium acidity. And of course, the reaction seems to be an easy reaction that could be catalysed by the clay systems since the activity is more than 80% in most cases. The Lewis and

Table 3.26 Cyclohexanol decomposition over Fe-Al systems

Catalyst	Conversion (%)	Product Distribution (%)			Selectivity	
		Cyclohexene	Cyclohexanone	Others	-ene	-one
M	29.49	28.10	1.39	-	95.29	4.71
AlPM	91.94	74.60	2.64	14.7	97.13	2.87
FeAl _{0.1} PM	88.01	70.83	1.08	16.1	98.77	1.23
FeAl _{0.2} PM	88.11	56.96	1.11	29.94	98.74	1.26
FeAl _{0.3} PM	90.11	59.02	1.01	30.08	98.88	1.12
FeAl _{0.4} PM	96.13	62.66	1.83	31.64	98.10	1.90
FeAl _{0.5} PM	94.62	58.70	1.00	34.92	98.94	1.06
FeAl _{1.0} PM	91.84	73.68	2.05	16.11	97.77	2.23
FePM	91.26	62.32	1.61	27.33	98.24	1.76

Table 3.27 Cyclohexanol decomposition over Cr-Al systems

Catalyst	Conversion (%)	Product Distribution (%)			Selectivity	
		Cyclohexene	Cyclohexanone	Others	-ene	-one
AlPM	91.94	74.60	2.64	14.7	97.13	2.87
CrAl _{0.1} PM	86.99	64.27	2.11	20.61	97.57	2.43
CrAl _{0.2} PM	80.76	56.79	2.98	20.99	96.30	3.70
CrAl _{0.3} PM	78.41	52.76	1.04	24.61	98.67	1.33
CrAl _{0.4} PM	70.10	43.00	2.01	25.09	97.13	2.87
CrAl _{0.5} PM	70.06	48.67	1.98	16.21	97.17	2.83
CrAl _{1.0} PM	84.61	62.76	2.44	19.41	96.11	3.89
CrPM	94.11	86.62	1.38	6.11	98.53	1.47

Table 3.28 Cyclohexanol decomposition over vanadia loaded iron pillared montmorillonites.

Catalyst	Conversion (%)	Product Distribution (%)			Selectivity	
		Cyclohexene	Cyclohexanone	Others	-ene	-one
FePM	91.26	62.32	1.61	27.33	98.24	1.76
2VFe	88.61	57.59	2.01	29.01	97.73	2.27
5VFe	95.39	57.79	2.98	34.62	96.88	3.12
7VFe	96.01	58.08	2.31	35.62	97.59	2.41
10VFe	83.00	49.44	2.56	31.00	97.82	3.08
15VFe	50.10	35.21	2.88	12.01	94.25	5.75
20VFe	33.11	20.33	2.88	9.90	91.30	8.70

Brønsted acidity in the weak and medium range seems promoting the conversion of cyclohexanol. The cyclohexene formed during the reaction is transforming to other products such as benzene, cyclohexane and methylcyclopentene. These changes are favoured by the strong acidity present on the systems. The very low percentage yield of cyclohexanone confirms the absence of enough basic sites on the catalyst. However, the presence of surplus acidity does not affect the conversion and dehydration activity. This can be evidenced by comparing the data for FeAl_{0.3}PM and FeAl_{0.4}PM. Though the sum of weak and medium acidity is two-fold greater for FeAl_{0.4}PM than FeAl_{0.3}PM, both have almost same conversion, thus the change in activity is not commensurating with the increase in acidity due to weak and medium strong acid sites. Comparing 7VFe and FePM, the acidity due to weak and medium strong acid sites is three times greater for the former than the latter. But the activities are not very different. This again suggests the non-requirement of surplus acidity for the reaction.

References

- [1] G. Johansson, *Acta. Chem. Scand.*, 14 (1960) 15.
- [2] B.O. A. Hedstrom, *Arkiv. Kemi*, 6 (1953) 1.
- [3] D.L. Zvyagintsev and S.B. Lyakhmanov, *Russ. J. Inorg. Chem.*, 13 (1968) 643.
- [4] J. Sutton, *Nature*, 169 (1952) 71.
- [5] A.R. Olsen and T. R. Simonson, *J. Chem. Phys.*, 17(1949) 1322.
- [6] M.M. Jones, E. A. Jones, D.E. Harman and R.T. Semmes, *J. Amer. Chem. Soc.*, 3 (1961) 2038.
- [7] L.N. Mulay and P.W. Selwood, *J. Amer. Chem. Soc.*, 77 (1955) 2693.
- [8] J. Bjerrum, G. Schwarzenbach and L.G. Silten, *Stabilizing Constants of Metal-Ion Complexes*, Spe. Pub. Chem. Soc., London, (1964) 17.
- [9] R. N. Sylva, *Rev. Pure Appl. Chem.*, 22 (1972) 115.
- [10] J. A. Laswick and R.A. Plane, *J. Amer. Chem. Soc.*, 81(1959).
- [11] H. Stünzi and W. Marty, *Inorg. Chem.*, 22 (1983) 2145.
- [12] H. Stünzi and L. Spiccia, R.P. Rotzinger and W. Marty, *Inorg. Chem.*, (1989) 2866.
- [13] D. Zhao, G. Wang, Y. Yang, X. Guo, Q. Wang and J. Ren, *Clays Clay Miner.*, 41 (1993) 317.
- [14] S. Yamanaka and H. Hattori, *Catal. Today*, 2 (1988) 261.
- [15] P. Canizares, J.L. Valverde, M.R. Sunkou and C.B. Molina, *Micropor. Mater.*, 29 (1999) 267.
- [16] D. Zhao, Y. Yang and X. Guo, *Zeolites*, 5 (1995) 58.
- [17] T.J. Pinnaivia, *Science*, 220 (1983) 365.
- [18] T. Blasco, J. Lopez-Nieto, A. Dejoz and M.I. Vasquet, *J. Catal.*, 159 (1995) 271.
- [19] J.R. Shon, S.G. Cho, Y.I. Pae and S. Hayashi, *J. Catal.*, 159 (1996) 170.
- [20] J.M. Lopez-Neito, G. Kremnik and J.L.G. Fiero, *Appl. Catal.*, 61 (1990) 235.
- [21] S. Narayanan and B.P. Prasad, *J. Mol. Catal.*, 96 (1995) 57.
- [22] S. Narayanan and K. Deshpande, *Appl. Catal. A Gen.*, 135 (1996) 125.
- [23] M. Thompson and R.E. Connick, *Inorg. Chem.*, 20 (1981) 2279.
- [24] L. Spiccia, W. Marty and R. Giovanoli, *Inorg. Chem.*, 27 (1988) 2660.
- [25] N.N. Greenwood and A. Earnshaw, *Chemistry of the Elements*, Pergamon Press, New York, 1984

- [25] N.N. Greenwood and A. Earnshaw, *Chemistry of the Elements*, Pergamon Press, New York, 1984
- [26] T. Mishra and K. Parida, *Appl. Catal. A Gen.*, 166 (1998) 123.
- [27] S. Narayanan, K. Deshpande and B.P. Prasad, *J. Mol. Catal.*, 88 (1984) L 271.
- [28] H. Ming-Yuan, L. Zhonghui and M. Enze, *Catal. Today*, 2 (1988) 321.
- [29] B.M. Reddy, M. Vijayakumar and K. Jeeva Ratnam, *Appl. Catal. A Gen.*, 181 (1999) 77.
- [30] A. Corma, *Chem. Rev.*, 95 (1995) 559.
- [31] P.A. Jacobs and C.F. Heylen, *J. Catal.*, 34 (1974) 267.
- [32] H. Knozinger, H. Kriwtenbrink and P. Ratnasamy, *J. Catal.*, 48 (1977) 436.
- [33] A. Corma, C. Rodellas and V. Fornes, *J. Catal.*, 88 (1984) 374.
- [34] H. Miyata and J.B. Moffat, *J. Catal.*, 62 (1980) 357.
- [35] A. Satsuma, Y. Kamiya, Y. Westi and T. Hattori, *Appl. Catal. A Gen.*, 194 (2000) 253.
- [36] P.L. Hall, *Clay Miner.*, 15 (1985) 321.
- [37] J.C. Davidtz, *J. Catal.*, 43 (1976) 260 .
- [38] S.M. Bradley and R.A. Kydd, *J. Catal.*, 141 (1993) 239.
- [39] S. Bodoardo, F.Figueras and E. Garroen, *J. Catal.*, 147 (1994) 223.
- [40] M.M. Khader, *J. Mol. Catal. A Chem.*, 104 (1995) 87.
- [41] J.J. Rooney and R.C. Pink, *Proc. Chem. Soc.*, (1961) 70.
- [42] D. Flockart, J.A.N.Scott and R.C. Pink, *Trans. Farad. Soc.*, 62 (1966) 730.
- [43] J. Kijenski and A. Baiker, *Catal. Today* (1989) 1.
- [44] T.J. Dines, C.H. Rochester and A.W. Ward, *J. Chem. Soc. Farad. Trans.*, 87 (1991) 1611.
- [45] M. Takalji, T.K. Qwai, M. Soma, Onoshi and K. Tamaru, *J. Phys. Chem.*, 80 (1976) 430.
- [46] M. Takalji, T.K. Qwai, M. Soma. Onoshi and K. Tamaru, *J. Catal.*, 50 (1977) 441.
- [47] M. Trombetta, G. Busca, M. Lenarda, L. Storaro, R. Ganzerla, L. Piovesan, A.J. Lopez, M. Alcantara Rodriguez and E.R. Castellon, *Appl. Catal. A Gen.*, 193 (2000) 550

- [51] T. Mishra and K. Parida, *Appl. Catal. A Gen.*, 174 (1988) 91.
- [52] T. Mishra and K. Parida, *Appl. Catal. A Gen.*, 166 (1998) 123.
- [53] A. Gil, L.M. Gandia and M.A. Vicente, *Catal. Rev. Sci. Engg.*, 42 (2000) 145.
- [54] S.M. Bradely and R.A. Kydd, *J. Catal.*, 141 (239) 1993.
- [55] P. Wu, T. Komatsu, T. Yashima, *Micropor. Mesopor. Mater.*, 22 (1998) 343.
- [56] S. Narayanan and K. Deshpande, *Appl. Catal. A Gen.*, 199 (2000) 1.
- [57] S.J. Kulkarni, R. Ramachandra Rao, M. Subrahmanyam and A.V. Rama Rao, *J. Chem. Soc. Chem. Commun.*, (1994) 273.
- [58] P. Bezouhanova, Chr. Dimitrov, V. Nenorva, Yu Kalvachev and H. Lechert, *Stud. Surf. Sci. Catal.*, 49 (2989) 1223.
- [59] M. Ai, *J. Catal.*, 40 (1975) 318.
- [60] M. Ai, *Bull. Chem. Soc. Jpn.*, 50 (1977) 2587.
- [61] N. John Febarathinam and V. Krishnaswamy, *Catalysis: Present and Futures* (P. Kanta Rao and B.S. Benwal (Eds.)), Publication and Information Directorate, New Delhi- p-288.

Catalytic Activity Of Pillared Clays In Liquid Phase And Vapour Phase Alkylation And Acylation Reactions

4.0 Friedel-Crafts Reactions

Friedel-Crafts reactions (alkylation and acylation of aromatic compounds) constitute a very important class of reactions, which are of common use in organic chemistry. Lewis acids such as AlCl_3 or BF_3 etc. are well-known for promoting Friedel-Crafts alkylation and acylation reactions [1-5]. Protonic acids such as HF and H_2SO_4 have also been extensively studied for the reaction [6]. However, because of the environmental problems posed by the use and disposal of these hazardous homogeneous acid reagents, there has been a growing interest in using alternatives. Active research has been directed at replacing the traditional homogeneous catalysts with heterogeneous ones such as clay minerals and zeolites [7]. Sulphated zirconia [8] and zinc chloride impregnated K10 montmorillonite [9] are found to be efficient heterogeneous catalysts in the Friedel-Crafts alkylation and acylation reactions. Zinc chloride impregnated K10 montmorillonite, called 'clayzic' is found to be the most efficient material that catalysed the alkylation of aromatics [9] and subsequently the process is commercialised. Materials such as pillared clays and rare-earth exchanged pillared clays, Keggin type heteropolyacids, sulphated zirconia and graphite have been proven to catalyse acylation reactions [10-13]. Acid molecular sieves have also been widely used as acylation catalysts and more specifically medium and large pore zeolites have been presented as the ultimate catalysts for the future industrial production of aromatic ketones [14].

He *et al.* studied alkylation reactions of benzene with benzyl chloride using iron containing mesoporous molecular sieve materials [15]. They found that iron containing mesoporous materials are very active benzylation catalysts with a monoalkylated product selectivity of 100% under the experimental conditions. Highly dispersed and/or impregnated Fe(III) species are found to be more responsible for catalytic activity than exchangeable Fe(III) species. Temperature and pore size are convinced to be two critical factors influencing the activities of the investigated

systems. They also found that these efficient catalysts could not catalyse the said reaction at temperatures $\leq 40^\circ\text{C}$. Following this observation, they suggested a redox mechanism operating during the reaction, which was previously suggested by Choudhary *et al.* [16]. This mechanism involves the homolytic rupture of the carbon-chlorine bond followed by the oxidation of the radical, to give the benzyl carbocation.

The redox mechanism is suggested by Choudhary *et al.* [16] after confirming the influence of iron content of the various clay samples on which they studied the benzylation reaction, on activity. Fe^{3+} is an easily reducible cation and the presence of larger amounts of this cation will lead to higher activity. Both the teams of Choudhary [16] and He [15] could not find any correlation with acidity and activity. Instead, they confirmed the influence of reducible cations and suggested the free radical mechanism.

Benzylation of aromatics over clays exchanged by various ions was studied by Cseri *et al.* [17] using two different benzylating agents, viz. benzyl alcohol and benzyl chloride. They have exchanged the clays with Fe^{3+} , Ti^{4+} , Zr^{4+} , Cu^{2+} , Zn^{2+} , Ce^{3+} , Cr^{3+} and Sn^{2+} ions and used for the reaction. They have established the influence of reducible cations and hence proposed the redox mechanism. When benzyl alcohol was used as the alkylating agent, the mechanism is purely ionic (a carbocation mechanism). But when the benzylating agent was benzyl chloride, a radical mechanism is found to be operating. The benzyl radical, being a powerful reductant, gets readily oxidised to benzyl cation in presence of reducible metallic ions such as Fe^{3+} , Sn^{4+} or Cu^{2+} . Hence activities were found to be high for systems containing these ions.

The catalytic activity for the alkylation reaction depended significantly on synthesis methods rather than structural differences for KIT-1, MCM-41 and MCM-48, the mesoporous silica molecular sieves over which benzylation of benzene, toluene and m-xylene were performed by Jun *et al.* [18].

Employing β -zeolites, acylation of toluene has been carried out by Botella *et al.* [19]. β -Zeolite is found to be a good catalyst for the acylation of toluene with acetic anhydride at low temperature (150°C). Though reasonable conversions with

very high selectivities to methylacetophenone are obtained, the poisoning of the active sites by adsorption of products and coke limit the extent of the reaction.

Baudry-Barbies *et al.* proved [20] that thermally activated rare-earth salts deposited on solid inorganic supports such as K10 montmorillonite and silica are very efficient catalysts for acylations of aromatic substrates. They have also found that K10 montmorillonite is a better support than silica for preparing effective catalysts.

Hino and Arata [21] employed solid superacids for acylation of toluene with acetic anhydride and benzoic acid. They confirmed that under the experimental conditions, the acid catalyst of ZrO_2 with an acid strength of $H_0 \leq -16.04$ is most effective in the reactions.

Benzoylation of *o*-xylene using various zeolite catalysts was reported by Jacob *et al.* They found the selective formation of 3,4-dimethylbenzophenone [22].

We report in this section of the chapter, the results of Friedel-Crafts alkylation (benzylation) and acylation (benzoylation) of toluene catalysed by the various pillared montmorillonites and modified pillared montmorillonites. We have also studied the influence of alkylating agent, temperature and moisture and the extent of metal leaching for the alkylation reaction of toluene.

4.1 Benzylation of Toluene

Benylation of toluene has been carried out using two different alkylating agents namely benzyl chloride and benzyl alcohol. The reaction between benzyl chloride or benzyl alcohol and toluene was carried out in liquid phase in a 50 mL round-bottomed flask, equipped with a magnetic stirrer, a thermometer and a reflux condenser with a $CaCl_2$ guard tube. The heating was done in an oil bath, the temperature of which was controlled by a dimmerstat. For each reaction, a mixture of substrate and alkylating agent was taken in the desired molar ratio and the activated catalyst was introduced into the reactor. After reaction, the mixture was analysed using gas chromatography.

4.1.1 Benzylation of Toluene with Benzyl Chloride

The essential feature of the alkylation reaction is the replacement of a hydrogen atom of an aromatic compound by an alkyl group derived from an

alkylating agent. A schematic representation of the reaction between toluene and benzyl chloride is shown below. The products identified were *ortho* and *para*-methyldiphenylmethane (*o*-MDPM and *p*-MDPM respectively).

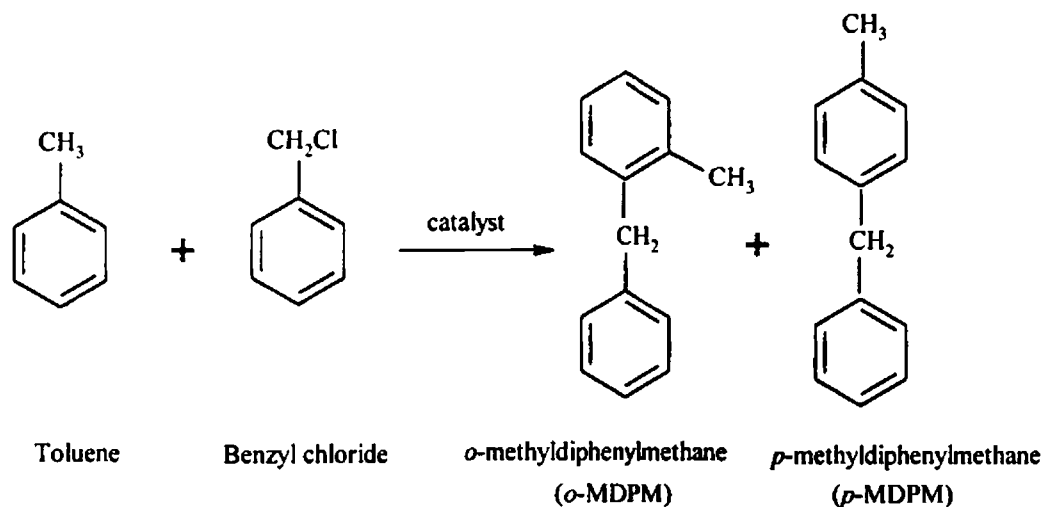


Figure 4.1 Benzylation of toluene with benzyl chloride

For process optimisation, we have studied the influence of the presence of a catalyst, temperature and moisture. We have tested the reaction for any metal leaching to assess whether truly heterogeneous reaction is taking place.

a) Presence of Catalyst

First of all, we made the reaction run using benzyl chloride and toluene in the absence of a catalyst (blank run) at the refluxing temperature of the mixture. In this case, we observed a percentage conversion of 11.79 after five minutes of reaction. However, when we tried the reaction using FePM catalyst, complete conversion of benzyl chloride was obtained within five minutes. The data are shown in Table 4.1. Low yield for the reaction in the absence of the catalyst is due to the higher activation

Table 4.1 Benzylation of toluene with benzyl chloride in the absence and presence of a catalyst (0.1 g FePM activated at 500°C, benzyl chloride: toluene molar ratio-1: 10, reaction temperature-110°C)

	Time of reaction (min)	Conversion (%)
Without catalyst	5	11.79
With catalyst	5	100

energy of the uncatalysed reaction. The addition of the catalyst significantly reduces the activation energy as the reaction now proceeds through a different path with a lower activation energy, resulting in a higher percentage conversion.

b) Effect of Temperature

To investigate the influence of temperature on the reaction between toluene and benzyl chloride, a series of experiments were carried out at different temperatures keeping other reaction conditions the same. The results are furnished in Table 4.2. We have observed only monoalkylated products; the products were identified as *o*-methyldiphenylmethane and *p*-methyldiphenylmethane. The temperatures selected for the study were in the range, 40 - 110°C. Complete conversion of benzyl chloride was observed for temperatures 80°C and above. Also, *p*-MDPM was formed selectively at these temperatures. Higher temperatures favour the formation of the more thermodynamically stable product namely *p*-MDPM. At a lower temperature of 70°C also, 100% selectivity was observed for *p*-MDPM, but complete conversion of benzyl chloride was not observed. At 60°C, the conversion was still low, but a distribution of products was established. However, *p*-MDPM was the major product. At temperatures 50°C and 40°C, conversion was very low compared to those at higher temperatures. Here also, the only product detected is *p*-MDPM.

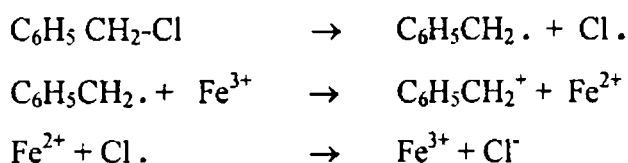
The data shown in Table 4.2 reveal that as the temperature increased from 50 to 60°C, the conversion jumped from 10.93 to 86.82%. But, the increase of temperature from 60 to 70°C caused the conversion to increase only by a small percentage. Thus it is clear that the sharp leap in conversion as the reaction temperature changes from 50 to 60°C is not merely due to a temperature effect. Some other cause such as a sudden turn in the reaction mechanistic route seems to apply here and hence it is relevant to probe into the reaction mechanism. Fe^{3+} is an easily reducible cation. The reduction potential for $\text{Fe}^{3+} \rightarrow \text{Fe}^{2+}$ is + 0.77 eV. This high reduction potential enables Fe^{3+} ion to accept a single electron easily, itself getting readily reduced to Fe^{2+} . This strongly suggests the possibility of a redox mechanism. The existence of the radicals was substantiated by ESR studies carried out by Cativiela *et al.* [23]. However, there is a large consensus that Friedel-

Crafts reaction proceeds through carbocations [24] and that radicals are powerful reductants, which should be readily be oxidised to cations in presence of reducible

Table 4.2 Data on the influence of temperature on benzylation of toluene with benzyl chloride (0.1 g FePM, benzyl chloride: toluene molar ratio-1: 10, 30 min. run)

Temperature (°C)	Conversion (%)	Selectivity (%)	
		<i>o</i> -MDPM	<i>p</i> -MDPM
110	100	-	100
80	100	-	100
70	94.59	-	100
60	86.82	23.5	76.5
50	10.93	-	100
40	2.10	-	100
30	-	-	-

metallic ions such as Fe^{3+} . In consonance with the above statement, we can propose a mechanism involving carbocations, the carbocations being formed by the oxidation of the radical in presence of the reducible metallic cation, Fe^{3+} . A sudden jump in conversion from 10.67 to 86.82% conversion when the temperature was increased from 50°C to 60°C could then be ascribed to a different initiation of the reaction. Homolytic rupture of the carbon-chlorine bond in benzyl chloride is the initiation reaction to form benzyl radical and chlorine radical. Benzyl radical then gets oxidised to benzyl cation as shown below.



Significant reaction occurred only at temperatures above 50°C. At 40°C, the conversion was negligible. Below 40°C, there was no conversion. This suggests that temperatures below 50°C are insufficient for starting the reaction. The formation of radicals is not activated at these temperatures. Thus it can be deduced that the energy required for the rupture of C-Cl bond will prevent it from taking place at temperatures below 50°C or below. There are enough evidences supporting this

acidity of the system, the latter being responsible for a carbocation mechanism. Instead, a direct relationship of activity with the reducibility of the cations is established. Iron-pillared clays were claimed to be efficient catalysts for Friedel-Crafts reactions by Choudhary *et al.* [16] and this is reasoned due to the easy reducibility of Fe^{3+} ion. They have well studied the influence of iron content and found that as the iron content increased, conversion also increased. As in the case of Cseri *et al.*, they also could not find any relationship between acidity and catalytic activity [17]. He *et al.* also proposed the redox mechanism for explaining their results, when they carried out the reaction over Fe containing mesoporous molecular sieves [15].

The cation thus formed by the oxidation of the radical attacks the *ortho* and *para* positions of the substrate and this results in the formation of *o*-MDPM and *p*-MDPM. The selectivities for the *ortho* and *para* products are also dependent on temperatures. Both of the products are formed only for an intermediate temperature of 60°C.

c) Effect of Metal Leaching

Benzylating toluene with benzyl chloride produces HCl as the by-product and this can cause acid-activation of the parent clay. Treatment of clay with an acid results in the removal of octahedral cations such as Al^{3+} and Fe^{3+} from the clay system. In the homogeneous Friedel-Crafts alkylation and acylation reactions, the reaction is generally performed with metal halides such as FeCl_3 or AlCl_3 as catalysts. When clays are used for the reaction with benzyl chloride, there is every possibility for the formation of FeCl_3 or AlCl_3 in the liquid phase by the combination of HCl formed during the reaction with the leached cation from the clay system. Hence a question arises whether the reaction proceeds in a purely heterogeneous manner or not. In view of this, we have removed the catalyst from the reaction mixture by filtration after 30 minutes of reaction and the filtrate was again subjected for reaction for 15 more minutes. The results are shown in Table 4.3. Even after removing the catalyst from the reaction medium, the reaction between benzyl chloride and toluene proceeded further to show a change in activity from 86.82 to 92.57%. A small amount of the filtrate is withdrawn from the reaction mixture and tested for the presence of Fe^{3+} ions by adding thiocyanate solution to it. A blood-red

colouration confirmed the presence of Fe^{3+} in solution. These ions in solution are responsible for the reaction between benzyl chloride and toluene even in the absence of the solid catalyst. From this, we can conclude that a 100% heterogeneous process is not taking place during the reaction. Instead, a small part of the reaction is occurring by the homogeneous catalysis as well.

Table 4.3 Metal leaching during benzylation of toluene with benzyl chloride (0.1 g FePM activated at 500°C, Benzyl chloride: toluene molar ratio: 1: 10, reaction temperature-60°C)

Time (min)	Conversion (%)	Selectivity (%)	
		<i>o</i> -MDPM	<i>p</i> -MDPM
30	86.82	23.50	76.50
45*	92.57	23.27	76.70

*After 30 minutes, the catalyst is filtered off and the filtrate is again subjected for reaction.

This conclusion is supported by the results obtained for Arata and coworkers when they carried out benzoylation reaction with sulphate and tungstate modified Fe_2O_3 [25]. The reaction mixture turned brown due to the presence of Fe^{3+} in the solution. They have confirmed the presence of Cl^- in the mixture. When the reaction was performed with another reagent, benzoic anhydride, for which there is no possibility of formation of HCl and hence Fe^{3+} in solution, the reaction stopped when the catalyst is removed from the medium.

d) Effect of Moisture

One of the disadvantages of homogeneous acid catalysts commonly practised in Friedel-Crafts type reactions is that these catalysts are highly moisture sensitive and hence demand moisture-free solvent and reactants, anhydrous catalyst and dry atmosphere for their handling. Developments of solid acid catalysts having high activity and little or no moisture sensitivity for liquid phase Friedel-Crafts reactions, is therefore of great practical importance. In this context, we have tried to study whether our catalysts are 'deactivated' by the presence of moisture.

To investigate the influence of moisture we have carried out two parallel runs: in one system, fresh catalyst was used and in the other, catalyst adsorbed with moisture was used. For adsorbing moisture on the catalyst, the catalyst was activated at the required temperature of 500°C and then placed into a desiccator saturated with

water vapour for 48 hours at room temperature. The substrate namely toluene was also kept inside the desiccator for making it saturated with water vapour.

0.1 g each of fresh catalyst and moisture adsorbed catalyst was put into the reaction mixture containing benzyl chloride and toluene with 1:10 molar ratio in separate R.B. flasks and the reaction was carried out at 60°C. At regular intervals of time, very small quantity of reaction mixture was withdrawn from each of the R. B. flasks and analysed by gas chromatography. The results are shown in Table 4.4 and Figure 4.2. The percentage conversion gradually increased as a function of time and became 100% at 50 minutes of the reaction, when fresh catalyst was used for reaction. But when the moisture-adsorbed catalyst was used for reaction, there was negligible conversion even after forty minutes. (At this time the conversion was 94.22% for the fresh catalyst). The percentage conversion suddenly raised from 5.29 to 69.99% in the time range 40-50 minutes. After this time, the conversion increased steadily and became 100% after 60 minutes. Thus there was a time period for which the catalyst was inactive towards reaction, when it is adsorbed with moisture. The moisture gets adsorbed on the active sites, (Fe^{3+} and Al^{3+}) present on the interlayer and surface of the pillared clay and prevents the benzyl chloride molecule to react over these sites. However, after the induction period, the reaction was as in the case of fresh catalyst itself.

Table 4.4 Data on the influence of moisture adsorption over the catalyst for benzylation of toluene with benzyl chloride (0.1 g FePM activated at 500°C, Benzyl chloride: toluene molar ratio-1: 10, reaction temperature-60°C)

Time (min)	Conversion (%)over fresh catalyst	Conversion (%)over catalyst adsorbed with moisture*
10	50.33	2.90
20	86.82	2.99
30	94.22	2.89
40	100	3.29
50	100	69.99
60	100	98.94
120	100	100

*The catalyst and toluene were kept in a desiccator containing water for 48 hours.

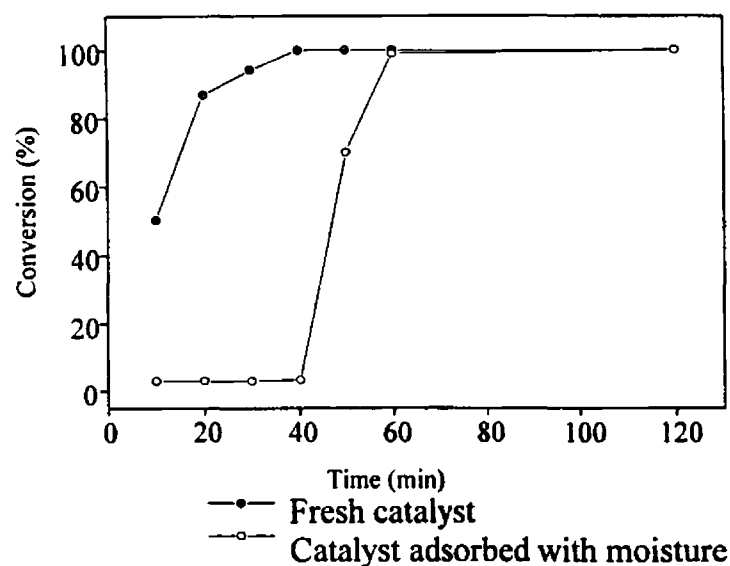


Figure 4.2 Conversions of benzyl chloride over fresh catalyst and catalyst adsorbed with moisture

This suggests that the benzyl chloride molecule is replacing the water molecules, which have been adsorbed on the active sites. Once the sites are freed from moisture, they are active towards the desired reaction. The induction period (Figure 4.2) can be defined as the time required for the reactant(s), here benzyl chloride, for replacing the adsorbed moisture on the catalyst to start the catalytic reaction [26]. From the results, we can conclude that these catalysts are active even in the presence of moisture.

e) Catalyst Comparison

Mixed iron-aluminium systems: Under optimised conditions such as a reaction temperature of 60°C, benzyl chloride: toluene molar ratio of 1: 10 and for a reaction time of 30 minutes, all the catalysts were tested for catalytic activity, after activating at a temperature of 500°C. The results for mixed Fe-Al systems are illustrated in Table 4.5. Iron incorporated systems showed excellent activity. The reaction yields only *ortho* and *para* isomers namely *o*-MDPM and *p*-MDPM, which are expected for a cationic mechanism. Besides, only monoalkylated products are detected during the reaction, which could be ascribed to the high substrate to alkylating agent molar ratio.

Iron incorporated systems show a percentage conversion of more than 50% whereas the parent montmorillonite (M) and aluminium-pillared montmorillonite (AlPM) show lesser conversion. Though M and AlPM originally possess iron contents of 10.73 and 10.23 wt% respectively, the reaction is sluggish. Hence it can be deduced that most of the iron present in these clays is not in the ion-exchanged positions and hence cannot take part in reaction. We have already proposed a different initiation for the formation of carbocations, the homolytic rupture of C-Cl bond of benzyl chloride. This rupture creates benzyl radical, which in presence of a reducible cation oxidises to benzyl cation. The low percentage conversion with M and AlPM suggest that the iron present in these systems is not active for the homolytic rupture of C-Cl bond in benzyl chloride. Incorporation of iron along with aluminium resulted in the placement of iron at the ion-exchanged positions. The Fe^{3+} ions having a high reduction potential ($\text{Fe}^{3+} \rightarrow \text{Fe}^{2+}$ reduction potential = + 0.77 eV) are sufficient to rupture the C-Cl bond homolytically and the benzyl radical formed will get converted to benzyl carbocation in presence of this reducible cation. The formation of carbocation results in the conversion of toluene to *o*-MDPM and

Table 4.5 Data on the benzylation of toluene with benzyl chloride over mixed Fe-Al systems. (0.1 g catalyst activated at 500°C, benzyl chloride: toluene molar ratio-1: 10, reaction temperature-60°C and time of reaction – 30 min.)

Catalyst	Conversion (%)	Selectivity (%)	
		<i>o</i> -MDPM	<i>p</i> -MDPM
M	3.10	16.62	83.38
AlPM	19.60	22.11	77.89
FeAl _{0.1} PM	50.60	24.32	75.68
FeAl _{0.2} PM	56.11	22.68	77.32
FeAl _{0.3} PM	65.66	25.01	74.99
FeAl _{0.4} PM	76.22	23.61	76.39
FeAl _{0.5} PM	80.12	22.90	77.10
FeAl _{1.0} PM	78.62	23.25	76.75
FePM	86.82	23.50	76.50

p-MDPM, the products that are expected for a carbocation mechanism. As the iron content increased, the percentage conversion also increased as illustrated in Figure 4.3. This is attributed to the formation of more benzyl radicals in presence of more Fe^{3+} ions in the ion-exchanged positions.

Acidity data for iron-aluminium systems (Tables 3.16 and 3.19) show that AlPM has more acidity than systems with low Fe/Al ratios. But all iron incorporated systems show very high activity than AlPM. No correlation can then be found between activity and acidity. AlPM possesses more than two-fold acidity (Table 3.16) than $\text{FeAl}_{0.1}\text{PM}$, but the latter exhibited more than two-fold activity compared to the former. For other systems also with less acidity than AlPM, the activity for converting benzyl chloride was more. ESR experiments indeed showed that Fe in the clay can be reduced and can produce radicals by interaction with anisole [23]. In view of all these facts, the high activity observed for iron incorporated systems can be ascribed to a different initiation of the reaction, for instance, homolytic rupture of C-Cl bond followed by the oxidation of the radical as shown in page number 139.

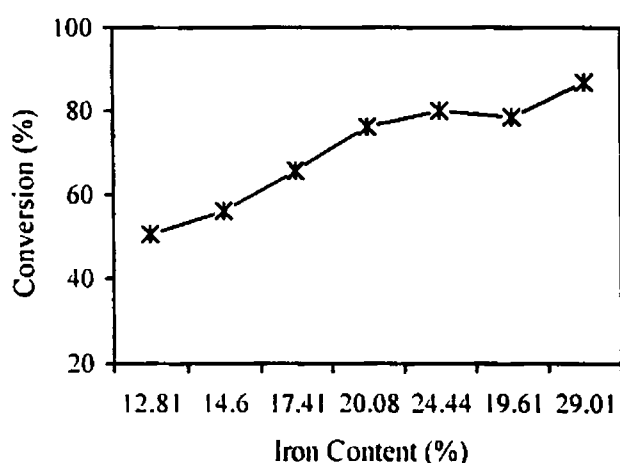


Figure 4.3 Influence of iron content of mixed iron-aluminium pillared montmorillonites on benzylation of toluene

Mixed Cr-Al systems: Table 4.6 gives the benzylation reaction data of toluene with benzyl chloride over the mixed Cr-Al systems. Comparing with mixed Fe-Al systems these catalysts show lesser percentage conversion. A redox mechanism can be ruled out in the case of Cr containing systems since the redox potential for $\text{Cr}^{3+} \rightarrow \text{Cr}^{2+}$ is -0.41 eV, which is much less than the redox potential of $(\text{Fe}^{3+}, \text{Fe}^{2+})$ system. Experiments conducted by Cseri *et al.* [17] using various cation exchanged clays

confirmed that in the presence of reducible cations such as Fe^{3+} , Sn^{4+} and Cu^{2+} , redox mechanism is operating. But in presence of cations such as Cr^{3+} , Zn^{2+} , Zr^{4+} , etc. redox mechanism is not operating since these cations are not easily reducible. This explains the low activity of Cr systems. However, among the Cr-Al pillared systems, to elucidate correlation between the catalytic activity and any property of the catalytic systems, we have examined the various types of acidity determined by the three independent methods namely the thermodesorption of DMPY, adsorption of perylene and TPD of NH_3 . We could not find any correlation between any of the types and region of acidity except the number of acidic sites in the strong region as determined by NH_3 -TPD method. The conversion of benzyl chloride is directly proportional to the density of acidic sites in the strong region, as shown in Figure 4.4. Among Cr-, Al- and Cr-Al pillared montmorillonites, CrPM possesses maximum number of strong acidic sites and essentially this catalyst showed maximum percentage conversion. AIPM possesses minimum number of strong acidic sites and it exhibits lowest activity. Benzyl chloride is getting adsorbed on strong acid sites and the benzyl cation is formed. The adsorption of benzyl chloride on the strong acid sites can be explained as follows. In spite of possessing lone pairs, owing to the high electronegative character of chlorine, it is reluctant to adsorb on weak sites. Sufficiently strong acidic sites are

Table 4.6 Benzylation of toluene with benzyl chloride over mixed Cr-Al systems (0.1 g catalyst activated at 500°C , benzyl chloride: toluene molar ratio-1: 10, reaction temperature- 60°C and time of reaction – 30 min.)

Catalyst	Conversion (%)	Selectivity (%)	
		<i>o</i> -MDPM	<i>p</i> -MDPM
AIPM	19.60	22.11	77.89
CrAl _{0.1} PM	28.301	20.61	79.39
CrAl _{0.2} PM	30.21	21.21	78.79
CrAl _{0.3} PM	31.03	22.01	77.99
CrAl _{0.4} PM	32.69	21.07	78.93
CrAl _{0.5} PM	25.02	23.00	77.00
CrAl _{1.0} PM	27.11	22.04	77.96
CrPM	38.61	21.51	78.49

required for adsorbing benzyl chloride through the lone pair of chlorine. Mechanism of the reaction is shown in Figure 4.5.

Thus we can conclude that in presence of a reducible cation such as Fe^{3+} , redox mechanism is operating whereas in its absence, strong acidity of the catalyst is responsible for reaction.

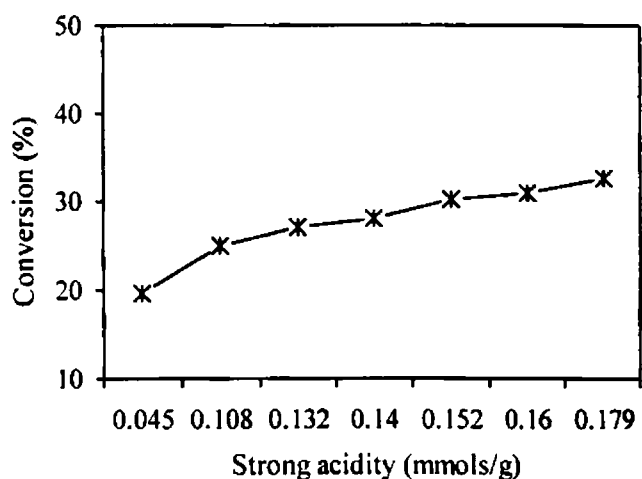


Figure 4.4 Influence of strong acidity on benzylation of toluene with benzyl chloride performed over mixed Cr-Al systems

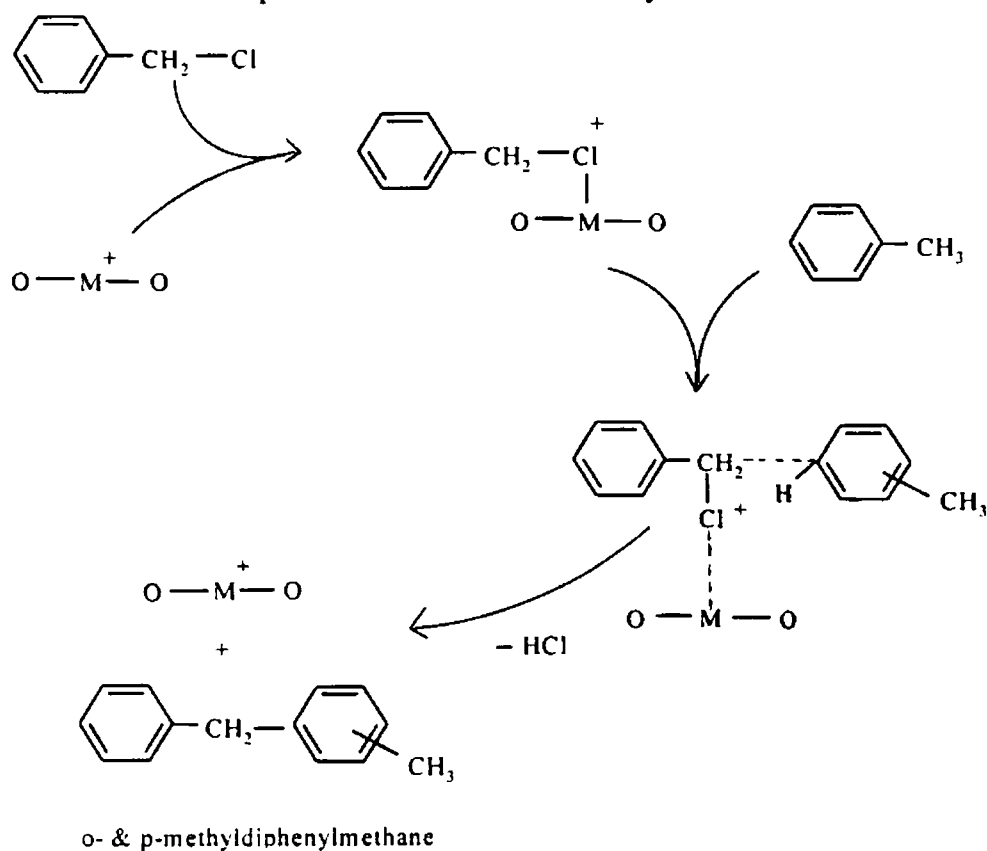


Figure 4.5 A plausible mechanism for benzylation of toluene with benzyl chloride involving the Lewis acid sites over pillared clays

Vanadia impregnated systems: The percentage conversion and selectivities of *o*-MDPM and *p*-MDPM over vanadia impregnated systems are shown in Table 4.7. The presence of iron in the systems makes these catalysts efficient towards benzylation of toluene. In addition, vanadia loading increased the number of strong acid sites considerably up to a vanadia loading of 7%. This increase in strong acidity is reflected in their activity as well. Catalysts having a vanadia loading of 7% or below, were found to be more active than FePM. Others showed lesser activity. After 10VFe, the selectivities also changed slightly. At higher vanadia loadings, the pores are almost blocked and this results in the large reduction in surface area and catalytic activity. Pore blockage leads to higher selectivity for *p*-MDPM than *o*-MDPM. However, the conversion were very low for systems with high vanadia loading such as 15 and 20%, compared to systems having low vanadia loadings.

Table 4.7 Data of benzylation of toluene with benzyl chloride over vanadia loaded FePM. (0.1 g catalyst activated at 500°C, benzyl chloride: toluene molar ratio-1: 10, reaction temperature-60°C and time of reaction – 30 min.)

Catalyst	Conversion (%)	Selectivity (%)	
		<i>o</i> -MDPM	<i>p</i> -MDPM
FePM	86.82	23.50	76.50
2VFe	87.81	22.10	77.90
5VFe	90.21	20.41	79.59
7VFe	92.11	21.68	78.32
10VFe	64.80	19.15	80.85
15VFe	50.10	14.10	85.90
20VFe	31.01	12.21	87.79

4.1.2 Benzylation of Toluene with Benzyl Alcohol

We have also carried out the Friedel-Crafts reaction using a different benzylating agent such as benzyl alcohol, the scheme of the reaction is shown in Figure 4.6. It is well established that the Brönsted acid sites present in a catalyst are taking part in the reaction when the benzylating agent is benzyl alcohol [17, 27]. Hence, in this case we have studied the influence of calcination temperature also to confirm the involvement of Brönsted acid sites. Apart from the influence of

calcination temperature, the influence of reaction temperature, metal leaching and moisture, have also been investigated. In addition, all the prepared catalysts were tested for catalytic activity under optimised conditions.

In a typical run, a mixture of toluene and benzyl alcohol in 10:1 molar ratio was allowed to react for the desired time in a 50 mL R.B after introducing 0.1 g of the activated catalyst, the reaction mixture being well stirred by means of a magnetic stirrer. At required time intervals, the reaction mixture was analysed by gas chromatography and the products identified were *o*-MDPM and *p*-MDPM along with dibenzyl ether.

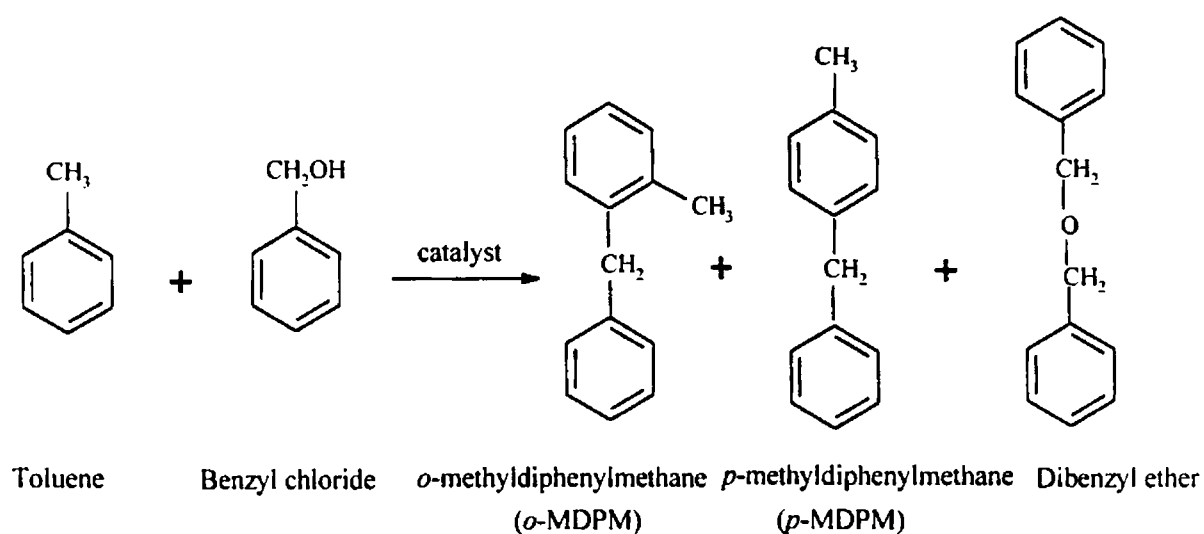


Figure 4.6 Benzylation of toluene with benzyl alcohol

For studying the influence of various reaction parameters, we have selected iron-pillared montmorillonite (FePM) and conducted the runs under desired conditions.

a) Presence of Catalyst

In a blank run, toluene and benzyl alcohol mixed in the molar ratio 10:1 was allowed to react in the absence of the catalyst for one hour. A parallel run was also carried out under similar conditions with the addition of 0.1g of activated FePM catalyst. A small amount from both of the reactors was withdrawn and analysed gas chromatographically. The results are furnished in Table 4.8. Without using a catalyst we observed a percentage conversion of 6.9 after one hour at refluxing condition.

p-Methyldiphenylmethane, along with dibenzyl ether were formed. The former has a percentage selectivity of 21.25%. 78.55% selectivity was observed for dibenzyl ether, which is formed by the self condensation of benzyl alcohol [8, 28]. When FePM was used as catalyst, a conversion of 47.14% was observed. Product selectivity for *o*-MDPM, *p*-MDPM and dibenzyl ether was 33.32, 51.72 and 14.45% respectively. Thus desirable product selectivity along with the sharp increase of conversion was obtained by using a catalyst. The formation of dibenzyl ether is very much suppressed by using a catalyst. The percentage conversion of benzyl alcohol is demandingly high because of the lower activation energy of a catalysed reaction compared to the uncatalysed one. In other words, catalyst works by permitting the reaction to occur by another reaction path that has a lower energy barrier. This is shown schematically in Figure 4.7 [29].

Table 4.8 Influence of catalyst on the benzylation of toluene with benzyl alcohol (0.1 g FePM, benzyl alcohol: toluene molar ratio-1: 10, reaction temperature-110°C)

	Time (min)	Conversion (%)	Selectivity (%)		
			<i>o</i> -MDPM	<i>p</i> -MDPM	Dibenzyl ether
Without catalyst	60	6.9	-	21.25	78.75
With catalyst	60	47.19	51.72	33.32	14.95

b) Effect of Metal Leaching

We have explored that there is metal leaching when the reaction between toluene and benzyl chloride was carried out using FePM as the catalyst. This was assigned to the evolution of HCl during the reaction, which leaches out the metal cation from the catalyst into the solution. In the case of benzyl alcohol and toluene reaction mixture also, we have attempted to study about metal leaching. The catalyst was removed from the reaction mixture after one-hour reaction and the filtrate was allowed to react further for one more hour. It is observed that there is negligible conversion after the removal of the catalyst, even after one more hour (Table 4.9). From this observation itself we can conclude that the catalyst is stable when the benzylating agent is benzyl alcohol, since no acid is generated during the course of the reaction. The filtrate was colourless when tested for metal ions, confirming the absence of metal ions in the solution.

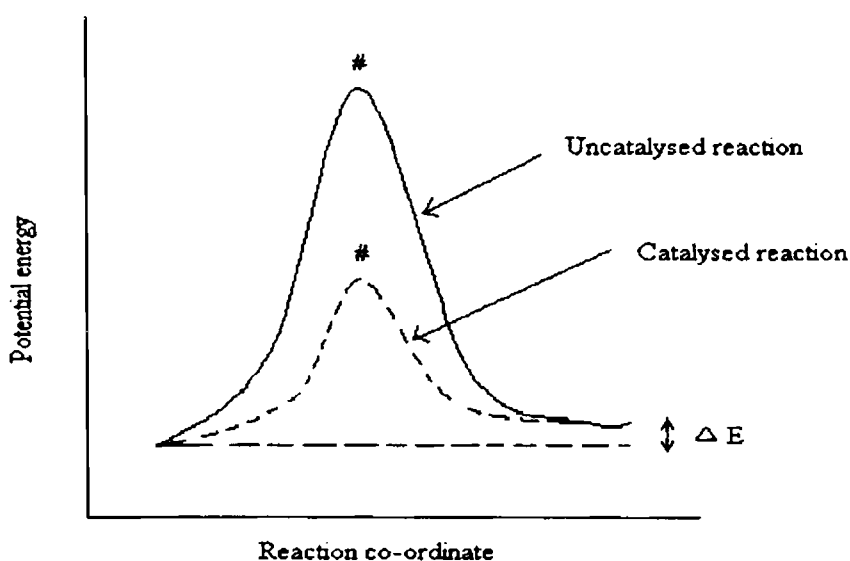


Figure 4.7 The lowering of energy barrier brought about by a catalyst

Table 4.9 Metal leaching during benzylation of toluene with benzyl alcohol. (0.1 g FePM activated at 500°C, Benzyl alcohol: toluene molar ratio: 1: 10, reaction temperature-110°C)

Time (min)	Conversion (%)	Selectivity (%)		
		o-MDPM	p-MDPM	Dibenzyl ether
60	47.19	51.72	33.32	14.95
120*	50.86	49.63	33.12	17.25

* After 60 minutes, the catalyst is filtered off and the filtrate is again subjected for reaction.

c) Effect of Calcination Temperature

In the set of experiments performed to understand the influence of calcination temperature, the catalyst calcined at various temperatures were used. Figure 4.8 reveals the variations in catalytic activity and selectivity due to changes in calcination temperatures. There is a steady decrease in percentage conversion as the calcination temperature increased. However, the selectivities for various products are not altered much. It is reported that Brönsted acid sites are catalysing the reaction of toluene with benzyl alcohol and the benzyl carbocation is formed by the interaction of OH groups in benzyl alcohol and the catalyst surface (Mechanism is shown in Figure 4.9)

[17, 27]. As the calcination temperature is increased, the number of Brønsted acid sites decreased due to dehydroxylation [30] and hence the catalytic activity is reduced. Hence, this series of experiments confirm the involvement of Brønsted acid sites for the reaction between benzyl alcohol and toluene.

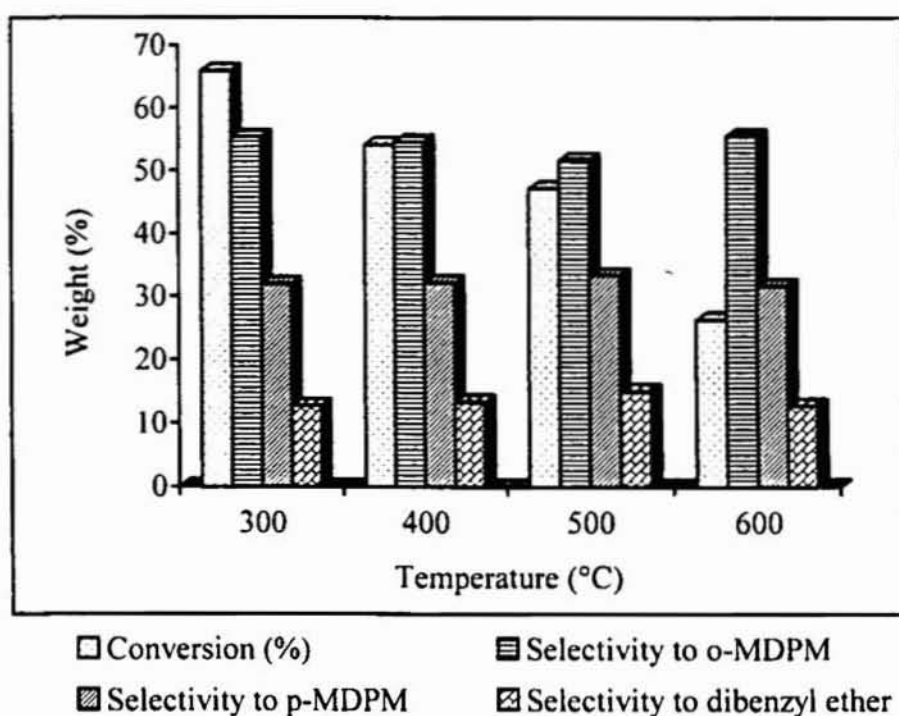


Figure 4.8 Influence of calcination temperature on benzylation of toluene by benzyl alcohol

d) Effect of Moisture

From the experiments performed by calcining the catalyst at various temperatures, we have concluded about the participation of Brønsted acid sites. Our study was then extended to the investigation on the influence of moisture. From the variation of conversion pattern, we can get further insight into the nature of active sites that are participating in the reaction. The procedures for moisture study with benzyl chloride as benzylating agent were repeated to perform the reaction. Fresh catalyst and moisture-adsorbed catalyst after activating at 500°C were used separately to carry out the reaction. The results are shown in Figure 4.10. Adsorption of moisture on the catalyst did not cause any decrease in catalytic activity. Instead, we noticed that the catalytic activity was higher when the catalyst was adsorbed with moisture. When we used the catalyst after adsorbing with moisture for carrying out the reaction between benzyl chloride and toluene, we have clearly

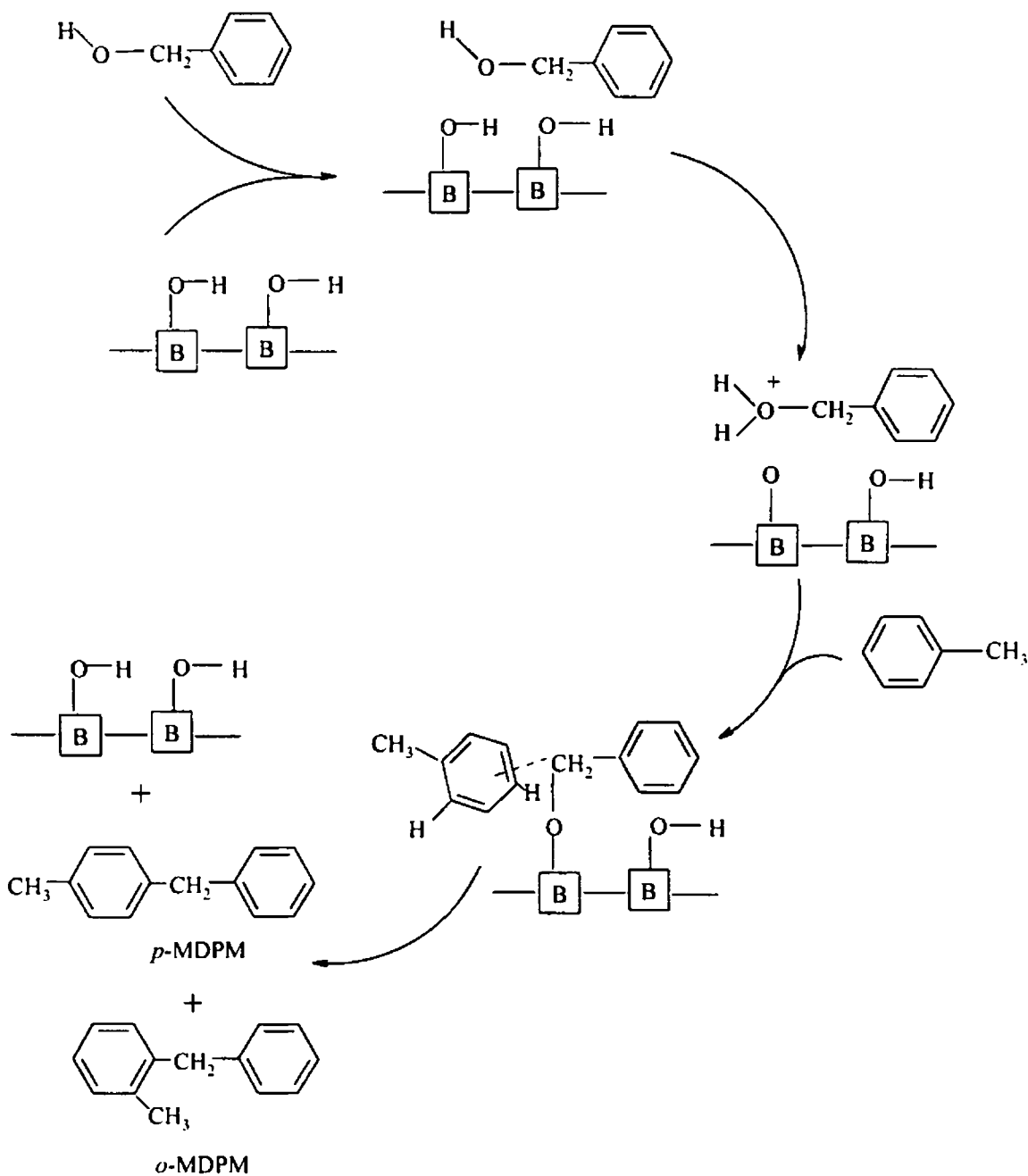


Figure 4.9 A plausible mechanism of benzylation of toluene with benzyl alcohol involving Brønsted acidic sites

noticed an "induction period" to start the catalytic reaction. In the present case, such an induction period is not at all observed. From the results obtained, we can record that moisture has a beneficial rate enhancement effect on the reaction. The enhancement effect of catalytic activity by adsorbing the catalyst with moisture can be explained as follows. Moisture is getting adsorbed on the metal ions (Lewis acid sites) present in the catalyst and in effect, these act as Brønsted acid sites [31]. By adsorbing on the electron deficient metal cations, the water molecules get polarised

and this polarisation effect makes them efficient to carry out the reaction (Figure 4.11) [31, 32]. Thus the number of Brönsted acid sites taking part in the reaction when the catalyst is adsorbed with moisture will be greater than those taking part in the absence of moisture. This leads to the higher percentage conversion when the reaction is carried out with a catalyst which is adsorbed with moisture.

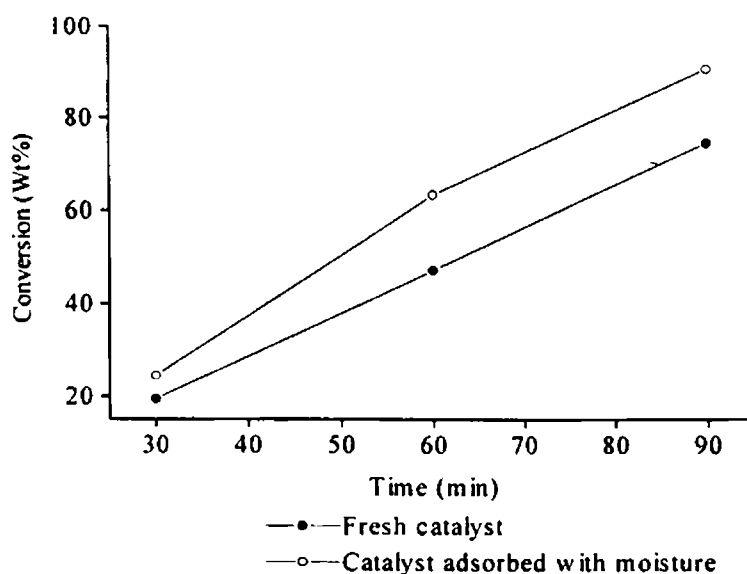


Figure 4.10 Conversions of benzyl alcohol over fresh catalyst and catalyst adsorbed with moisture (0.1 g FePM, benzyl alcohol: toluene molar ratio-1: 10, reaction temperature-110 °C)

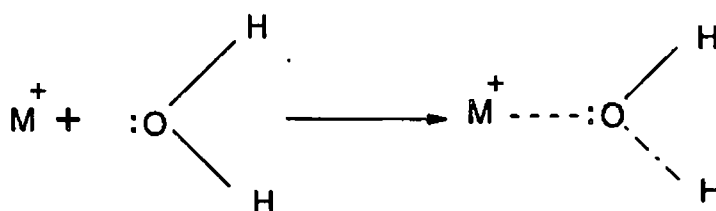


Figure 4.11 Polarisation of water molecule when adsorbed over a Lewis acidic site

e) Effect of Reaction Temperature

Table 4.10 shows the influence of reaction temperature on the catalytic activity and selectivity. As the temperature is increased, there was a steady increase in conversion. Maximum conversion is obtained at the refluxing temperature. A

more desirable product selectivity was also obtained at this temperature of reaction. As the temperature of reaction was lowered, the percentage selectivity for the formation of ether increased whereas those of *o*-MDPM and *p*-MDPM decreased. In a pillared clay system there are fewer numbers of Brönsted acid sites and these actively participate in catalytic reaction only at a higher temperature. Hence the self condensation of benzyl alcohol to dibenzyl ether is more favoured at low temperatures. The fewer number of Brönsted acid sites can be attributed to the higher activation temperature (500°C) of the catalyst, which leads to the reduction of the Brönsted acid sites.

Table 4.10 Influence of temperature on benzylation of toluene with benzyl alcohol (0.1 g FePM activated at 500°C, benzyl chloride: toluene molar ratio-1:10, time of reaction -60 min)

Temperature (°C)	Conversion (%)	Selectivity (%)		
		<i>o</i> -MDPM	<i>P</i> -MDPM	Dibenzyl ether
110	47.19	51.72	33.32	14.95
100	40.01	48.78	30.01	21.21
80	29.66	45.12	24.04	26.84
60	13.11	39.64	19.68	40.68

f) Catalyst Comparison

Tables 4.11 to 4.13 show the catalytic activity of mixed iron-aluminium, chromium-aluminium and vanadia impregnated iron-pillared montmorillonites. A rough correlation with Brönsted acidity could be obtained within a series of systems but could not be applied among the various systems. Mixed Fe-Al systems showed higher activity than Cr-Al systems. The ionic radius of Cr³⁺ is 94pm and that of Fe³⁺ is 78.5pm (23). Hence the charge to ionic radius for Fe³⁺ is higher than that for Cr³⁺. The higher charge to ionic radius ratio of the Fe³⁺ cation leads to the higher interlayer acidity of the iron-pillared and the mixed Fe-Al pillared montmorillonites [34, 35]. Vanadia addition enhanced the Brönsted acidity of the system with 7% vanadia loading and the catalytic activity was found to be more than the other loaded systems. For high vanadia loaded systems such as 15 and 20VFe, very low conversion was observed owing to their low surface areas.

Table 4.11 Data on benzylation of toluene with benzyl alcohol over mixed Fe-Al systems. (0.1 g catalyst activated at 500°C, benzyl alcohol: toluene molar ratio-1:10, reaction temperature-110°C and time of reaction – 60 min.)

Catalyst	Conversion (%)	Selectivity (%)		
		<i>o</i> -MDPM	<i>p</i> -MDPM	Dibenzyl ether
M	3.10	23.11	-	76.89
AlPM	61.01	41.11	23.21	35.68
FeAl _{0.1} PM	56.62	46.62	26.55	26.84
FeAl _{0.2} PM	55.62	50.72	33.00	16.28
FeAl _{0.3} PM	55.68	40.18	28.20	31.62
FeAl _{0.4} PM	50.62	51.22	30.18	18.59
FeAl _{0.5} PM	48.21	53.66	33.08	13.26
FeAl _{1.0} PM	56.82	49.62	30.08	20.29
FePM	47.19	51.72	33.32	14.95

Table 4.12 Benzylation of toluene with benzyl alcohol over mixed Cr-Al systems. (0.1 g catalyst activated at 500°C, benzyl alcohol: toluene molar ratio-1:10, reaction temperature-110°C and time of reaction – 60 min.)

Catalyst	Conversion (%)	Selectivity (%)		
		<i>o</i> -MDPM	<i>p</i> -MDPM	Dibenzyl ether
AlPM	61.01	41.11	23.21	35.68
CrAl _{0.1} PM	42.90	46.11	28.72	25.17
CrAl _{0.2} PM	40.60	48.21	26.66	25.13
CrAl _{0.3} PM	37.19	49.62	25.31	25.07
CrAl _{0.4} PM	37.14	44.61	24.14	31.25
CrAl _{0.5} PM	39.89	49.62	23.66	26.72
CrAl _{1.0} PM	42.11	48.54	25.62	25.84
CrPM	44.62	46.55	25.15	28.30

Table 4.13 Benzylation of toluene with benzyl alcohol over vanadia loaded FePM (0.1 g catalyst activated at 500°C, benzyl alcohol: toluene molar ratio- 1:10, reaction temperature-110°C and time of reaction – 60 min.)

Catalyst	Conversion (%)	Selectivity (%)		
		<i>o</i> -MDPM	<i>p</i> -MDPM	Dibenzyl ether
FePM	47.19	51.72	33.32	14.95
2VFe	27.84	50.11	37.58	12.31
5VFe	31.92	50.65	36.23	13.12
7VFe	50.21	54.62	34.17	11.21
10VFe	41.62	39.21	42.15	18.64
15VFe	21.11	22.62	37.10	40.28
20VFe	9.62	18.19	22.37	59.44

4.1.3 Influence of Benzylating Agent

Table 4.14 gives the details of results for reactions conducted with different benzylating agents. At 110°C, we observed a complete conversion of benzyl chloride with 100% selectivity to *p*-methyldiphenylmethane after a reaction time of 30 minutes. At the same temperature of reaction, even after 60 minutes, the percentage conversion for benzyl alcohol was only 47.19%. In this case both *o*-MDPM and *p*-MDPM were produced, *ortho* being formed predominantly. At reaction temperature of 60°C, the percentage conversions were 86.82 and 13.11 for benzyl chloride and benzyl alcohol respectively. *p*-MDPM is the major product with benzyl chloride whereas *o*-MDPM is the major product with benzyl alcohol. We have proposed a free radical mechanism (Section 4.1.1 b) for the reaction between benzyl chloride and toluene and a purely carbocation mechanism (Section 4.1.2 c) for the reaction between benzyl alcohol and toluene. The homolytic rupture of C-Cl bond in benzyl chloride takes place at a sufficiently high temperature (60°C) and the free radicals thus produced enables the reaction to proceed at a faster rate. Even at a higher temperature of 110°C, the lesser number of Brønsted acid sites restricts the reaction and hence a relatively low catalytic activity is noticed. It is worthwhile to note that even though a free radical mechanism is not operating in case of Cr-systems, these systems also showed complete conversion of benzyl chloride

Table 4.14 Benzoylation of toluene with different benzoylating agents

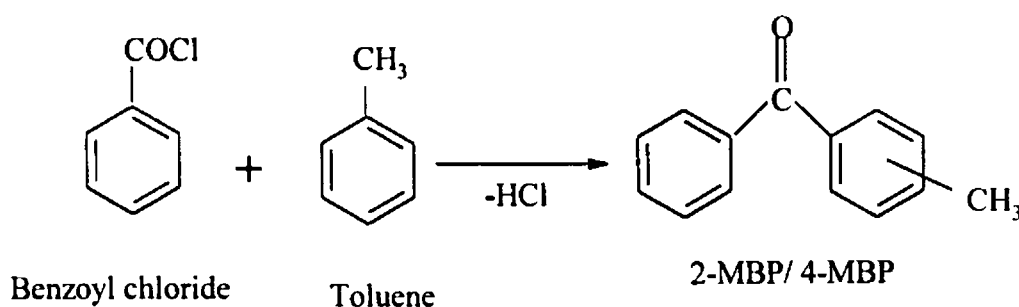
Benzoylating agent	Temperature of reaction (°C)	Time of reaction (min.)	Conversion (%)	Selectivity to MDPMs (%)
Benzyl chloride	110	30	100	100 (0, 100)*
Benzyl alcohol	110	60	47.19	85.1 (60.8, 39.2)
Benzyl chloride	60	30	86.82	100 (23.5, 76.5)
Benzyl alcohol	60	60	13.11	59.32 (66.8, 33.2)

*Figures in parenthesis give the selectivity of *o*-MDPM and *p*-MDPM respectively.

even before 30 minutes when the reaction was conducted at 110°C. Under these conditions the conversion of benzylalcohol is very less and this suggest the limited number of Brønsted sites over the pillared clays, when compared to the Lewis sites.

4.2 Benzoylation of Toluene

Liquid phase benzoylation was conducted by refluxing a mixture of toluene and benzoyl chloride in a 50 mL round bottomed flask. The refluxing was done in an oil bath at the boiling point of the mixture. We had optimised the conditions of the reaction such that a reaction time of 1 h yielded a sufficient range of products and a proper comparison of the various catalyst systems could be made. The products in the reaction mixture were analysed by using GC employing an SE-30 column and flame ionisation detector. The reaction yielded only two products namely 2-methylbenzophenone (2-MBP or *ortho* product) and 4-methylbenzophenone (4-MBP or *para* product). The reaction can be depicted as shown below.

**Figure 4.12** Schematic representation of the benzoylation of toluene

4.2.1 Influence of Molar Ratio

In a set of experiments, toluene and benzoyl chloride were taken in different molar ratios and the percentage conversion was calculated. As the toluene/benzoyl chloride ratio increased, we could find a decrease in the percentage conversion of benzoyl chloride. For FePM system, the conversion was 98.21% for the toluene/benzoyl chloride molar ratio of 5. The conversion decreased to 53.11% as the molar ratio was increased to 20. The results are shown in Table.4.15.

Table 4.15 Influence of molar ratio on benzoylation of toluene with benzoyl chloride 0.1 g FeAl_{0.3}PM activated at 500°C and reaction temperature-110°C)

Toluene/benzoyl chloride molar ratio	Conversion (%)	Selectivity (%)	
		2-MBP	4-MBP
5	98.21	16.51	83.49
10	81.82	18.00	82.00
15	69.94	18.54	81.46
20	53.11	17.01	82.99

Two reasons can be stipulated for the observation of decreasing percentage conversion with increasing toluene/benzoyl chloride molar ratio.

1. As the toluene/benzoyl chloride molar ratio increased, toluene may get adsorbed over the catalyst surface, suppressing the adsorption of benzoyl chloride.
2. At high toluene/benzoyl chloride molar ratios, the effective concentration of benzoyl chloride will be less, which leads to lesser conversion. According to the law of mass action, rate of reaction is proportional to the concentration of the reactant. Toluene is taken in excess and as the concentration of toluene is increased in the mixture, the effective concentration of benzoyl chloride in the mixture is reduced. This, we can call as a dilution effect.

Between the two reasons pointed above, since toluene is a non-polar molecule, the first one can be ruled out. It is very unlikely that toluene get adsorbed on the catalyst surface, even in the presence of large excess of toluene. Hence we can conclude that the reduction in the percentage conversion is merely due to the 'dilution' effect.

4.2.2 Influence of Catalyst Composition

The benzylation activity of different catalysts is depicted in Tables 4.16-4.18. The parent montmorillonite did not exhibit any activity towards the reaction under optimised conditions. It is due to the unavailability of enough number of acidic sites and its very low surface area. Among the various Fe-Al pillared montmorillonites, FeAl_{0.5}PM exhibited maximum activity for the benzylation of toluene. The total acidity as well as the strong acidity is found to be high for this system, as determined from ammonia TPD method (Table. 3.19). Lewis acidity from perylene adsorption method (Table. 3.16) also was maximum for this system. Thus it is forced to say that strong acid sites are involved in the benzylation reaction. However, it is to be noted that FeAl_{0.3}PM exhibited a better conversion than FeAl_{0.2}PM and FeAl_{0.4}PM, though all these three catalysts possessed almost similar perylene adsorption values. The strong and total acidity values of the former were intermediate between the latter two. Thus it becomes subtle to assign a particular type of acidic sites, which are responsible for the reaction. There are several articles stating the involvement of strong Lewis acidic sites in the reaction. The confusion doubles when we compare the benzylation activity of Fe-Al and Cr-Al systems. The

Table 4.16 Data of benzylation of toluene over mixed Fe-Al pillared systems. (0.1 g catalyst, toluene: benzoyl chloride molar ratio 1: 10, reaction temperature-110 °C)

Catalyst	Conversion (%)	Selectivity (%)	
		2-MBP	4-MBP
M	-	-	-
AlPM	44.58	16.01	83.99
FeAl _{0.1} PM	56.95	8.03	91.96
FeAl _{0.2} PM	65.43	16.33	83.66
FeAl _{0.3} PM	81.31	15.81	84.19
FeAl _{0.4} PM	63.22	19.94	80.05
FeAl _{0.5} PM	84.34	16.26	83.74
FeAl _{1.0} PM	76.65	14.98	85.02
FePM	81.82	18.00	82.00

Cr-Al systems showed much more number of perylene adsorption sites (Lewis sites) than Fe-Al systems. Still they showed lesser activity. We may get a little more insight into the reaction if we could find the distribution of the Lewis acid sites present in the catalyst. Even though, a distribution of acid sites may be possible by ammonia TPD method as weak, medium and strong, this method does not differentiate between Lewis and Brønsted acidic sites. The value obtained at the strong region may contribute both strong Lewis and Brønsted acid sites.

Table 4.17 Data of benzylation of toluene over mixed Cr-Al pillared systems (0.1 g catalyst, toluene: benzoyl chloride molar ratio 1: 10, reaction temperature-110 °C and time of reaction-60 min.)

Catalyst	Conversion (%)	Selectivity (%)	
		2-MBP	4-MBP
AlPM	44.58	16.01	83.99
CrAl _{0.1} PM	41.14	17.48	82.52
CrAl _{0.2} PM	55.32	15.38	84.62
CrAl _{0.3} PM	56.38	15.52	84.48
CrAl _{0.4} PM	60.26	16.44	83.55
CrAl _{0.5} PM	31.16	16.99	83.01
CrAl _{1.0} PM	56.46	20.19	79.81
CrPM	29.34	0.00	100

Although very good correlation between acidity and benzylation activity of Fe-Al and Cr-Al systems is not obtained, a comparison of the benzylation activity of the various vanadia loaded iron-pillared montmorillonites is more consolable. Table 4.18 allows a comparison of activity with the different types of acidity. All the vanadia-loaded samples displayed lesser activity than the parent iron-pillared montmorillonite. The limiting amount of perylene adsorbed over the catalyst also showed a similar trend. This observation confirms the involvement of Lewis acidic sites in the reaction. The data in Table 4.18 reveal that both the total and strong acidity are increasing up to a vanadia loading of 7%. However, this does not favour the reaction. Instead, a steady decline of activity is noted. We have already observed the role of strong acid sites in the reaction by comparing various Fe-Al and Cr-Al

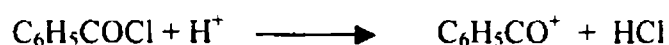
systems. By comparing the various vanadia-loaded systems, it is deduced that Lewis acidity is playing a major role in the reaction.

Table 4.18 Comparison of the benzoylation activity with various types of acidity of the different vanadia loaded FePMs

Catalyst	Conversion (%)	Strong acidity (mmol/g)	Total acidity (mmol/g)	Limiting amount of perylene adsorbed (10^{-2} mmol/g)
FePM	81.82	0.1163	0.5881	1.2104
2VFe	74.11	0.1314	0.5909	1.1010
5VFe	70.71	0.3726	1.2214	0.9088
7VFe	56.11	0.6186	1.9280	0.7316
10VFe	41.14	0.3754	1.0324	0.4140
15VFe	28.29	0.0534	0.5524	0.3421
20VFe	12.91	0.0190	0.3011	0.2461

4.2.3 Mechanism of Benzoylation Reaction

Many of the earlier studies of the benzoylation of toluene by heterogeneous catalysts involve superacidic sulphated metal oxides as catalysts [21, 25, 36, 37]. Benzoylation of toluene according to some authors [21, 36, 37] takes place through the creation of benzoyl cation by the reaction of superacidic Brönsted sites of the catalyst with benzoyl chloride according to the reaction step,



However, there is no superacidity in our catalytic systems. From our studies we have established the involvement of Lewis acidic sites in the reaction. As the reaction mixture has a net non-polar nature, a complex between the catalyst and $\text{C}_6\text{H}_5\text{COCl}$ is a more likely intermediate than a free benzoyl cation. A plausible mechanism is depicted in Figure 4.13.

The formation of predominant para isomer is due to steric considerations. The formation of only *ortho* and *para* isomers as the main products can be rationalised by considering the symmetry of the highest occupied molecular orbital (HOMO) of toluene involved in the interaction with the intermediate complex. An

interaction can take place only on bonds formed by orbitals bearing the same sign, i.e., 1-2, 1-6, 3-4 and 4-5, but not 2-3 and 5-6. Of the four allowed sets, the attack on the former two can lead only to *ortho* substitution whereas the latter two will give the *para* isomer and less *meta* [40]. This is evident from the Figure 4.14.

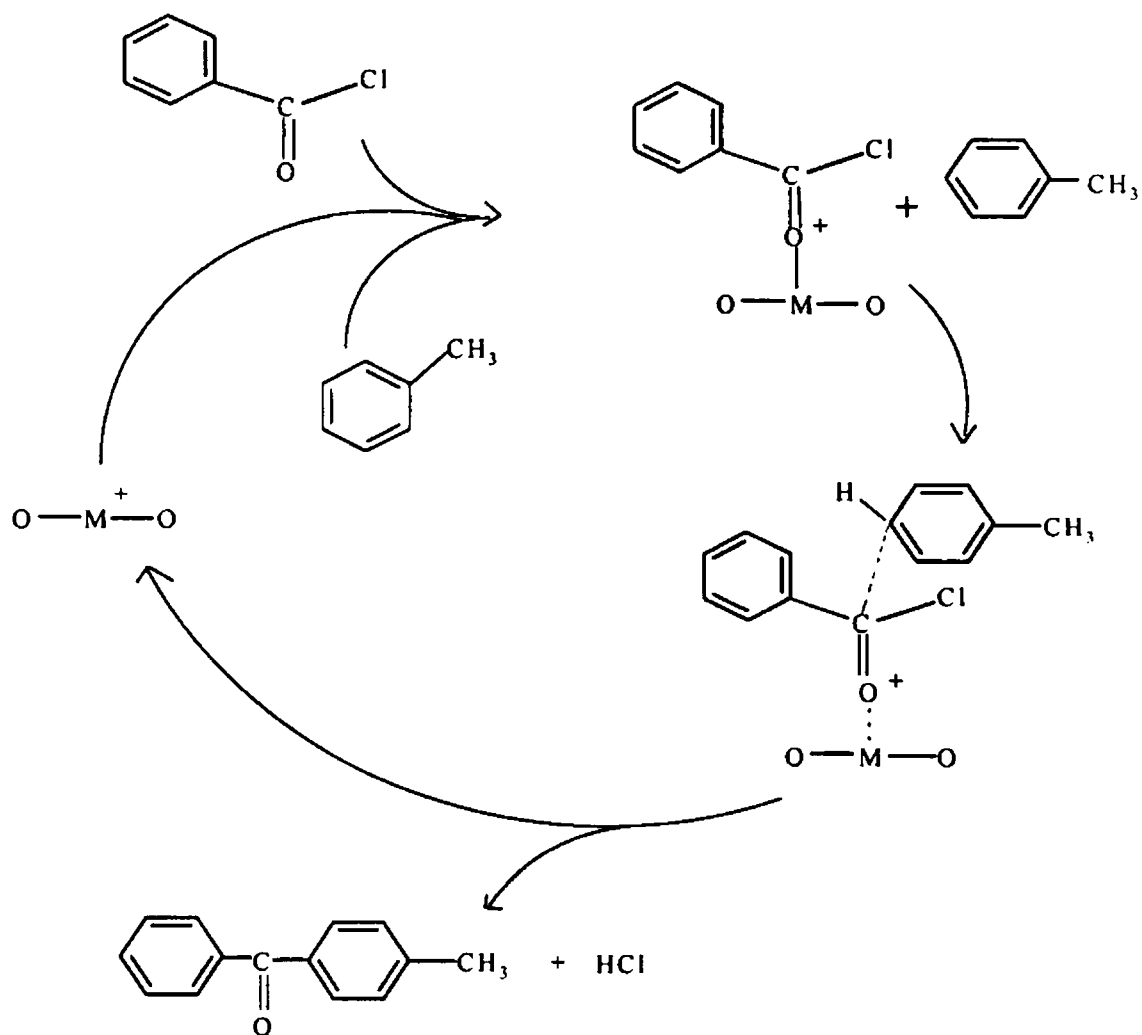


Figure 4.13 A plausible mechanism for the benzoylation of toluene with benzoyl chloride as reagent

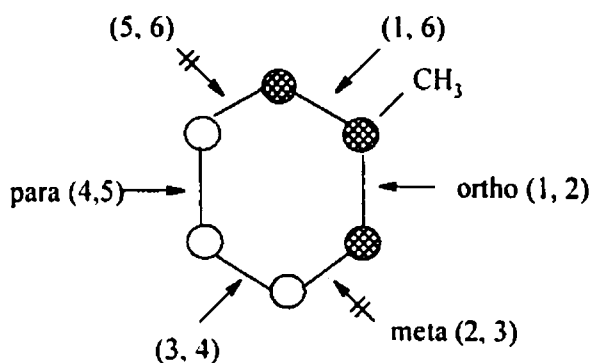


Figure 4.14 The HOMO of toluene suggesting only the *ortho* and *para* substituted products

4.3 Alkylation of Aniline

Alkyl anilines viz., N-methylaniline (NMA), N,N'-dimethylaniline (NNDMA), N-ethylaniline, N, N'-diethylaniline and 2,6-dimethylaniline are important intermediates for the manufacture of dyes and pharmaceuticals. These compounds are generally prepared by the catalytic alkylation of aniline with methanol or ethanol [39, 40]. Methylation of aniline is a multistep sequential reaction, the main reaction scheme of which can be represented as follows.

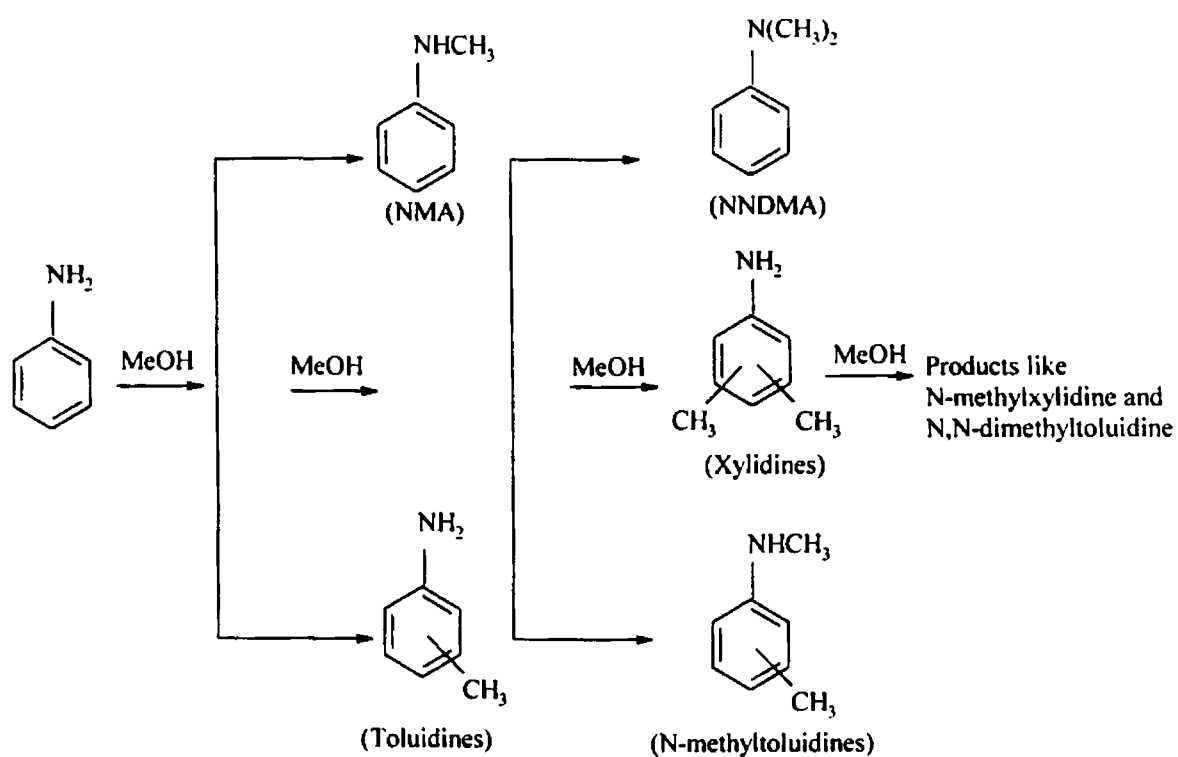


Figure 4.15 Reaction scheme of aniline alkylation using methanol as the alkylating agent

Extensive research regarding the alkylation of aniline has been performed by various researchers over different solid acid catalysts. Studies on metallosilicates have suggested that the weak acidity of the catalyst helps N-alkylation [41]. Hill *et al.* suggested that a low temperature normally favours N-alkylation and high temperature favours ring alkylation by Hoffmann-Martius rearrangement [42].

Yuvaraj and Palanichamy studied the reaction over Li-exchanged Y-zeolite for various Si/Al ratios [43]. They have also studied the influence of temperature and feed rate on this reaction. Maximum selectivity for N-alkylaniline around 90% is obtained at low temperature. The percentage conversion first increases and then decreases with the increase in temperature for the reaction. At higher temperatures,

both the side reactions of ethanol and the deposition of coke on the active sites account for the reduction in conversion. Aniline conversion and selectivity for N,N'-diethylaniline and C-alkylated products decreased with increase in WHSV. A similar trend is observed for the increase of SiO₂/Al₂O₃ ratio [43].

Singh *et al.* studied the reaction over AlPO-11, SAPO-11 and MASPO-11 catalysts in detail [44]. They have concluded that relatively stronger acid sites must be present for the consecutive methylation of aniline in N,N'-dimethylaniline formation. A direct relationship of aniline conversion to reaction temperature and methanol concentration is also established.

Prasad and Rao suggested the mechanism of aniline alkylation with methanol by carrying out the reaction on AlPO₄-5 catalysts [45]. They cited that NNDMA is, to a large extent, responsible for the increase in the yield of N-methyltoluidine. This occurs via N → C shift, which is favoured at high temperatures.

Thus majority of the literature gives evidence that the formation of the primary product namely NMA is always associated with the formation of NNDMA and C-alkylated products. Though metal oxides were reported to exhibit better selectivity for N-alkylation over C-alkylation, usually many such systems afford both mono and disubstitution on nitrogen leading to poor selectivity for the synthetically more important mono-substituted product. However, very high selectivity for N-monomethylation of aniline is observed with spinal systems [40, 46, 47].

Narayanan *et al.* extensively studied aniline alkylation reaction over various pillared montmorillonites [28, 48]. As the OH/Al ratio in the pillaring agent increases, they found that conversion reduces but selectivity to NMA increases. Ce-exchanged Al pillared montmorillonite showed excellent conversion compared to Al pillared montmorillonite, though the selectivity was less.

Aniline alkylation studies over modified silica and K10 montmorillonite [48, 49] suggest that although the presence of a certain amount of weak and medium acidity is essential for reaction, surplus acidity does not affect the conversion. By studying the reaction over modified zeolite and aluminium-pillared montmorillonites of different OH/Al ratios, they also observed that the porosity of the pillared clays affects the conversion of aniline, but not the selectivity pattern [48].

In the following sections we discuss the results of methylation of aniline performed over the present systems. Influence of various reaction parameters are also discussed in detail.

4.3.1 Process Optimisation

a) Effect of Flow Rate

A series of experiments were conducted at a reaction temperature of 350°C and with aniline to methanol molar ratio of 1: 7. The flow rate is varied from 4 to 6 mL h⁻¹. The catalyst was activated at 500°C before every catalytic run.

Table 4.19 shows the effect of flow rate on aniline conversion and selectivity. As the flow rate increases from 4 to 6 mL h⁻¹ the conversion steadily declines from 62% to 41%. The feed rate alters the contact time and at high flow rates, the encounter of the reactants and products with the catalyst surface will be less compared to that at lower flow rates. This results in lower conversions at higher flow rates. However, the selectivity for NMA reaches a maximum of 79.86% at a flow rate of 6 mLh⁻¹. The selectivity and yield for NNDMA and toluidines decreases as the flow rate increases. The contact time becomes insufficient for the successive alkylation of NMA to NNDMA, at high flow rates. The lower yield of NNDMA explains the lower yield of N-methyl p-toluidine since the latter is formed by the N → C shift of methyl group in the former [41].

Table 4.19 Effect of flow rate on aniline methylation reaction (0.5g FeAl_{0.3}PM activated at 500°C, reaction temperature- 350°C, aniline: methanol molar ratio- 1: 7, TOS- 2 h)

Flow rate (mL h ⁻¹)	Conversion (%)	Selectivity (%)			
		NMA	NNDMA	NMT	Others
4	62.03	53.54	36.51	4.50	5.45
		(33.21)*	(22.65)	(2.79)	(3.39)
5	52.19	65.24	29.49	2.36	2.91
		(34.04)	(15.39)	(1.23)	(1.52)
6	41.28	79.86	16.05	1.93	2.16
		(32.97)	(6.625)	(0.797)	(0.892)

* Figures in parenthesis give product distribution.

b) Effect of Reaction Temperature

The reaction is carried out at various reaction temperatures in the range of 300-450°C. Figure 4.16 shows the influence of reaction temperature on the

conversion and the product distribution. The general trend for the alkylation reaction is that the conversion usually increases with increase in temperature and reaches a steady state at high temperatures. In the present study, as the temperature increased from 300-350°C, the conversion and yields of both NMA and NNDMA increased apparently. Furthermore, a small but significant increase in the amount of ring alkylation was also observed. Maximum yield of both NMA and NNDMA were observed at 350°C. Increasing the temperature above 350°C did not improve alkylation activity. Both at 400°C and 450°C, the percentage conversion and the yields were lower than those at 350°C. This is because of the increased rate of decomposition of methanol at high temperatures resulting in the formation of side products such as CO, CO₂ and traces of C-1 and C-2 hydrocarbons.

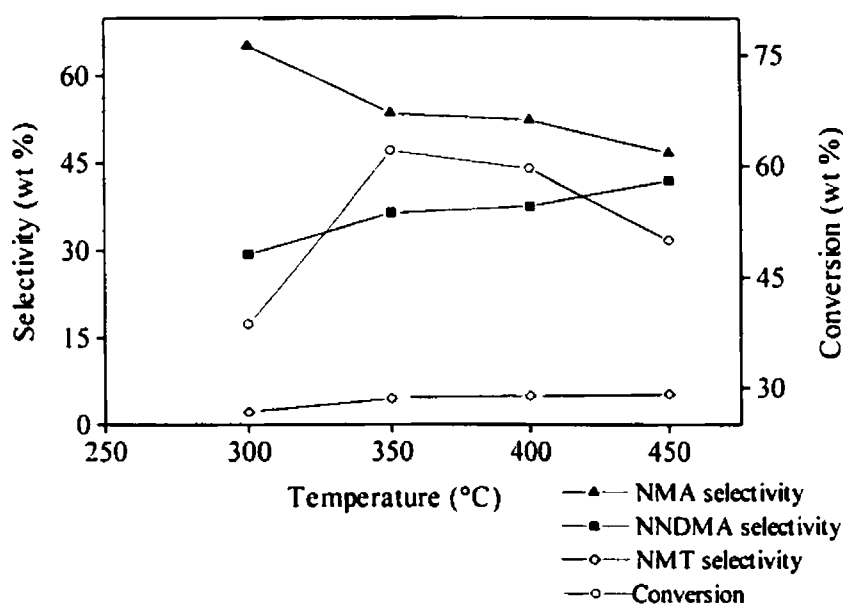


Figure 4.16 Methylation of aniline as a function of temperature (catalyst-0.5 g FeAl_{0.3}PM; reaction temperature- 350°C, aniline: methanol molar ratio- 1: 7, TOS- 2 h)

From these experimental data, it can be concluded that in the methylation of aniline, formation of NMA is favoured at low temperature. This is subsequently converted to NNDMA as the temperature is increased which is evident from its increased yields at higher temperatures.

c) Effect of Methanol to Aniline Molar Ratio

In order to understand the optimum feed-mix ratio, a series of experiments

were performed at 350°C with various molar ratios of methanol to aniline over FeAl_{0.3}PM. Methanol to aniline molar ratios varying from 1 to 9 is selected for study. Selectivity of products and aniline conversion is plotted against the methanol to aniline molar ratio in Figure 4.17. As the molar ratio increases, conversion increases up to a molar ratio of 7. However, further increase of molar ratio reduces the conversion. Both the NNDMA selectivity and the yield continuously increase throughout the range of molar ratio from 1 to 9. This indicates that consecutive methylation of NMA is more and more favoured at sufficiently large amount of the alkylating agent. However, excess of methanol beyond 7:1 molar ratio lowered the conversion because the alcohol probably underwent side reactions leading to the formation of other products. At high concentration of methanol, competitive adsorption of methanol may be preventing the adsorption of aniline over the catalyst surface. This also may be contributing to the reduction in percentage conversion.

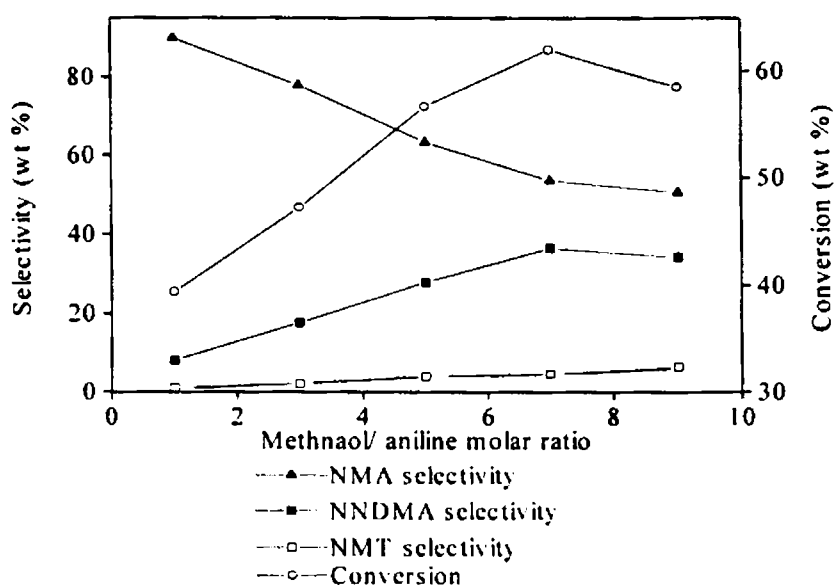


Figure 4.17 Methylation of aniline as a function of aniline to methanol molar ratio (catalyst-0.5 g FeAl_{0.3}PM, reaction temperature- 350°C, Flow rate-5 mLh⁻¹, TOS- 2 h)

d) Effect of Time on Stream

Performance of the reaction for a continuous five hours run, tests the deactivation of the catalyst. The products were collected and analysed after every one hour. It is seen that the conversion continuously declines from 62% to 49%. During the final stage, the activity remained more or less constant (Table 4.20).

However, the NMA yield remains almost constant throughout the reaction (Figure 4.18). This shows that the activity of the catalyst for monomethylation of aniline is retained even on its prolonged use. The gradual reduction in catalytic conversion is due to the deposition of coke formed during the course of reaction on the active sites, thus decreasing the number of available active sites.

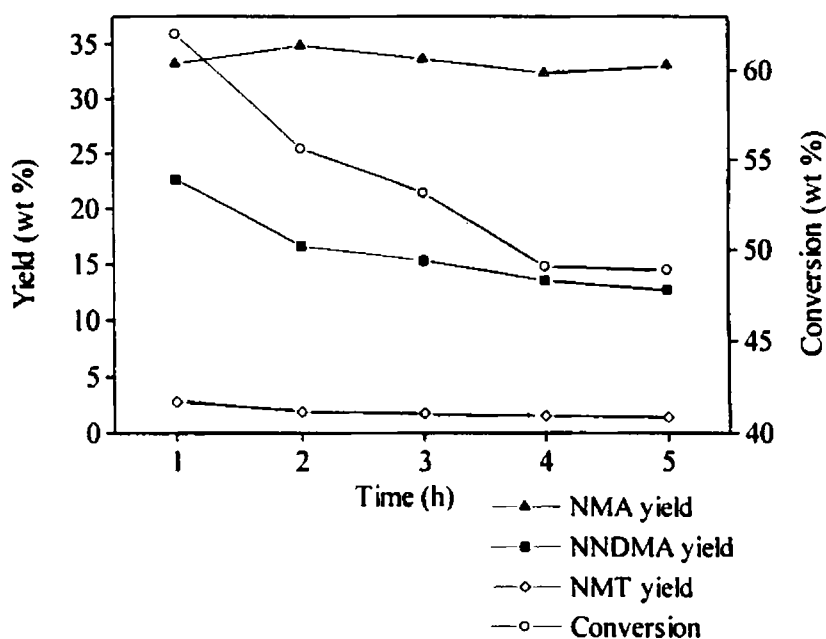


Figure 4.18 Deactivation study of aniline methylation reaction.

Table 4.20 Time on stream study of aniline methylation reaction (catalyst- 0.5g FeAl_{0.3}PM activated at 500°C, reaction temperature- 350°C, flow rate- 4 mLh⁻¹, aniline: methanol molar ratio- 1: 7)

Time (h)	Conversion (%)	Selectivity (%)			
		NMA	NNDMA	NMT	Others
1	62.03	53.54	36.51	4.50	5.45
2	55.61	62.63	28.83	3.40	3.89
3	53.15	63.23	28.82	3.32	4.63
4	49.07	65.89	27.63	3.10	3.78
5	48.91	67.63	26.01	2.95	3.41

4.3.2 Catalyst Comparison

a) Mixed Fe-Al systems: From the optimisation process we have seen that both monomethylation and dimethylation are taking place on the nitrogen of aniline to yield NMA and NNDMA respectively. Ring alkylation is also taking place to a small extent to give toluidines. Maximum conversion was obtained at a flow rate of 4 mLh^{-1} and at an aniline to methanol molar ratio of 1:7. Also, the methanol decomposition rate was minimum at a reaction temperature of 350°C (Figure 4.16). Hence the reaction is carried over the catalyst systems under these optimised conditions.

Aniline alkylation is an acid catalysed reaction and the amount and distribution of the acidity influence the conversion of aniline and selectivity pattern of the alkylanilines. Table 4.21 gives the reaction data over the parent and Fe-Al pillared systems. NMA and NNDMA are formed to a large extent. In most cases, the selectivity to N-alkylation is more than 90%. Due to the adsorption of aniline over the catalyst surface, alkylation usually yields N-alkylated products. (Mechanism will be discussed later). The parent montmorillonite showed only very little activity owing to its very low surface area and acidity. Mixed Fe-Al systems exhibited better activity compared to the single pillared systems namely, FePM and AlPM.

Table 4.21 Aniline methylation data over mixed Fe-Al systems (0.5 g activated at 500°C , reaction temperature- 350°C , molar ratio-1: 7, flow rate- 4 mL h^{-1} and TOS – 2h)

Catalyst	Conversion (%)	Yield of			Selectivity to N-alkylation
		NMA	NNDMA	Others (C-alkylation)	
M	5.62	3.12	1.70	0.80	85.77
AlPM	30.32	16.15	12.16	2.01	93.37
FeAl _{0.1} PM	52.30	28.13	29.63	3.54	93.23
FeAl _{0.2} PM	52.05	26.39	20.70	4.95	90.49
FeAl _{0.3} PM	62.03	33.21	22.65	6.18	90.03
FeAl _{0.4} PM	70.49	28.15	30.72	11.14	84.20
FeAl _{0.5} PM	64.82	17.65	25.81	21.36	67.05
FeAl _{1.0} PM	62.87	34.03	26.06	2.78	95.57
FePM	48.91	24.02	17.18	7.17	85.34

Comparing the C-alkylated products obtained over the systems, $\text{FeAl}_{0.5}\text{PM}$ gives a significantly higher yield for the same. This may be due to the larger number of strong acidity of that system. The strong acid sites favour C- alkylation [42]. Correspondingly, the yield for the N- alkylated products is comparatively less. It is reported that surplus acidity does not favour aniline alkylation, but a moderate acidity in the weak and medium region is sufficient for a good catalytic conversion [48]. Among all the mixed Fe-Al systems, $\text{FeAl}_{0.4}\text{PM}$ gave the maximum conversion with desirable product selectivity. The weak plus medium acidity is maximum for this system among the various mixed Fe-Al systems and hence maximum conversion is observed for this system..

AIPM showed a lesser conversion, namely 30.32%. We can see from the Table 3.19 that AIPM possesses enough active sites in the weak and medium region. However, there is not a correspondingly high activity. This can be due to the presence of more number of Brönsted acidic sites as can be seen from Table 3.13. At this stage it is relevant to discuss the mechanism of the reaction in detail.

Mechanism of Methylation of Aniline

The orientation effect in the aromatic ring is closely related to the electropolar nature of the previously introduced group. Due to the delocalisation effect of the unshared pair of electrons over the amino group into the benzene ring, it exerts an *ortho/para* orientation effect. As a result, the *ortho* and *para* positions of the ring become more susceptible to the electrophilic substitution and the expected major product is the *ortho* and/or *para* C-alkylated aniline. But due to the adsorption of aniline (owing to the presence of lone pair on nitrogen) over the surface, alkylation usually yields N-alkylated products. The catalyst also plays a major role in releasing the electrophile from the alkylating agent, namely methanol. Comparing aniline and methanol, aniline being a stronger base, gets adsorbed preferentially over the Lewis sites. The high electronegativity of the oxygen of methanol, leads to hydrogen bonding with hydroxyl protons of the Brönsted sites and thus methanol is adsorbed over the Brönsted sites as shown in the Figure 4.19. Protonation of alcohol, dehydration and subsequent formation of ether linkage of the released carbocation may follow. On the Lewis site, the adsorbed aniline may lose a proton to balance the positive charge developed on the nitrogen. The high electronegativity of oxygen in the ether linkage results in the development of partial positive charge on the alkyl

side chain, initiating heterolytic cleavage of polar O-C bond and shift of alkyl carbocation to nitrogen.

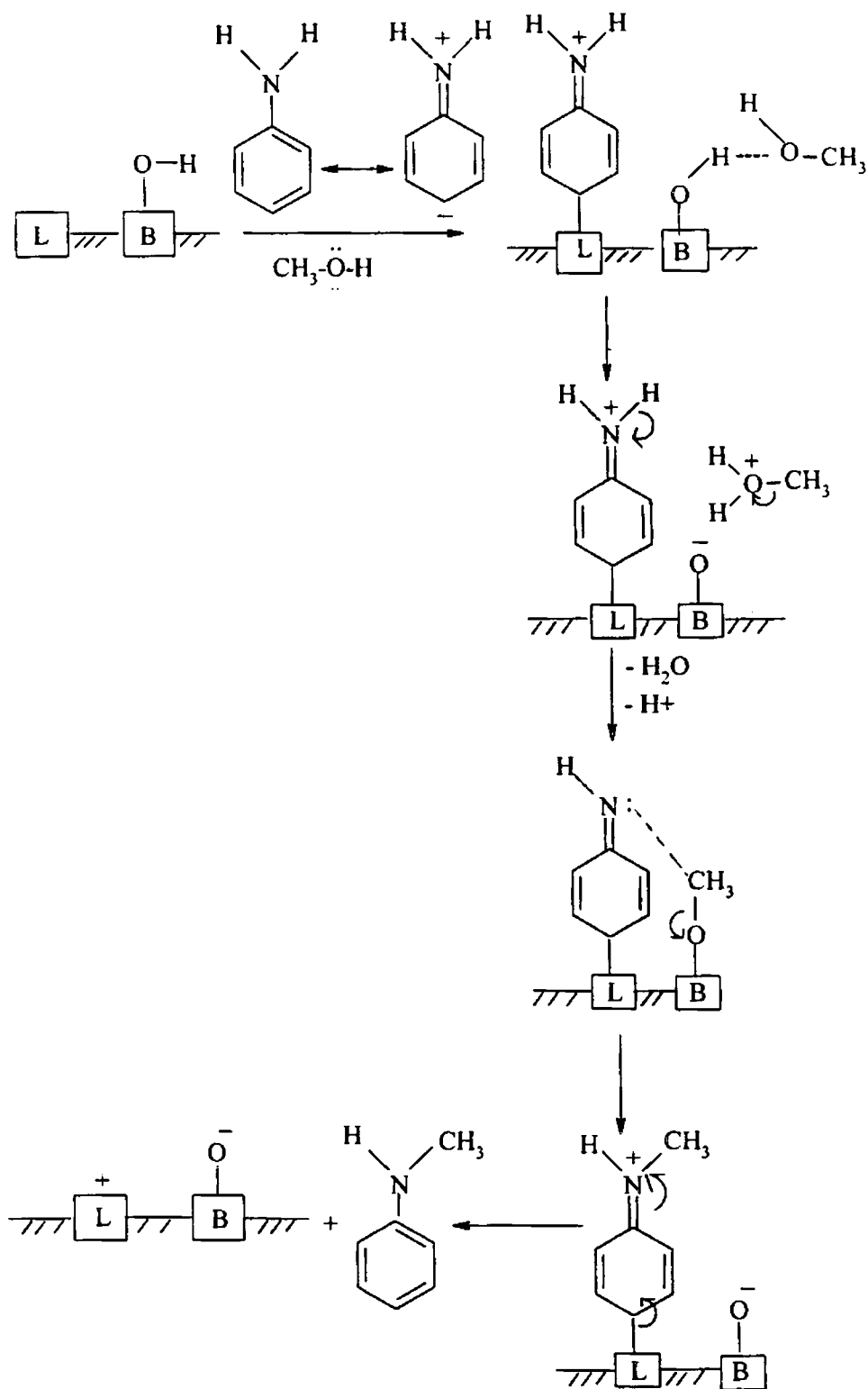


Figure 4. 19 Mechanism of aniline methylation over pillared clays involving both Brønsted acidic sites and Lewis acidic sites.

Thus we can infer that, for the reaction to take place in the desired direction, aniline should adsorb on Lewis sites and methanol on Brönsted sites. However, in the presence of a larger number of Brönsted acidic sites, the possibility of adsorption of aniline over these sites cannot be ruled out which in turn reduces the percentage conversion. In AIPM, there is a larger number of Brönsted acidic sites and due to the inhibiting effect imparted by the adsorption of aniline over these sites, the catalytic activity is found to be less.

b) Mixed Cr-Al systems: The data for aniline methylation reaction over Cr-Al systems is shown in Table 4.22. We can see that these mixed systems are very efficient for converting aniline to NMA and NNDMA. A combination of Brönsted and Lewis acidity in the weak and medium region is required for the reaction [48]. We could not get a clear-cut dependence of the activity with the acidity measured by employing the various techniques. Compared to iron systems, chromium systems exhibited higher percentage conversion, though the acidity determined by TPD of ammonia is less for the chromium systems. This is suggestive of the fact that only weak to moderate acidity favour the reaction and the presence of a certain minimum number of acidic sites is enough to trigger the reaction. Any excess number of acid sites even if present, will not be involved in the reaction and will be superfluous.

Table 4.22 Data of aniline methylation reaction over mixed Cr-Al systems (0.5 g activated at 500°C, reaction temperature-350°C, molar ratio-1: 7, flow rate- 4 mL h⁻¹ and TOS – 2h)

Catalyst	Conversion (%)	Yield of			Selectivity to N-alkylation
		NMA	NNDMA	Others (C-alkylation)	
AIPM	30.32	16.15	12.16	2.01	93.37
CrAl _{0.1} PM	74.47	34.74	31.62	7.75	89.59
CrAl _{0.2} PM	75.11	32.58	30.16	12.36	83.54
CrAl _{0.3} PM	79.74	43.03	29.99	6.71	91.59
CrAl _{0.4} PM	81.49	38.61	25.07	8.37	89.73
CrAl _{0.5} PM	78.90	38.46	28.35	12.01	84.78
CrAl _{1.0} PM	61.17	28.87	23.36	8.93	85.40
CrPM	62.73	27.08	20.39	15.65	75.05

c) *Vanadia impregnated iron-pillared systems*: Table 4.23 explains the results for the reaction when carried over the vanadia loaded samples. It can be seen from the table that as the percentage of vanadia loading increases, the conversion also increases up to 7% loading, thereafter a decrease is observed. Due to the blocking of acidic sites at higher loadings and also the reduction in surface area at high vanadia loadings the activity is less. Vanadia addition improves the Brönsted acidity and

Table 4.23 Aniline methylation reaction data over vanadia loaded FePM (0.5 g activated at 500°C, reaction temperature-350°C, molar ratio-1: 7, flow rate- 4 mL h⁻¹ and TOS – 2h).

Catalyst	Conversion (%)	Yield of			Selectivity to N-alkylation
		NMA	NNDMA	Others (C-alkylation)	
FePM	48.91	24.02	17.18	7.17	85.34
2VFe	48.90	18.85	20.27	8.54	82.53
5VFe	58.82	29.19	25.89	13.74	76.64
7VFe	60.24	22.72	20.34	17.18	71.48
10VFe	40.04	20.28	12.96	6.80	83.01
15VFe	39.92	22.70	15.61	1.59	96.49
20VFe	10.77	6.46	2.64	1.67	84.49

creates Lewis acidity [48]. Table 3.21 shows that the weak plus medium acidity of 7VFe is more than two times the value of FePM. Though the activity is increasing with the increase in acidity, the increase in acidity does not commensurate with the increase in activity. Thus once again we can conclude that only a moderate acidity is required for the reaction.

To conclude, an acceptable correlation between the weak plus acidity is obtained for mixed Fe-Al pillared systems and vanadia loaded iron pillared systems within each set of systems, but may not be applicable to the acidity/alkylation activity of two different sets or types of catalysts.

References

- [1] G.A. Olah, *Friedel-Crafts and Related Reaction*, Intersciences (Ed.), Vol. 111, Part 1, New York, 1964.
- [2] J.N. Kim, K.H. Chung and E.K. Ryu, *Tetrahedron Lett.*, 35 (1994) 903.
- [3] K.H. Chung, J.N. Kim and E.K. Ryu, *Tetrahedron Lett.*, 35 (1994) 2913.
- [4] S.H. Back, *J. Chem. Res. (S)* (1994) 451.
- [5] S. Pivsa-Art, K. Okuro, M. Miura, S. Murata and M. Nomura. *J. Chem. Soc. Perkin Trans. I* (1994) 1703.
- [6] G.A. Olah, G.K.S. Prakash and J. Sommer, *Super acids*, Wiley-Interscience, New York, Brisbane, Toronto, 1985.
- [7] J.C. Jansen, E.J. Geyghton, S.L. Njo, H. Van Koningsveld and H. Van Bekkum, *Catal. Today*, 38 (1997) 205.
- [8] G.D. Yadav, T.S. Throat and P.S. Kumbhar, *Tetrahedron Lett.*, 34 (1993) 529.
- [9] J.H. Clark, S.R. Cullen, S.J. Barlow and T.W. Bastock, *J. Chem. Soc. Perkin Trans. II* (1994) 1117.
- [10] P.R. Kurek, *US Patent*, 5 126 489 (1992).
- [11] M. Misono, *Adv. Catal.*, 41 (1996) 113
- [12] S. Getto, M. Getto and Y. Fimura, *React. Kinet. Catal. Lett.*, 41 (1991) 27.
- [13] S. Kodomari, Y. Suzuki and Y. Yoshida, *Chem. Commun.*, 1567 (1997).
- [14] M. Spagnol, L. Gilbert and D. Alby in "The Roots of the Organic Development" (J.R. Desmurs and S. Ratton (Eds.)), *Industrial Chemistry Library*, Vol. 8, p-29, Elsevier, Amsterdam, 1996.
- [15] N. He, S. Bao and Q. Xu, *Appl. Catal. A Gen.*, 169 (1998) 29.
- [16] B.M. Choudhary, M.L. Kantam, M. Sutesh, K.K. Rao and P.L. Santhi, *Appl. Catal. A Gen.*, 149 (1997) 25.
- [17] T. Cseri, S. Bekassy, F. Figueras and S. Rizner, *J. Mol. Catal. A Chem.*, 98 (1995) 101.
- [18] S. Jun and R. Ryoo, *J. Catal.*, 195 (2000) 237.
- [19] P. Botella, A. Corma, J. M. Lopez-Nieto, S. Valencia and R. Jacquot, *J. Catal.*, 195 (2000) 161.
- [20] D. Bandry-Barbier, A. Dormont and F. Duriau-Montagne, *J. Mol. Catal. A Chem.*, 149 (1999) 215.

- [21] M. Hino and K. Arata, *J. Chem. Soc. Chem. Commun.*, (1985) 112.
- [22] B. Jacob, S. Sugunan and A. P. Singh, *J. Mol. Catal. A Chem.*, 139 (1999) 43.
- [23] C. Cativiela, J.M. Fraile, J.I. Gracia, J.A. Mayoral, F. Figueras, L.C. de Menorval and M. Shouji, *Appl. Catal. A Gen.*, 197 (2000) 213
- [24] G.A. Olah, *Friedel-Crafts Chemistry*, Wiley Intersciences, New York, London, Sydney, Toronto, 1973.
- [25] K. Arata, H. Nakamura and M. Shouji, *Appl. Catal. A Gen.*, 197 (2000) 213.
- [26] V.R. Choudhary, S.K. Jana and B. P. Kiran, *J. Catal.*, 182 (2000) 257.
- [27] H.H.P. Yiu and D. R. Brown, *Catal. Lett.*, 56 (1998) 57.
- [28] S. Narayanan and K. Deshpande, *Appl. Catal. A Gen.*, 193 (2000) 17
- [29] K.J. Laidler and J.H. Meiser, in "Physical Chemistry" CBS Publishers and Distributors, New Delhi, p-442.
- [30] F. Figueras, *Catal. Rev. Sci. Engg.*, 30 (1988) 457.
- [31] K. Arata, M. Hino and N. Yamagata, *Bull. Chem. Soc. Jpn.*, 63 (1990) 21.
- [32] B.M. Choudhary, V. Bhaskar, M.L. Kantam, K.K. Rao and K. V. Raghavan, *Green Chemistry*, (2000) 67.
- [33] J.E. Huhee, E.A. Kieter and R.L. Keiter, "Inorganic Chemistry Principles of Structure and Reactivity", Fourth Edn., Addison-Wesley Publishing Company, Tokyo, Milan, Paris, New York, 1993, p- 114.
- [34] R. D. Laura, *Clay. Miner.*, 11 (1976) 331.
- [35] T. J. Pinnavaia, *Science*, 220 (1983) 365.
- [36] K. Arata and M. Hino, *Appl. Catal.*, 59 (1990) 197.
- [37] Y. Xia, W. Hua and Z. Gao, *Catal. Lett.*, 55 (1998) 101.
- [38] G.A. Olah, S. Kobayashi and M. Tashoro, *J. Amer. Chem. Soc.*, 94 (1972) 7448.
- [39] S. Narayanan, B.P. Prasad and V. Viswanathan, *React. Kinet. Catal. Lett.*, 48 (1992) 561.
- [40] K. Sreekumar, T.M. Jyothi, M.B. Talawar, B.P. Kiran, B.S. Rao and S. Sugunan, *J. Mol. Catal. A Chem.*, 152 (2000) 225.
- [41] Y.K. Park, K.U. Park and S.I. Woo, *Catal. Lett.*, 26 (1994) 169.
- [42] A.G. Hill, J.H. Shippe and A.J. Hill, *Ind. Eng. Chem.*, 43 (1951) 1579.

- [43] S. Yuvaraj and M. Palanichamy, *Catalysis: Modern Trends*, (N.M. Gupta and D.K. Chakrabarthy (Eds.)) Narosa Publishing House, New Delhi, India, 1995.
- [44] P.S. Singh, R. Bandopadhyay and B.S. Rao, *Appl. Catal.*, 136 (1996) 177.
- [45] S. Prasad and B.S. Rao, *J. Mol. Catal.*, 62 (1990) L 17.
- [46] K. Sreekumar, Ph. D. Thesis, Cochin university of Science and Technology, 1999.
- [47] K. Sreekumar, T. Raja, B.P. Kiran, S. Sugunan and B.S. Rao, *Appl. Catal. A Gen.*, 182 (1999) 327.
- [48] S. Narayanan and K. Deshpande, *Appl. Catal. A.Gen.*, 193 (2000) 17.
- [49] S. Narayanan and K. Deshpande, *Appl. Catal. A. Gen.*, 199 (2000) 1.
- [50] S. Narayanan and K. Deshpande, *Micropor. Mater.*, 11 (1997) 77.

Pillared Clays As Efficient Catalysts For Liquid Phase Catalytic Wet Peroxide Oxidation Of Phenol

5.0 Introduction

In recent years, the problem of disposing waste-water containing toxic organic pollutants has become increasingly acute due to the tightening of environmental regulations. Catalytic wet peroxide oxidation (CWPO) using heterogeneous catalysts is being developed as a powerful technique for the treatment of dilute aqueous waste streams contaminated by a variety of organic pollutants. The complete oxidation of phenol and other organic compounds in waste-water stream is achieving considerable attention in recent years. Phenol is an important environmental waste pollutant. It is a very simple organic compound, easily soluble in water at different conditions of acidity. It will be of added advantage, if this phenol is converted to useful products. The oxidation of phenol by H_2O_2 is a widely applied process in chemical industry for the production of hydroxylation derivatives, namely catechol and hydroquinone (diphenols). These hydroxylation products are extensively used as photographic developers, ingredients for food and pharmaceutical applications and antioxidants. Hence, much attention is being paid to the production of diphenols from phenol employing the catalytic wet peroxide method. Till date, different types of solids were proposed as catalysts for the oxidation of phenol [1-5].

$HClO_4-H_3PO_4$ and $Fe(III)/Co(II)$ catalysts are used conventionally for the oxidation of phenol. But obvious shortcomings of these homogeneous catalysts prevent their wide use in diphenol production [6, 7]. To date, many researchers have been interested in the development of heterogeneous catalysts for hydroxylation of phenol in the liquid phase with H_2O_2 as oxidising agent. These catalysts include TS-1 [8, 9], TS-2 [10, 11], Ti-MCM-41 [12], Cu-ZSM-5 [13], etc. Simple metal oxides and supported metal oxides are also found to catalyse phenol hydroxylation [14, 15]. All these systems have one or other limitations. Even though attractive catalytic activities were shown by the transition metal containing zeolites, their drawback is that they are often expensive and relatively difficult to synthesise. The slower

reaction rate also limits their wide application in industrial production. Simple and supported metal oxides have poor catalytic activity and low diphenol selectivity.

A number of factors such as calcination conditions [16], nature of solvent [17], reaction temperature, concentration of H_2O_2 [18], procedure for H_2O_2 addition [19] and crystal size [20] have been identified as the key parameters for phenol hydroxylation reaction. However, even today, various aspects of the phenol hydroxylation, such as the reaction mechanism, contribution of the external surface, and diffusion of the reactants and products are not yet fully understood.

Generally the catalytic activity and product selectivity in phenol hydroxylation by hydrogen peroxide are strongly influenced by surface area of the catalyst, nature of solvent, reaction time, reaction temperature, molar ratio of phenol to hydrogen peroxide and catalyst amount. Several research articles have been published related to this field [17, 18, 21]. Xiong *et al.* synthesised different Fe-based complex oxide catalysts and studied the reaction [22]. They found that Fe-Mg-Si-O complex catalyst is a new hopeful catalyst to replace TS-1 in the diphenol production industry. They also noticed an induction period at the beginning of the reaction. The induction period was shortened when the crystallite size was smaller. They concluded that the heterogeneously catalysed aqueous phase oxidation of phenol proceeds by a free radical mechanism, involving initiation on the catalyst surface followed by homogeneous or heterogeneous propagation in the liquid phase. The phenoxy radicals initiate the reaction chain in the solution.

Yu *et al.* [23] established that a catalyst of V-Zr-O complex was more active than the respective simple oxides and their mechanical mixture. They studied the influence of solvents on the reaction and found acetonitrile to be a better solvent than acetone. This was attributed to the increased polarity of acetonitrile over acetone.

The same team systematically studied the influence of reaction time, reaction temperature and molar ratio of phenol to H_2O_2 on the reaction and made the following observations- (a) low residence time led to relatively low phenol conversion as well as undesirable product selectivity, (b) high reaction temperatures increased the phenol conversion and (c) as the amount of H_2O_2 is increased, the phenol conversion first increased and then decreased [21].

Van der Pol *et al.* [18] studied the reaction over titanium silicate-1 samples and concluded that the catalytic activity strongly depended on the particle size of the catalyst. The higher activity of smaller catalyst particles is not caused by a larger contribution of the outer surface of the catalyst particles, but by a higher catalyst efficiency as a result of less pore diffusion limitation. These authors excluded a major influence of external surface activity.

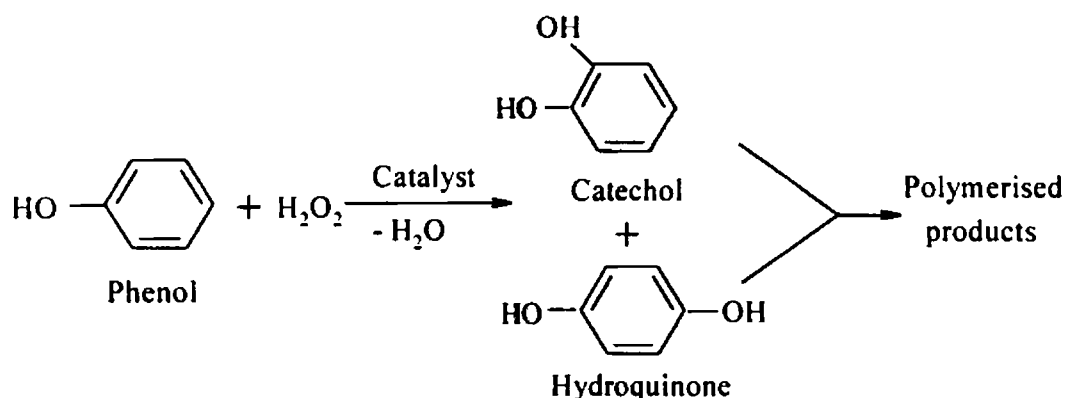
The hydroxylation of phenol to catechol and hydroquinone using aqueous H₂O₂ over TS-1 catalyst has been studied by Tuel *et al.* also [24]. They have found that both external and internal catalytic sites of TS-1 play an important role in the oxidation of phenol with H₂O₂. Inside the channels, the production of hydroquinone prevails whereas outside the channels, the major product formed is catechol. Furthermore, they showed that the catalytic processes can be influenced and thereby the selectivity can be varied using appropriate solvents.

Phenol hydroxylation reaction has been performed over various pillared clays also. Reports on clay based catalysts pillared by Fe- hydroxo complexes [25], mixed Al-Cu [1] and Al-Fe complexes [26] have shown that the mixed pillared clays exhibit the most promising results for the total oxidation of organic compound in water, using H₂O₂ as the oxidant. The influence of solvent in the hydroxylation of phenol on titanium pillared montmorillonite have been studied by Castello *et al.* [27]. Studies over Al-Fe pillared clay catalyst have shown that the catalyst could be one of the most promising catalysts for an industrial de-pollution process [26]. Over this catalyst, under mild reaction conditions, about 80% of the initial amount of phenol was found to be transformed into CO₂, at 70°C, in two hours under atmospheric pressure. However, more stress is given to the disposal of phenol from waste-water than the selective synthesis of catechol and hydroquinone.

We have carried out the catalytic wet peroxide oxidation of phenol over the various pillared clay systems due to the following reasons.

- (1) Phenol is a major water pollutant.
- (2) Phenol hydroxylation yields industrially important chemicals such as catechol and hydroquinone.
- (3) To check the prepared catalysts' activity towards oxidation reaction, since the phenol hydroxylation is extremely sensitive to the quality of the catalyst [1].

The reaction scheme is depicted below.



Schematic representation of hydroxylation of phenol

We have tried to understand the influence of the parameters such as reaction temperature, solvent used and concentration of H₂O₂ on hydroxylation of phenol. After optimising the conditions, we have tested the catalytic activity of all the pillared and vanadia impregnated clay samples.

1 mL of phenol and 5 mL of the solvent was introduced into a 50 mL round bottomed flask equipped with a magnetic stirrer and an air condenser. Desired amount of 30% H₂O₂ was added to the flask as a whole. 0.1 g of the catalyst was then introduced into the reactor and the components were allowed to react for one hour. After one hour, the liquid sample was withdrawn and filtered. The components in the withdrawn liquid were then analysed using gas chromatography. We have observed tar formation due to the over oxidation of products in all cases. However, the formation of tar is neglected and only the phenol conversion towards diphenol formation is taken into account.

5.1 Process Optimisation

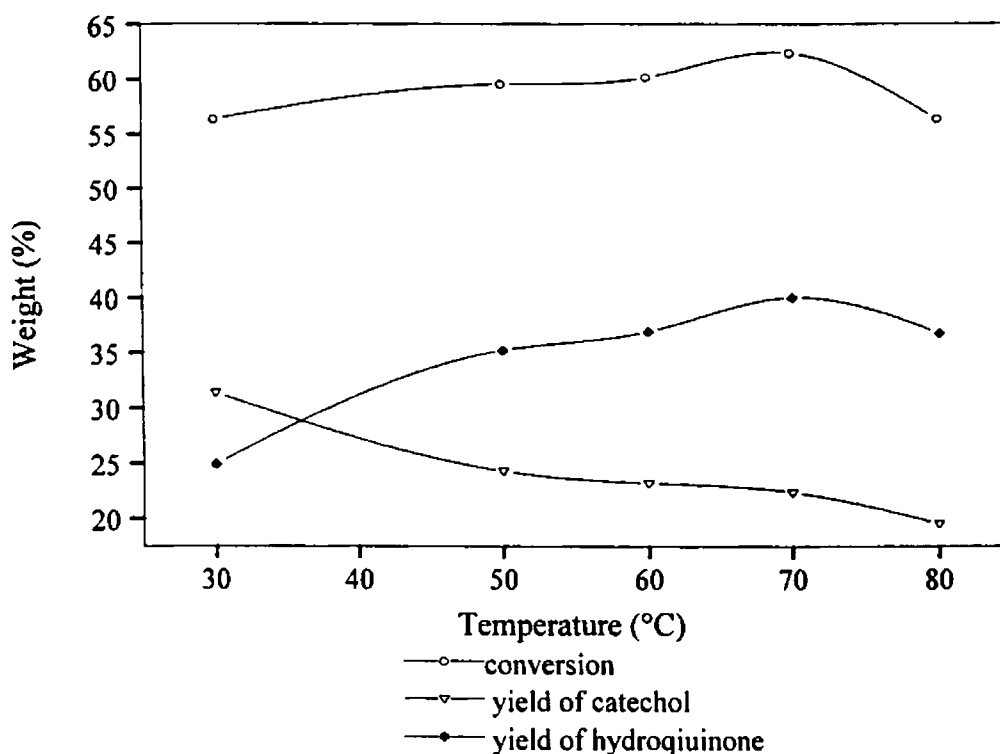
Hydroxylation of phenol can be performed under atmospheric pressure. This reaction is extremely sensitive to the reaction conditions and the quality of the catalyst. A detailed discussion on the optimization process is presented below.

5.1.1 Effect of Reaction Temperature

A set of experiments was carried out using FeAl_{0.5}PM as catalyst for studying the influence of temperature. Temperatures from 30 to 80°C were selected. The

Table 5.1 Influence of temperature on hydroxylation of phenol over $\text{FeAl}_{0.5}\text{PM}$ (5 mL H_2O_2 , 1 mL phenol, 5 mL water, room temperature)

Temperature (°C)	Conversion (%)	Selectivity	
		Catechol	Hydroquinone
30	56.33	55.75	44.25
50	59.53	40.86	59.14
60	60.15	38.62	61.38
70	62.38	35.89	64.11
80	56.31	34.71	65.29

**Figure 5.1** Effect of temperature on wet peroxide oxidation of phenol over $\text{FeAl}_{0.5}\text{PM}$

results are furnished in Table 5.1 and Figure 5.1. A steady increase of conversion with increase in temperature, as is usually the case, is not observed here. The percentage conversion not only increased very insignificantly, but also decreased by increasing the temperature above 70°C. As the temperature is increased, decomposition of H_2O_2 to molecular oxygen will increase. This side effect suppresses

the increase in conversion with increase in temperature. Molecular oxygen or air is not found to be effective for phenol hydroxylation reaction, as is being confirmed by our experiments. Instead of H_2O_2 we have used air as an oxidant and it is found that the phenol is neutral towards hydroxylation when air/ O_2 was used as the oxidant. Similar results were reported by Dubey *et al.* [28].

At a high temperature of 80°C , the decomposition of H_2O_2 is very high and the net result is decrease in conversion. However, the data on the selectivity patterns of diphenols (Table 5.1) show that, as the temperature is increased, there is a gradual increase of selectivity to hydroquinone with a concomitant decrease in selectivity to catechol. It is reported that, in the case of zeolites and molecular sieves as catalysts catechol is formed on the external surface of the catalyst whereas hydroquinone is formed inside the pores [16, 24]. Since pillared clays also have a porous structure, we can propose that, on the external surface catechol is formed and inside the pores hydroquinone is formed. As the temperature is increased, diffusion from the pores is more favoured. This is clear from the increase in yield of hydroquinone with the increase in temperature.

5.1.2 Effect of Solvent

It has been mentioned in several articles that phenol conversion and product selectivity are sensitive to the nature of the solvent used [21, 24, 29]. We have employed different solvents such as water, methanol, acetonitrile and acetone for the reaction. The influence of solvent on the phenol hydroxylation is summarised in Table 5.2. The reaction is performed at room temperature using the catalyst $\text{FeAl}_{0.5}\text{PM}$. There was no conversion for phenol when acetone was used as a solvent. With acetonitrile as solvent, a slight conversion of phenol, namely 1.72% was observed with 100% selectivity to catechol. The catalytic reaction showed much higher conversion when methanol and water were used as solvents. Among all the solvents studied, water is found to be the best solvent. Phenol conversion was 56.33% with water as solvent whereas it was only 22.02% with methanol as solvent. The highest activity with water can be ascribed to the strong adsorption of phenol on the catalyst in this solvent, which is driven by the non-ideality of the water-phenol solution. At the same mole fraction, the calculated activity coefficient of phenol using UNIFAC software [30] is much higher in water than in the other solvents. The

activity coefficients are shown in Table 5.3. The high activity coefficient of phenol in water leads to the strong adsorption of phenol over the catalyst. This, in fact, can be taken as a driving force in eliminating phenol from waste-water using these catalysts. Hence a higher amount of adsorbed phenol and low H_2O_2 concentrations as a result of competitive adsorption effects, are expected with water as solvent. This leads to a higher percentage conversion of phenol in water.

It should also be noticed that as the polarity of the solvent increases, phenol conversion also increases [21]. Among the different solvents studied, the polarity is of the order- water > methanol > acetonitrile > acetone. The phenol conversion also follows the same order as evident from Table 5.2.

Among the organic solvents, methanol is found to be better than acetonitrile and acetone. The absence of activity with acetone as a solvent can be attributed to the possible side reactions between H_2O_2 and acetone yielding hydroxy hydroperoxy propane and derived products (Figure 5.2) [31, 32]. This results in a lower concentration of free H_2O_2 at or near the active sites of the catalyst.

Table 5.2 Influence of solvent on phenol hydroxylation reaction (0.1 g $\text{FeAl}_{0.5}\text{PM}$, room temperature, 5 mL H_2O_2 , 1mL phenol, 5 mL solvent and time of reaction-1 h).

Solvent	Conversion (%)	Selectivity	
		Catechol	Hydroquinone
Water	56.33	55.75	44.25
Methanol	22.02	25.83	74.17
Acetonitrile	1.72	100	-
Acetone	-	-	-

With water, an almost equimolar mixture of catechol and hydroquinone was formed during the reaction, *o/p* ratio being 1.26 (yield of catechol is little more than that of hydroquinone). When methanol was used, the *para* product, namely hydroquinone was formed as the major product (*o/p* = 0.348). Thus, a replacement of water by methanol resulted in a significant decrease of the *o/p* hydroxylation selectivity. Enhanced *para* selectivity in methanol solvent is confirmed by various literature reports [16, 19, 24]. Catechol formation mainly takes place over the

external surface and hydroquinone formation takes place inside the pores, i.e., on the internal surface. In water, the consumption of phenol takes place relatively more on the external surface, as can be deduced from the slightly larger yield of catechol. The relatively small contribution of the internal surface to the rate of consumption of phenol can be explained by the strong adsorption of phenol in the catalyst using water as a solvent. Due to the competitive adsorption, the concentration of hydrogen peroxide near the active sites inside the pore system of the catalyst (internal surface) will be very low. This will result in a low observed rate for the consumption of phenol in the pores. However, with methanol as the solvent, the data clearly indicate that a relatively larger consumption of phenol is taking place inside the pores to yield around 74% selectivity towards hydroquinone formation.

Table 5.3 Activity coefficient of phenol in the different solvents

Solvent	Activity coefficient (Y)
Water	9.0535
Methanol	0.5943
Acetone	0.3047

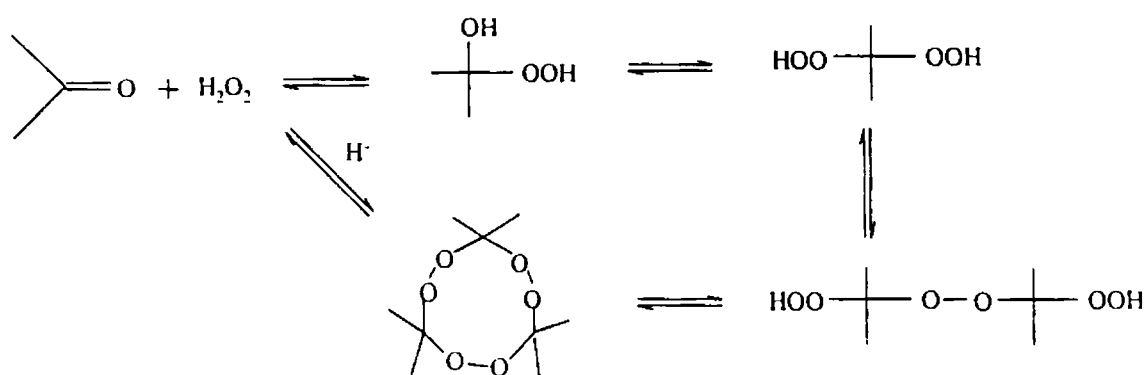


Figure 5.2 Formation of alkylidene peroxides from acetone and hydrogen peroxide

5.1.3 Effect of Amount of Hydrogen Peroxide

Table 5.4 summarises the catalytic hydroxylation results under various molar ratios of phenol to H_2O_2 . Three molar ratios were selected and the reactions were carried out using water as solvent. It is found that the phenol conversion and proportion of the products are sensitive to variation in phenol to H_2O_2 molar ratio (Table 5.4). 1 mL phenol was used in all cases with the amount of H_2O_2 varied as 3, 5 and 10 mL corresponding to H_2O_2 /phenol molar ratios of 8.61, 14.32, and 28.69 respectively. As the H_2O_2 amount changed from 3 to 5 mL, the conversion increased from 10.14 to 56.33%. However, further increase of H_2O_2 only reduced the conversion to 20.84%. A very significant reduction of the yield (Figure 5.3) is observed when a large excess of H_2O_2 is used. Similar results were observed by Neumann *et al.* [29] and Yu *et al.* [21]. Neumann *et al.* explain the decreased yield on the basis of the negative influence of the large amount of water accompanying the H_2O_2 sample. However, in other reports [33], even if large amount of water was used as solvent, phenol conversion was found to be satisfactory. The negative effect of water accompanying the hydrogen peroxide may be, of course, a minor reason for the decrease in conversion with high H_2O_2 /phenol molar ratio. We propose two major reasons for the decreased yield at higher H_2O_2 concentration viz., a) the large excess of H_2O_2 leads to deep oxidation of the products and b) the large excess of the H_2O_2 leads to the increased H_2O_2 decomposition as a result of which the yield of diphenols reduced remarkably. Although the tar selectivity is not determined quantitatively, the excessive formation of tar is observed during reaction with large amount of H_2O_2 . This also contributes to the decreased yield of diphenols.

Table 5.4 Effect of amount of H_2O_2 on phenol hydroxylation reaction (0.1 g of $\text{FeAl}_{0.5}\text{PM}$, room temperature, 5 mL water as solvent)

H_2O_2 /phenol molar ratio	Conversion (%)	Selectivity	
		Catechol	Hydroquinone
8.61 (3 mL /1 mL)	10.14	83.41	16.59
14.32 (5 mL /1 mL)	56.33	55.75	44.25
28.69 (10 mL /1 mL)	20.84	60.55	39.45

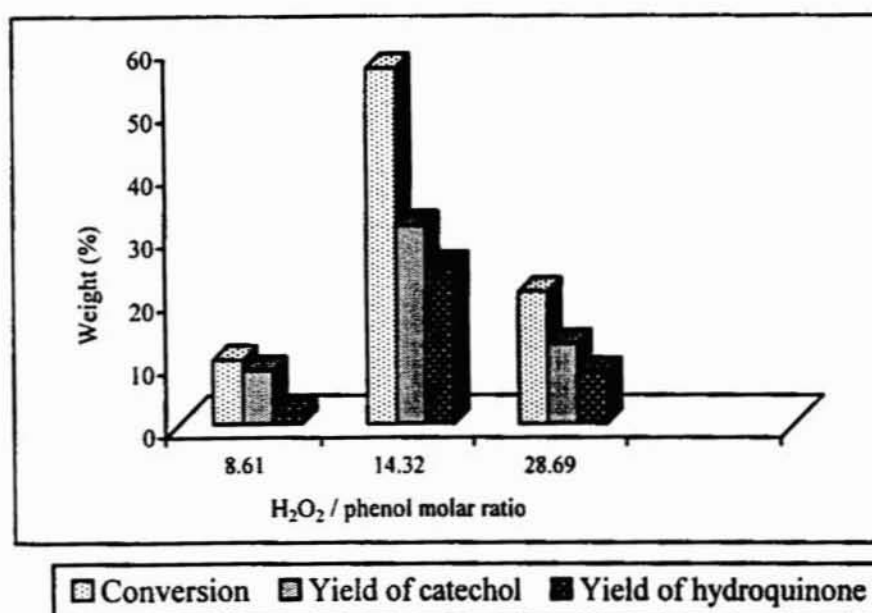


Figure 5.3 Influence of H₂O₂/phenol molar ratio on hydroxylation of phenol

5.1.4 Effect of Reaction Time

Table 5.5 summarises phenol hydroxylation data with time on stream over the catalyst. There is an induction period at the beginning of the reaction (Figure 5.4) and the phenol conversion increases exponentially, after the induction period. After a

Table 5.5 Time on stream study of hydroxylation of phenol over FeAl_{0.5}PM (0.1 g, 1 mL phenol, 5 mL H₂O₂, 5 mL water, room temperature)

Reaction time (min.)	Conversion (%)	Selectivity		Hydroquinone/ catechol
		Catechol	Hydroquinone	
10	0	0	0	-
20	0	0	0	-
30	0	0	0	-
40	12.31	56.68	43.32	0.764
50	28.11	53.00	47.00	0.887
60	56.33	50.75	49.25	0.970
70	59.21	40.18	59.82	1.49
120	60.11	28.75	71.25	2.478

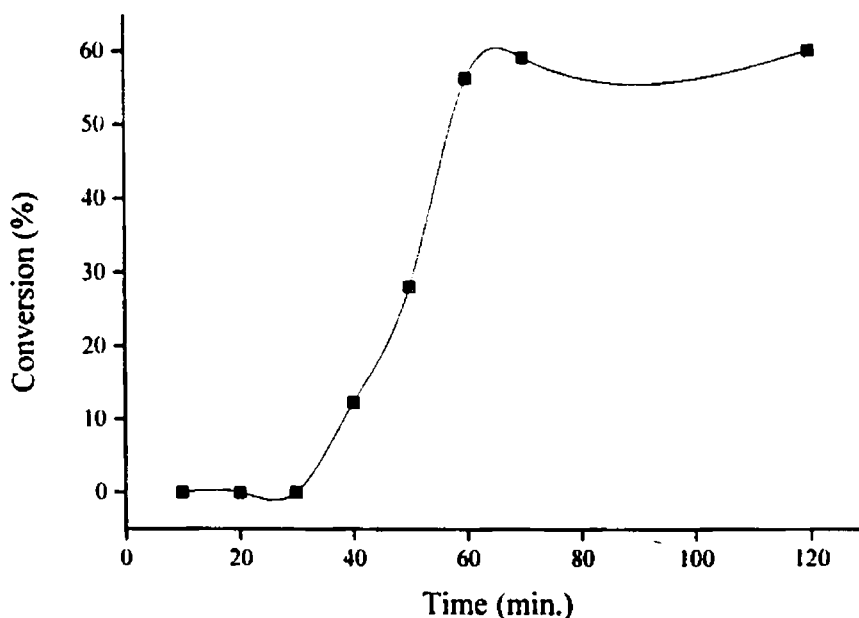


Figure 5.4 Induction period during the hydroxylation of phenol over $\text{FeAl}_{0.5}\text{PM}$ at room temperature

particular conversion level, the phenol conversion is nearly constant. The occurrence of an induction period is indicative of the involvement of free radical mechanism for the reaction. It should also be noticed that as the phenol conversion increases, the hydroquinone to catechol ratio increases. As time progresses, the catechol formation is suppressed whereas the hydroquinone formation is more favoured. This can be the result of poisoning of the external surface by the unwanted formation of the tarry products [34].

5.2 Catalytic Reaction over Various Fe-Al Pillared Montmorillonites

Table 5.6 shows the results of the reaction carried over the various iron-aluminium pillared montmorillonites. There was negligible reaction over parent montmorillonite and aluminium pillared montmorillonite after one hour of reaction. But the percentage conversion dramatically increased by the incorporation of iron into the systems. The influence of the reaction time is discussed in the earlier section. An induction period is clearly observed for the reaction. The catalyst AlPM cannot overcome the induction period within one hour whereas the induction period is much below this duration for all the iron incorporated systems. However, almost similar conversion and selectivity pattern are exhibited by all iron incorporated systems. This

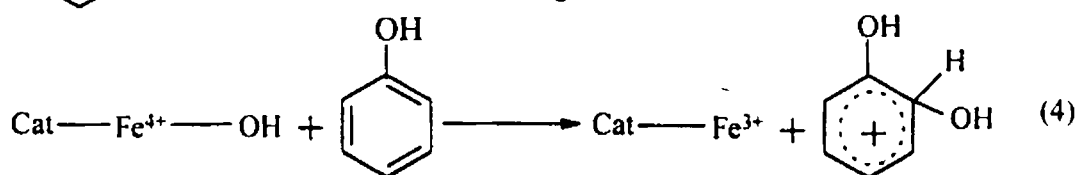
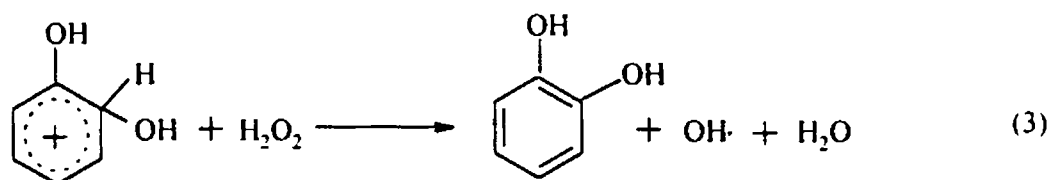
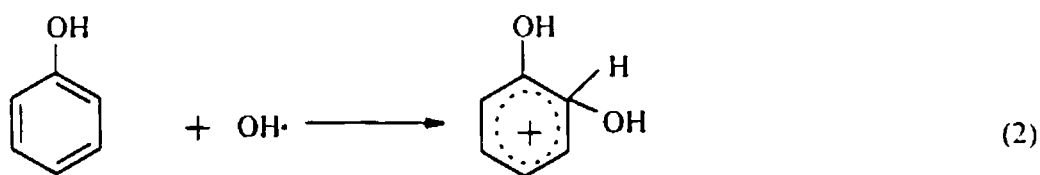
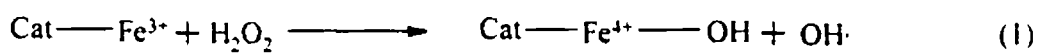
Table 5.6 Phenol hydroxylation data over mixed Fe-Al pillared montmorillonites (0.1 g catalyst, room temperature, 1 mL phenol, 5 mL water and 5 mL H₂O₂, 1 h run)

Catalyst	Conversion (%)	Selectivity (%)	
		Catechol	Hydroquinone
AIPM	3.00	100	0
FeAl _{0.1} PM	54.94	56.40	43.60
FeAl _{0.2} PM	62.13	58.40	41.61
FeAl _{0.3} PM	58.78	55.70	44.30
FeAl _{0.4} PM	56.77	56.80	43.20
FeAl _{0.5} PM	56.33	50.75	49.25
FeAl _{1.0} PM	57.90	57.27	42.74
FePM	55.15	55.76	44.24

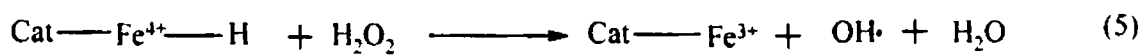
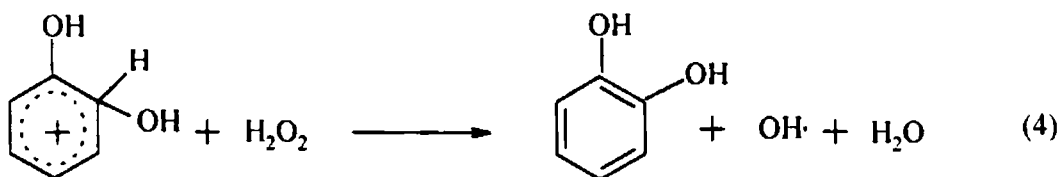
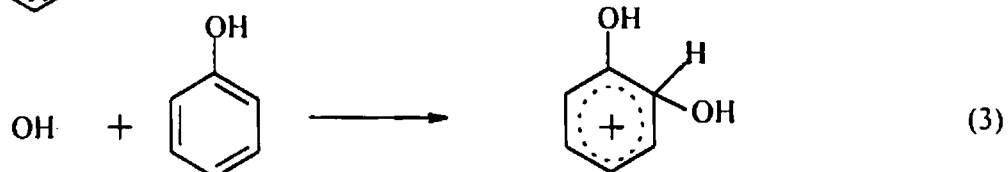
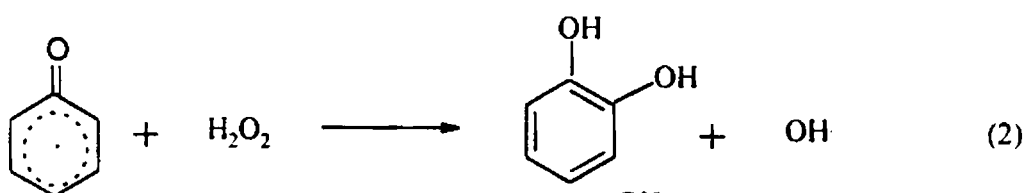
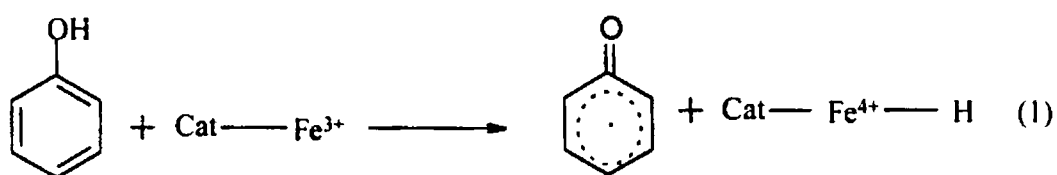
is indicative of the fact that only a minimum concentration of iron is required for carrying out the reaction and this is satisfied by all the prepared iron systems. Almost similar selectivity pattern is exhibited by all the iron containing catalysts.

5.3 Mechanism of Phenol Hydroxylation

Many mechanisms of phenol hydroxylation have been put forward, such as free radical mechanism [35], peronium salt mechanism [36], etc. The occurrence of an induction period (Figure 5.4) is clearly an indicative of a free radical mechanism. During our catalytic activity studies, we observed a vigorous and violent reaction of the mixture after a particular time of reaction. Analysis of the reaction mixture before this bursting did not give any phenol conversion, whereas the reaction took place all of a sudden during this bursting. In the case of hydroxylation of phenol with H₂O₂ as oxidant, free radicals can be generated on the solid catalyst surface in two ways as shown in scheme I and scheme II. In scheme 1, the initiation step is the formation of hydroxyl free radical, OH[•] from H₂O₂. OH[•] shows the characteristic of electrophilic substitution in the hydroxylation of the aromatic ring to yield the diphenols. It is assumed that the production of hydroquinone proceeds in the same manner as that of catechol.

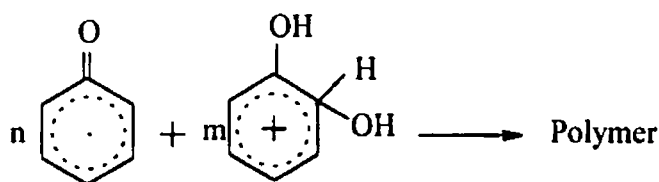


Scheme I



Scheme II

In scheme II, the initiation step is the formation of phenoxy radical from the reaction between phenol and catalyst. This phenoxy radical initiates the formation of OH free radical which is the active species for the reaction. Due to the competitive adsorption effects, the initiation step can be thought to be the formation of phenoxy radicals. These phenoxy radicals are involved in the propagation of the reaction chain. In all the cases of catalytic activity studies of phenol hydroxylation, the solution became dark brown after reaction. This can be the result of formation of tarry products from the reaction intermediates formed in the scheme II. This reaction, which is perhaps the main side reaction, is shown in Scheme III.



Scheme III

Thus we can conclude that the heterogeneously catalysed aqueous phase oxidation of phenol proceeds by a free radical mechanism, with an induction period before the steady state regime is achieved. The mechanism involves initiation on the catalyst surface followed by homogeneous or heterogeneous propagation in the liquid.

5.4 Catalytic Activity Studies over Other Systems

The time on stream study of phenol hydroxylation reaction over various Cr-Al pillared montmorillonites are shown in Figure 5.5. We can see that an appreciable conversion for the reaction is attained only around the third hour of reaction. This is the case with AlPM also. This means that the induction period is too large in the case of aluminium and mixed Cr-Al systems, compared to mixed Fe-Al systems. The incorporation of iron into the system thus helps to reduce the induction period. Once the reaction starts, the conversion level does not vary very much with time.

The reaction data over various vanadia loaded iron pillared montmorillonites are shown in Table 5.7. These data reveal that the selectivity patterns are very much affected by the vanadia incorporation. At low vanadia loadings the selectivity towards hydroquinone is more than that towards catechol. This is very much predominant in the case of 2VFe, where the selectivity for hydroquinone is 73.7%. At low vanadia loadings, vanadia blocks the active sites on the surface and hence catechol formation is retarded and more selectivity towards hydroquinone is observed. However, as the loading increases, more and more vanadia enter into the pores and an equimolar mixture of catechol and hydroquinone are observed. At much higher loadings such as 15VFe and 20VFe, only catechol is formed, which suggests that the reaction takes place only on the external surface sites only. It is noteworthy that, as the vanadia content increases, due to the blocking of active sites, the conversion decreases.

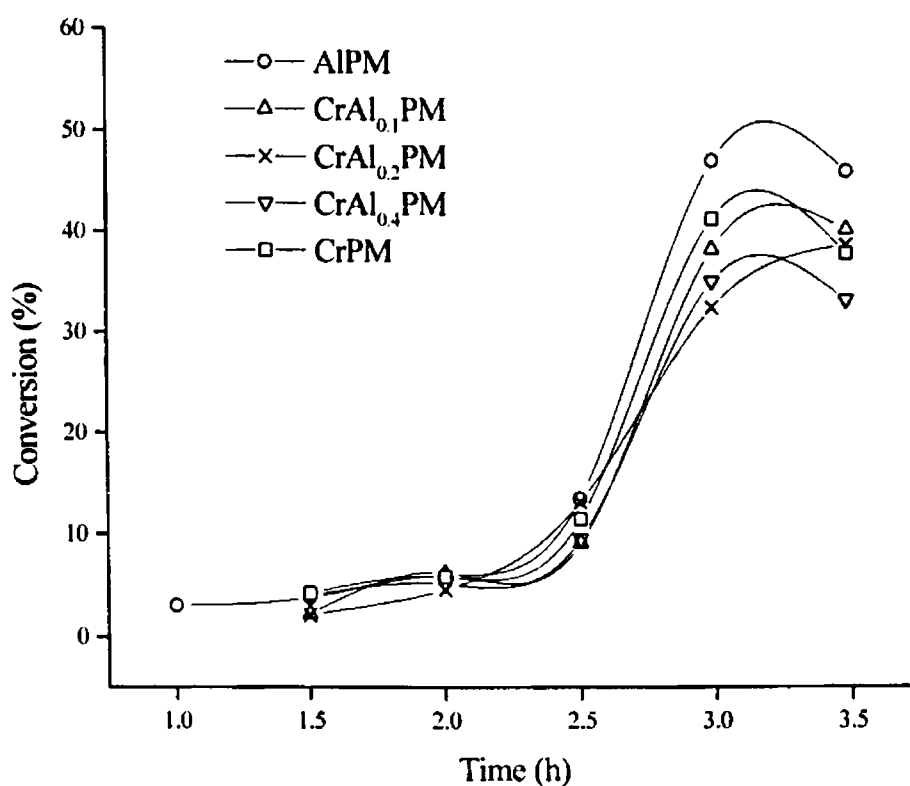


Figure 5.5 Phenol hydroxylation reaction over mixed Cr-Al pillared systems

Table 5.7 Catalytic wet peroxide oxidation data over various vanadia loaded FePMs

Catalyst System	Conversion (%)	Selectivity (%)	
		Catechol	Hydroquinone
FePM	56.33	50.75	49.25
2VFe	50.11	26.30	73.70
5VFe	50.32	44.76	55.26
7VFe	46.28	65.61	34.39
10VFe	20.11	74.21	25.79
15VFe	10.24	100	0
20VFe	5.62	100	0

Analysis of the reaction mixture after a prolonged time of 5-6 h showed that the percentage of catechol or hydroquinone in the reaction mixture is almost zero. This suggests the over-oxidation of the products to tarry products [34]. Also the formation of carbon oxides, which accompanies the reaction, is not quantitatively estimated. It must be stated that an increasing amount of carbon oxides can be formed by increasing the temperature. The complete oxidation of phenol to carbon oxides (wet oxidation in water) is possible on these catalyst systems, as indicated by this study. So, by optimising reaction conditions, it would be possible to purify water containing small amounts of phenol over these catalysts.

The study of the catalytic oxidation by hydrogen peroxide of an aqueous solution of phenol on various pillared clays has shown that, under mild reaction conditions, these solids work as efficient catalysts and can be successfully used as depollution catalysts. Among different solvents tried, water is found to be the best solvent to carry out the reaction. All catalysts showed an induction period for the reaction, suggesting a free radical initiation for the reaction. The induction period for iron systems were found to be very low compared to other systems.

References

- [1] J. Barrault, C. Bouchoule, K. Echachoui, N. Frini-Srasra, M. Trabelsi and F. Bergaya, *Appl. Catal. B Environ.*, 15 (1998) 269.
- [2] M. Abdellaoui, J. Barrault, C. Bouchoule, N. Frini-Srasra, and F. Bergaya, *J. Chim. Phys.*, 96 (1999) 419.
- [3] M. Falcon, K. Fajerweg, J.N. Foussard, E. Peuch-Coster, M.T. Maurette and H. Debellefontaine, *Environ. Technol.*, 16 (1995) 501.
- [4] K. Fajerweg and H. Debellefontaine, *Appl. Catal. B Environ.*, 10 (1996) L 229.
- [5] C. Hemmert, M. Renz and B. Meunier, *J. Mol. Catal.*, 137 (1999) 205.
- [6] H. Jeifert, W. Waldmann and W. Sch Weidel, *Ger. Patent* 2 410 742 (1975).
- [7] P. Maggioni, *US Patent*, 3 914 323 (1975).
- [8] M. Taramasso, G. Perego and B. Notari, *US Patent* 4 410 501 (1983).
- [9] A. Thangaraj, R. Kumar and P. Ratnasamy, *Appl. Catal.*, 57 (1990) L 1.
- [10] J.S. Reddy, R. Kumar and P. Ratnasamy, *Appl. Catal.*, 58 (1990) L 1.
- [11] J. S. Reddy and S. Sivasankar, *Catal. Lett.*, 11 (1994) 241.
- [12] K.R. Jiri, Z. Amost and H. Jiri, *Collect. Czech.Chem. Commun.*, 60 (1995) 451.
- [13] J.F. Yu, C.L. Zgang, Y. Yang and T.H. Wu, *J. Catal.*, 18 (1997) 230.
- [14] S. M. Imamura, *Gijustu* 22 (1981) 201.
- [15] N. Al-Hayck, *Water Res.*, 19 (1985) 657.
- [16] J.A. Martens, P. Buskens, P.A. Jacobs, A. van der Pol, J.H.C. Vant Hoff, C. Ferrini, H.W. Kouwenhoven, P.J. Kooyman and H. van Bekkum, *Appl. Catal. A Gen.*, 99 (1992) 71.
- [17] A. Thangaraj, R. Kumar, S.P. Mirajkar and P. Ratnasamy, *J. Catal.*, 130 (1991) 1.
- [18] A. van der Pol, A. J. Verduyn and J.H.C. Vant Hoff, *Appl. Catal. A Gen.*, 92 (1992) 113.
- [19] A. Thangaraj, R. Kumar and P. Ratnasamy, *J. Catal.*, 131 (294) 1991.
- [20] T. Blasco, A. Cambor, A. Corma, P. Esteve, J.M. Guil, A. Martinez, J. A. Perdigon-Melon and S. Valencia, *J. Phys. Chem. B*, 102 (1998) 75.
- [21] R. Yu, F. Xiao, D. Wang, J. Sun, Y. Liu, G. Pang, S. Feng, S. Qiu, R. Xu and C. Fang, *Catal. Today*, 51 (1999) 39.

- [22] C. Xiong, Q. Chen, Weiran Lu, H. Gao, W. Lu and Z. Gao, *Catal. Lett.*, 69 (2000) 231.
- [23] R. Yu, F. Xiao, D. Wang, Y. Liu, G. Pang, S. Feng, S. Qiu and R. Xu, *Catal. Lett.*, 49 (1997) 49.
- [24] A. Tuel, S. Moussa-Khouzami, Y. Ben Taarit and C. Naccache, *J. Mol. Catal.*, 68 (1991) 45.
- [25] D.H. Doff, N.H. Gangas, J.E. Allan and J.M. Coey, *Clay Miner.*, 23 (1988) 367.
- [26] J. Barrault, M. Abdellaoui, C. Bouchoule, A. Majesti, J.M. Tatibouet, A. Louloudi, N. Papyannakos and N.H. Gangas, *Appl. Catal. B Environ.*, 27 (2000) L 225.
- [27] H.L.D. Castello, A. Gil and P. Grange, *Clays Clay Miner.*, 44 (1996) 706.
- [28] A. Dubey, V. Rives and S. Kannan, *Fifteenth Ind. Nat. Symp. on Catal.*, Pune, India, 2000.
- [29] R. Neumann and M. Levin-Elad, *Appl. Catal. A Gen.*, 122 (1995) 85.
- [30] S. I. Saudler, "Chemical and Engineering Thermodynamics", 2nd Edn., Elsevier, 1992.
- [31] A. G. Davies, "Organic Peroxides" Butterworth, 1961.
- [32] M.C.V. Sauer and J.O. Edwards, *J. Phys. Chem.*, 75 (1971) 3004.
- [33] P.R. Hari, P. Rao and A.V. Ramaswamy, *Appl. Catal. A Gen.*, 93 (1993) 123.
- [34] U. Wilkenhoner, G. Laughendries, F. van Laar, G.V. Baron, D.W. Gammon, P.A. Jacobs and E. van Steen, *J. Catal.*, (In Press).
- [35] C. Meyer, G. Clement and J.C. Balaceanu in " Proc. 3rd Int. Cong. on Catalysis" Vol.1 (1965) p- 184.
- [36] C.B. Liu, Z. Zhao, X.G. Yang, Y.K. Ye and Y. Wu, *J. Chem. Soc. Chem. Commun.*, (1996) 1019.

Summary and Conclusions

6.1 Summary of the Work

Since the first report of synthesis of montmorillonite pillared with heat stable inorganic cation complexes of Zr, these modified materials have been the subject of intense research efforts in both industrial research laboratories and academia. Pillaring of montmorillonite with stable oxides of other metals such as Al, Fe, Cr, etc resulted in the conversion of inexpensive and thermally unstable clay minerals into highly porous and stable structures. In this process, robust oxide particles are formed between the clay layers resulting in layer expansion and higher surface area. The open microporous structures which contain both Brønsted and Lewis acid sites are accessible for catalysis. This has given a new impetus to the study of catalytic activities of pillared clay minerals.

The present work is devoted to the synthesis and modification of various pillared montmorillonites. Single oxide pillaring with Al, Fe and Cr as well as pillaring of montmorillonite with mixed oxides of a) Al and Fe and b) Al and Cr are attempted. Modification of iron-pillared montmorillonite by vanadia impregnation is also tried. Various characterisation techniques have been used to evaluate the structural and textural properties of these solids. Finally, the catalytic activities of these materials in various industrially important reactions are investigated. The present thesis comprises of six chapters expounding the introduction, experimental and results and discussion parts.

In **Chapter 1** a brief introduction to heterogeneous catalysis is given. A detailed description of the clay structure and its modification by pillaring covers a major part of this chapter. A brief literature survey on the catalysis by single and mixed pillared clays is also included. Determination of acidity by different techniques, including alcohol and cumene test reactions is discussed. A brief introduction about certain catalytic reaction such as Friedel-Crafts alkylation and acylation, aniline methylation and catalytic wet peroxide oxidation of phenol is also included in this chapter.

Chapter II deals with the various experimental procedures adopted for the synthesis, characterisation and catalytic activity studies of the different single, mixed and modified pillared montmorillonites. It also gives a brief account of the relevant theory of each method of characterisation employed.

Chapter III is devoted to giving and discussing the results of the various characterisation techniques. The results and discussion are conveniently given under three headings, Fe-Al pillared montmorillonites, Cr-Al pillared montmorillonite and vanadia impregnated iron pillared montmorillonites. The XRD results and the surface area and pore volume results are considered as the prime evidences for efficient pillaring of the parent montmorillonite. The EDX results give the chemical composition of each pillared and modified montmorillonite and confirm the incorporation of the employed metals' oxide into the clay structure. Vanadia impregnation over the iron-pillared montmorillonite is suggested by the XRD and EDX results. FT-IR analysis of the pillared montmorillonites confirms that the structure of the clay layers is not altered by pillaring. Dispersion of vanadia as V_2O_5 crystals over iron-pillared montmorillonite is evidenced by FTIR analysis. TGA proves that dehydroxylation of pillared materials takes place much below a temperature at which the parent clay dehydroxylates. Surface acidity measurements have revealed that pillaring enhanced both Brönsted acidity and Lewis acidity of the samples. Vanadia impregnation also resulted in the modification of the acidity pattern of the parent iron-pillared montmorillonite. Thermodesorption of 2,6-dimethylpyridine and electron accepting studies by perylene gives the Brönsted acidity and Lewis acidity of the samples respectively. Temperature programmed desorption of ammonia performed over the various catalysts gave the acidity distribution and total acidity of the samples. The results of cumene cracking reaction which is performed as a test reaction for acidity determination, agree to the generally accepted view that cracking proceeds over Brönsted sites whereas dehydrogenation proceeds over Lewis acidic sites.

In chapter IV, we have furnished the results and discussion of liquid phase Friedel-Crafts benzylation and benzoylation of toluene and vapour phase methylation of aniline. Benzylation of toluene with two different reagents namely benzyl chloride and benzyl alcohol established that the former reaction is catalysed by Lewis acidic sites and the latter by Brönsted acidic sites. When benzyl chloride is used for the

reaction, a free radical mechanism is observed in the presence of reducible cations like Fe^{3+} . In the absence of reducible cations, strong acid sites are responsible for catalysing the reaction. Between benzyl chloride and benzyl alcohol, in catalysis point of view, benzyl alcohol is found to be a better reagent, though conversion is lower when compared to the conversion with benzyl chloride. This is because of the fact that the catalysts are less stable in presence of benzyl chloride due to the evolution of HCl during the reaction. A true heterogeneous reaction is observed with benzyl alcohol while a 100% heterogeneous reaction is not occurring with benzyl chloride as reagent. For acylation of toluene, benzoyl chloride is used. It is found that benzylation is catalysed by the strong Lewis acid sites present in the catalyst. Chapter IV also narrates the results of methylation of aniline which is conducted in the vapour phase. The results revealed that a moderate acidity is required for a better catalytic reaction. Surplus acidity does not seem to favour the conversion of aniline.

In Chapter V, the efficiency of pillared clays in catalytic wet peroxide oxidation of phenol is discussed. Iron pillared clays are found to be very effective for the catalytic wet peroxide oxidation of phenol. An induction period is noted for the reaction. The influence of solvent, temperature and phenol to H_2O_2 molar ratio are also discussed. It is found that certain optimum parameters are required for the better performance of the catalysts in the catalytic wet peroxide oxidation of phenol.

In the present chapter, Chapter VI, the summary and conclusions of the work done are given.

6.2 Conclusions

The following conclusions are drawn from the present work.

- Pillaring of montmorillonite with polyoxocations of metals resulted in the satisfactory incorporation of metals into the clay layers.
- Maximum incorporation of metal takes place for an optimum Fe(Cr)/Al ratio in the case of mixed pillared clays.
- Pillared and modified pillared solids were thermally stable.
- Enhancement of surface area and pore volume and shift of XRD peak towards lower 2θ region suggest efficient pillaring.
- Vanadia is dispersed as V_2O_5 over the iron pillared montmorillonite and becomes detectable by XRD after 7% loading.

- Both pillaring of montmorillonite and vanadia modification over pillared montmorillonite increased the acidity (both Brønsted and Lewis) of the systems.
- Iron incorporated systems are found to be very active for benzylation of toluene with benzyl chloride; in that case a free radical mechanism is found to be operating.
- Brønsted acidity decides the activity towards benzylation of toluene with benzyl alcohol.
- Catalysts are active even in the presence of moisture for benzylation of toluene. An induction period is noticed for the reaction between benzyl chloride and toluene in presence of moisture. Moisture has a beneficial effect for the reaction between benzyl alcohol and toluene.
- Truly heterogeneous reaction is operating when benzyl alcohol is the reagent for benzylation. A 100% heterogeneous reaction is not taking place with benzyl chloride. During the reaction between benzyl chloride and toluene, the HCl evolved during the reaction leaches some of the metal ions into the solution and homogeneous reaction is also occurring to some extent.
- In general, stronger Lewis acidic sites are found to be required for the benzylation of toluene.
- Moderate acidity in the weak plus medium region decides aniline conversion; stronger sites lead to C-alkylation.
- In almost all cases, more than 80% selectivity is observed for N-alkylated products which are industrially very important.
- Pillared clays are found to be very effective for the catalytic wet peroxide oxidation of phenol. The induction period noted for the reaction is found to be very low with iron systems compared to Al and Cr systems. Water is found to be the most effective solvent whereas methanol is the most selective solvent.

SCOPE FOR FURTHER WORK

The present thesis describes the catalytic reactions such as Friedel-Crafts alkylation and acylation, methylation of aniline and catalytic wet peroxide oxidation of phenol. We have found that the pillared clays are efficient catalysts for all the reactions. In the case of benzylation of toluene, though catalyst is not very stable in presence of benzyl chloride as reagent, the catalyst is found to be stable with benzyl alcohol. Hence the work can be extended to study the alkylation of other aromatic molecules with different substituents using benzyl alcohol as reagent. Other novel alkylation reactions can be tried over the pillared clays.

An interesting property of pillared clays is that their pore size can be tuned by choosing appropriate pillaring precursors. Hence shape selectivity could be achieved and pillared clays could be used for shape selective catalysis.

We have found that the pillared clay catalysts are promising ones for the hydroxylation of phenol. Prolonged reaction is found to remove all the phenol present in the reaction mixture. Mild conditions yield hydroxylated derivatives whereas prolonged reactions resulted in the formation of carbon oxides and tar. Study of the reaction using pillared clays for the removal of phenol present in ppm levels in waste-water is a fruitful scope of the present investigation. These investigations could be extended for the catalytic wet peroxide oxidation of other organic pollutants.